Virulence and required genes in the fish pathogen *Vibrio anguillarum*

Stuart McMillan

B. Sc. Applied Marine Biology

A thesis submitted for the degree of doctor of philosophy

Institute of Aquaculture

University of Stirling

Oct, 2016

Declaration

I, Stuart McMillan, hereby certify that this thesis, which is approximately 48,000 words in length, has been written by me, that it is the record of work carried out by me and that it has not been submitted in any previous application for a higher degree.

Stuart McMillan

Date

Acknowledgements

First and foremost, thank-you to Laura, my wife, who has put up with a lot over the past four years but has supported me all the way.

A huge thank-you to all the staff at Fishers in the City, Edinburgh, for keeping me sane and providing some much needed balance.

For keeping me fit and healthy, and providing the best banter in Stirling, thank-you to Marie, Sanne, Andre, Matt, Neila and Sean. I would not have been able to do this without you guys.

To Matt in Manchester, thank-you for all the pub crawls and good-natured political debate. You are a legend.

Thank-you to Jacquie, Kerry, Elsbeth, John, Michael, Debbie and Jan for all their help in the lab along the way. Likewise, thank-you to Shirley Graham (University of St Andrews, UK) for her advice on point mutagenesis procedure.

For kindly gifting the bacterial strains, thank-you to Dr Dawn Austin (Heriot Watt University, UK), Professor Debra Milton (Umea University, Sweden) and Professor David Nelson (University of Rhode Island, US).

Finally, special thanks to my supervisors, Brian, David, Andrew and Jason, but most of all Dr. Andrew Desbois, who allowed me to embark upon this adventure and has taught me how to write proper.

Abstract

Vibrio anguillarum infects many fish species in aquaculture, reducing farm productivity and negatively impacting fish welfare. Deeper understanding of the biology of *V. anguillarum*, particularly during infections *in vivo*, will help to improve disease prevention and control. Thus, the aim of this thesis was to provide further insight into the infection biology of *V. anguillarum* with a view to identifying better ways to reduce the impact of this pathogen in aquaculture. Conventional studies on virulence, particularly those aiming to identify novel virulence factors, often employ transposon mutagenesis where the functions of individual genes in the bacterium are disrupted. These mutant libraries are screened to identify those with attenuated virulence, allowing subsequent identification of the gene responsible. Usually the native fish host would be used but such studies are increasingly difficult to perform due to regulations on vertebrate experiments and ethical concerns. As a result, alternative invertebrate hosts are now an important means to studying microbial infections, but few models have been assessed for bacterial pathogens of fish. In this thesis, larvae of the greater wax moth *Galleria mellonella* were evaluated as an alternative host to investigate *V. anguillarum* virulence. Wild-type *V. anguillarum* isolates killed larvae in a dose-dependent manner, replicated in the haemolymph, and larvae infected with a lethal dose of bacteria could be rescued by antibiotic therapy, thus indicating that *V. anguillarum* established an infection in *G. mellonella*. Crucially, virulence of 11 wild-type *V. anguillarum* isolates correlated

significantly between larva and Atlantic salmon infection models, and studies with isogenic mutants knocked out for various virulence determinants revealed conserved roles for some in larva and fish infections, including the pJM1 virulence plasmid and *rtxA* toxin. Thereafter, 350 strains from a *V. anguillarum* random transposon insertion library were screened for attenuated virulence in *G. mellonella*. In total, 12 strains had reduced virulence and in these mutants the transposon had inserted into genes encoding several recognised and putative virulence factors, including a haemolytic toxin (*vah1*) and proteins involved in iron sequestration (*angB/G* and *angN*). Importantly, the transposon in one strain had inserted into an uncharacterised hypothetical protein. Preliminary investigations found this putative novel virulence factor to contain a GlyGly-CTERM sorting domain motif, with sequence similarity to *VesB* of *Vibrio cholerae* which is involved in post-translational processing of cholera toxin. Finally, three transposon insertion libraries were mass sequenced on a MiSeq platform to identify *V. anguillarum* genes lacking transposon insertions. These genes were assumed to be 'required' for viability in the conditions under which the mutants were selected, in this case tryptone soya agar. In total, 248 genes lacked a transposon insertion and were the putative 'required' genes, and these may be important chemotherapeutic targets for new approaches to combat *V. anguillarum* infections. This thesis has furthered our understanding of the biology of the important fish pathogen *V. anguillarum* using an ethically acceptable approach, and the findings

may assist with new ways to reduce the burden of this bacterium in aquaculture.

Table of contents

Chapter 1.

Introduction **1**

1.1.	Aquaculture and current challenges	1
1.2.	*Vibrio anguillarum*	2
1.2.1.	General background	2
1.2.1.1.	Biotype	3
1.2.1.2.	Serotype	4
1.2.1.3.	Plasmids in *Vibrio anguillarum*	5
1.2.2.	Virulence mechanisms of *Vibrio anguillarum*	7
1.2.2.1.	Iron acquisition	7
1.2.2.2.	Motility and chemotaxis	16
1.2.2.3.	Lipopolysaccaride	17
1.2.2.4.	Protease	18
1.2.2 5.	Haemolysins	19
1.2.2.6.	Exopolysaccaride	20
1.2.2.7.	Regulation and communication	21
1.2.3	*Vibrio anguillarum*: Current status, treatment and prevention	22
1.3	Alternative Hosts	24
1.3.1.	Selecting an alternative host	24
1.3.1.1.	Protozoans	27
1.3.1.2.	Nematodes	27
1.3.1.3.	Zebrafish embryo	28
1.3.1.4.	Insects	29
1.3.2.	Alternative hosts used in the study of bacterial fish pathogens	30
1.3.3.	The alternative host *Galleria mellonella*	31
1.3.4.	Previous study of pathogens in *Galleria mellonella*	33
1.4.	Transposon mutagenesis	36
1.5.	Transposon insertion sequencing	38
1.5.1.	Transposon mutagenesis and massively parallel sequencing	38
1.5.2.	Tn-seq in *Vibrio* spp.	43
1.6	Aims and objectives of this thesis	44

Chapter 2.

Standard procedures and identification of *Vibrio anguillarum* and mutant genotypes **45**

2.1.	**Introduction**	**45**
2.2.	**Materials and methods**	**46**
2.2.1.	Chemicals, reagents and media	46
2.2.2.	Bacteria	47
2.2.3.	*Galleria mellonella* larvae	48
2.2.3.1.	Larval injections	48
2.2.4.	Preparation of calibration curves	52
2.2.5.1.	DNA extraction	53
2.2.5.2.	Primers	54
2.2.5.3.	Polymerase chain reaction (PCR)	54
2.2.5.4.	Gel electrophoresis	57
2.2.6.	Confirmation of cultures as *Vibrio* spp.	58
2.2.7.	Confirmation of cultures as *Vibrio anguillarum*	59
2.2.7.1.	Latex agglutination test	59
2.2.7.2.	Optimisation of *Vibrio anguillarum* specific PCR	60
2.2.7.3.	*Vibrio anguillarum* identification by PCR	62
2.2.8.	Confirmation of pJM1-like virulence plasmid in wild-type serotype O1 *Vibrio anguillarum* isolates	62
2.2.9.	Confirmation of *Vibrio anguillarum* mutant genotypes	62
2.3.	**Results**	**67**
2.3.1	Generation of calibration curves	67
2.3.2.	Identification and confirmation of colonies as *Vibrio* spp.	67
2.3.3.	Identification of *Vibrio anguillarum*	67
2.3.4.	*Vibrio anguillarum* serotype O1 isolates carrying the pJM1-like virulence plasmid	73
2.3.5.	Confirmation of *Vibrio anguillarum* mutant genotypes	75
2.4.	**Discussion**	**79**

Chapter 3.

Evaluation of *Galleria mellonella* as an alternative host for studying the pathogenicity and virulence of *Vibrio anguillarum* **86**

3.1.	**Introduction**	**86**
3.2.	**Materials and methods**	**87**

3.2.1.	Minimum inhibitory concentration (MIC) of antibiotics	87
3.2.2.1.	Wild type challenge and correlation with virulence in *Salmo Salar*	89
3.2.2.2.	Heat-killed bacterial challenge	89
3.2.2.3.	Antibiotic rescue of infection	90
3.2.3.	*Vibrio anguillarum* burden in *Galleria mellonella*	90
3.2.3.1.	*Vibrio anguillarum* burden in *Galleria mellonella* haemolymph	91
3.2.3.2.	*Vibrio anguillarum* burden in *Galleria mellonella* tissues	92
3.2.4	*In vitro* growth curve in 96-well plate	93
3.2.5.	Mutant challenge	93
3.2.6.	Recovery and confirmation of *Vibrio anguillarum*.	94
3.2.6.1.	Recovery of *Vibrio anguillarum* from infected *Galleria mellonella*.	94
3.2.7.	Statistical analyses	94
3.3.	**Results**	**95**
3.3.1.	Minimum inhibitory concentration (MIC) of antibiotics	95
3.3.2.	*Vibrio anguillarum* establishes an infection in *Galleria mellonella*	97
3.3.3.	Only viable *Vibrio anguillarum* cells caused mortality of larvae	97
3.3.4.	Antibiotic rescue of infection	97
3.3.5.	Positive correlation in virulence of *Vibrio anguillarum* isolates in *Salmo salar* and *Galleria mellonella* infection models	102
3.3.6.	Recovery of *Vibrio anguillarum* from infected *Galleria mellonella*.	102
3.3.7.	*Vibrio anguillarum* burden in haemolymph and tissue	105
3.3.7.	Isogenic knockout mutant challenge	108
3.4.	**Discussion**	**110**

Chapter 4.

Identification of genes required for virulence in *Vibrio anguillarum* using transposon mutagenesis. **115**

4.1.	**Introduction**	**115**
4.2	**Materials and Methods**	**120**
4.2.1.	Strains and plasmids	120

4.2.2.	Susceptibility of test strains to antibiotics	120
4.2.3.	Curing *Escherichia coli* SM10λpir of plasmid pSC189	124
4.2.4.	Generation and screening of *Vibrio anguillarum* streptomycin-resistant mutants	124
4.2.4.1.	Generation of *Vibrio anguillarum* streptomycin resistant mutants	124
4.2.4.2.	Spontaneous mutant challenge in wax moth	125
4.3.4.3.	*In vitro* growth of *Vibrio anguillarum* NB10Sm	126
4.2.5.	Generation and validation of *Vibrio anguillarum* NB10Sm random transposon insertion mutant library	126
4.2.6.	Individual transposon mutant challenge	128
4.2.6.1.	Preparation of mutant inoculums for virulence assessment in *Galleria mellonella*	128
4.2.6.2	Assessment of virulence in *Galleria mellonella*	129
4.2.7.	PCR validation of *V. anguillarum* transposon mutants	130
4.2.7.1	Transposon integration into genomic DNA	131
4.2.7.2.	Loss of pSC189 plasmid backbone	131
4.2.7.3.	Retention of p67-NB10 virulence plasmid	131
4.2.7.4.	Non-transfer of bacteriophage Mu	134
4.2.8.	Identification of transposon insert locations by arbitrary PCR	134
4.2.8.2.	Arbitrary PCR to amplify the transposon-host DNA junction in transposon mutants	134
4.2.8.3.	PCR clean-up	137
4.2.8.4.	Lightrun sequencing	138
4.2.8.5.	Identification of insert location	138
4.2.9.	Characterisation of three *Vibrio anguillarum* random transposon insertion mutants	139
4.2.9.1	Retention of transposon insertions in the strains during *in vivo* infection of *Galleria mellonella*	139
4.2.9.2.	*In vitro* growth of transposon insertion mutants compared to the parent strain	140
4.2.9.3.	*In silico* analysis of uncharacterised protein	140
4.2.9.4.	Biolog profile	141
4.2.10.	Statistical analysis	142
4.3	**Results**	**143**
4.3.1.	Curing *Escherichia coli* SM10λpir of pSC189 plasmid.	143

4.3.2.	Antibiotic selection of *Vibrio anguillarum* transposon insertion mutants	143
4.3.3.	Generation of *Vibrio anguillarum* streptomycin-resistant (STR^r) spontaneous mutant for subsequent use in transposon insertion mutant library preparation	148
4.3.4.	Generation and selection of *Vibrio anguillarum* transposon mutants	156
4.3.5.	Virulence assessment of transposon insertion mutants in *G. mellonella*	156
4.3.6.	Examination of transposon mutants by PCR.	158
4.3.7.	Identification of transposon insertion locations	160
4.3.8.	Further characterisation of Tn73, Tn100 and Tn205 *Vibrio anguillarum* transposon insertion mutants	163
4.4	**Discussion**	**173**

Chapter 5.

Determination of genes required for growth and virulence of *Vibrio anguillarum* by transposon insertion sequencing		**179**
5.1.	**Introduction**	**179**
5.2.	**Materials and methods**	**181**
5.2.1.	Isolates and plasmids	181
5.2.2.	Preparation of competent *Escherichia coli* cells	181
5.2.3.	DNA quantification by Qubit®	183
5.2.4.	Purification of PCR products using magnetic beads	184
5.2.5.1.	Site-directed point mutagenesis of the pSC189 plasmid	185
5.2.5.2.	Digestion of template DNA and transformation back into donor strain	187
5.2.5.3.	Plasmid transformation into delivery vector	191
5.2.5.4.	Confirmation of point mutation	192
5.2.6.	Preparation of transposon mutant libraries	193
5.2.6.1	Transposon mutagenesis	193
5.2.6.2.	Library preparation	195
5.2.7.	Processing of random transposon mutant libraries for Tn-seq	195
5.2.7.1.	Library selection	195
5.2.7.2.	Library DNA Extraction	196
5.2.7.3.	Confirmation of DNA integrity	197

5.2.7.4.	Library digestion and purification	198
5.2.7.5.	Ligation of adapter	199
5.2.7.6.	Insert fragment amplification and addition of Nextera adapter sequences	200
5.2.7.7.	Processing and loading onto MiSeq	203
5.2.8.	Data analysis	204
5.3.	**Results**	**205**
5.3.1.	Site-directed point mutagenesis of the pSC189 plasmid	205
5.3.2.	Preparation of transposon mutant libraries	206
5.3.3.	Transposon library quality and yield	208
5.3.4.	Ligation of Illumina and Illumina Nextera index adapters by PCR	208
5.3.5.	MiSeq run performance and processing of raw reads	214
5.3.6.	Tn-seq analysis	214
5.4.	**Discussion**	**227**

Chapter 6.
General Discussion **235**

References **243**

Appendices **268**

I	Consumables and equipment suppliers	283
II	Molecular buffers and reagents	284
III	Growth curve in shakeflask	287
IV	Hamilton® syringe wash procedure	288
V	Heat killing of *Vibrio anguillarum*	290
VI	Effect of penicillin in media	291
VII	Mariner transposon mutagenesis of *E. coli* recipient	292
VIII	Isolation of pSC189 and pUC18 plasmids	295
IX	Essential genes of *Vibrio anguillarum* NB10Sm	300

List of tables:

Table 1.1	*Vibrio anguillarum* virulence mechanisms, genes and functions.	8-11
Table 1.2.	Practical and functional parameters of various alternative hosts for studying microbial pathogens.	26
Table 1.3.	Previous studies using transposon sequencing (Tn-seq).	42
Table 2.1.	Isolates and plasmids used in this study.	48-49
Table 2.2.	Primers used to confirm *Vibrio anguillarum* wild-type and mutant isolates.	56-57
Table 2.3.	Primer annealing temperatures used in gradient polymerase chain reaction	61
Table 3.1.	Minimum inhibitory concentrations and minimum bactericidal concentrations of 11 *Vibrio anguillarum* isolates to kanamycin, penicillin G, streptomycin and tetracycline.	96
Table 3.2.	Burden of *Vibrio anguillarum* viable colonies within infected *Galleria mellonella*; comparison of haemolymph and whole body homogenate.	104
Table 3.3.	Comparison of virulence of *Vibrio anguillarum* parent and isogenic mutant strains lacking virulence factors in *Galleria mellonella* larva and fish models of infection.	96
Table 4.1.	Bacterial isolates and plasmids used in Chapter 4	123-124
Table 4.2.	Primers used to validate *Vibrio anguillarum* NB10Sm transposon insertion mutants.	133
Table 4.3.	Primers used for arbitrary PCR amplification of transposon-host DNA.	135
Table 4.4.	Minimum inhibitory concentrations (MICs) and minimum bactericidal concentrations (MBCs) of 8 *Vibrio anguillarum* isolates and *Escherichia coli* SM10λpir to ampicillin (AMP) following 24 h incubation.	146
Table 4.5.	Minimum inhibitory concentrations (MICs) and minimum bactericidal concentrations (MBCs) against kanamycin (KAN) of *Vibrio anguillarum* NB10 and the spontaneous streptomycin-resistant mutant (*V. anguillarum* NB10Sm), and *Escherichia coli* SM10λpir (pSC189).	147
Table 4.6.	Spontaneous mutation frequency of selected *Vibrio anguillarum* isolates on agar containing streptomycin.	149

Table 4.7.	Virulence of selected *Vibrio anguillarum* parent and spontaneous STR^r mutants in *Galleria mellonella*.	151
Table 4.8.	Transposon insertion locations in the *Vibrio anguillarum* NB10Sm genomic DNA.	162
Table 4.9.	Abilities of the *Vibrio anguillarum* NB10Sm parent and the transposon insertion mutant *V. anguillarum* Tn100 to utilise various carbon sources.	169-171
Table 4.10.	*Vibrio anguillarum* spontaneous mutant NB10Sm and transposon mutant derivative Tn100 sensitivities to chemicals, pH and differential NaCl concentrations.	172
Table 5.1.	Isolates and plasmids used in Chapter 5.	182
Table 5.2.	Oligonucleotides used in Chapter 5.	192
Table 5.3.	*Vibrio anguillarum* transposon (Tn) libraries and Illumina® Nextera XT index number and sequences.	202
Table 5.4.	Estimated number of *Vibrio anguillarum* NB10Sm random transposon mutants recovered from matings with *Escherichia coli* SM10 (pSC189_5').	207
Table 5.5.	Transposon library DNA concentration and purity.	210
Table 5.6.	Coverage of TA dinucleotide transposon insertion sites in *Vibrio anguillarum* NB10Sm genomic DNA.	216
Table 5.7.	Distance between TA dinucleotide sites with transposon insert within *Vibrio.anguillarum* NB10Sm genomic DNA.	217
Table 5.8.	Dinucleotide TA sites in *Vibrio anguillarum* NB10Sm identified to have been disrupted by transposon insertion.	218
Table 5.9.	Number of different transposon Tn-seq insert reads mapped to *Vibrio anguillarum* genomic DNA.	220-221
Table 5.10.	Putative required genes and gene products of *Vibrio anguillarum* NB10Sm with sequence similarity to a required gene of *Vibrio cholerae* E7946.	229

List of Figures:

Figure 2.1	*Galleria mellonella* larvae, in final instar stage, highlighting the abdominal prolegs into which inoculums are administered.	51
Figure 2.2	Confirmation of targeted mutations in *Vibrio anguillarum* genes.	64-65
Figure 2.3	Relationship between colony forming units per mL and cell suspension absorbance at 600 nm for *Vibrio anguillarum* and *Vibrio ordalii* isolates.	68
Figure 2.4.	Growth of *Vibrio anguillarum* on TCBS agar.	69
Figure 2.5.	Growth of *Vibrio anguillarum* on media with vibriostatic agent 0129 discs.	70
Figure 2.6.	*Vibrio anguillarum* specific temperature gradient PCR.	72
Figure 2.7.	Presence of pJM1-like virulence plasmid in *Vibrio anguillarum* serotype O1 isolates.	74
Figure 2.8	Presence of pJM1-like virulence plasmid in *Vibrio anguillarum* serotype O1 mutant knockout isolates.	76
Figure 2.9.	Confirmation of knockout mutation by allelic exchange in *Vibrio anguillarum* isolates.	78
Figure 2.10.	Confirmation of knockout mutation by plasmid insertion in *Vibrio anguillarum* isolates.	80-81
Figure 3.1.	Survival of groups of *Galleria mellonella* larvae injected with culture filtrate, viable CFU, and heat-killed CFU of eleven wild-type *Vibrio anguillarum* isolates.	98-99
Figure 3.2.	Survival of *Galleria mellonella* larvae injected with 1 x10^7 CFU of eleven wild-type *Vibrio anguillarum* isolates and treated at 2 h, 24 h and 48 h with tetracycline.	100-101
Figure 3.3.	Pearson correlation of virulence of 11 wild-type *Vibrio anguillarum* isolates in the *Galleria mellonella* larva and in a *Salmo salar* infection model.	103

Figure 3.4. Replication of 11 wild-type *Vibrio anguillarum* isolates in the haemolymph of *Galleria mellonella*. 106

Figure 3.5. In vitro growth of 11 *Vibrio anguillarum* wild-type isolates. 107

Figure 4.1. Workflow schematic illustrating the different stages required to complete a random transposon insertion mutant screen for *Vibrio anguillarum.* 116

Figure 4.2. Diagrammatic representation of targets in PCR assays to confirm transposon mutants in *Vibrio anguillarum.* 132

Figure 4.3. Diagrammatic representation of arbitrary PCR and insertion sequencing workflow. 136

Figure 4.4. *Escherichia coli* SM10λpir colonies sub-cultured onto antibiotic selective agar plate, to identify strains cured of the pSC189 plasmid. 144

Figure 4.5. Agarose gel electrophoresis of *Escherichia coli* SM10λ*pir* isolates, to confirm loss of AMP^r pSC189 plasmid following curing experiments. 145

Figure 4.6. Survival of *Galleria mellonella* injected with 1 $x10^5$ CFU of spontaneous streptomycin-resistant mutant strain *Vibrio anguillarum* NB10Sm and the *V. anguillarum* NB10 parent strain during 120 h at 15°C. 152

Figure 4.7. Growth of spontaneous STR^r mutant *Vibrio anguillarum* NB10Sm compared to the *V. anguillarum* NB10 parent. 153

Figure 4.8. Correlation between colony forming units per mL (CFU/mL) and culture absorbance at 600 nm (A_{600}) for *Escherichia coli* SM10 (pSC189). 154

Figure 4.9. Growth of transposon donor strain *Escherichia coli* SM10λ*pir* and *Vibrio anguillarum* NB10Sm recipient. 155

Figure 4.10. Transposon mutagenesis workflow illustrating the different stages of experiment. 157

Figure 4.11. Agarose gel electrophoresis of PCR products from presumed *Vibrio anguillarum* NB10Sm transposon insertion mutants. 159

Figure 4.12. Agarose gel electrophoresis of PCR products from *Vibrio anguillarum* NB10Sm transposon insertion mutants to confirm retention of the pJM1-like virulence plasmid. 161

Figure 4.13.	Growth of three transposon insertion mutants *Vibrio anguillarum* (Tn73, Tn100 and Tn205) compared to the *V. anguillarum* NB10Sm parent.	164
Figure 4.14.	Predicted amino acid sequence of putative uncharacterised protein of *Vibrio anguillarum* Tn100.	165
Figure 4.15.	Predicted structure of putative uncharacterised protein into which transposon TnSC189 inserted in *Vibrio anguillarum* Tn100.	166
Figure 4.16.	BLAST® tree showing similarity of the putative uncharacterised protein found in *Vibrio anguillarum* Tn100 to proteins found in other *Vibrio* spp.	168
Figure 5.1.	Transposon sequencing (Tn-seq) workflow.	180
Figure 5.2.	Point mutation of the pSC189 plasmid and confirmation of the C→A single substitution.	186
Figure 5.3.	Workflow of Tn-seq library preparation and sequencing.	188-189
Figure 5.4.	Agarose gel electrophoresis of *Vibrio anguillarum* NB10Sm random transposon libraries DNA.	209
Figure 5.5.	Agarose gel electrophoresis of *Vibrio anguillarum* NB10Sm random transposon library products following Illumina primer ligation.	212
Figure 5.6.	Agarose gel electrophoresis of *Vibrio anguillarum* NB10Sm random transposon library products following Illumina index PCR.	213
Figure5.7.	Mean quality score of reads across all bases when the DNA fragments were sequenced.	215
Figure 5.8.	Coverage of transposon insertions into *Vibrio anguillarum* NB10Sm Chromosome I.	222
Figure 5.9.	Coverage of transposon insertions into *Vibrio anguillarum* NB10Sm Chromosome II.	223
Figure 5.10.	Coverage of transposon insertions into the *Vibrio anguillarum* NB10Sm p67-NB10 virulence plasmid.	224
Figure 5.11.	Coverage of transposon insertions into the *Vibrio anguillarum* NB10Sm plasmid NC_019325.	225

Figure 5.12. Coverage of transposon insertions into the *Vibrio anguillarum* NB10Sm plasmid NC_009531. 226

Figure 5.13. Putative required genes of *Vibrio anguillarum* NB10Sm and *Vibrio cholerae* E7946. 228

Abbreviations

Cultures media and chemical solutions

AMP	Ampicillin
CHL	Chloramphenicol
CIP	Calf-intestinal phosphatase
DH_2O	Distilled water
EDTA	Ethylenediaminetetraacetic acid
EtBr	Ethidium bromide
EtOH	Ethanol
KAN	Kanamycin
KCl	Potassium chloride
KH_2PO_4	Potassium dihydrogen phosphate
LB	Miller's Luria-Bertani Broth
LB20	1% NaCl supplemented Miller's Luria-Bertani Broth
LBA	Miller's Luria-Bertani Agar
LBA20	1% NaCl supplemented Miller's Luria-Bertani Agar
MHA	Mueller-Hinton Agar
MHB	Mueller-Hinton Broth
$Na_2HPO_4 \cdot 2H_2O$	Disodium hydrogen phosphate dehydrate
NaCl	Sodium chloride
PBS	Phosphate-buffered Saline
PEN	Penicillin G
SAM	S-adenosylmethionine
SDS	Sodium dodecyl sulphate
STE	Sodium chloride-Tris-EDTA
STR	Streptomycin
TAE	Tris-acetate-EDTA
TCBS	Thiosulphate-citrate-bile salts-sucrose agar

TE	Tris-EDTA
TSA20	1.5% NaCl supplemented tryptone soy agar
TSB20	1.5% NaCl supplemented tryptone soy broth
U	Unit

Units of measurement

°C		Degrees centigrade
µ	g	Microgram
µ	L	Microlitre
µ	m	Micrometre
AU		Absorbance units
CFU		Colony forming units
g		G-force
g		Gram
Hr.		Hours
mg		Milligram
Min.		Minutes
mL		Millilitre
mm		Millimetre
ng		Nanogram
nm		Nanometre
pH		Potential Hydrogen
pmol		Picomole
rpm		Revolutions per minute
Sec.		Seconds
Temp.		Temperature
T_m		Melting temperature
U		Unit
V		Volts

Miscellaneous

A_{600}		Absorbance at 600 nm
bca		Base call accuracy
bp		Base pairs
DNA		Deoxyribonucleic acid
HF		High fidelity
HPLC		High performance liquid chromatography
HPSF		High purity salt free
kb		Kilobase pair
MBC		Minimum bactericidal concentration
mbp		Megabase pair
MIC		Minimum inhibitory concentration
NTC		No Template Control
OD		Optical density
*O*ri		Origin of replication
PCR		Polymerase chain reaction
spp.		Species
UK		United Kingdom
US		United States
w/	v	weight per volume

1. Introduction

1.1. Aquaculture and current challenges

Aquaculture is a rapidly growing industry which now accounts for over 44% of global fish production (FAO, 2016a) and produced annual expansion of 5.8%, through 2010-2014 (FAO, 2016b). Within Europe, UK farmed finfish production, which is dominated by Atlantic salmon (*Salmo salar*) production, is only surpassed by Norway (FAO, 2016a) and has increased by 30% in the decade up to 2014 (FEAP, 2015). This expeditious expansion has brought many problems around environmental impacts, concerns with animal welfare, and disease transmission. In particular, disease has a devastating global economic impact in aquaculture that is estimated at $3.2 billion annually (FAO, 2012).

The fight against bacterial disease and economic losses has led to wide scale use of antibiotic therapy resulting in chemical residues persisting in flesh and pathogens gaining resistance to certain compounds, both of which are of concern to human health particularly where antibiotics against human pathogens have been used or resistance has been selected in zoonotic pathogens (FAO, 2012). In addition, it has been suggested that climate change could increase disease incidence (Lehane and Rawlin, 2000) as higher water temperatures lead to faster bacterial growth, increased geographical range of pathogens and stress on animals, all of which can increase host susceptibility to infection (Callaway et al., 2012). Furthermore, the growth of aquaculture has been driven by anthropogenic

introduction of non-native fish species which has introduced new and emerging diseases to farm stocks and this, coupled with high stocking densities, genetic homogeneity of fish and poor water quality, can lead to greater prevalence of infections (Peeler and Feist, 2011).

1.2. *Vibrio anguillarum*

1.2.1. General background and classification

One important pathogen that continues to create new challenges is *Vibrio anguillarum*, one of the aetiological agents of vibriosis in fish. This microbe was first reported in 1893 by Canestrini, who named the organism *Bacterium anguillarum* after isolating the bacterium from diseased migrating eels *Anguilla anguilla* (Canestrini, 1893). Sometime later, the same pathogen was again isolated from *A. anguilla* by Bergman in Sweden who contrived the name, *Vibrio anguillarum* (Bergman, 1909). Vibriosis is primarily a haemorrhagic septicaemia with typical gross signs of pathogenesis, including skin discolouration, ulceration, weight loss and lethargy (Frans et al., 2011). *V. anguillarum* is responsible for this infection in over 50 species of wild and farmed fish, bivalves and crustaceans within marine, brackish or fresh water and continues to cause severe economic losses worldwide (Actis et al., 2011; Frans et al., 2011; Kitao et al., 1983; Paillard et al., 2004).

V. anguillarum is a gram negative, motile, fermentative and facultatively anaerobic, rod-shaped bacterium (approximately 0.5 × 1.5 μm) and has two chromosomes in accordance with most other *Vibrio* spp. (Austin and Austin,

2007; Frans et al., 2011; Okada et al., 2005). When cultured, colonies are typically round and cream coloured, with an optimal growth temperature of approximately 25°C, and can be recovered onto rich media, such as tryptone soy agar (TSA) supplemented with 1.5-2 % sodium chloride (NaCl) (Frans et al., 2011; Gratacap, 2008). Chromosome 1, of approximately 3.2 megabase pairs (mbp) in size, harbours the majority of genes that encode for essential cell functions and virulence factor proteins, while chromosome 2 (approximately 1 mbp) contains more hypothetical genes (Naka et al., 2011), which has led some workers to speculate that it may have originated from a plasmid (Jha et al., 2012). To date, three publically-available complete genome sequences are available for serotype O1 strains (*V. anguillarum* 775, M3 and NB10), of which 775 is the most completely annotated (Holm et al., 2015; Li et al., 2013a; Naka et al., 2011), though the number of genomes available is expected to increase rapidly.

1.2.1.1. Biotype

Primordial genotype and phenotype profiling of *V. anguillarum* has revealed a distinct heterogeneity between isolates, prompting the designation of classical biotype 1 and atypical biotype 2 (Schiewe et al., 1977). Furthermore, comparison of biochemical and genotypic characteristics of these two biotypes led to the reclassification of *V. anguillarum* biotype 2 to *Vibrio ordalii* (Schiewe et al., 1981). Whereas *V. anguillarum* has a global distribution, *V. ordalii* infections usually originate within salmonid populations around the Pacific rim; however, recent work suggesting *V.*

ordalii infection of cod (*Gadus morhua*) in the North Atlantic requires further taxonomic confirmation (Actis et al., 2011; Ruiz et al., 2016; Steinum et al., 2016).

V. anguillarum biotype 1 was reclassified in 1985 based on 5S ribosomal RNA sequence analysis to *Listonella anguillarum* (Macdonell and Colwell, 1985); however, this was not widely adopted and a recent investigation suggested that this microbe be reclassified as *Vibrio anguillarum*, based on phylogenetic 16S rRNA, genomic and phenotypic comparison with other *Vibrio* spp. (Austin and Austin, 2007; Frans et al., 2011; Macdonell and Colwell, 1985; Thompson et al., 2011).

1.2.1.2. Serotype

Serological classification of *V. anguillarum*, predominantly based on the presence of O-antigens, was originally frustrated by different research groups promoting contrasting systems, and it wasn't until 1986 that a single system consolidated all of the schemes into 10 distinct serogroups (Gratacap, 2008; Sorensen and Larsen, 1986). A total of 23 serotypes of *V. anguillarum* have now been described (Larsen et al., 1994; Pedersen et al., 1999b). However, isolates, which are mainly environmental and are not typable within the present system, are not uncommon, indicating the existence of further *V. anguillarum* O-serotypes (Colquhoun and Lillehaug, 2014; Pedersen et al., 1999b). Serotype O2 isolates have been further categorised into sero-subtypes O2α and O2ß using polyclonal antibodies (Bolinches et al., 1990). All *V. ordalii* that have been serotyped belong to the

sero-subtype O2α (Austin et al., 1997; Larsen et al., 1994). Furthermore, additional O2 sero-subtypes have been reported in isolates recovered from Atlantic cod which contrast with sero-subtypes O2α and O2ß serologically, phenotypically and genotypically (Mikkelsen et al., 2011; Mikkelsen et al., 2007; Tiainen et al., 1997).

The causative agents of vibriosis in fish are predominantly serotypes O1 and O2 (and occasionally O3), while strains belonging to the remaining serogroups are pathogenic only rarely and are mostly environmental isolates recovered from plankton, sediment or seawater (Frans et al., 2011; Pedersen et al., 1999b). Serotype O1 is predominantly isolated from infected salmonids and turbot (*Scophthalmus maximus*), while sero-subtype 02α strains are usually isolated from salmonids and marine fish, and serotype O2ß is isolated primarily from non-salmonids, especially cod (Mikkelsen et al., 2007). Historically, serotype O3 has been isolated from infected eels (*A. anguilla*) but has also been recovered from other fish species including sea-bass (*Dicentrarchus labrax*) and salmonids (Larsen et al., 1994; Silva-Rubio et al., 2008; Tiainen et al., 1997).

1.2.1.3. Plasmids in *Vibrio anguillarum*

Numerous serotype O1 strains carry a virulence plasmid of approximately 65 kilobase pairs (kbp), which encodes many genes required for proliferation within an iron limited environment, and as a result this plasmid is an important virulence determinant in *V. anguillarum* (Naka and Crosa, 2011). Plasmid pJM1 was the first to be described, and this plasmid was

demonstrated to be essential for virulence in a fish challenge comparing the wild-type *V. anguillarum* 775 and a plasmid-cured derivative (Crosa, 1980; Crosa et al., 1980). Consequently, pJM1 was sequenced to reveal a total of 59 open reading frames (ORFS), including those needed for replication and partition and a large proportion (32%) required for iron metabolic functions (Di Lorenzo et al., 2003). Although there are some differences between pJM1-like plasmids in different strains of *V. anguillarum* anguibactin biosynthesis and transport virulence related genes (see below) are highly homologous and found on all pJM1-like plasmids (Wu et al., 2004; Castillo et al., 2017). The presence of extremely homologous insertion sequences (ISV-A1 and ISV-A2) on pJM1 and pJM1-like plasmids suggest a modular construction, favouring genes required for iron acquisition, acquired over time by horizontal transfer from different geographical locations (Di Lorenzo et al., 2003; Stork et al., 2002). Plasmid pJM1 has a copy number of 1-2 and two origins of replication; *ori1* can replicate within *Escherichia coli*, but *ori2* can only replicate within *V. anguillarum* (Naka et al., 2012).

Although, only serotype O1 isolates have been reported with pJM1-like virulence plasmids, non-pJM1-like plasmids have been found in many different *V. anguillarum* serotypes including O1 isolates with and without pJM1-like plasmids (Austin et al., 1995; Naka et al., 2013).

1.2.2. Virulence mechanisms of *Vibrio anguillarum*

Several key virulence mechanisms of *V. anguillarum* have been identified and characterised and these are detailed below and in Table 1.1. The recent

escalation in the availability of molecular tools has accompanied an increase in our understanding of *V. anguillarum* virulence (Naka and Crosa, 2011). However, a recent study using 15 different *V. anguillarum* strains found that genotypic and phenotypic traits do not correlate with virulence, suggesting that virulence of this bacterium is multifactorial (Frans et al., 2013). Thus, pathogenesis cannot be attributed to any single virulence mechanism.

1.2.2.1. Iron acquisition

Iron is essential for the metabolism of *V. anguillarum*, and consequently this bacterium possesses both siderophore-dependent and heme systems to scavenge this metal from the surrounding environment (Naka and Crosa, 2011). These mechanisms circumvent non-specific host immune defence mechanisms, which maintain low iron availability through the production of iron-binding proteins, including transferrin and lactoferrin, to combat microbial invaders (Crosa, 1980; Lemos et al., 2010).

Siderophore mediated iron-sequestration

Within iron limited environments metal chelators, termed siderophores, are secreted into the external environment, such as within an infected fish host, to harvest ferric (Fe^{3+}) iron; before transport back into the cell via a ferric uptake complex (Stork et al., 2002; Wilson et al., 2016).

Table 1.1 *Vibrio anguillarum* virulence mechanisms, genes and functions. Genes implicated with a specific virulence mechanism are presented, along with the proteins they encode and the proposed function. In addition, the outcome of any fish challenge trial of knockout mutants for specific genes, injected by the intraperitoneal route, is also included.

Mechanism	Gene/ operon	Product	Function	Mutant reduced in virulence	Reference
Ferric iron acquisition and transport (plasmid)	*fatDCBA - angRT*	Anguibactin Receptor (*fatA*) siderophore biosynthesis (*angRT*)	Ferric siderophore transport and Anguibactin biosynthesis	✓(Δ*angR*)	Stork et al. (2007a); Zhang et al. (2015)
	fatE	ATPase	Ferric anguibactin transport		Naka et al. (2013b)
	angB/G	isochorismate lyase	anguibactin biosynthesis		Welch et al. (2000)
	angD	Phosphopantetheinyl transferases (PPTases)	Catalyse post translational modification.		Liu et al. (2005)
Ferric iron acquisition and transport (chromosomal)	*tonB1-exbB1-exbD1*	*tonB* system	Ferric anguibactin transport	× (Δ*tonB1*)	Stork et al. (2004)
	fvtA	Vanchrobactin receptor	Vanchrobactin transport		Balado et al. (2009)
	fvtB, fvtD, fvtC, fvtE	ABC transporter system	Ferric anguibactin, vanchrobactin, enterobactin transport		Naka et al. (2013)
	tonB2-exbD2-exbB2	tonB system	Ferric anguibactin transport	✓ (Δ*tonB2*)	Stork et al. (2004)
	orf2 (ttpC)	tonB2 system	Ferric anguibactin transport		Stork et al. (2007)
	fetA		Ferric enterobactin transport		Naka and Crosa. (2012)

Mechanism	Gene/ operon	Product	Function	Mutant reduced in virulence	Reference
Heme acquistion	*huvA*	heme receptor	iron transport	✓(Within an iron rich environment)	Mazoy et al. (2003)
	huvAZBCD	heme utilisation system	iron acquisition		Mourino et al. (2004)
	huvS	heme receptor	iron transport		Mourino et al. (2005)
Motility and chemotaxis	*flaA*	Flagellin subunit	Motility	✓ (polar and C-terminus mutations) × (C-terminal mutation)	Milton et al. (1996)
	flaB	Flagellin subunit	Motility	×	McGee et al. (1996)
	flaC	Flagellin subunit	Motility	×	McGee et al. (1996)
	flaD	Flagellin subunit	Motility	✓ (5'end mutation only)	McGee et al. (1996)
	flaE	Flagellin subunit	Motility	✓ (5'end mutation only)	McGee et al. (1996)
	cheR	methyltransferase	Chemotaxis	×	O'Toole et al. (1996)
	motY	Stator	Flagellar motor	×	Ormonde et al. (2000)
Lipopolysaccharide	*virA*		O-antigen biosynthesis	✓	Norqvist and Wolfwatz. (1993)
	virB		O-antigen biosynthesis	✓	Norqvist and Wolfwatz. (1993)
	virC		O-antigen biosynthesis	✓	Milton et al. (1995)
	rmlBADC	O side chain precursor dTDP-rhamnose	dTDP-rhamnose biosynthesis	✓ (*rmlD*)	Welch and Crosa. (2005)

Mechanism	Gene/ operon	Product	Function	Mutant reduced in virulence	Reference
Lipopolysaccharide	*wzm-wzt-wbhA*	ABC transporters (*wzm* and *wzt*) and methyltransferase (*wbhA*)	O-antigen transport		Lindell et al. (2012)
Protease	*empA*	Zinc metalloprotease	Host invasion	×	Norqvist et al. (1990); Milton et al. (1992)
	(epp/prtV)	EmpA processing protease	Host invasion	✓	Varina et al. (2008); Mo et al. (2010)
Haemolysin	*vah1*	Haemolysin	Haemolysin	✓	Hirono et al. (1996); Rock et al. (2006)
	vah2	Haemolysin	Haemolysin	✓	Rodkhum et al. (2005)
	vah3	Haemolysin	Haemolysin	✓	Rodkhum et al. (2005)
	vah4	Haemolysin	Haemolysin	✓	Rodkhum et al. (2005)
	vah5	Haemolysin	Haemolysin	✓	Rodkhum et al. (2005)
	plp	phospholipase	Repression of *vah1 and llpA*	×	Rock et al. (2006)
	llpA	Lactonizing lipase	Possible haemolysin	×	Rock et al. (2006)
	rtxA	Repeat-in-Toxin	haemolysin	×	Li et al. (2008)
	hns	Histone-like nucleoid structuring protein	Negatively regulates haemolysin clusters		Mou et al. (2013)
	mtlD	lytic murein transglycosylase	hemolytic, phospholipase, gelatinase and diastase activities	×	Wang et al. (2009); Xu et al. (2011)

Mechanism	Gene/ operon	Product	Function	Mutant reduced in virulence	Reference
Exopolysaccaride	*wza*	secretin	Exopolysaccharide (EPS) transport	✓	Croxatto et al. (2007)
	wzb	Tyrosine kinase	EPS transport	✓	Croxatto et al. (2007); Weber et al. (2010)
	wzc	Tyrosine phosphatase	EPS transport	✓	Croxatto et al. (2007); Weber et al. (2010)
	wbfD	Lipoprotein	EPS biosynthesis	×	Croxatto et al. (2007)
	orf1-wbfD-wbfC-wbfB operon	Exopolysaccaride operon	EPS biosynthesis	✓	Croxatto et al. (2007)
Regulation	*hfq*	RNA chaperone	RNA binding protein	✓	Weber et al. (2008); Weber et al. (2010)
	rpoN	Alternative σ^{54} sigma factor 54	Transcriptional activator	×	O'Toole et al. (1997)
				✓ (intramuscular injection)	Hao et al. (2010)
	rpoS	σ^{38} sigma factor	Transcriptional regulator	✓	Weber et al. (2008); Ma et al. (2009)
	vanT	Quorum sensing master regulator	Transcriptional activator	×	Croxatto et al. (2002)
Communication	*vanI*	*N*-acylhomoserine lactone (AHL) synthesis	*N*-acylhomoserine lactone (AHL) synthesis		Milton et al. (1997)
	vanR	Transcriptional activator	Transcriptional activator		Milton et al. (1997)

Siderophores are categorised according to their iron binding moieties (metal chelating functional groups), namely catecholate, hydroxyamate, phenolate or carboxylate, although many siderophores have mixed moiety (Wilson et al., 2016). Many isolates of *V. anguillarum* possess siderophore systems encoded on the pJM1-like virulence plasmid or chromosome (Naka et al., 2013).

Anguibactin

Serotype O1 strains of *V. anguillarum* carrying a pJM1-like virulence plasmid possess an anguibactin siderophore complex (Naka et al., 2013a). Anguibactin is synthesised from precursors 2,3-dihydroxybenzoic acid (DHBA), cysteine and histidine and uniquely contains catecholate and hydroxyamate metal-chelating functional groups (Naka et al., 2013a; Tolmasky et al., 1995; Wertheimer et al., 1999). The majority of genes required for this system are encoded on the pJM1-like plasmid at two major loci, the iron transport biosynthesis operon (ITBO) and *trans*-acting factor (TAF) [Naka et al., 2013]. The ITBO contains anguibactin biosynthesis genes *angR* and *angT*, in addition to anguibactin transport genes *fatD*, *fatC*, *fatB*, *fatA*, and is up-regulated by *fur* (ferric uptake regulator protein) under iron-limiting conditions (Di Lorenzo et al., 2003; Tolmasky et al., 1994). The AngR protein is probably bifunctional, as it has been linked with the activation of cysteine and regulation of the ITBO, whereas AngT may be responsible for release of anguibactin from AngM (Wertheimer et al., 1999). Furthermore, regulation of ITBO is also controlled by two antisense RNAs

(RNAα and RNAß) encoded on the opposite strand of this operon (Naka et al., 2013).

The TAF locus of pJM1-like plasmids is spilt into two regions: TAFb and TAFr (Welch et al., 2000). Many genes required for anguibactin synthesis, including *angC*, *angE*, *angB/G* and *angD*, are found in TAFb (Welch et al., 2000). Whereas the anguibactin precursor DHBA is synthesised by chromosome-encoded proteins in *V. anguillarum* 775 (Chen et al., 1994), many other pJM1-like strains use plasmid-encoded *angB/G* (Welch et al., 2000). Other genes required for anguibactin synthesis encoded on the pJM1-like plasmid include *angM*, *angU*, *angN*, *angH*, *angL* and *angI* (Naka et al., 2013a). The *angH* gene, encoding a histidine decarboxylase, is essential for the biosynthesis of anguibactin and virulence of *V. anguillarum* within histamine limiting conditions (Tolmasky et al., 1995). Furthermore, *angH* is also essential for producing histamine in *V. anguillarum*, a potential virulence determinant (Barancin et al., 1998).

Vanchrobactin

Serotype O2 and plasmidless serotype O1 isolates of *V. anguillarum* produce vanchrobactin, a DHBA-based catechol siderophore, via a chromosome I encoded system, which is conserved but redundant in serotype O1 strains carrying the pJM1-like virulence plasmid (Balado et al., 2006, 2008; Naka et al., 2008). Furthermore, representatives of serogroups O3 to O10 all possess genes for vanchrobactin synthesis and transport (Balado et al., 2009).

Vanchrobactin is produced by biosynthesis of DBHA which is activated by the *vabE* product and requires *vabA*, *vabB* and *vabC*, and finally *vabF* which codes for a non-ribosomal peptide synthase possibly involved in assembly of the component parts (Balado et al., 2006). It has been hypothesised that a transposon from pJM1 inserts into chromosomal *vabF* (a vanchrobactin biosynthesis gene) to inactivate the vanchrobactin siderophore system in strains synthesising anguibactin - a more efficient iron chelator. (Naka et al., 2008). Furthermore, some serotype O2 strains harbour ferric anguibactin genes encoded on the chromosome but these are inactivated by a transposon insertion (Balado et al., 2009).

Siderophore-independent iron acquisition

In addition to siderophore-dependent iron-uptake mechanisms, *V. anguillarum* possesses a system that facilitates the utilisation of free heme and some heme-containing proteins, although the components of these systems vary between different serotypes (Mourino et al., 2004; Mourino et al., 2005). HuvA is the outer membrane receptor involved in heme uptake and a mutation in this gene reduces virulence in fish pre-treated with hemin or haemoglobin (Mazoy et al 2003). The complete serotype O1 *huvAZBCD* and *huvX* system has been characterised and all genes except *huvX* play an essential role in heme utilisation (Mourino et al., 2004). Furthermore, *huvA* is not present in the genome of many serotype O3 isolates, while a second heme receptor (*huvS*) is a functional analogue but shares little (39 %) sequence homology (Mourino et al., 2005).

Iron uptake

Two ABC (ATP binding cassette) transporters involved with iron transport across the cytoplasmic membrane are found in *V. anguillarum* (Naka et al., 2013b). The first, found on the serotype O1 pJM1-like plasmid, incorporates FatBCD and FatE encoded by genes within the iron transport and biosynthesis operon (ITBO) and TAFb region respectively (Naka et al., 2013a). The outer membrane protein FatA, encoded within the ITBO, transports the ferric anguibactin into the periplasm where it binds with FatB (a protein anchored to the inner cytoplasmic membrane) and is transported across the inner membrane into the cytoplasm by essential FatC and FatD proteins (Naka et al., 2010). FatE encodes the ATPase (ATP-binding protein) which completes the ABC transporter (Naka et al., 2013b). The second and homologous ABC transport system, FvtBCDE, is encoded on chromosome II and is responsible for transporting ferric-vanchrobactin and enterobactin across the cytoplasmic membrane (Naka et al., 2013b). These transport systems are specific for their respective siderophores except that FatE and FvtE can both facilitate ferric-anguibactin transport meaning that *fatE* is not essential for anguibactin internalization (Naka et al., 2013b). In addition, a second chromosomal exogenous ferric entorobactin receptor called FetA has been found in serotype O1 strains (Naka and Crosa, 2012).

Energy is required for internalizing various iron compounds and in *V. anguillarum* two membrane bound TonB systems (TonB1 and TonB2), each transcribed as operons, expedite this using membrane proton motive force (Stork et al., 2004). Part of the *huvAZBCD* and *huvX* heme uptake

cluster, the TonB1 system consists of TonB1 and associated proteins ExbB1 and ExbB2 (Mourino et al., 2004). In contrast, the TonB2 (TonB2, ExbB2 and ExbB2) includes an additional gene (*orf2*) which encodes TtpC and is essential for ferric anguibactin transport (Stork et al., 2007). Both these systems can function in the transport of heme and ferrichrome, while transport of siderophores is only achieved with a functional TonB2 system (Stork et al., 2004).

1.2.2.2. Motility and chemotaxis

Flagella act in host attachment and invasion and, combined with chemotaxis, constitute an important virulence mechanism required for infection of fish skin (McGee et al., 1996; Ormonde et al., 2000). The flagellum of *V. anguillarum* is powered by a flagellar motor encoded by *motY*, and it consists of four subunits (FlaA, FlaB, FlaC and FlaD) while a putative fifth subunit encoded by *flaE* remains unconfirmed (McGee et al., 1996; Milton et al., 1996; Ormonde et al., 2000). Skin colonisation may be a more important infection route compared to crossing the intestine, however functional motility and chemotaxis are not required for the latter (O'Toole et al., 2004; Weber et al., 2010). Furthermore, mucus, bile salts and cholesterol each increase motility of *V. anguillarum* (Li et al., 2015).

Non-motile aflagellate or chemotaxis (*cheR*) null mutants of *V. anguillarum* demonstrate attenuated virulence during immersion challenge trials, but show virulence similar to wild-type when administered by intraperitoneal injection, suggesting that neither is essential for dissemination and

persistence within the host (O'Toole et al., 1996; O'Toole et al., 1997). However, further work has demonstrated that a polar mutant of *flaA* and carboxy terminal deletions of *flaA*, *flaD* and *flaE* showed decreased virulence compared to wild-type by both immersion and intraperitoneal routes; though surprisingly, separate mutant isolates, each with a single full gene deletion for either of the five flagellum subunits, each produced wild-type virulence phenotypes via intraperitoneal infection (McGee et al., 1996; Milton et al., 1996).

1.2.2.3. Lipopolysaccaride

Serotype O1 isolates of *V. anguillarum* have an O-antigen that completely covers the cell surface and flagella sheath, and this O- antigen is one of the three domains that compose lipopolysaccharide (LPS), along with the outer membrane lipid A region and the KDO-core oligosaccharide region (Stroeher et al., 1998). One suggested mechanism for the rearrangement of *V. anguillarum* and *Vibrio cholerae* O-antigen side chains, which are responsible for serotype specificity, is the insertion sequence IS1358, a putative transposon element (Jedani et al., 2000; Stroeher et al., 1998). Isolates of *V. anguillarum* smooth serotype O1 are able to prevent classical complement-mediated killing despite activation of the complement system, and a positive correlation exists between O-antigen size and resistance to serum killing in rainbow trout (*Oncorhynchus mykiss*) (Boesen et al., 1999). Furthermore, O-antigen polysaccharides are required to evade phagocytosis by rainbow trout epithelial cells and protect against antimicrobial peptides

and lysozyme, and it is also possible that the serotype O1 side chain is required to stabilise the outer membrane ferric anguibactin receptor FatA (Lindell et al., 2012; Welch and Crosa, 2005).

Transposon mutagenesis and a screen of virulence attenuated mutants with rabbit polyclonal antibodies was used to identify genes *virA* and *virB* as putative components of a major surface antigen lipopolysaccharide, and further study suggests that a third gene, named *virC*, may also be involved in virulence (Milton et al., 1995; Norqvist and Wolfwatz, 1993). Moreover, the *rmlBADC* cluster is reputed to be involved in the synthesis of dTDP-rhamnose, a precursor to the O side chain (Welch and Crosa, 2005). Transport of the O-antigen putatively requires the *wzm-wzt-wbhA* operon, which encodes two ABC transporters and a methyltransferase (Lindell et al., 2012).

1.2.2.4. Protease

The zinc metalloprotease EmpA was first characterised by Norqvist et al. (1990) who found reduced proteolytic but not haemolytic activity when this protein was knocked out, suggesting a role in mucus degradation and invasion of the host. Furthermore, *V. anguillarum* protease activity is induced at stationary phase when grown in culture containing Atlantic salmon mucus (Denkin and Nelson, 1999). Zinc metalloprotease EmpA is translated as a preproenzyme which is putatively modified posttranslationally by cleavage of pre- and propeptides during secretion, followed by EmpA processing protease (Epp or PrtV) within the

extracellular environment (Milton et al., 1992, Mo et al., 2010; Staroscik et al., 2005; Varina et al., 2008). Knockout of the gene encoding metalloprotease EmpA in wild-type *V. anguillarum* NB10 produced a strain designated *V. anguillarum* NB12, but this knockout strain has similar virulence to the parent in rainbow trout (*Oncorhynchus mykiss*) when infected by intraperitoneal injection (IP), thus questioning the role of this protein in virulence (Milton et al., 1992). However, a further study comparing the virulence of these strains in an Atlantic salmon model infected by IP injection found a significant reduction of virulence in *V. anguillarum* NB12 compared to the parent strain (Denkin and Nelson, 2004), and this contrasting observation was attributed to investigations in different fish species.

1.2.2.5. Haemolysins

Haemolytic activity of *V. anguillarum* is believed to be responsible for the haemorrhagic septicaemia observed during infection of fish (Hirono et al., 1996). The first haemolysin reported for this bacterium was *vah1* (Hirono et al., 1996); however, since then further haemolysins (*vah2*, *vah3*, *vah4* and *vah5*) with strong similarities to haemolysins in *Vibrio vulnificus* (*vah2*) and *V. cholera* (*vah3*, *vah4* and *vah5*) have been proposed to contribute to virulence in fish (Rodkhum et al., 2006b). Two haemolysin clusters have been characterised: the Repeat-in-Toxin (*rtxACHBDE*) operon, which is regulated by metal-regulated transcriptional regulatory protein (HlyU) (Li et al., 2011; Li et al., 2008), and the *vah1* cluster (Rock and Nelson, 2006).

Within the first cluster Repeat-in-Toxin RtxA is matured post-translationally by the activating acylase RtxC, while *rtxBDE* encode the RtxA ABC transporters (Li et al., 2008). Phospholipase Plp of the *vah1* cluster represses *vah1* expression, though it does exert haemolysin activity itself, though Δ*plp* strains show no reduction in virulence compared to parent strains (Li et al., 2013b). Furthermore, histone-like nucleoid structuring protein (H-NS), a global regulator found in most *Vibrio* spp., represses expression of both *rtxACHBDE* and *vah1-plp* gene clusters (Mou et al., 2013). Despite this role in negative regulation, a Δ*hns* mutant was attenuated in virulence compared to wild-type, possibly because the change in virulence gene expression may negatively impact on overall fitness (Mou et al., 2013). Finally, a knockout mutant of membrane-bound haemolysin, lytic murein transglycosylase (*mltD*), had increased virulence compared to wild-type parent (Xu et al., 2011).

1.2.2.6. Exopolysaccharide

Two separate operons of *V. anguillarum* encode putative exopolysaccharide production systems (Croxatto et al., 2007). First, the *wza-wzb-wzc* operon encodes an exopolysaccharide transport operon secretin, tyrosine kinase and tyrosine phosphatase respectively, and these proteins are required for attachment to fish skin and a mutant of *wza* shows reduced exopolysaccaride production and exoprotease activity (Croxatto et al., 2007). Moreover, single-gene Δ*wza, Δwzb* and *Δwzc* knockout mutants are each attenuated in virulence compared to parent strains (Weber et al., 2010). The

second operon (*orf1-wbfD-wbfC-wbfB*) encodes proteins of unknown function, although they share sequence similarity to those of *V. cholera* O139, and mutations in both *orf1* and *wbfD* cause a decrease in exopolysaccaride biosynthesis, while only the *orf1* mutant shows a reduction in exoprotease activity (Croxatto et al., 2007). Furthermore, a mutant prepared with a knockout of the global regulator alternative σ^{54} sigma factor *rpoN* has reduced expression of *wbdF* in addition to a reduced ability to form biofilm, a process known to involve exopolysaccharide production in other bacteria (Hao et al., 2013).

1.2.2.7. Regulation and communication

N-acylhomoserine lactones (AHLs), which are synthesised by *VanI* and *VanM* in *V. anguillarum*, are a group of secreted (diffusible) autoinducers that monitor self population density, a mechanism called quorum sensing (Hardman et al., 1998; Milton, 2006; Milton et al., 1997). The transcriptional regulator VanT is believed to negatively regulate its own expression by binding to and repressing to its own promoter, and binding to and then upregulating the *vanOU* promoter (Croxatto et al., 2004). The VanO protein then activates expression of various small RNAs (sRNAs) which, working with RNA chaperone Hfq, destabilises *vanT* mRNA (Weber et al., 2008). *VanT* is also regulated by sigma factor RpoS, and itself regulates various physiological responses to stress from the surrounding environment, most notably positively modulating *empA* expression but also

serine, pigment and biofilm production (Croxatto et al., 2002; Weber et al., 2008).

Temperature has also been shown to regulate virulence. *V. anguillarum* M3 has been found to kill flounder (*Paralichthys olivaceus*) more quickly at higher temperatures (22-24°C) than at the lower temperature of 16-18°C (Mo et al., 2001), and high protease activity corresponds with faster growth in warmer temperatures (Mo et al., 2002). Chemotaxis is temperature dependent in *V. anguillarum* with cells incubated at 25°C moving towards serine faster than at 15°C or 5°C (Larsen et al., 2004). Furthermore, it has been reported that *in vitro* expression of *empA* is increased in one strain and *toxR*, *fur* and *tonB* are increased in a second strain at 15°C compared to 25°C (Crisafi et al., 2014).

1.2.3. *V. anguillarum*: Current status, treatment and prevention

Despite successful therapeutics and vaccines, *V. anguillarum* is still a major problem to European fisheries, and infections caused by *Vibrio* spp. are expected to increase with rising sea temperatures, which is linked to climate change (LeRoux et al., 2015). Outbreaks have been reported in captive Ballan wrasse (*Labrus bergylta Ascanius*), a wild caught cleaner fish species cultured alongside *S. salar* to combat the sea lice problem that threatens to devastate Atlantic salmon production (Beiring et al., 2016). Moreover, there is additional concern regarding possible transfer of *V. anguillarum* between these fish species during co-habitation, although there is no evidence of transmission at present (Treasurer, 2012). In

addition, *V. anguillarum* has been recovered from wild caught black-spotted seabream (*Pagellus bogaraveo*) destined for an aquaculture facility (Mancuso et al., 2015), and this outbreak was attributed to post-capture storage stress and highlights one of the main challenges to developing *P. bogaraveo* and other novel species for aquaculture.

It is likely that new and existing vaccines will play a role in preventing emerging disease problems, as they have done in the past. Vaccinating fish against *V. anguillarum* remains highly successful, especially when delivered by intraperitoneal injection, although this method has its drawbacks: it is relatively labour intensive and potentially stressful to fish which could leave them more susceptible to other infections (Frans et al., 2011). Moreover, some fish may be too small for intraperitoneal injection when it is required (Colquhoun and Lillehaug, 2014). In addition, different fish species may require different vaccine formulations, methods of administration, and delivery regimes (Gudmundsdottir et al., 2009).

Despite characterisation of many key *V. anguillarum* virulence determinants, the virulence mechanisms of this pathogen remain relatively poorly understood. However, recent work has elucidated a number of putative virulence factors using novel molecular methods including genome sequencing and *in vivo*-induced antigen technology (IVIAT) (Rodkhum et al., 2006b; Zou et al., 2010). This latter process involves screening for potential virulence genes that are expressed *in vivo* using a library of antibodies that only react with proteins specifically expressed during

infection (Handfield et al., 2005). Therefore, novel and cost effective research techniques are required to elucidate and characterise these and other suspected novel *V. anguillarum* virulence determinants, as improved knowledge of these factors will lead to new vaccine targets and potentially permit the development of non-antibiotic chemotherapeutants where vaccine approaches are ineffective or impractical. However, experiments using fish are becoming increasingly restrictive due to financial and ethical concerns connected with stricter legislation. Thus, there is strong justification to pursue alternative infection models when studying microbial pathogens of farmed fish.

1.3. Alternative Hosts

1.3.1. Selecting an alternative host

To address microbial disease problems, there is a requirement for deeper understanding of the pathogen during infection, as this may facilitate the development of improved treatments, vaccines and management practices. *V. anguillarum* is no exception and, to this end, many studies have been performed in native fish hosts, including Atlantic salmon (*Salmo salar*), rainbow trout (*Oncorhynchus mykiss*), European sea bass (*Dicentrarchus labrax*) and zebra fish (*Danio rerio*) (Denkin and Nelson, 2004; Frans et al., 2013; Mou et al., 2013; Sullivan and Kim, 2008; Xu et al., 2011). However, these experiments require specialist infrastructure such as aquaria and biosecurity measures to ensure the safety of workers and aquatic animal stocks, particularly when studying zoonotic pathogens (Froquet et al., 2007).

In addition, whole-animal studies are often costly, do not permit high-throughput approaches, and may be covered by strict legislation (Chamilos et al., 2007; Zak and Oreilly, 1991). Furthermore, good practice prescribes that researchers should adhere to the principles of the 3Rs, i.e., the replacement, reduction and refinement of experiments on animals (Schaeck et al., 2013).

Alternative infection models can be used because many innate immune responses are functionally conserved across phyla, and pathogens often employ similar mechanisms to exploit different hosts (Chamilos et al., 2007). Furthermore, *V. anguillarum* is ideal for alternative host validation because a range of strains and genetic resources are available and much is known of its key virulence mechanisms (Austin et al., 1995; Frans et al., 2011; Naka and Crosa, 2011). Many alternative hosts are associated with various shortcomings such as the need for time-consuming training to achieve competence, a requirement for tissue culture or aquarium facilities, the lack of important aspects of immune complexity, or being unsuited to the study of certain pathogen virulence traits (Desbois and Coote, 2012; Ott et al., 2012). Furthermore, attributes of specific alternative hosts, such as low cost or availability of molecular tools, makes them suitable for specific applications, as detailed in Table 1.2. Thus, consideration must be given to which host will best accommodate the intended experimental aims.

Table 1.2. Practical and functional parameters of various alternative hosts for studying microbial pathogens.

	Acanthamoeba castelanii	***Dictyostelium discoideum,***	***Caenorhabditis elegans***	***Panagrellus redivivus***	***Danio rerio* (embryo)**	***Drosophila melanogaster***	***Bombyx mori***	***Galleria mellonella***
Genome available	×	✓	✓	×	✓	✓	✓	×
Molecular tools	×	✓	✓	×	✓	✓	✓	×
Easy to handle	×	×	×	×	×	×	✓	✓
Fully automated process	✓	✓	✓	✓	✓	×	×	×
Minimal maintenance and training	✓	✓	×	×	×	×	×	✓
Delivery of precise inoculations	×	×	×	×	✓	×	✓	✓
Inexpensive	✓	✓	×	×	×	×	✓	✓
Requires minimal space	✓	✓	✓	✓	✓/×	×	✓	✓
Possible batch variation	×	×	×	✓	×	✓	✓	✓
Study of phagocytosis	✓	✓	×	×	✓	✓	✓	✓
Testing antimicrobials	×	×	✓	×	✓	✓	✓	✓
High throughput screens possible	✓	✓	✓	✓	✓	✓	✓	✓
Tissue recovery	×	×	×	×	×	✓	✓	✓
Transparent	✓	✓	✓	✓	✓	×	×	×
Efficacy of drug combinations	×	×	✓	×	✓	✓	✓	✓

1.3.1.1. Protozoans

Unicellular organisms such as the amoeba *Dictyostelium discoideum and Acanthamoeba castelanii* can phagocytose particles, including yeasts, fungi and bacteria (Steenbergen et al., 2003), which has seen the use of these microbes as alternative hosts for investigating this immune mechanism. However, as investigations using amoeba hosts are limited mainly to phagocytosis, these hosts are more useful for investigations of intracellular pathogens (Dorer and Isberg, 2006). Several studies investigating pathogen internalisation and survival have found that the lipopolysaccharide O-antigen plays a key role (Riquelme et al., 2016; Steenbergen et al., 2001). Furthermore, amoebae are useful for primary screening assays before progressing to a more complex animal. For instance, a *Mycobacterium marinum* transposon mutant library was screened in *D. discoideum* to select for isolates with attenuated virulence for subsequent investigation in a zebra fish model (Alibaud et al., 2011). However, delivering precise doses of a pathogen is not possible with amoeba models and the unicellular anatomical simplicity restricts the host-pathogen interaction parameters that can be investigated.

1.3.1.2. Nematodes

Nematode hosts have many benefits, including transparency (beneficial for microscopy), a fast reproductive cycle, genetic tractability, long-term storage of progeny in liquid nitrogen, and the potential to perform fully-automated high-throughput assays incorporating specimen sorting, feeding, and

administration of pathogens and test compounds (Yanik et al., 2011). This has made *Caenorhabditis elegans* an important model in drug discovery (O'Reilly et al., 2014). Furthermore, the *C. elegans* genome is available and substantial genetic resources for several nematodes are publicly available on the WormBase website (Yook et al., 2012). However, when studying comparative immune function, nematode models are limited by their anatomical simplicity, especially the absence of specific cellular components and phagocytosis (Balboa et al., 2007; Desalermos et al., 2012; Schulenburg et al., 2004). Other significant deficiencies of nematodes as an alternative host are the inability to deliver specific inoculums of pathogens or antimicrobials (Desbois and Coote, 2012) and difficulties with quantifying tissue burden of compounds and infectious organisms (Glavis-Bloom et al., 2012).

1.3.1.3. Zebrafish embryo

The zebrafish (*Danio rerio*) embryo is a very successful model for studying immune responses, as the innate immune system is functional during the embryonic phase (Magnadottir, 2006) and the animals are transparent and malleable at this early stage (Sullivan and Kim, 2008). *D. rerio* embryos can be accommodated in multi-well plates and are amenable for mechanised, high-throughput experiments and flow cytometry applications (Yanik et al., 2011). Furthermore, many molecular and genetic manipulation tools are available for *D. rerio*, including inactivation of genes and transgenic fluorescence tagging to examine gene regulation (Lin et al., 2016). Despite

these benefits, embryonic stage *D. rerio* can only be infected by a limited number of pathogen species by immersion challenge and, even in the event of successful immersion challenge, it is not possible to accurately quantify the infective dose or therapeutant uptake (Meijer and Spaink, 2011). An alternative approach that addresses this shortcoming, microinjection, is slow when performed manually, although fully mechanised systems are available (Yanik et al., 2011). Regardless, these automated systems are expensive, as is the training of personnel, husbandry and equipment required to maintain adult *D. rerio* to produce embryos, thus making this host impractical for many applications.

1.3.1.4. Insects

The availability of a complete and well annotated genome makes *Drosophila melanogaster* an attractive host when studying specific virulence factors and their interaction with corresponding host immune pathways. Famously, research on *D. melanogaster* elucidated pathways leading to the production of antimicrobial peptides (AMPs) (Hoffmann et al., 1996). When using Toll-deficient *D. melanogaster* mutants, virulent strains of *Aspergillus fumigatus* produced high mortality similar to virulence observed in a murine model (Lionakis and Kontoyiannis, 2010). This work used oral and rolling infection models which stimulate epithelial entry of a pathogen. However, *D. melanogaster* requires anaesthetic prior to injecting precise inoculums (Khalil et al., 2015) and a further limitation is the requirement

for a fly room (Desalermos et al., 2012). Moreover, non-virulent bacteria can kill *D. melanogaster* via the injection route of infection (Jensen et al., 2007).

Precise inoculation doses can be delivered to silkmoth (*Bombyx mori*) larvae by injection and a correlation exists between *Staphylococcus aureus* virulence in this host and in mice (Kaito et al., 2005). *B. mori* larvae have also been useful for virulence gene discovery in bacterial pathogens, including *S. aureus* and *E. coli* (Miyashita et al., 2012; Miyazaki et al., 2012). Moreover, *B. mori* is amenable to histopathological examination and is genetically malleable (Kaito et al., 2002). Although *B. mori* larvae are readily available as reptile feed, they are marketed within the UK only in their first instar stage, while it is the fifth instar that is used for infection experiments (Kaito et al., 2012). Furthermore, to progress through developmental stages these animals require a mulberry leaf diet or a specialist artificial feed (Banno et al., 2010), which are expensive or unavailable within the UK.

1.3.2. Alternative hosts used in the study of bacterial fish pathogens

Alternative hosts for the study of pathogen virulence are a welcome addition to the laboratory toolbox. Still, relatively few studies have described alternative infection models for investigating microbial pathogens of fish, but those available include cell culture (Li et al., 2008; Mou et al., 2013; Ormonde et al., 2000), which bridges the gap between *in vitro* and true *in vivo* host models; the amoeba *D. discoideum* (Froquet et al., 2007); the nematode *C. elegans* (Brackman et al., 2011); the freshwater ciliate

Tetrahymena thermophila (Pang et al., 2012); the crustacean *Artemia franciscana* (Defoirdt et al., 2005); and *D. rerio* larvae (Harvie et al., 2013; van Soest et al., 2011).

1.3.3. The alternative host *Galleria mellonella*

The larva of the greater wax moth (*Galleria mellonella*) is one alternative model attracting much attention in part due to the simplicity and reliability of establishing infections in this insect (McMillan et al., 2012). This insect occurs naturally as a pest in bee hives (Olsen et al., 2011) and has been used as an experimental infection model for over a century (Metalnikoff, 1906). The larvae are a convenient size for manipulation (2 to 3 cm in length), do not need feeding, require little space or specialist infrastructure, and are inexpensive to purchase (Desbois and Coote, 2012). Furthermore, unlike *B. mori,* they are sold in their final instar stage, which is desirable for experimental work (Desbois and McMillan, 2015), as rearing in-house would take up significant laboratory space, manpower and resources. Nevertheless, relatively small variations in susceptibility to infection can occur between batches of larvae from the same supplier and such variation probably arises from factors such as age, size and nutritional status on receipt; conditions encountered during transit to the laboratory; and the presence of any underlying natural infections (Desbois and McMillan, 2015).

Injection of *G. mellonella* through the prolegs (Kavanagh and Reeves, 2004) allows for relatively easy delivery of precise doses of inoculums and antimicrobials. Moreover, the short life cycle of *G. mellonella* makes them

suitable for high-throughput studies (Tsai et al., 2016). In addition, the training needed to work with this alternative host can be performed quickly, and studies on this model are ethically more acceptable than working with vertebrates (Desbois and Coote, 2012). Notably, the *G. mellonella* model presents a low biohazard risk because no liquid systems are required and the larvae are kept in Petri dishes; thus, the relatively small volumes of infected material produced can be made safe by autoclaving. In addition, this model has been used successfully to study virulence of various human pathogens and the efficacy of antibiotic therapies (Desbois and Coote, 2011; Desbois and Coote, 2012).

Recent work has elucidated much needed immune gene and transcriptomic data in this insect (Vogel et al., 2011); however, the lack of a fully sequenced and annotated genome for *G. mellonella* remains a limitation for genetic studies of immune responses (Cook and McArthur, 2013). Nevertheless, a project to sequence the *G. mellonella* genome and 5000 other Arthropoda is due for completion soon (http://arthropodgenomes.org/wiki/i5K), and this is expected to lead to a huge increase of information on the Insect Innate Immunity Database (IIID) (Brucker et al., 2012), thereby facilitating new research on the immune genes of these insects and permitting more informative host-pathogen interaction studies.

Importantly, insects rely solely on the innate immune system to fight pathogens, and there is functional similarity in the innate immune responses to invasive infection between insects and fish with respect to

pathogen recognition, expression of antimicrobial peptides, generation of reactive oxygen species, phagocytosis of invading microbes, and initiation of clotting cascades (Agius and Roberts, 2003; Cytrynska et al., 2007; Jiang et al., 2010; Magnadottir, 2006; Neumann et al., 2001). In addition, the fish adaptive response is slow compared to other more complex higher vertebrates as a result of their evolutionary status and poikilothermic nature; accordingly, the innate system, which is the foundation of all vertebrate immune systems, is especially crucial in fish (Magnadottir, 2006). Thus, *G. mellonella* warrants evaluation as an alternative host for investigations of pathogenicity and virulence of aquatic pathogens.

1.3.4. Previous study of pathogens in *Galleria mellonella*

Previous literature using *G. mellonella* as an alternative infection model is extensive. *G. mellonella* has been used previously to replace mammalian hosts in studies of human pathogens (Brennan et al., 2002; Jander et al., 2000; Olsen et al., 2011). Mutants of *Pseudomonas aeruginosa,* a common opportunistic environmental pathogen and important source of nosocomial infections, exhibit significant positive correlation of virulence when tested in mice and *G. mellonella* (Jander et al., 2000). Correlations of virulence in *G. mellonella* and conventional host models have also been shown with Group A Streptococcus (Olsen et al., 2011) and the fungus *Candida albicans* (Brennan et al., 2002). A negative correlation has been demonstrated between *C. albicans* virulence and *G. mellonella* haemocyte density, and highly virulent strains proliferate within the larvae and reduce host

haemocyte numbers (Bergin et al., 2003). Furthermore, *G. mellonella* is a valuable tool for evaluating experimental antibiotic treatments (Desbois and Coote, 2012) and multiple compounds can be tested for synergistic or antagonistic effects (Desalermos et al., 2012). Excluding published sections of experiments described within this thesis (McMillan et al., 2015), there is only one other report describing the use of *G. mellonella* as an alternative host to investigate *Vibrio* spp.: an indole-signalling mutant of *V. cholerae* has attenuated virulence compared to its wild-type parent strain (Nuidate et al., 2016).

Thermotolerance is a beneficial attribute in an alternative host because bacterial transcriptomes can alter at different temperatures (Smoot et al., 2001), and certain species, including *Yersinia pestis*, can survive within poikilothermic insects and homeothermic humans and express different virulence factors in each organism (Konkel and Tilly, 2000). Furthermore, *Yersinia entomophaga* kills *G. mellonella* by *per os* infection when incubated at 25°C but not at 37°C (Hurst et al., 2015). However, possible variation in immune parameters must be accounted for when examining a pathogen within *G. mellonella* at different temperatures, as experiments have shown increased resistance to infection and elevated immune function after incubation at 4°C compared to animals incubated at 30°C (Mowlds and Kavanagh, 2008).

Fish challenge experiments using *V. anguillarum* are normally completed at 15°C despite the bacterium being routinely cultured at 22°C (Austin et al.,

1995; Pedersen et al., 1997). Thus, it would be beneficial if any alternative host for *V. anguillarum* could also be incubated at 15°C. Despite a previous report suggesting *G. mellonella* has an experimental temperature range of between 25°C-37°C (Desalermos et al., 2012) there is no reason why these animals cannot be successfully used in infection trials at temperatures of 4°C and above, meaning that this insect could be suited, at least in terms of temperature, to study almost any bacterium infecting fish, including cold water fish pathogens such as *Vibrio salmonicida*, which is pathogenic below 10°C (Guijarro et al., 2015).

Experimental planning must include consideration of standardised storage, handling of animals and experimental conditions to improve reproducibility and reduce variance within the data acquired from experiments. Immunomodulation of *G. mellonella*, in response to stress including temperature or starvation, can lead to reduced survival, alterations in haemocyte densities, and changes in AMP expression (Banville et al., 2012; Mowlds and Kavanagh, 2008). Notably, physical stress can enhance the immune response and survival (Mowlds et al., 2008). Furthermore, the duration of pre-challenge incubation may also affect the outcome of bacterial and fungal challenges in *G. mellonella* (Browne et al., 2015). Thus, when planning experiments standardised storage, handling of animals and experimental conditions is essential to improve reproducibility and reduce variance within experimental data.

New techniques for use within *G. mellonella* continue to emerge, including real-time imaging of infection progression using luciferase fused to a protein expressed on the pathogen cell surface (Delarze et al., 2015), investigating *in vivo* horizontal gene transfer between bacteria (Gottig et al., 2015), and enrichment of pathogen RNA recovered from infected insect haemolymph for RNA-seq assessment (Amorim-Vaz et al., 2015b). Amorim-Vaz et al. (2015b) also demonstrated a correlation between the *C. albicans* transcriptome during infection of *G. mellonella* and mice. The same research group also completed a virulence screen of 51 *C. albicans* transcription factor mutants in *G. mellonella* (Amorim-Vaz et al., 2015a), thus demonstrating the potential to accomplish a large-scale screening within this host. This would make *G. mellonella* well suited to screening a random transposon mutant library, which could elucidate novel virulence mechanisms.

1.4. Transposon mutagenesis

Identifying and characterising novel bacterial virulence factors is crucial to assisting the development of new chemotherapeutic and vaccine targets (Wu et al., 2008). To accomplish this objective, many new procedures have been developed including genome sequencing (Rodkhum et al., 2006b), IVIAT (Handfield et al., 2005) and representational difference analysis (Choi et al., 2002). Random transposon mutagenesis is one such powerful technique for bacterial virulence gene discovery

Transposons or 'jumping genes' are genetic elements that have the ability to replicate and relocate within or between genomes (Skipper et al., 2013), a process known as horizontal transfer. Transposons were first described in maize by Barbara McClintock in the 1940's and were originally called 'controlling elements' (Kidwell and Lisch, 2001). Since then they have been identified in all branches of the tree of life (Tellier et al., 2015). Moreover, transposable elements are believed to have transplanted into almost every living organism and they account for 50% of the human genome, although most are dormant fossil remnants (Skipper et al., 2013). Although they have been used to manipulate bacterial DNA since the mid-1970s (Kleckner et al., 1977), it was the advent of whole genome sequencing that, coupled with transposon mutagenesis, expedited the study of genotype-phenotype relationships (van Opijnen and Camilli, 2013).

Transposon elements relocate using either replicative or cut-and-paste systems facilitated using the enzyme transposase, which recognises the inverted repeats at either end of the transposon and the target sequence (Craig, 1997). This makes them advantageous for the random mutation of organisms (Choi and Kim, 2009). One transposon family which is especially useful for random mutagenesis is *Mariner*, as these transposons insert into DNA at TA dinucleotide recognition sequences (Tellier et al., 2015) that are relatively evenly distributed throughout most genomes, and thus this system generates transposon insertion libraries with random and even distribution throughout the genome (Chiang and Rubin, 2002; Robertson, 1995). *Mariner* elements are part of the IS630-Tc1-*mariner* (ITm) family of

transposons found in most eukaryotic genomes, and these are defined by a transposase gene bordered by a pair of terminal inverted repeats (Tellier et al., 2015). Individual screening of transposon mutants for a specific phenotype is followed by sequencing of sections of DNA containing the transposon insert which can then be mapped to the host genome. One example is the screening of bacterial transposon mutants in *C. elegans* to reveal genes that confer a reduction in virulence within this model (Agnoli et al., 2012). Although a similar screen of transcription factor insertion mutants to identify those with attenuated virulence has been completed in *G. mellonella* (Amorim-Vaz et al., 2015a), the insect has not been used to screen libraries of random transposon mutants. Thus, using *G. mellonella* to screen transposon mutations in *V. anguillarum* for reduced virulence would demonstrate an additional application for this alternative host.

1.5. Transposon insertion sequencing

1.5.1. Transposon mutagenesis and massively parallel sequencing

Next or second generation sequencing (NGS) platforms have catalysed a rapid increase in sequenced genomes available and potential applications of the data generated, chiefly arising from reductions in cost and time required to operate these systems (Land et al., 2015; Morey et al., 2013). Indeed, one high-throughput next-generation platform, developed by Solexa and now produced by Illumina, incorporates a technique called massively parallel sequencing (MPS), a method of sequencing by synthesis named reversible termination, to sequence upwards of a billion short nucleotide reads

simultaneously, which can be achieved subsequent to the fragmentation, indexing and amplification of template DNA (Loman et al., 2012).

One area that has been revolutionised by the emergence of NGS is the field of transposon mutagenesis. This technique has been combined with MPS to produce transposon insertion sequencing (TIS), which involves the analysis of whole libraries of transposon insertion mutants concurrently before mapping the insertion sites to the genome to identify genotype-phenotype relationships (van Opijnen and Camilli, 2013). There are now several separate methods to process transposon insertion mutant library DNA for sequencing, including four approaches published by different research groups in 2009 (Chao et al., 2016).

First, high-throughput insertion tracking by deep sequencing (HITS) involves shearing of transposon library DNA, before end repair and ligation of poly (A) tails, then addition of adapter and amplification of fragments containing the transposon/genomic DNA junction by polymerase chain reaction (PCR), and these PCR products are selected by size on agarose gel and sequenced (Gawronski et al., 2009). Transposon-directed insertion site sequencing (TraDIS) is broadly similar, except the post PCR size selection step is omitted (Langridge et al., 2009).

Two further methods take advantage of an MmeI restriction enzyme site, which can be added to a *Mariner* transposon terminal inverted repeat site by introducing a single point mutation (van Opijnen and Camilli, 2013). This Type II restriction enzyme, derived from *Methylophilus*

mephylotrophus, has the longest distance between recognition site and cut location (20-bp) of any enzyme in its class (Morgan et al., 2009). Thus, when the recognition site is located at the end of the terminal inverted repeat region it produces a staggered cut approximately 16-bp downstream of the insert location (van Opijnen and Camilli, 2013). Transposon library DNA is digested by MmeI before ligating an adapter to the cut site sticky end in both insertion sequencing (INseq) (Goodman et al., 2009) and transposon sequencing (Tn-seq) (van Opijnen et al., 2009). Then, the appropriate fragments containing the transposon/genomic DNA junction are amplified by PCR, gel purified or size selected then sequenced.

Recently two additional methods, described as modifications to Tn-seq but actually more similar to HITS and TraDIS, have been detailed. The Tn-seq circle technique involves shearing of transposon library DNA and then ligation of adapters to the free ends, before restriction enzyme digestion at a known site in the transposon (Gallagher et al., 2011). These products are denatured before the fragment containing the transposon end and a single remaining adapter is circularised by templated ligation, and all non-circularised DNA is degraded by exonuclease activity (Gallagher et al., 2011). Then, remaining transposon-genome junctions are amplified using a quantitative PCR (qPCR) step that adds a second adapter for sequencing. Finally, another technique uses the enzyme terminal deoxynucleotidyl transferase (TdT) to add a poly-C tail of approximately 20 deoxycytidine nucleotides to the 3' ends of sheared transposon library fragments (Klein et al., 2012; Lazinski and Camilli, 2013). Then, two rounds of PCR are

performed: the first PCR amplifies the correct fragment using poly-C-specific and transposon-specific primers, while the second PCR incorporates additional Illumina-specific sequences to permit subsequent sequencing.

All of these methods can facilitate the identification of 'required' (or 'essential') genes within a library of transposon mutants because cells disrupted at required loci will not replicate and consequently will be lost from a population. Thus, when a transposon library is sequenced and mapped to the genome, required genes will contain no insertions and will be revealed by negative selection (Chao et al., 2016). Henceforth this section will concentrate on the applications of Tn-seq, as this technique is best suited for this present study because all reads are of the same size, which prevents bias during PCR amplification (Kwon et al., 2016).

The Tn-seq technique can be applied to annotate required or conditionally essential loci in bacteria from libraries generated under various selection conditions, including different media (Lee et al., 2015), different chemical and physiological parameters (van Opijnen and Camilli, 2012), and *in vivo* (Crimmins et al., 2012). Furthermore, Tn-seq data can reveal fitness of specific mutants under different conditions, as this is proportional to the number of reads when analysing whole libraries (Pritchard et al., 2014). Amongst the many other applications of Tn-seq (Table 1.3) are identification of virulence factors in *Burkholderia pseudomallei* (Gutierrez et al., 2015) and cell wall biogenesis factors in *Bacillus subtilis* (Meeske et al., 2015).

Table 1.3. Previous studies using transposon sequencing (Tn-seq). This table covers applications using the Tn-seq technique only (van Opijnen and Camilli, 2010) and not similar methods of preparing transposon libraries for sequencing.

Organism	Experimental target	Library selection conditions	Reference
Streptococcus pneumoniae	Gene fitness	Todd Hewitt Broth (THY).	van Opijnen et al. (2009)
Yersinia pseudotuberculosis	Gene fitness to identify putative virulence factors	Mouse spleen and liver.	Crimmins et al. (2012)
Burkholderia pseudomallei	Gene fitness to identify putative virulence factors	Mouse lung, spleen and liver.	Gutierrez et al. (2015)
Bacillus subtilus	Cell wall biogenesis factors	Wild-type and multidrug/oligosaccharide-lipid/polysaccharide (MOP) exporter superfamily knockout mutants.	Meeske et al. (2015)
Streptococcus pneumoniae	Virulence mechanism and conditionally essential genes	Semi-defined minimal media (SSMM) with either glucose, fructode, mnannose, galactose, N-acetylglocosamine, sialic acid, sucrose, maltose, cellobiose, raffinose,. SSMM + glucose and either 2,2'-Bipyridyl, Methyl methanesulfonate, H_2O_2, pH6, temperature stress and antibiotic exposure DNA transformation. Mouse lung and nasopharynx.	van Opijnen et al. (2012)
Shewanella oneidensis	Essential genes involved in carbon metabolism	*Shewanella* basal medium (SBM; Covington et al. [2010]) agar and broth.	Brutinel et al. (2012)
Streptococcus pyogenes (GAS)	Essential genes	Comparison of two GAS isolates in Todd-Hewitt yeast (THY) medium.	Le Breton et al. (2015)
Bacillus subtilus	Genes involved in conjugation	A Δ*yvbJ* (penicillin binding protein which inhibits conjugation).	Johnson et al. (2014)

1.5.2. Tn-seq in *Vibrio* spp.

Studies of required or essential genes within *Vibrio* spp. are restricted to two previous reports for *Vibrio cholera.* The first of these studies used transposon insertion libraries of *V. cholerae* El Tor C6706 that were processed by the HITS method combined with hidden Markov model-based analysis, a data examination technique that reduces the effects of noise and enables fine-scale mapping independent of genomic annotation (Chao et al., 2013). The second study used transposon insertion libraries of *V. cholerae* El Tor E7946 prepared by the Tn-seq TdT method to investigate gene fitness within a rabbit model or pond water subsequent to passage through the rabbit or incubation in rich media (LB), and this revealed the different gene requirements for each condition (Kamp et al., 2013). Furthermore, Kamp et al. (2013) compared the required gene sets of *V. cholerae* El Tor E7946 and *V. cholerae* El Tor C6706 (Chao et al., 2013), and this produced an 87% overlap (361/414) between the two strains.

Additional studies of *V. cholerae* transposon insertion libraries has identified genotypes involved with antibiotic resistance (Dorr et al., 2014; Dorr et al., 2016) and regulation of cell envelope stress (Chao et al., 2015). Combined, these examples of successful transposon sequencing in *V. cholerae* suggest that *V. anguillarum* could be investigated by a similar approach. Furthermore, this technique could be combined with the *G. mellonella* host model to produce an ethically acceptable and low

maintenance system for identifying pathogen genes important for bacterial survival and prosperity *in vivo*.

1.6. Aim and objectives of this thesis

Knowledge of *V. anguillarum* pathogenicity and virulence remains limited (Frans et al., 2011) and further insight into the mechanisms underlying infection of fish is required to address problems caused by this bacterium. Therefore, the broad aim of this thesis is to further our knowledge on the virulence mechanisms employed by *V. anguillarum* using an invertebrate alternative host and a transposon insertion mutagenesis approach.

This aim will be achieved by completing the following objectives:

1. To evaluate *G.mellonella* as an alternative host for studying the virulence of *V. anguillarum*;
2. To prepare a random tagged-transposon insertion libraries of *V. anguillarum* and screen mutantss in *G. mellonella* to identify novel virulence genes;
3. To perform massively parallel sequencing of *V. anguillarum* random tagged-transposon insertion libraries to identify required genes under *in vitro* conditions.

Chapter 2. Standard procedures and identification of *Vibrio anguillarum* and mutant genotypes.

2.1. Introduction

This chapter aims to outline the general materials and methods used throughout this thesis and steps taken towards their improvement and optimisation. The microbiological resources will be described, including the identities of bacterial isolates; their culture, storage and re-isolation; methods to confirm the phenotypic traits and genotypic properties; and protocols for enumerating colony-forming units (CFU) and preparing standardised cell suspensions. Moreover, methods developed to evaluate the acceptibility of a *Galleria mellonella* infection model for *Vibrio anguillarum* virulence will be described, including handling and storage procedures; injection of liquids and cell suspensions; and determining larva survival.

Development and application of protocols to identify *V. anguillarum* isolates are essential. However, previously published polymerase chain reaction (PCR) protocols for *V. anguillarum* diagnostics have major shortcomings including the use of just one *V. ordalii* isolate (Gonzalez et al., 2003; Hirono et al., 1996; Hong et al., 2007) to confirm lack of cross-reactivity with this closely-related species (Fernandez and Avendano-Herrera, 2009) and reported primers that have no matches in published *V. anguillarum* genome sequences (Gonzalez et al., 2003). Thus, an optimised PCR assay developed in this chapter aimed to improve on existing methods.

2.2. Materials and methods

All consumables and equipment suppliers used throughout this thesis are listed in Appendix I.

2.2.1. Chemicals, reagents and media

Unless stated otherwise, all chemicals and reagents were purchased from Sigma-Aldrich (Poole, United Kingdom [UK]) and made with nuclease free Milli-Q water (Millipore Ltd, Watford, UK), while culture media were purchased from ThermoFisher Scientific (Renfrew, UK) and prepared with distilled water (dH_2O). Phosphate-buffered saline (PBS) was prepared to contain 8 g NaCl, 0.2 g KCl, 1.78 g $Na_2HPO_4 \cdot 2H_2O$ and 0.24 g KH_2PO_4 per litre and then corrected to pH 7.4 with 1M HCl. Preparation of ethylenediaminetetraacetic acid (EDTA), Tris, acetate and EDTA (TAE), NaCl-Tris-EDTA (STE) and Tris-EDTA (TE) buffers is described in Appendix II.

Unless stated otherwise, bacteria were cultured routinely on 1.5% sodium chloride (NaCl)-supplemented tryptone soy agar (TSA20) and broth (TSB20) or 1% NaCl-supplemented Miller lysogeny agar (LBA20) and broth (LB20); with '20' relating to the final concentration of NaCl in parts per thousand. Mueller-Hinton broth (MHB) and agar (MHA), supplemented with 2% NaCl where required, were used for determining minimum inhibitory concentration (MIC) and minimum bactericidal concentration (MBC) values, respectively. Thiosulphate-citrate-bile salts-sucrose agar (TCBS) was prepared according to the manufacturer's instructions.

All solutions and culture media (except TCBS agar which was brought to the boil on a hotplate) were sterilized by autoclaving at 121°C for 15 minutes. Where required, medium was supplemented after autoclaving with antibiotics ampicillin (AMP), chloramphenicol (CHL), kanamycin (KAN), penicillin G (PEN) or streptomycin (STR), to final concentrations (μg/mL) indicated by superscript, by aseptic addition of filter-sterilised (0.22-μm polyethersulfone; Millipore., Watford, Hertfordshire, UK) stock solutions prepared in dH_2O (or absolute ethanol for CHL) and stored routinely at -20°C.

2.2.2. Bacteria

Bacterial isolates (Table 2.1) were kept routinely at -70°C in 15:85 glycerol:PBS (1×10^9 CFU/mL). Before use, bacteria were recovered initially on to appropriate agar (Table 2.1), incubated (22°C, 48 h for *V. anguillarum*; 22°C, 72 h for *V. ordalii*; 22°C, 48 h for *Yersinia ruckeri*; 37°C, 24 h for *Escherichia coli*), and then single colonies inoculated into 5 mL of appropriate broth (Table 2.1). Cultures were incubated at 150 rpm (22°C, ~16 h for *V. anguillarum* and *V. ordalii*; 37°C, ~12 h for *E. coli*) until mid- to late-exponential phase, which was derived from experimental growth curve (Appendix III) and then cells were harvested by centrifugation ($2600 \times g$; 15 minutes; 4°C). The cell pellet was washed by re-suspension in PBS, before an identical second wash was performed after re-centrifugation and re-suspension in PBS. Finally, cell density of the suspension was determined by measuring absorbance at 600 nm (A_{600}) with a spectrophotometer

Table 2.1. Isolates used in this study.

Isolate or plasmid[a]	Characteristic(s)[b]	Serotype	Culture medium[cd]	Source or Reference
Isolates				
Vibrio anguillarum				
Dawn Austin, Heriot Watt University, Edinburgh, UK				
VIB 1 (ATCC 43305)	Wild type isolated from *Oncorhynchus mykiss*, Denmark	O1	TSA20/TSB20	Austin et al. (1995)
VIB 39 (UB 178/90)	Wild type isolated from *Dicentrarchus labrax*, Greece	O1	TSA20/TSB20	Austin et al. (1995)
VIB 44 (UB 261/91)	Wild type isolated from *D. labrax*, Italy	O1	TSA20/TSB20	Austin et al. (1995)
VIB 56 (UB 601/91)	Wild type isolated from *D. labrax*, Italy	O1	TSA20/TSB20	Austin et al. (1995)
VIB 64 (UB A023)	Wild type isolated from *Scophthalmus maximus*, Spain	O1	TSA20/TSB20	Austin et al. (1995)
VIB 79 (LMG 12101)	Unknown	O1	TSA20/TSB20	Austin et al. (1995)
VIB 85 (RVAU 87-9-117)	Wild type isolated from *O. mykiss*, Italy	O1	TSA20/TSB20	Austin et al. (1995)
VIB 87 (NCIMB 1873)(T265)[e]	Wild type isolated from *Salmo Salar*, UK	O1	TSA20/TSB20	Austin et al. (1995)
VIB 88 (RVAU 51/82/2)	Wild type isolated from *O. mykiss*, Germany	O1	TSA20/TSB20	Austin et al. (1995)
VIB 93 (RVAU 850610-1/6a)	Wild type isolated from *O. mykiss*, Denmark	O1	TSA20/TSB20	Austin et al. (1995)
VIB 134 (RVAU 91-8-178)	Wild type isolated from *Sc. maximus*, Norway	O1	TSA20/TSB20	Austin et al. (1995)
Debra Milton, Umea University, Sweden				
NB10	Wild type environmental isolate from Gulf of Bothnia, Sweden	O1	TSA20/TSB20	Norqvist et al. (1989)
NB10 cured	NB10 cured of p67-NB10 virulence plasmid	O1	TSA20/TSB20	Weber et al. (2010)
NB12	CHL^r NB10 derivative carrying a plasmid insertion in *empA*	O1	TSA20/TSB20 + CHL^5	Milton et al. (1992)
DM1	CHL^r NB10 derivative carrying a plasmid insertion in *virC* This strain has lost p67-NB10 virulence plasmid	O1	TSA20/TSB20 + CHL^5	Milton et al. (1995)
DM16	NB10 derivative with 153bp 3'-end in frame deletion within *flaA*	O1	TSA20/TSB20	Milton et al. (1996)
KD12	NB10 derivative with 180bp 5'-end in frame deletion within *flaD*	O1	TSA20/TSB20	McGee et al. (1996)
KD27	NB10 derivative with 180bp 5'-end in frame deletion within *flaE*	O1	TSA20/TSB20	McGee et al. (1996)

David Nelson, University of Rhode Island, US

M93Sm	Spontaneous STR^r mutant of wild type M93 isolated from *Plecoglossus altivelis*	J-O-1[f]	LBA20/LB20 + STR^{200}	Denkin and Nelson. (1999)
M99	STR^r and CHL^r M93Sm derivative carrying a plasmid insertion in *empA*	J-O-1[f]	LBA20/LB20 + STR^{200} + CHL^5	Denkin and Nelson. (2004)
JR1	STR^r and CHL^r M93Sm derivative carrying a plasmid insertion in *vah1*	J-O-1[f]	LBA20/LB20 + STR^{200} + CHL^5	Rock and Nelson. (2006)
S123	STR^r and CHL^r M93Sm derivative carrying a plasmid insertion in *rtxA*	J-O-1[f]	LBA20/LB20 + STR^{200} + CHL^5	Li et al. (2008)
S183	STR^r, CHL^r and KAN^r M93Sm derivative carrying a plasmid insertion	J-O-1[f]	LBA20/LB20 + STR^{200} + CHL^5+ KAN^{80}	Li et al. (2008)
S262	STR^r and CHL^r M93Sm derivative carrying a plasmid insertion in *plp*	J-O-1[f]	LBA20/LB20 + STR^{200} + CHL^5	Li et al. (2013)

Vibrio ordalii

Dawn Austin, Heriot Watt University, Edinburgh, UK

VIB 2 (ATCC43306)[h]	Wild type isolated from *Gadus morhua*, Denmark	O2a[i]	TSA20/TSB20	Austin et al. (1995)
VIB 307^T ($LMG\ 13544)^T$	Wild type isolated from *Oncorhynchus kisutch*, US	O2a[i]	TSA20/TSB20	Austin et al. (1995)
VIB 679 (Muroga PT-81025)	Wild type isolated from *Plecoglossus altivelis*, Japan	O2a[i]	TSA20/TSB20	Austin et al. (1995)

Yersinia ruckeri

Lab collection, University of Stirling, UK

YR1	Wild type isolated from *Oncorhynchus mykiss*, UK	O1	TSA	Tinsley et al. (2011)

a Strain numbers in brackets refer to the original holding institutions collections: ATCC, American Type Culture Collection; UB, University of Barcelona, Spain; LMG, Laboratorium voor Mikrobiologie, University of Gent, Gent, Belguim; RVAU, Royal Veterinary and Agricultural University, Copenhagen, Denmark; NCIMB, National Collection of Industrial Food and Marine Bacteria, Aberdeen, UK; Eaves, Dr. L. Eaves, Animal Research Institute, Yeerongpilly, Queensland, Australia; Muroga, Dr. K. Muroga, Hiroshima University, Hiroshima, Japan.

b AMP^r, ampicillin-resistant CHL^r, chloramphicol-resistant; KAN^r, kanamycin-resistant; STR^r, streptomycin-resistant.

c TSA20, tryptone soya agar + 1.5 % NaCl; TSB20, tryptone soya broth + 1.5 % NaCl; LBA (20), Luria-Bertani agar, Miller (+ 1 % NaCl); LB (20) Luria-Bertani broth, Miller (+ 1 % NaCl).

d Concentrations of AMP, CHL, KAN and STR were added to medium at the concentrations (µg/mL) in superscript.

e T265 (Pedersen et al., 1997) confirmed as VIB 87 by personal communication with author.

f Japanese serotype which likely corresponds to serotype O2a of Danish system (Fujiwara-Nagata et al., 2003; Grisez and Ollevier, 1995; Miyamoto and Eguchi, 1996).

h Listed by ATCC and reference above as *Vibrio (Listonella) anguillarum*. However this strain has been reclassified as *V.ordalii* (Dawn Austin, personal communication).

i Refers to the *V. anguillarum* serogrouping system (Austin et al., 1997).

(CE 2041; Cecil Instruments Ltd, Cambridge, UK). Bacterial suspensions were diluted with PBS to the desired colony-forming units per millilitre (CFU/mL) using data from calibration curves determined previously (Section 2.2.4.). Prior to use, the CFU/mL of cell suspensions were confirmed by serial dilution in PBS in quadruplicate and plating onto appropriate agar.

2.2.3. *Galleria mellonella* larvae

Larvae in their final instar stage were purchased from UK Waxworms Ltd (Sheffield, UK) and stored at 4ºC for up to 14 days before use. The wax moth life cycle spanning egg to final instar stage (5 day duration at 25°C) lasts approximately 5 weeks at 25°C (Ramarao et al., 2012). Only uniformly cream-coloured larvae (uniform groups of larvae with no markings are suggested to support reproducible results; Fuchs et al., 2010) of 20-25 mm in length and approximately 220 mg in mass, were selected for inclusion in experiments. Larvae were sorted at least 24 h prior to use in procedures.

2.2.3.1. Larval injections

Culture, antibiotics, culture supernatant or PBS (10 µL) were administered to the larvae by injection into the posterior left abdominal proleg (Figure 2.1) using a 50-µL Hamilton® syringe (McMillan et al., 2015). The syringe was cleaned and sterilised before the first injection, between experimental groups, and after the final injection in the experiment by three full-syringe volumes of 1% (w/v) sodium hypochlorite, followed by three full-syringe

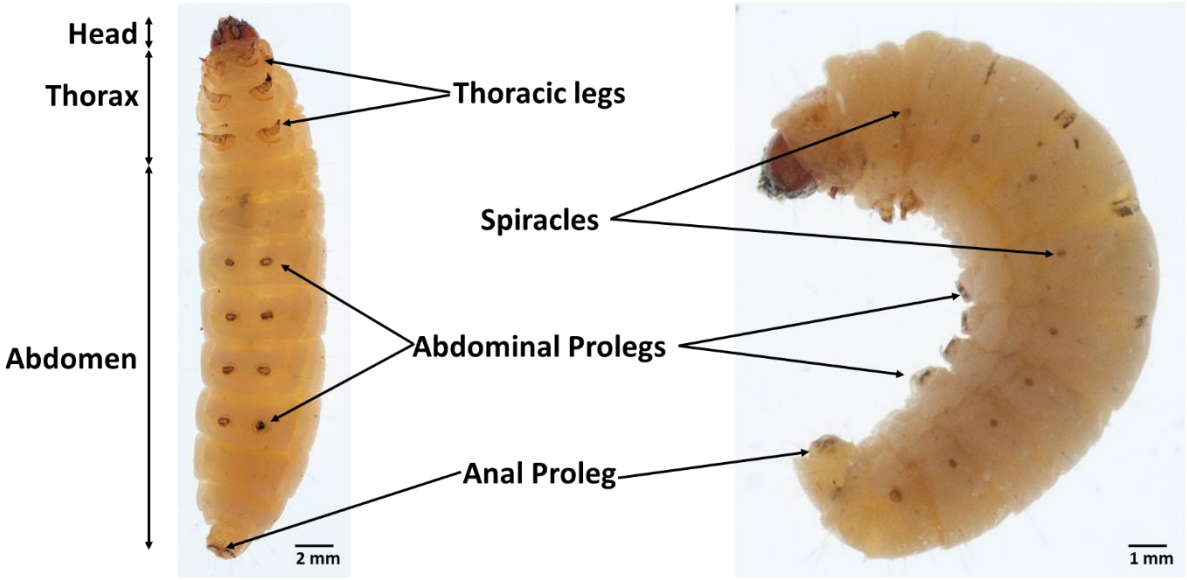

Figure 2.1 *Galleria mellonella* larva, in final instar stage, highlighting the abdominal prolegs into which inoculums are administered.

volumes of 70% ethanol, and finally six full-syringe volumes of PBS. This regime was derived empirically (Appendix IV).

Where larvae required more than one injection, further injections were made into different prolegs by working up the body beginning with the posterior right proleg. All experiments included a group of larvae injected with PBS only to control for the trauma of injection(s) and a group of larvae that underwent no manipulation to control for any background mortality in the batch.

Larvae were routinely incubated at 15ºC and this reduced incubation temperature, compared to *in vitro* culture, was used to imitate previous challenge work in fish (Pedersen et al., 1997). Challenge experiments were completed over 120 h and percentage survival in groups was recorded every 24 h, with larvae considered to be dead if they did not react to gentle probing with a sterile inoculation loop for two minutes. Unless stated otherwise, all experiments were repeated once with a different batch of larvae.

2.2.4. Prepartion of calibration curves

Duplicate cultures of *V. anguillarum* VIB1, VIB 39, VIB 87, and VIB 93 and *V. ordalii* VIB 2 were cultured from single colonies for 14 h (150 rpm, 22ºC) in 10 mL of TSB20 (Table 2.1). The *V. anguillarum* isolates were selected to represent an equal number of pathogenic and non-pathogenic strains in a previous *Salmo salar* challenge model (Pedersen et al., 1997). *V. ordalii* VIB 2 was included to investigate differences in culture absorbances between

these related species. Cells from single cultures of each strain were harvested and washed as described in Section 2.2.2 before re-suspension in 5 mL PBS and determination of A_{600}. Then this crude bacterial suspension was diluted four times 1:10 in PBS and the A_{600} of each suspension determined. Finally, to obtain an accurate estimate of CFU/mL quadruplicate aliquots of 10 µL of each suspension were serially diluted 1:10 in PBS and plated onto TSA20. Agar plates were incubated as described in Section 2.2.2 until colonies formed. The dilutions from each series giving ca. 30–300 CFU were counted and plotted against A_{600} of each suspension (Excel; Microsoft, Redmond, US) and a straight line of best fit through the origin applied. The equations of the lines of best fit were used to calculate CFU/mL of bacterial suspensions from A_{600} values.

2.2.5.1. DNA extraction

Single colonies of culture(s) of interest were inoculated into sterile universal bottles containing approximately 5 mL of appropriate broth (Table 2.1) and incubated overnight as described in Section 2.2.2. Cells from 1.5 mL of culture were harvested by centrifugation (4000 ×*g*, 3 minutes) in an Eppendorf tube. The supernatant was discarded while the cell pellet was suspended in 1 mL STE buffer. Then the cells were re-pelleted by centrifugation (13000 ×*g,* 1 minute) and the supernatant removed carefully by pipette and discarded. The cell pellet was re-suspended in 100 µL of TE buffer and placed on a heat block at 95ºC for 10 minutes before placing immediately on ice. Once cooled, the sample was centrifuged (13000 ×*g,* 1

minute) before 50 µL of supernatant (containing the DNA) was transferred to a fresh Eppendorf tube and kept on ice.

Following mixing by vortex and brief centifugation (1 s, 3000 ×*g*), the sample was read by nanodrop spectrophotometer (NanoDrop 1000; ThermoScientific, Wilmington, US), as a crude indicator of DNA content, using 1.7 µL of sample to determine absorbance ratios at 260:280 nm and 260:230 nm, respectively compared to an identical volume of TE buffer as control, before storing the sample at -20ºC.

2.2.5.2. Primers

Where required, novel primers were designed using Primer-BLAST (https://www.ncbi.nlm.nih.gov/tools/primer-blast/index.cgi?LINK_LOC=BlastHome) and synthesised as high-purity and salt-free (HPSF) by Eurofins Genomics (Ebersberg, Germany) unless stated otherwise. Primers (Table 2.2) were routinely dissolved in nuclease free water to 100 pmol/µL (on ice), before working stocks were prepared in water at 10 pmol/µL. Aliquots of primers were stored at -20ºC until needed.

2.2.5.3. Polymerase chain reaction (PCR)

Specific DNA sequences were amplified in 10 µL reactions prepared on ice with each reaction containing 5 µL 2× MyTaq mix (Bioline, London, UK), 0.4 µL of each primer at 10 pmol/µL, 1 µL of DNA sample at 50 ng/µL, and nuclease free water to make up the final volume. After mixing by gently flicking the bottom of the tube then briefly pulsing tubes in a centrifuge

(1 s, 3000 ×*g*), the reaction was run on a thermocycler (TProfessional; Biometra, Göttingen, Germany) operating the following conditions (unless stated otherwise): 95ºC for 1 minute; 30 cycles of denaturation at 95ºC for 15 s, annealing at the desired annealing temperature for 15 s, and extension at 72ºC for 20 s; a final extension of 72ºC for 2 minutes; then 10ºC for 30 s to rapidly cool the reaction. The thermocycler lid was set to 99ºC throughout all PCR cycles and reaction tubes were put on ice immediately after cessation of the run. A no template control (NTC) containing each reagent in the reaction, except sample DNA, was included in each PCR run.

2.2.5.4. Gel electrophoresis

For products expected to be >200 base pairs (bp) long, samples were routinely run on a 1% w/v (weight/volume) agarose gel made with 0.75× TAE. The agarose was dissolved in TAE buffer by microwave heating (700 W, 45 s), and then allowed to cool to approximately 50ºC before the desired volume of 5 mg/mL ethidium bromide (EtBr) stock solution was added in fume hood to give a final concentration in the gel of 0.05 µg/mL. The molten agarose was poured into a gel tray that had been sealed at either end with masking tape. Then, a comb with 2 × 1 mm teeth was added to form the wells and the gel was allowed to set for 1 h in a fume hood. Prior to loading, the gel was submerged in a tank of 0.75× TAE for at least 10 minutes.

Meanwhile, each sample for gel electrophoresis was prepared on ice and this consisted of 0.5 µL PCR reaction product, 1 µL of 6× loading dye

Table 2.2. Primers used to confirm *Vibrio anguillarum* wild-type and mutant isolates.

Target	Primer	5'-3'	Amplicon Length (bp)	Annealing temp. (°C)	Source or Reference
V. anguillarum specific *amiB* – N-acetylmuramoyl-L-alanine amidase	**van-ami8** **van-ami417**	**F:** ACATCATCCATTTGTTAC **R:** CCTTATCACTATCCAAATTG	429	55	**Hong et al. (2007)** **Hong et al. (2007)**
V. anguillarum specific *rpoN* – cellular factor σ^{54} subunit	**rpoN1SMF** **rpoN1SMR**	**F:** GGATGATGTCTACAGCGCGA **R:** ACGCTGTCGGGGTTTATTGT	612	54	**This study** **This study**
V. anguillarum specific *rpoN* – cellular factor σ^{54} subunit	**rpoN-ang5'** **rpoN2SMR**	**F:** GTTCATAGCATCAATGAGGAG **R:** TGCCGAGCAGATCAATATGT	538	62	**Gonzalez et al. (2003)** **This study**
V. anguillarum empA plasmid insertion	**NB12F** **pNQ705-R**	**F:** AACAAAAGCAAGCGGTT **R:** GCGTAACGGCAAAAGCACCGCCGGACATCA	638	52	**Milton et al. (1992)** **Milton et al. (1992)**
V. anguillarum virC plasmid insertion	**DM1F** **pNQ705-R**	**F:** TGGGTTGAAAGGGCGAGTTTA **R:** GCGTAACGGCAAAAGCACCGCCGGACATCA	359	64	**This study** **Milton et al. (1992)**
V. anguillarum flaE in frame deletion	**KD27flaESMF** **KD27flaESMR**	**F:** TATGTATGGTGTGGCGGACG **R:** GCCGCAACATAGCTAAAGCC	589	56	**This study** **This study**
V. anguillarum flaA in frame deletion	**DM16flaASMF** **DM16flaASMR**	**F:** AATCAGCAAACGGCACCAAC **R:** CCTAACCCACGTCTGAGCTG	735	57	**This study** **This study**
V. anguillarum flaD in frame deletion	**KD12flaDSMF** **KD12flaDSMR**	**F:** AGCATTGGCCTTACTTCGCT **R:** TCGCTACACGGTCTGCTTTT	419	57	**This study** **This study**
V. anguillarum angR on pJM1 like virulence plasmid	**angRSMF** **angRSMR**	**F:** AAGACGTGACCCGATTGCTT **R:** TATCGATGCTTCGGTGGCTC	247	55	**This study** **This study**
V. anguillarum fatE on pJM1 like virulence plasmid	**fatESMF** **fatESMR**	**F:** TTTTGTCCATGGCTTCACGC **R:** TGGATGACAAGCACTACGGC	454	57	**This study** **This study**
V. anguillarum vah1 plasmid insertion	**vah1JR1SMF** **pNQ705-R**	**F:** CGTAGTACGGCCAGTATGGT **R:** GCGTAACGGCAAAAGCACCGCCGGACATCA	773	63	**This study** **Milton et al. (1992)**
V. anguillarum empA plasmid insertion	**M99SMF** **pNQ705-R**	**F:** GTTGAACAAAAGCAGGCGGT **R:** GCGTAACGGCAAAAGCACCGCCGGACATCA	743	61	**This study** **Milton et al. (1992)**

V. anguillarum plp plasmid insertion	**S262SMF** **pNQ705-R**	**F:** TGATCGTTCACACCCGTCAG **R:** GCGTAACGGCAAAAGCACCGCCGGACATCA	699	64	**This study** **Milton et al. (1992)**
V. anguillarum rtxA plasmid insertion	**vah1JR1SMF** **pNQ705-R**	**F:** CGTAGTACGGCCAGTATGGT **R:** GCGTAACGGCAAAAGCACCGCCGGACATCA	559	63	**Nelson, D., Per. Communication** **Nelson, D., Per. communication**
V. anguillarum vah1 in frame deletion	**vah1S183SMF** **vah1S183SMR**	**F:** ATAATTCGCCACAAAGGTGCC **R:** CTTACTTAACGCCACCGTGC	2534	56	**This study** **This study**

(ThermoFisher) and 4.5 µL nuclease free water. Molecular weight markers were included in the first well of each gel and each of these consisted of 0.2 µL of 100-bp DNA ladder (0.5 µg/µL; ThermoFisher), 1 µL of 6× loading dye and 4.8 µL nuclease free water. After mixing by vortex and briefly pulsing in a centrifuge (1 s, 3000 ×*g*), the samples were loaded into the wells of the gel while molecular weight markers were added last. The gel was run at 10 /cm until the ladder products had migrated and separated sufficiently along the gel to be distinguishable. Each gel was photographed in a UV transilluminator using the Genesnap v.7.12.06 software (Syngene, Cambridge, UK.). Products expected to be >1 kb were run as above except that 2 µL of 1-kb ladder (0.1 µg/µL) containing 6× loading dye was run in the first and last well of each gel.

2.2.6. Confirmation of cultures as *Vibrio* spp.

Cultures were confirmed initially as *Vibrio* spp. by spreading three distinct colonies onto TCBS agar (Kobayashi et al., 1963) and incubating at 22ºC for 72 h, as *Vibrio* spp. form colonies of a characteristic yellow colour. The constituents of TCBS agar make it highly alkaline (pH 8.6) and saline (1%) which suits the mildly halophilic and facultatively anaerobic *V. anguillarum*. Next, *Vibrio* spp. were confirmed by growth inhibition by Vibrio static agent 0/129 (i.e., 2,4-diamino-6,7-di-iso-propylpteridine phosphate; Fisher Scientific), as species from this genera are susceptible to this agent (Shewan et al., 1954). Briefly, 2-3 colonies from a 'pure' culture was added to 2 mL PBS and re-suspended by aspiration with a pipette and

mixing by vortex. Then 50 μL of cell suspension was spread evenly onto a TSA20 plate and discs containing 10 μg and 150 μg of Vibrio static agent 0/129 were placed on the agar surface. The plate was incubated (22ºC; 24 h) before being examined for growth inhibition around the discs. Control cultures of *V. anguillarum* NB10 (positive), *Y. ruckeri* YR1 (negative) and *E. coli* SM10λ*pir* (negative) were used for both assays.

2.2.7. Confirmation of cultures as *Vibrio anguillarum*

2.2.7.1. Latex agglutination test

A commercially available latex agglutination test (MONO-AQUA; Bionor, Skien, Norway) gives a positive reaction (i.e., agglutination) in the presence of *V. anguillarum* serotypes O1 and O2, and this test was performed according to the manufacturer's instructions. Briefly, a small drop of test reagent (approximately 5 μL, 1-2 mm in diameter) was placed onto an analysis card and then 1-3 colonies were added to the liquid and mixed with an inoculation loop for 30 s to observe for signs of agglutination. If agglutination occurred then a further 1-3 colonies were mixed with the control reagent, which should not agglutinate and thus confirm a specific response. Again, control cultures of *V. anguillarum* NB10 (positive), *Y. ruckeri* YR1 (negative) and *E. coli* SM10λ*pir* (negative) were used in this assay.

2.2.7.2. Optimisation of *V. anguillarum* specific PCR

Next, it was desirable to confirm identification of cultures as *V. anguillarum* by PCR amplification of *V. anguillarum* specific DNA sequences. However, the specificity of existing protocols for this purpose (Gonzalez et al., 2003; Hirono et al., 1996; Hong et al., 2007) was not fully verified, as these previous studies had tested primers for negative amplification against only one *V. ordalii* isolate, a species very closely related to *V. anguillarum* (Fernandez and Avendano-Herrera, 2009). Furthermore, the reverse primer from one protocol (Gonzalez et al., 2003) did not complement the *V. anguillarum rpoN* sequence as claimed. Thus, it was decided to develop a new protocol.

Initially this process was optimised, in a temperature gradient PCR programme, to select the most specific primers and annealing temperature for *V. anguillarum* DNA amplification whilst reducing false positive signals from *V. ordalii*. Products of DNA extracted (2.2.5.1) from *V. anguillarum* strains VIB 39, VIB 87, NB10 and M93Sm and *V. ordalii* VIB 2, VIB 307^{t}, and VIB 679 were PCR amplified (2.2.5.3) using 3 different primer sets (van-ami8/van-ami417 targeting amiB, an N-acetylmuramoyl-L-alanine amidase, and rpoN1SMF/R and rpoN-ang5'/rpoN2SMR both targeting rpoN, the cellular factor σ54 subunit; Table 2.2). Each primer set was run, with all samples, at three different annealing temperatures (Table 2.3) before visualising PCR products on agarose gel (2.2.5.4).

Table 2.3. Primer annealing temperatures used in gradient polymerase chain reaction (PCR). These conditions were used to optimise *Vibrio anguillarum*-specific diagnostic assay.

Primer pair	Target gene	T_m[a] forward primer (°C)	T_m reverse primer (°C)	Temperature 1 (°C)	Temperature 2 (°C)	Temperature 3 (°C)
van-ami8/van-ami417	*amiB*	46.9	51.1	46.1	51.7	55.9
rpoN1SMF/rpoN1SMR	*rpoN*	59.4	57.3	51	54.4	57
rpoN-ang5'/rpoN2SMR	*rpoN*	55.9	55.3	52.1	57.7	61.9

a Primer melting temperature

2.2.7.3. *V. anguillarum* identification by PCR

DNA extracts (2.2.5.1) were confirmed as *V. anguillarum* by PCR and visualisation of a band of approximately 538 bp on agarose gel (according to Sections 2.2.5.3 and 2.2.5.4) using rpoN-ang5' and rpoN2SMR primers (Table 2.2) and a PCR annealing temperature of 62°C.

2.2.8. Confirmation of pJM1-like virulence plasmid in wild-type serotype O1 *V. anguillarum* isolates

To investigate which wild-type *V. anguillarum* serotype O1 isolates carried the pJM1-like virulence plasmid a PCR assay was completed using two specific primer pairs designed against the *angR* (Genbank locus tag: VANGNB10_67p038; angRSMF/R; Table 2.2), and *fatE* (Genbank locus tag: VANGNB10_67p010; fatESMF/R; Table 2.2) genes located on opposing sides of *V. anguillarum* NB10 p67-NB10 (pJM1-like) plasmid. DNA was extracted from all wild-type *V. anguillarum* serotype O1 isolates (Table 2.1) according to previous methods (Section 2.2.5.1. and Section 2.2.5.3) using *V. anguillarum* NB10 template DNA as a positive control. These products were then run on an agarose gel following Section 2.2.5.4. Plasmidless *V. anguillarum* M93Sm template DNA was used as an additional negative control.

2.2.9. Confirmation of *V. anguillarum* mutant genotypes

To confirm that mutant isolates (Table 2.1) had retained their expected genotypes, each strain was subjected to a specific PCR assay. Specific sequences expected to be present in each knockout mutant were amplified

by PCR following the cycle parameters detailed previously (Section 2.2.5.3), except that the extension step was increased to 1 minute for confirmation of *V. anguillarum* S183 (Li et al., 2008). This time increase reflects the expected 2534 bp size of *V. anguillarum* S183 PCR product. Completed PCR reactions were run on 1% agarose gels as described in Section 2.2.5.4. Primer pairs and annealing temperatures are given in Table 2.2.

To detect the p67-NB10 (pJM1-like) virulence plasmid in *V. anguillarum* NB10 derivatives a PCR confirmation was completed following Section 2.2.8. DNA extracted from a strain of *V. anguillarum* NB10 that had been cured of p67-NB10 (Weber et al., 2010) was assayed to confirm loss of the plasmid, while DNA extracted from each mutant derived from *V. anguillarum* NB10 (McGee et al., 1996; Milton et al., 1992; Milton et al., 1995; Milton et al., 1996) was included to confirm that each of isolate had retained the p67-NB10 plasmid, as loss of this plasmid during mutant strain construction may underlie, at least in part, observed reductions in virulence in *in vivo* infection trials. In addition to NTC, wild-type parent strain *V. anguillarum* NB10 and plasmidless *V. anguillarum* M93Sm were used as positive and negative controls, respectively.

For mutants created by allelic exchange and in-frame deletion (McGee et al., 1996; Milton et al., 1996; Li et al., 2008), primer pairs were designed against regions up- and downstream of the affected sites (Figure 2.2). In these cases, parent and mutant strains would be expected to generate products of different lengths, thus mutant *V. anguillarum* KD27 would yield

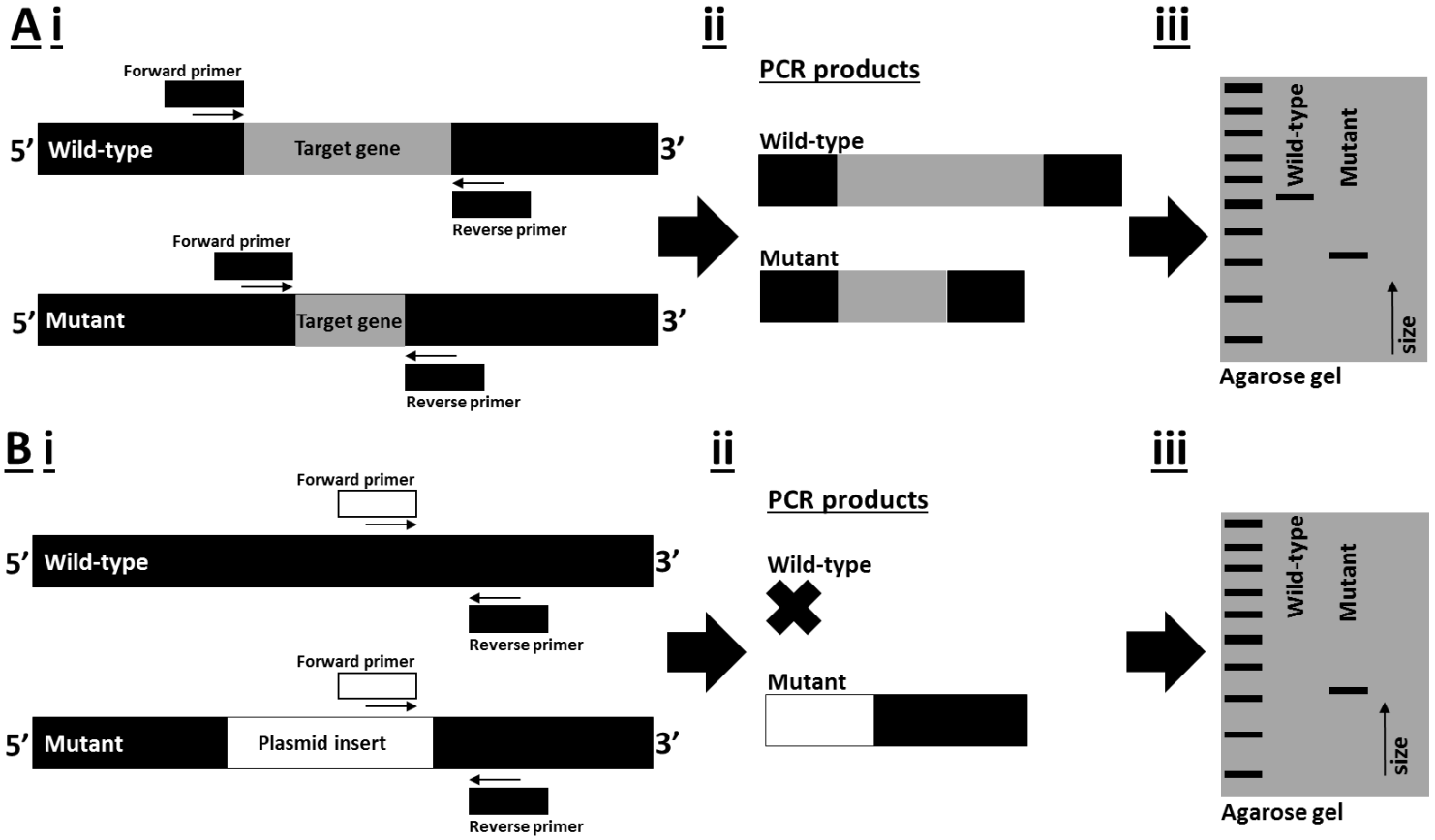
A i
ii
iii
Forward primer
5'
Wild-type
Target gene
3'
Reverse primer
Forward primer
5'
Mutant
Target gene
3'
Reverse primer
PCR products
Wild-type
Mutant
Wild-type
Mutant
size
Agarose gel
B i
ii
iii
Forward primer
5'
Wild-type
3'
Reverse primer
Forward primer
5'
Mutant
Plasmid insert
3'
Reverse primer
PCR products
Wild-type
Mutant
Wild-type
Mutant
size
Agarose gel

Figure 2.2 Confirmation of targeted mutations in *Vibrio anguillarum* genes. Gene deletions or insertions were confirmed by agarose gel electrophoresis of PCR products generated from DNA extracted from *Vibrio anguillarum* isolates with specific mutations. A) Mutations by allelic exchange were produced by overlap PCR which deletes a section of the target gene. i) To confirm this mutation, primers complementary to either side of this disruption amplify PCR products containing the sequence where the deleted section should be. ii) This product will be shorter than that of the wild-type; iii) and is confirmed by gel electrophoresis of PCR products. B) Mutations by plasmid insertion were produced by amplifying and inserting a section of target gene into a plasmid suicide vector. Then the plasmid was recombined into the chromosome following conjugation at a position within the cloned region. B) To confirm these mutations, a primer was designed complementary to a region of the plasmid ~80–170 bp up- or downstream from the cloned-plasmid insertion site; and a second within a region of the disrupted gene ~25–105 bp up- or downstream from the 3' or 5' end of the cloned product. ii) Thus, PCR product should only be generated from DNA of mutants with the insertion and not the wild-type. iii) This is confirmed by gel electrophoresis of PCR products.

a 589-bp product compared to a 779-bp product from the *V. anguillarum* NB10 parent; while *V. anguillarum* DM16 should yield a 735-bp compared to a 888-bp product from the *V. anguillarum* NB10 parent; and *V. anguillarum* KD12 should yield a 419-bp product compared to a 599-bp product from the *V. anguillarum* NB10 parent; and finally *V. anguillarum* S183 should yield a 2534-bp product compared to a 2789-bp product from the *V. anguillarum* M93Sm parent.

Mutants constructed by insertion of phenotype-disrupting sequences into the chromosome (Denkin and Nelson., 2004; Li et al., 2008; Li et al., 2013; Milton et al., 1992; Milton et al., 1995; Rock and Nelson, 2006), all had a section of the target gene amplified and inserted into a plasmid suicide vector. Then the plasmid was recombined into the chromosome following conjugation at a position within the cloned region. Thus, for mutants created by plasmid insertion into the chromosome, primer pairs were designed against i) a region of the plasmid ca. 80-170-bp up- or downstream from the cloned-plasmid insertion site; and ii) a region of the disrupted gene ca. 25-105 bp up- or downstream from the 3' or 5' end of the cloned product (Figure 2.2). Detection of a PCR product of the expected size confirmed the presence of the mutation and respective parent strains were used as negative controls in each assay.

2.3. Results

2.3.1. Generation of calibration curves

Calibration curves and equations for the lines of best fit were determined for *V. anguillarum* VIB 1, VIB 39, VIB 87, VIB 93 and *V. ordalii* VIB 2 and these permitted the accurate estimation of CFU/mL from culture A_{600} values (Figure 2.3).

2.3.2. Identification and confirmation of colonies as *Vibrio* spp.

All wild-type *V. anguillarum* and *V. ordalii* isolates (Table 2.1), formed yellow colonies on TCBS agar (Figure2.4), which is characteristic for *Vibrio* spp., although *V. anguillarum* VIB 79 formed colonies more slowly than the other isolates; meanwhile, *Y. ruckeri* YR1 and *E. coli* SM10*λpir* formed green colonies (Figure 2.4). Each *V. anguillarum* and *V. ordalii* isolate was susceptible to vibriostatic O/129 agent in a dose-dependent manner, as evidenced by a larger growth inhibition zone around the disc containing the greater dose of O/129 (Figure 2.5). Meanwhile, *Y. ruckeri* YR1 and *E. coli* SM10λ*pir* were not susceptible to the growth inhibitory action of the O/129 agent.

2.3.3. Identification of *V.anguillarum*

All wild-type *V. anguillarum* isolates caused agglutination of the test reagent in the MONO-AQUA latex agglutination analysis, while *Y. ruckeri* YR1 and *E. coli* SM10*λpir* did not cause agglutination. Interestingly, the three *V. ordalii* isolates tested (VIB 2 and VIB 307^T and VIB 679) also

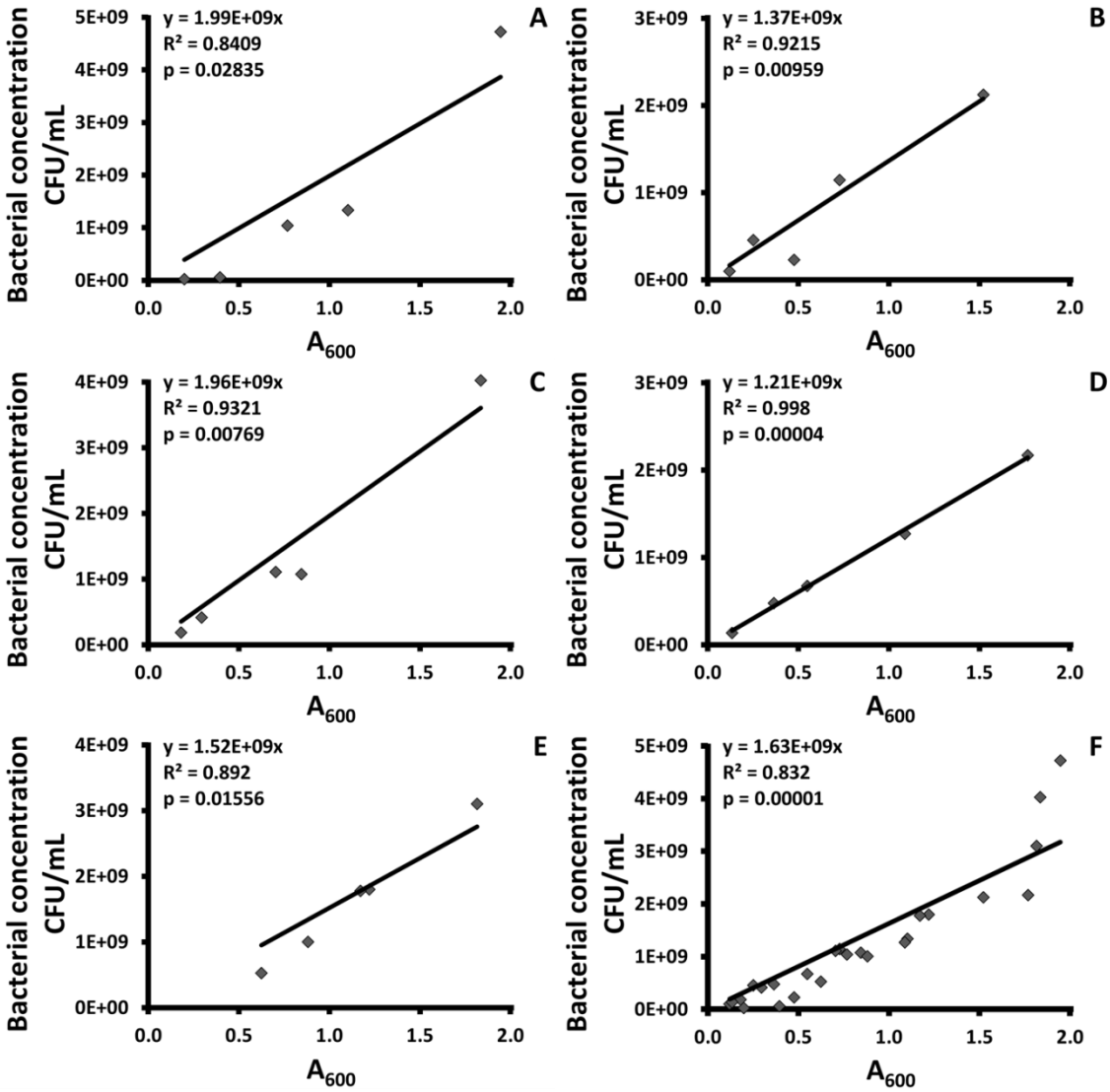

Figure 2.3. Relationship between colony forming units per mL (CFU/mL) of cell suspension absorbance at 600 nm (A_{600}) for *Vibrio anguillarum* VIB 1 (A), VIB 39 (B), VIB 87 (C), VIB 93 (D), *Vibrio ordalii* VIB 2 (E) and combined data for all isolates, including *V. ordalii* VIB 2 (F). Line, on each chart, intercepts the origin and p values are calculated from the Pearson's correlation coefficient R^2 value. n = 5, except F where n = 25.

.

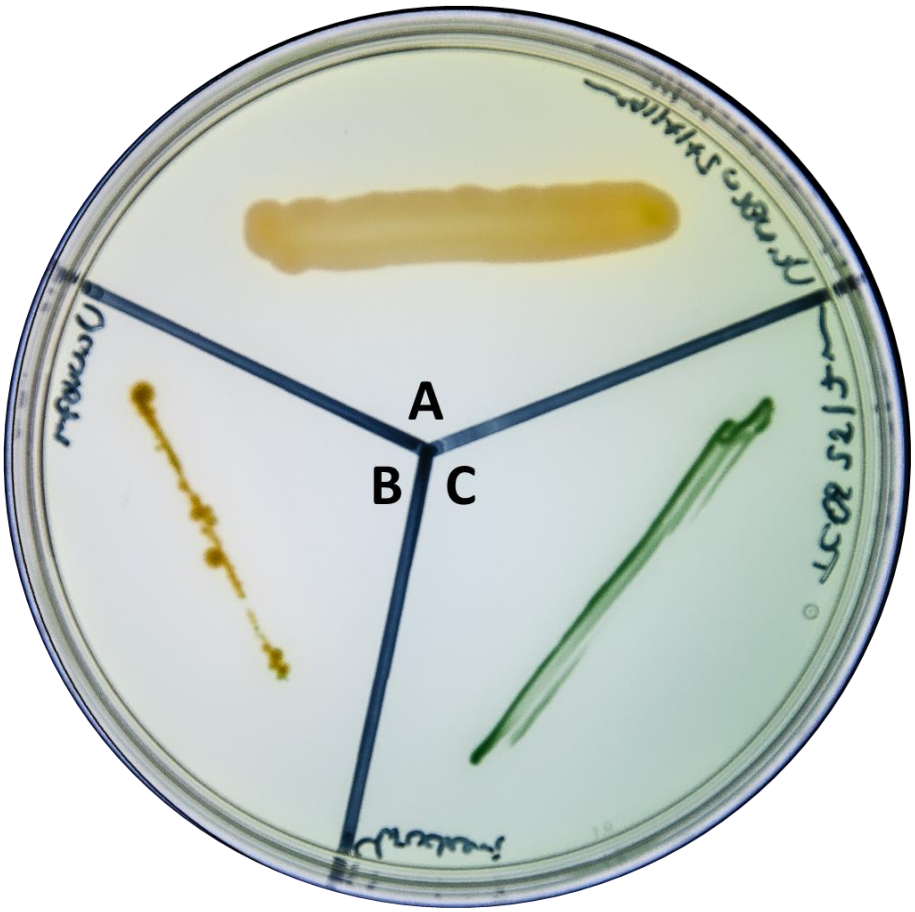

Figure 2.4. Representative colonies of *Vibrio anguillarum* NB10 (A), *V. anguillarum* VIB 79 (B) and *Yersinia ruckeri* (C) on TCBS agar showing that *V. anguillarum* form characteristic yellow colonies on this agar compared to most non-*Vibrio* spp. that form green colonies on this agar.

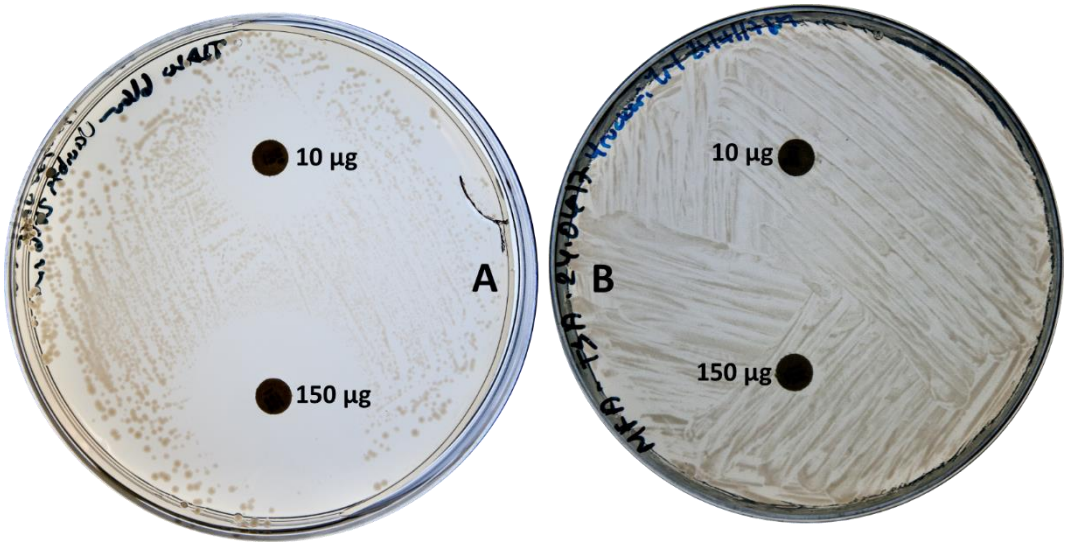

Figure 2.5. *V. anguillarum* VIB 79 (A) and *Y. ruckeri* YR1 (B) growth on TSA20 (*V. anguillarum*) and TSA (*Y. ruckeri*) agar with 10 µg and 150 µg of vibriostatic agent 0/129 discs which select for susceptible *Vibrio* spp.

caused agglutination, indicating this method is unable to distinguish *V. anguillarum* from *V. ordalii* isolates. As expected, none of the colonies causing a positive reaction for the test reagent subsequently caused the control reagent to agglutinate.

Primer pairs (van-ami8/van-ami417, rpoN1SMF/R, rpoN-ang5'/rpoN2SMR; Table 2.2) designed to amplify *V. anguillarum*-specific DNA sequences gave products of the expected sizes on agarose gels at each of the selected annealing temperatures (T_a) from template DNA extracted from four wild-type *V. anguillarum* isolates (M93Sm, VIB39, VIB 87 and NB10) (Figure 2.6). However, the product yielded using DNA from all *V. anguillarum* isolates was visibly reduced at the highest T_a when amplified with the van-ami8/van-ami417 and rpoN-ang5'/rpoN2SMR primer pairs. Visible bands of PCR product were produced from *V. ordalii* VIB 2 template DNA using each primer pair and T_a value tested. Only a single treatment failed to produce any detectable PCR product using *V. ordalii* VIB 307^T template DNA; primer pair rpoN-ang5' and rpoN2SMR at a T_a of 62°C. In contrast, only primer pair rpoN1SMF and rpoN1SMR at a single T_a of 51°C produced a visible PCR product using *V. ordalii* VIB 679 DNA template. As expected, the NTC reactions yielded no detectable PCR product. In conclusion, primer pair rpoN-ang5' and rpoN2SMR, using an annealing temperature of 62°C, was used in future work to distinguish between *V. anguillarum* and *V. ordalii* because both remaining primer sets produced more false positive products from *V. ordalii* DNA template.

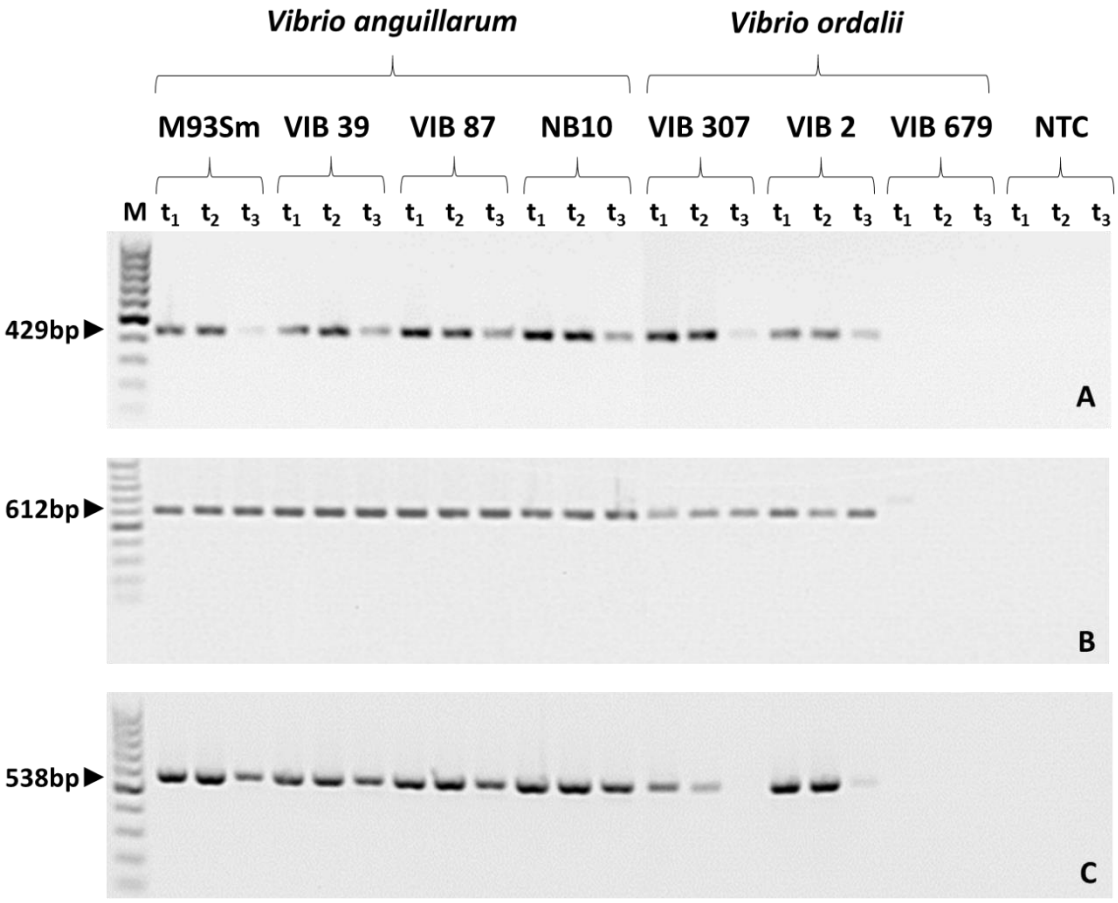

Figure 2.6. Agarose gel electrophoresis of PCR products generated from DNA extracted from four *Vibrio anguillarum* isolates (M93Sm, VIB 39, NB10 and VIB 87) and amplified using primers (A) van-ami8 and van-ami417, (B) rpoN1SMF and rpoN1SMR and (C) rpoN-ang5' and rpoN2SMR. Each template and a no template control (NTC) was added to PCR reactions performed at three different annealing temperatures (t_1, t_2 and t_3), as indicated in Table 2.3. Three *Vibrio ordalii* isolates (VIB 2, VIB 307^T and VIB 679) were included to investigate the ability of the primers pairs to discriminate these isolates from *V. anguillarum*. M, 100-bp DNA ladder.

2.3.4. *V. anguillarum* serotype O1 isolates carrying the pJM1-like virulence plasmid

To investigate which of twelve serotype O1 *Vibrio anguillarum* wild-type isolates carried the pJM1-like virulence plasmid two PCR assays were used to amplify products from primers targeting two separate genes (*angR* and *fatE*). These genes are located within the iron transport operon (ITBO; *angR*) and *trans*-acting factor (TAF; *fatE*) region on opposing sides of the p67-NB10 (pJM1-like) virulence plasmid of *V. anguillarum* NB10. DNA extracted from nine serotype O1 *V. anguillarum* isolates (VIB 1, VIB 39, VIB 44, VIB79, VIB 85, VIB 88, VIB 93 VIB 134 and NB10) revealed both products of the expected size (454 bp using primers fatESMF and fatESMR; 247 bp using primers angRSMF and angRSMR) on agarose gel suggesting they maintain a pJM1-like plasmid (Figure 2.7). This is particularly interesting regarding *V. anguillarum* VIB 88 as a previous study suggested that this isolate was plasmidless (Pedersen et al., 1997). Furthermore, DNA extracted from *V. anguillarum* VIB 64 generated a product, of the expected size, from primers specific for *angR* but not *fatE,* while in contrast DNA extracted from *V. anguillarum* VIB 87 generated a product, of the expected size, from primers specific for *fatE* but not *angR.* In both cases this is understandable as previous work has shown that *V. anguillarum* VIB 64 and *V. anguillarum* VIB 87 carry plasmids of 26 kbp and 53 kbp respectively instead of the 67 kbp approximate size indicative of pJM1-like plasmid (Pedersen et al., 1997). No products were amplified from

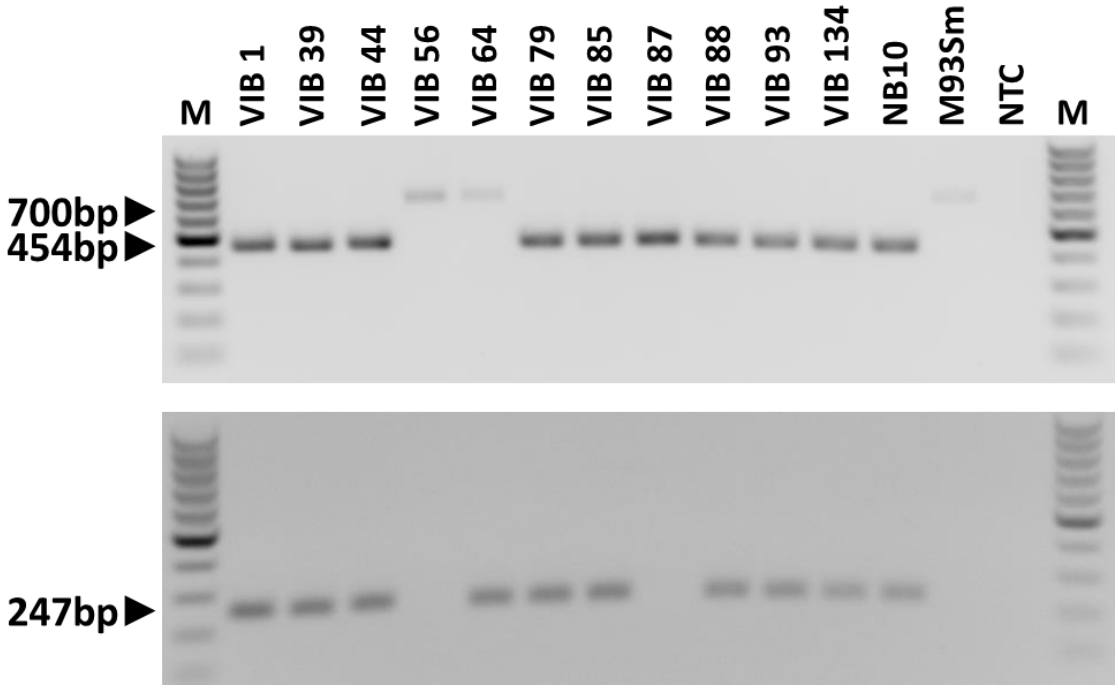

Figure 2.7. Agarose gel electrophoresis of PCR products generated from DNA extracted from eleven serotype O1 *Vibrio anguillarum* wild-type isolates (VIB 1, VIB 39, VIB 44, VIB 56, VIB 64, VIB 79, VIB 85, VIB 87, VIB 88, VIB 93, VIB 134 and NB10) and amplified using primers (A) fatESMF and fatESMR, (B) angRSMF and angRSMR. Both primer sets were used in PCR reactions at an annealing temperature of 56°C to amplify gene targets exclusive to the pJM1-like plasmid; carried by many serotype O1 *V. anguillarum* strains. A single plasmidless serotype J-O-1 *V. anguillarum* strain (M93Sm) was included as a negative control.
M, 100 bp DNA ladder.

DNA extracted from the final *V. anguillarum* serotype O1 isolate (VIB 56) in either assay despite previous work reporting that it carries a 67 kbp plasmid (Pedersen et al., 1997). Finally, DNA extracted from *V. anguillarum* VIB 56, *V. anguillarum* VIB 64 and plasmidless *V. anguillarum* serotype J-O-1 M93Sm isolates all produced bands for a single product at approximately 700 bp in assay targeting *fatE* (Figure 2.7) indicating amplification of a potential related gene. No further products were amplified in reactions containing either NTC or plasmidless *V. anguillarum* M93Sm.

2.3.5. Confirmation of *V. anguillarum* mutant genotypes

Each mutant *V. anguillarum* strain formed yellow colonies on TCBS agar, reacted positively in the MONO-AQUA latex agglutination test, and yielded PCR products of the expected size when amplified with the *V. anguillarum*-specific assay conditions (primers rpoN-ang5' and rpoN2SMR with a T_a of 62°C).

To verify that the *V. anguillarum* NB10 cured strain did not contain the p67-NB10 virulence plasmid, DNA was extracted from cells and a PCR performed to amplify sequences specific for sections of *angR* and *fatE* located on this plasmid. No bands corresponding to the expected sizes of *angR* and *fatE* sequences were visualised on agarose gels when DNA from the *V. anguillarum* NB10 cured strain was subjected to PCR, indicating that this isolate had been cured of the p67-NB10 virulence plasmid (Figure 2.8).

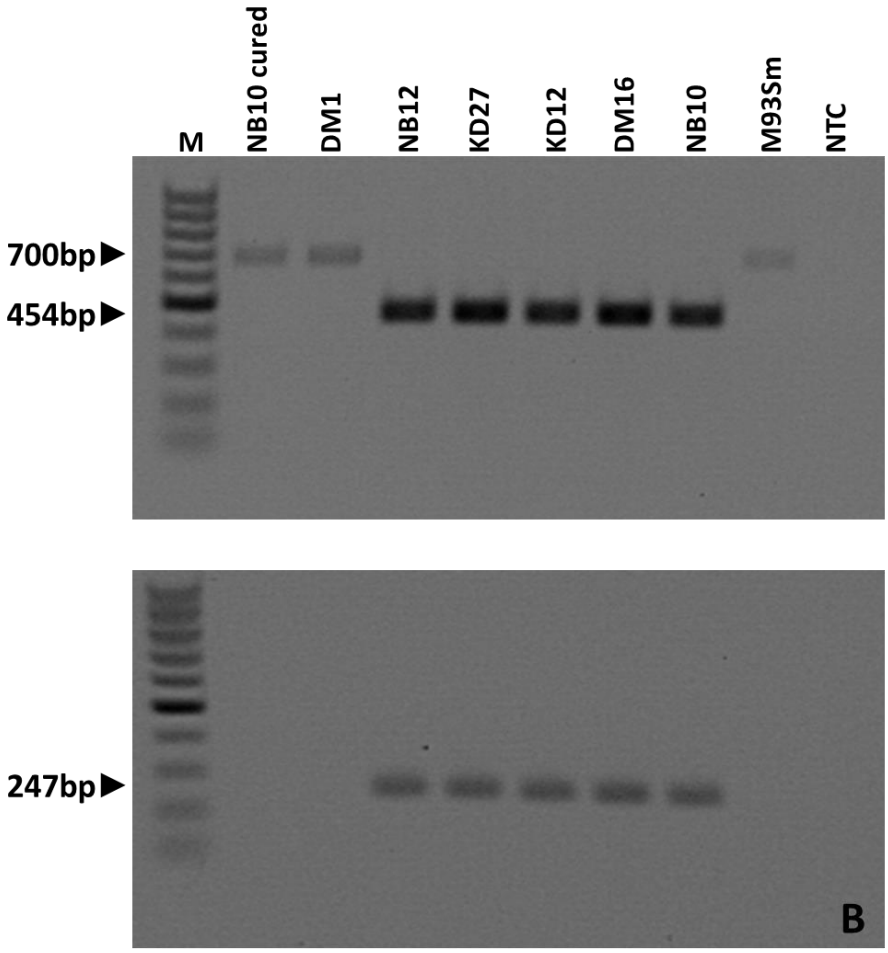

Figure 2.8 Agarose gel electrophoresis of PCR products generated from DNA extracted from six mutant serotype O1 *Vibrio anguillarum* wild-type isolates (NB10 cured, DM1, NB12, KD27, KD12 and DM16) and amplified using primers (A) fatESMF and fatESMR, (B) angRSMF and angRSMR. Both primer sets were used in PCR reactions at an annealing temperature of 56°C to amplify gene targets exclusive to the plasmid pNB10-67. Wild-type *V. anguillarum* (NB10) and plasmidless serotype J-O-1 *V. anguillarum* strain (M93Sm) were included as positive and negative control respectively. M, 100-bp DNA ladder.

Meanwhile, these PCR assays were repeated for DNA extracted from each of the other mutant strains and, with the exception of *V. anguillarum* DM1, all other strains generated PCR products of the expected sizes corresponding to partial sequences of *angR* and *fatE*, thus confirming the presence of the p67-NB10 plasmid (Figure 2.8). Positive control *V. anguillarum* NB10 generated products of the expected sizes for both plasmid target sequences, while the negative control and plasmidless *V. anguillarum* M93Sm yielded no detectable PCR products (Figure 2.8). However, *V. anguillarum* M93Sm, *V. anguillarum* NB10 cured and *V. anguillarum* DM1 all produced bands for a single product at approximately 700 bp, in assay targeting *fatE*, (Figure 2.8) indicating amplification of a potential related gene.

PCR products generated from DNA extracted from *V. anguillarum* mutants created by deletion within the target gene (KD12, KD27, DM16 and S183) all produced bands of smaller size than the respective parent strains, thus confirming deletions in the expected genes of each of the mutants (Figures 2.9). Furthermore, *V. anguillarum* mutants created by plasmid insertion (NB12, DM1, M99, JR1, S262, S123, and S183) yielded bands of expected sizes on agarose gels for the bespoke primer pairs designed for each strain, indicating that each strain still contained the insertion sequence at the expected location (Figure 2.10). Meanwhile, no PCR products were detected in each of the respective parent strains for any of these assays (Figure 2.10).

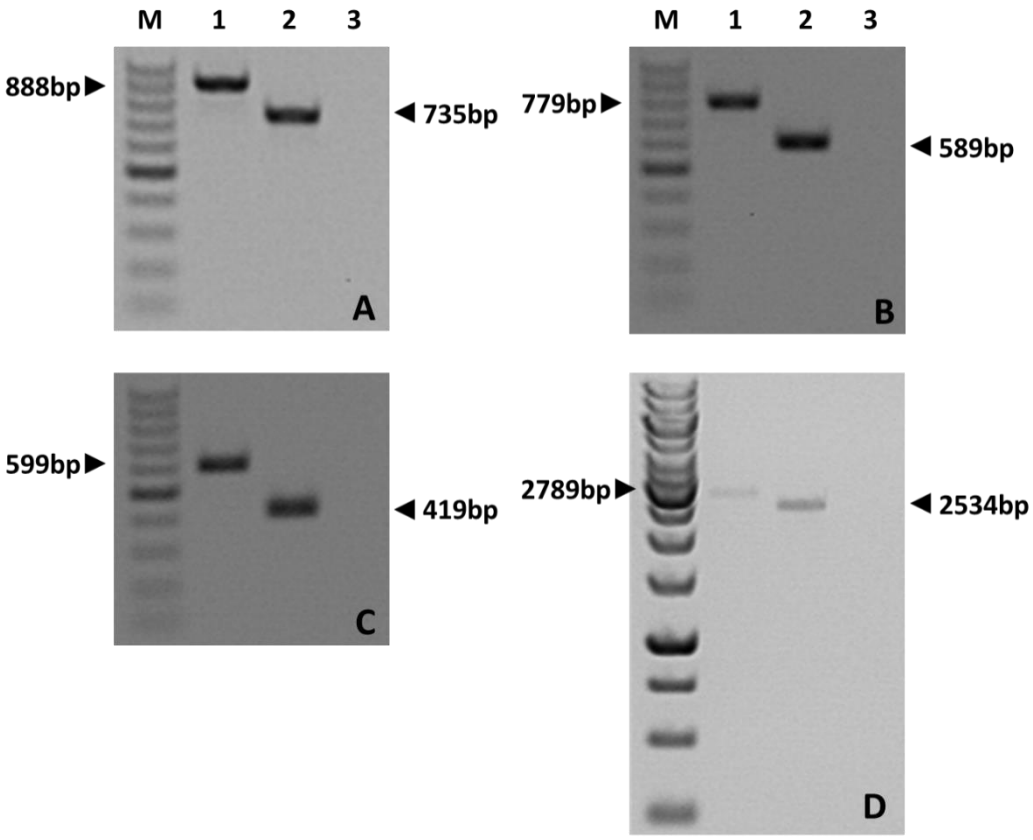

Figure 2.9. Agarose gel electrophoresis of *Vibrio anguillarum*, wild-type and mutant isolate, PCR products amplified from extracted DNA, to confirm deletions by allelic exchange. DM16 (A) Δ*flaA* mutation was confirmed using DM16flaASMF and DM16flaASMR primers at an annealing temperature of 57°C. KD27 (B) Δ*flaE* mutation was confirmed using KD27flaESMF and KD27flaESMR primers at an annealing temperature of 56°C. KD12 (C) Δ*flaD* mutation was confirmed using KD12flaDSMF and KD12flaDSMR at an annealing temperature of 57°C. S183 (D) *vah1* deletion was confirmed using primers vah1S183SMF and vah1S183SMF at an annealing temperature of 56°C. M, 100bp (A, B and C) or 1kb (D) DNA ladder; lane 1, wild-type NB10 (A, B and C) or M93sm (D); lane 2, DM16 (A), KD27 (B), KD12 (C) or S183 (D); lane 3, no template control.

2.4. Discussion

The aim of this chapter was to outline the general materials and methods used throughout this thesis and steps taken towards their improvement and optimisation. Previous studies that investigated Group A Streptococcus (GAS, *Streptococcus pyogenes*) infection of *G. mellonella* produced conflicting results (Loh et al., 2013; Olsen et al., 2011), potentially due to differing storage conditions and dietary circumstances. Changes to individual parameters, including storage temperature, feeding, storage time pre-challenge and handling, can alter infected larvae survival rates and immune function (Banville et al., 2012; Browne et al., 2015; Mowlds et al., 2008; Mowlds and Kavanagh, 2008). Results like these have driven some authors to argue for the introduction of global standard nutritional and storage parameters to facilitate inter-laboratory comparisons (Banville et al., 2012; Cook and McArthur, 2013; Desbois and McMillan, 2015; Junqueira, 2012). However, these steps cannot account for the source of the insects and transit conditions (Desbois and McMillan, 2015). In this present study, the virulence of wild-type *V. anguillarum* strains was assessed in *G. mellonella* at 15°C because the earlier *S. salar* trials were performed at this temperature (Pedersen et al., 1997), thus mitigating the effects of differential expression of temperature-regulated bacterial virulence factors.

V. anguillarum colonies grow yellow on TCBS agar, indicating acid production via sucrose fermentation (Balboa et al., 2012). However, a high frequency of non-*Vibrio* spp. can recover onto TCBS, which a recent study emphasised when reporting 39 % of growth was not from the target genus

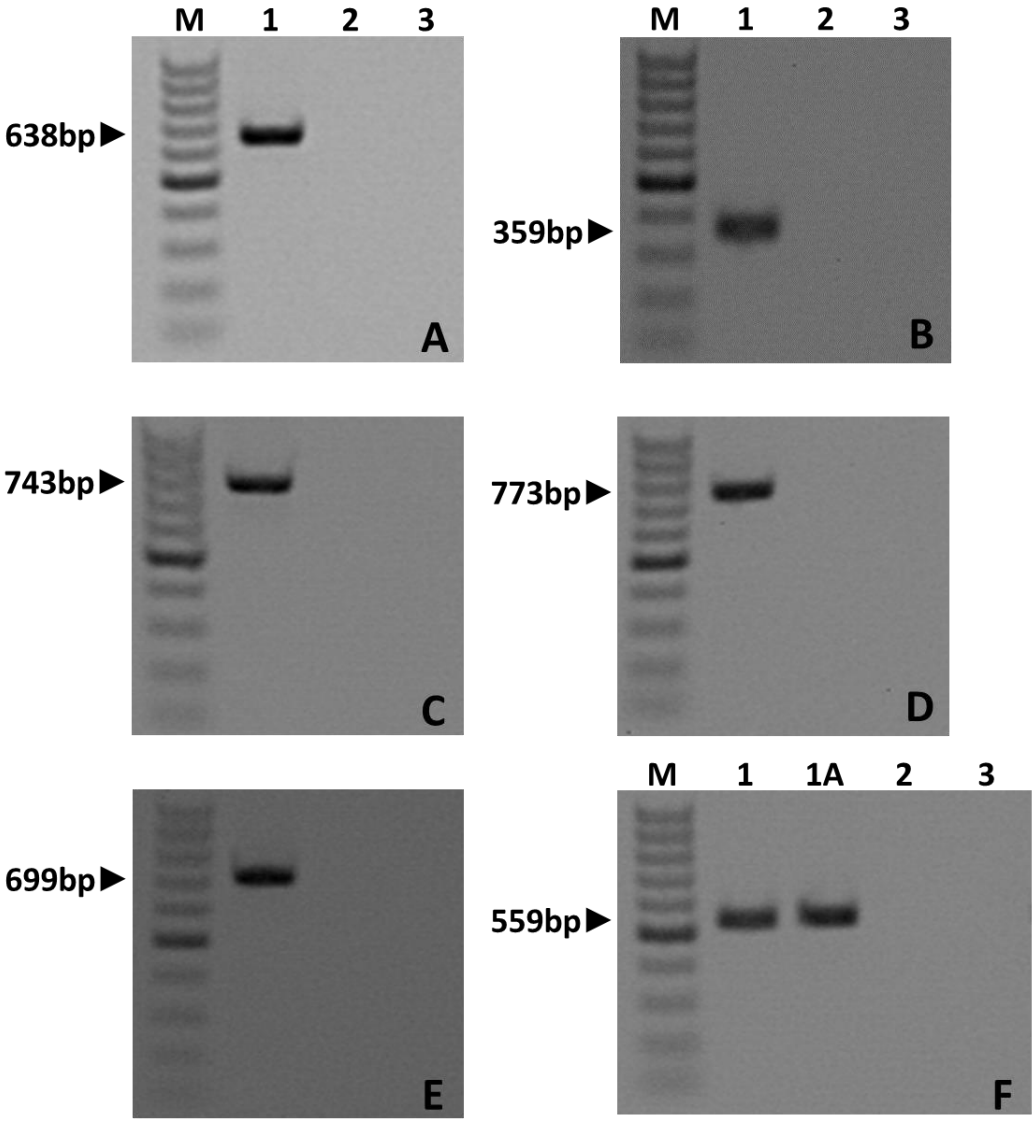
M 1 2 3
638bp
A
M 1 2 3
359bp
B
743bp
C
773bp
D
699bp
E
M 1 1A 2 3
559bp
F

Figure 2.10. Agarose gel electrophoresis of *Vibrio anguillarum*, wild-type and mutant isolate, PCR products amplified from extracted DNA, to confirm plasmid insertions into genes of interest. NB12 (A) Δ*empA* mutation was confirmed using primers NB12F and pNQ705-R at an annealing temperature of 52°C. DM1 (B) Δ*virC* mutation was confirmed using primers DM1F and pNQ705-R at an annealing temperature of 64°C. M99 (C) Δ*empA* mutation was confirmed using primers M99SMF and pNQ705-R at an annealing temperature of 61°C. JR1 (D) Δ*vah1* mutation was confirmed using primers vah1JR1SMF and pNQ705-R at an annealing temperature of 63°C. S262 (E) Δ*plp* mutation was confirmed using primers S262SMF and pNQ705-R at an annealing temperature of 64°C. S123 and S183 (F) Δ*rtxA* mutations were confirmed using primers rtxAflankF and pNQ705-R1 at an annealing temperature of 63°C.

M, 100bp DNA ladder; lane 1, NB12 (A), DM1 (B), M99 (C), JR1 (D), S262 (E) and S123 (F); lane 1A, S183 (F only); lane 2, wild-type NB10 (A and B) or M93Sm (C, D, E and F) negative controls; lane 3, no template control.

(Pfeffer and Oliver, 2003). One alternative to TCBS is *Vibrio anguillarum* medium (VAM) which contains ampicillin and a high salt content for selection; however, not all *V. anguillarum* isolates recover onto this agar and it is not commercially available (Alsina et al., 1994). Therefore, isolation on selective agar is only suitable as the first in a series of diagnostic tests before proceeding to the more reliable vibriostatic O/129 diagnostic test.

Neither method used to diagnose *V. anguillarum* to species level (commercial latex agglutination kit or PCR) was completely specific. First, the three *V. ordalii* isolates tested (VIB 2 and VIB 307^T and VIB 679) also agglutinated the MONO-AQUA test reagent, suggesting this method is unable to distinguish *V. anguillarum* from *V. ordalii* isolates despite a previous showing the type strain (VIB 307^T) testing negative (Romalde et al., 1995), and manufacturer recommendations that MONO-AQUA *V. anguillarum* latex agglutination reagent is specific for *V. anguillarum* serotypes O1, O2 and O3 only. However, perhaps this cross-reaction is unsurprising given that the three *V. ordalii* isolates used here have previously been classified as serotype O2a using the *V. anguillarum* serotyping system (Austin et al., 1997). Furthermore, positive MONO-AQUA agglutinates for *V. anguillarum* serotypes O3 to O10 have been reported previously (Romalde et al., 1995), suggesting that this assay may not be as specific as claimed.

Molecular identification of *V. anguillarum* by PCR amplification of specific DNA sequences is an established diagnostic technique that has been designed for many different gene targets, including the haemolysin *vah1* (Hirono et al., 1996), peptidoglycan hydrolase *amiB* (Hong et al., 2007) and cellular sigma factor σ^{54} *rpoN* (Gonzalez et al., 2003); however, these earlier studies only tested against a single *V. ordalii* isolate to demonstrate lack of cross-reactivity with this species. This present work assayed three primer sets, including *amiB* primers (Hong et al., 2007), and all yielded PCR products for at least one *V. ordalii* isolate, including for *V. ordalii* VIB 307^T under PCR conditions that produced a negative result previously (Hong et al., 2007), which may be due to differences in procedures, DNA quality and reagents. Therefore, none of the assays described can differentiate *V. anguillarum* from *V. ordalii* unequivocally. However, whole genome analysis has revealed many genes, including those encoding the biofilm-forming Syp system, are found in *V. ordalii* only and not in *V. anguillarum* (Naka et al., 2011). Thus, the Syp system would be an ideal candidate to include within a multiplex PCR to identify *V. anguillarum*, although the cluster is found in many other pathogenic *Vibrio* species (Naka et al., 2011) and additional controls would be required.

To detect the presence of a p67-NB10 plasmid in each *V. anguillarum* isolate (an important determinant of virulence in this species; Crosa, 1980), a PCR method was developed to amplify two sequences at distinct locations on the plasmid. The plasmid was not detected in *V. anguillarum* DM1, a Δ*virC* mutant, suggesting that this strain did not contain a p67-NB10

virulence plasmid (Figure 2.6). Thus, *V. anguillarum* DM1 was not used hereon, as changes in virulence compared to the parent that harbours the p67-NB10 virulence plasmid may be due to loss of this plasmid and not necessarily loss of a functional *virC*.

A final result of interest are the non-specific products generated from DNA of plasmidless isolates by primers designed for *fatE* located on p67-NB10 virulence plasmid (Figure 2.7 and Figure 2.8). The intensity of bands demonstrates that less product was amplified compared to the intended target sequence. This requires further investigation and may be linked to similar genes involved in iron acquisition found on chromosomal DNA. Furthermore, a 65% section of the chromosomal *fvtE* gene sequence was found to have 84% similarity with pJM1 plasmid encoded *fatE* (Naka et al., 2013b), both of which code for functional ATPase homologues for ferric-anguibactin transport. This strongly suggests that *fvtE* may be the non-specific product amplified in this assay and sequencing of this band would confirm this. Alternatively, the presence of pJM1-like plasmids could be confirmed by miniprep plasmid DNA extraction and running of products on agarose gel (Austin et al., 1995). This approach would have the additional advantage of producing complete plasmid profiles for all isolates, instead of merely the presence or absence of pJM1-like plasmids.

This chapter has examined standard techniques for *G. mellonella* challenge and the preparation and identification of bacteria to be used in this thesis. However, *V. anguillarum* diagnostic techniques have highlighted major

deficiencies in the specificity of current assays implying that a combination of multiple tests should be used to confidently identify *V. anguillarum* before more stringent tests are developed. Moving forward, the methods presented and developed in this chapter will be applied initially to evaluate whether *G. mellonella* larvae are a suitable alternative host to fish for studying the pathogenicity and virulence of *V. anguillarum*.

Chapter 3. Evaluation of *Galleria mellonella* as an alternative host for studying the pathogenicity and virulence of *Vibrio anguillarum*

3.1. Introduction

The aim of this chapter was to evaluate the larva of the greater wax moth, *Galleria mellonella*, as an alternative host to study pathogenicity and virulence of the fish pathogen, *Vibrio anguillarum*. New alternative hosts need to be validated for studying each particular pathogen to ensure that: an infection occurs and is dose dependent; infection can be rescued by an appropriate therapeutant if this is attainable in the native host; the infectious agent replicates within the host; virulence correlates with that observed in the native host, and; conserved virulence mechanisms are important during infection of alternative and native hosts.

To do this, initial investigations assessed whether *V. anguillarum* killed *G. mellonella* after injection into the insect and that the extent of killing occurred in a dose-dependent manner. Thereafter, it was important to check that live bacteria were necessary for killing *G. mellonella* by injecting heat-killed *V. anguillarum*, while antibiotic treatment of insects injected with an otherwise lethal inoculum would further confirm that live and replicating bacteria were required to cause death.

Subsequently, it was important to recover *V. anguillarum* from dead *G. mellonella* and confirm this as the causative agent. Examination of the bacterial burden data of different isolates during *G. mellonella* infection would elucidate whether discrepancies in virulence are related to the ability

of the pathogen to replicate *in vivo*. Prior to investigating the relationship between virulence and *V. anguillarum* burden in *G. mellonella*, an assessment of bacterial load in haemolymph and whole-body homogenate was required to determine where the bacteria aggregate within the insect. In this chapter, a number of strains with historical virulence data in fish (Pedersen et al., 1997) were used to challenge *G. mellonella* larvae, so to observe any differential virulence between strains and whether there is correlation between mortality in *G. mellonella* and Atlantic salmon.

Finally, to assess the importance of various virulence factors known to play a role in infection of native hosts, the virulence of isogenic mutant and parent strains was assessed within the *G. mellonella* host. Taken together these experiments aimed to characterize and validate the *G. mellonella* infection model for investigating *V. anguillarum* virulence. Moreover, this initial work will hopefully establish the strengths and limitations of this alternative host, which can be exploited when considering future research questions.

3.2. Materials and methods

3.2.1. Minimum inhibitory concentration (MIC) of antibiotics

To identify a suitable antibiotic to administer to infected *G. mellonella* larvae in an attempt to rescue them from a lethal dose of *V. anguillarum*, minimum inhibitory concentrations were determined for kanamycin (KAN), penicillin (PEN), streptomycin (STR)and tetracycline (TET) according to a method modified from the Clinical and Laboratory Standards Institute

(CLSI; Miller et al., 2014). Briefly, the wells in the last column of a flat-bottomed polystyrene 96-well microtitre plate (Sarstedt) were dispensed with 100 µL Mueller-Hinton broth (MHB; supplemented with 2% NaCl) containing antibiotic at double the greatest desired concentration for the assay. Two-fold dilutions were performed across the plate in fresh MHB (supplemented with 2% NaCl) and the final column contained just 100 µL MHB (no antibiotic control). Each *V. anguillarum* isolate to be tested was cultured, washed and diluted to 1 $\times 10^7$ CFU/mL according to Section 2.2.2, and then 5 µL of this bacterial suspension was added to each well of a row on the plate; bringing the final concentration in each well to approximately 5 $\times 10^5$ CFU/mL. An accurate estimate of CFU/mL in each inoculum suspension was determined by diluting and plating across TSA20 according to Section 2.2.2. Microtitre plates were incubated (24 h; 180 rpm; 22°C) and then examined for turbidity, by visually inspecting wells, which indicated bacterial growth. The MIC is the lowest concentration at which no turbidity is observed. To determine minimum bactericidal concentration (MBC), 10 µL of contents from each of the wells showing no visible growth were plated onto MHB (supplemented with 2% NaCl) and incubated (22°C, 48 h). Viable colonies were counted and the MBC is the minimum concentration of antibiotic at which 99.9 % of the inoculum is killed. The column containing broth lacking antibiotic confirmed that the isolate had grown. In addition, a row on each plate was incubated without bacterial incoculum to confirm the absence of any contaminants in the broth. All MIC and MBC determinations were run in duplicate for each strain.

3.2.2.1. Wild type challenge and correlation with virulence in *Salmo Salar*

The relative virulence of 11 wild-type *V. anguillarum* strains (VIB 1, VIB 39, VIB 44, VIB 56, VIB 64, VIB 79, VIB 85, VIB 87, VIB 88, VIB 93 and VIB 134; Table 1.1) that had been assessed for virulence in an earlier *Salmo salar* infection trial (Pedersen et al., 1997) was assessed in the *G. mellonella* alternative host. All isolates of *V. anguillarum* were grown, harvested and washed (according to Section 2.2.2), except that culture supernatant was retained and passed through a sterile polyethersulfone 0.22-µm filter (Millipore), to capture and remove any remaining cells. Cell suspensions were prepared in PBS at 1×10^5, 1×10^7 and 1×10^9 CFU/mL using the calibration curves determined in Section 2.3.1. For each *V. anguillarum* isolate, larvae in groups of ten were injected (according to Section 2.2.3) with each of the cell suspensions or sterile culture filtrate.

3.2.2.2. Heat-killed bacterial challenge

To assess whether inactivated *V. anguillarum* would be able to kill *G. mellonella*, bacterial suspensions were prepared and then heat-killed before injection into groups of ten larvae following Section 2.2.3.

To inactivate, *V. anguillarum* cultures were grown to stationary phase (20 h) then washed and adjusted to 5×10^9 CFU/mL with PBS following Section 2.2.2. Bacterial cultures were grown to stationary phase, as opposed to the exponential phase described in a previous method (Section 2.2.2), to increase the CFU concentration. Culture density was confirmed by plating onto TSA20 at 10^{-6} dilution. Three millilitres of each bacterial suspension

were put into sterile glass universal bottles and incubated in a water bath (60°C; 25 min), as these conditions were shown to successfully inactivate the cells (Appendix V). Heat killing of cells was confirmed by the absence of colonies forming after 100 µL of bacterial suspension was spread onto TSA20 agar and incubated at 22°C for 48 h. Furthermore, heat-killed bacterial suspensions were incubated during the experiments at the same temperature as the *G. mellonella* larvae, before plating again, as above, to confirm that reactivation did not occur over time.

3.2.2.3. Antibiotic rescue of infection

To confirm that antibiotic therapy could rescue larvae from lethal *V. anguillarum* infection, larvae were inoculated with 1×10^7 CFU and then treated sequentially at 2 h, 24 h and 48 h with tetracycline (TET: 1 µg/g of larva) in 10 µL PBS. An additional control group was assessed for TET toxicity.

3.2.3. *V. anguillarum* burden in *G. mellonella*

To determine whether the bacteria were replicating inside the haemolymph of *G. mellonella*, burden was assessed after infection with each of the 11 wild-type *V. anguillarum* isolates used in Section 3.2.2.1. Initially, a preliminary investigation with *V. anguillarum* VIB 79 compared the haemolymph and whole-body homogenate burden within *G. mellonella* at 24 h to reveal the locality of the majority of infective bacteria.

3.2.3.1 *V. anguillarum* burden in *G. mellonella* haemolymph

Groups of four *G. mellonella* larvae were injected with 1 ×10^5 CFU of *V. anguillarum* (according to Sections 2.2.2. and 2.2.3) and incubated at 15ºC. A control group of unmanipulated *G. mellonella* and a further group inoculated with sterile PBS were included in all burden experiments. Then at 2, 4, 8, 24, 48, 72, 96 and 120 h post-infection four surviving larvae, if available, were selected for bacterial load determination of haemolymph.

The last abdominal segment of each larva was removed with sterile scissors and the haemolymph (approximately 5 - 20 µL) was harvested into a well of a sterile 96-well plate by gently squeezing the body. Of this, 5 µL was serially diluted in PBS (1:10) and plated onto TSA20 supplemented with 2 µg/mL penicillin G as this antibiotic prevented the growth of occasional contaminants introduced from the larval surface and gut during sampling, but had no effect on colony formation by each of the *V. anguillarum* isolates tested here (Appendix VI). If four surviving animals were not available, in the group selected, the remaining larvae were selected from the next group, and so forth, until the correct number was collected. If a group contained more animals than required for sampling a black mark was drawn on the top of the petri dish which was then shaken, and the animal closest to this mark was used.

In addition to sampling surviving larvae, haemolymph from dead larvae inoculated with VIB 1, VIB 44, VIB 56, VIB 79 and VIB 85 was harvested at 48 h, while dead larvae inoculated with VIB 93 were sampled at 96 h, and

VIB 64 and VIB 88 were sampled at 120 h respectively (all dead larvae sampled were alive at the time point 24 h previous). Haemolymph was diluted and plated as described above. To assess potential contamination, control groups of four unmanipulated *G. mellonella* larvae and the same number inoculated with sterile PBS were processed in the same way, except that haemolymph was plated without dilution.

3.2.3.2.. *V. anguillarum* burden in *G. mellonella* tissue

A single group of four *G. mellonella* larvae were injected with 1×10^5 CFU of *V. anguillarum* VIB 79 (according to Sections 2.2.2. and 2.2.3.1) then incubated at 15°C for 24 h. Subsequent to collection and plating of haemolymph, as described above (Section 3.2.3.1), *G. mellonella* were homogenised individually in 500 µL PBS in screw cap microcentrifuge tube for 30 s, using a motorised sterile pestle (Pellet Pestle Motor; Kimble Chase, Rockwood, US). Homogenates (5 µL) were plated onto TSA20 + PEN[2] at 1:10 dilutions in PBS of 10^{-3} - 10^{-6}. The mass of PBS and each larva was used to calculate a ratio of larval tissue to PBS, in each sample, which was applied to produce approximate burden values of CFU/mL. To assess potential contamination, control groups of four unmanipulated *G. mellonella* larvae and the same number inoculated with sterile PBS were processed in the same way, except that homogenates were plated without dilution.

3.2.4 In vitro growth curve in 96-well plate

Growth curves were completed in a 96-well plate format to investigate whether *in vitro* replication of *V. anguillarum* correlated with the same isolate *in vivo*. The same 11 wild-type *V. anguillarum* isolates, used to quantify in vivo haemolymph burden (Section 3.2.3.), were cultured and washed as described in Section 2.2.2. and then re-suspended to approximately 1 $\times 10^8$ CFU/mL in TSB20 before 15 µL of corrected culture was added to 135 µL TSB20 in a colourless, flat-bottomed 96-well polystyrene microtitre plate (Sarstedt). Three wells were prepared for each isolate. A_{600} was recorded on a microplate reader (Synergy HT; Biotek, United States) after shaking (10 s, medium speed) before each read. Then plates were incubated (15°C; 170 rpm) and A_{600} readings collected at 11 h and then every hour until cultures reached stationary phase. This experiment was completed in triplicate.

3.2.5. Mutant challenge

To assess the importance of various virulence factors known to play a role in infection of native hosts, the virulence of isogenic mutant and parent strains (NB10 cured, NB12, M99, DM16, KD12, KD27 and parent strain NB10; M99,S123, JR1, S183, S262 and parent strain M93Sm; Table 2.1) was compared. With the exception of NB10 cured each pair of parent and knockout mutant had been tested for virulence in various fish models previously (Denkin and Nelson., 2004; Li et al., 2008; Li et al., 2013; McGee et al., 1996; Milton et al., 1992a; Milton et al., 1996; Rock and Nelson, 2006;

Weber et al., 2010). All virulence gene knockouts were located on the bacterial chromosomes. Challenge followed the same infection process as that of Section 3.2.2.1. except that only one treatment was used; an inoculum of approximately 1 $\times 10^7$ CFU/mL. Virulence of each mutant was compared to its parent.

3.2.6. Recovery and confirmation of *Vibrio anguillarum*.

3.2.6.1. Recovery of *Vibrio anguillarum* from infected *G. mellonella*.

Bacteria from *G. mellonella* larvae infected with wild-type and mutant isolates were recovered from haemolymph, as described in Section 3.2.3.1., onto TSA20 + PEN[2] then sub-cultured onto TCBS as described previously (Section 2.2.6) before confirmation as *V. anguillarum* by latex agglutination (Section 2.2.7.1.) and PCR and gel electrophoresis (Sections 2.2.5.3. and 2.2.5.4) using DNA extracted from recovered colonies (Section 2.2.5.1) and primers rpoN-ang5' and rpoN2SMR (Table 2.2) with an annealing temperature of 62°C.

3.2.7. Statistical analyses

Statistical tests were performed using SPSS v17.0 for Windows (SPSS Inc., Chicago, IL, USA). *G. mellonella* group survival was plotted according to the Kaplan-Meier method (Kaplan and Meier, 1958). Where desired, survival differences between groups of larvae were compared for significance with the logrank test (Mantel, 1966) and $p < 0.05$ was considered to indicate a

significant difference between two groups and multiple comparisons were accounted for by applying Holm's correction (Holm, 1979).

To investigate any relationship between virulence of the 11 wild-type *V. anguillarum* isolates in *S. salar* and *G. mellonella* models of infection relative virulence in the insect was calculated for each strain as the cumulative area under a Kaplan-Meier survival plot (Kaplan and Meier, 1958). These data were plotted against previous LD_{50} values of same strains challenged in Atlantic salmon (Pedersen et al., 1997) then the r^2 value, generated from the line of best fit, was used to determine Pearson's correlation coefficient (Pearson, 1895).

3.3. Results

3.3.1. Minimum inhibitory concentration (MIC) of antibiotics

To select a suitable antibiotic for rescuing *G. mellonella* from a lethal inoculum of *V. anguillarum*, the susceptibility of 11 wild-type *V. anguillarum* isolates were assayed against KAN, PEN, STR and TET (Table 3.1). Each *V. anguillarum* isolate was most susceptible to TET (MICs = 0.0125 - 0.025 μg/mL) than the other antibiotics tested (Table 3.1). Therefore, TET was selected to rescue larvae from lethal inoculums of *V. anguillarum*. Furthermore PEN was consistently the antibiotic to which all *V. anguillarum* isolates assayed were least susceptible (Table 3.1). Thus, PEN was selected for addition to TSA20 in *V. anguillarum* burden experiments, to minimise recovery of other contaminants from *G. mellonella*.

Table 3.1. Minimum inhibitory concentrations (MICs) and minimum bactericidal concentrations (MBCs) of 11 *Vibrio anguillarum* isolates to kanamycin (KAN), penicillin G (PEN), streptomycin (STR) and tetracycline (TET). Wells containing the four greatest antibiotic concentrations with no visible growth were plated to determine MBC and > indicates that less than 99.9% of the inoculum was killed in the well containing the greatest concentration of antibiotic plated. Assays were performed in duplicate and in the event of a differing result between replicates, it is the greater concentration that is given as the MIC and/or MBC.

Isolate	Kanamycin (KAN)		Penicillin (PEN)		Streptomycin (STR)		Tetracycline (TET)	
	MIC (µg/mL)	MBC (µg/mL)	MIC (µg/mL)	MBC (µg/mL)	MIC (µg/mL)	MBC (µg/mL)	MIC (µg/mL)	MBC (µg/mL)
VIB 1	16	64	32	128	8	> 64	0.13	4
VIB 39	32	64	64	128	16	64	0.13	> 4
VIB 44	16	64	64	> 128	16	64	0.13	4
VIB 56	128	128	64	128	16	32	0.25	> 4
VIB 64	32	128	64	> 128	16	> 128	0.25	> 4
VIB 79	16	64	64	> 128	16	64	0.25	2
VIB 85	16	64	64	> 128	16	> 128	0.25	> 4
VIB 87	8	64	64	> 128	16	32	0.25	> 4
VIB 88	16	32	64	128	16	> 128	0.25	> 4
VIB 93	8	32	64	128	16	32	0.25	> 4
VIB 134	16	64	64	> 128	16	128	0.25	> 4

3.3.2. *V. anguillarum* establishes an infection in *G. mellonella*.

To assess whether *G. mellonella* would be suitable for studying virulence of *V. anguillarum*, it was necessary to confirm that this bacterium established an infection in this insect. Initial challenge experiments with 11 wild-type 'VIB' isolates demonstrated that there was dose-dependent killing of the *G. mellonella* larvae for each isolate, meaning that greater inocula caused faster and greater mortality in groups (Figure 3.1).

3.3.3. Only viable *V. anguillarum* cells caused mortality of larvae.

Injection of larval groups with 5 x10^7 CFU heat-killed bacteria had no significant effect on survival during 120 h compared to PBS-only injected controls, and typically showed fewer deaths than groups challenged with the lowest dose of live bacteria (1 x10^3 CFU), suggesting that larval deaths were not occurring due to non-specific toxicity of bacterial cells, and viable bacteria were required to cause mortal events (Figure 3.1). Moreover, sterile culture filtrate from each isolate had no significant effect on larval survival, indicating that toxic extracellular metabolites were not being produced in vitro at sufficiently high concentrations to kill the larvae and further confirming viable bacteria were required to bring about death (Figure 3.1).

3.3.4. Antibiotic rescue of infection

For all strains, treatment of infected larvae with 1 µg/g TET significantly increased survival, compared to infected larvae treated with PBS only, and thus showing that larvae could be rescued from infection with an antibiotic

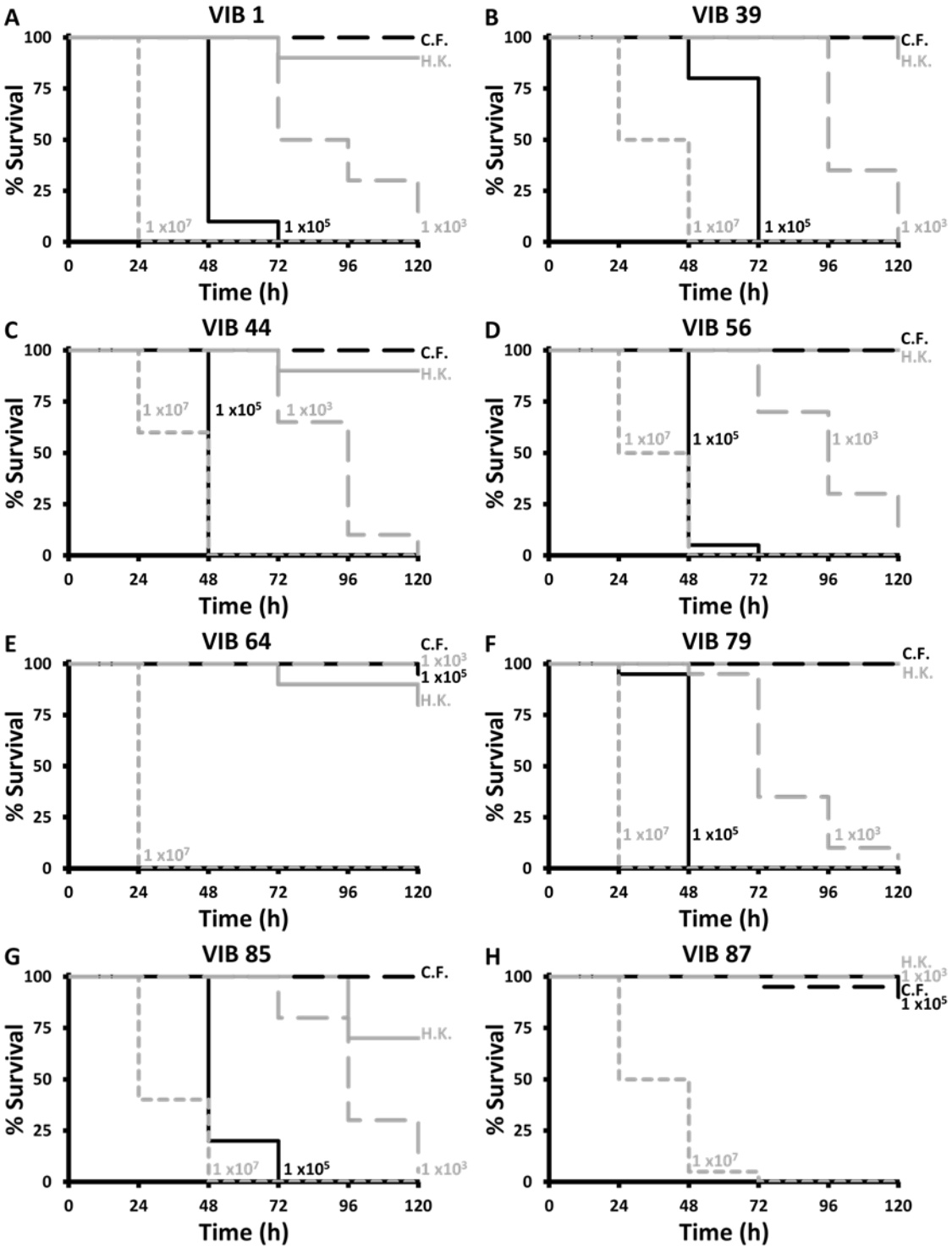
A
VIB 1
B
VIB 39
C
VIB 44
D
VIB 56
E
VIB 64
F
VIB 79
G
VIB 85
H
VIB 87
% Survival
Time (h)
C.F.
H.K.
1 x10^7
1 x10^5
1 x10^3

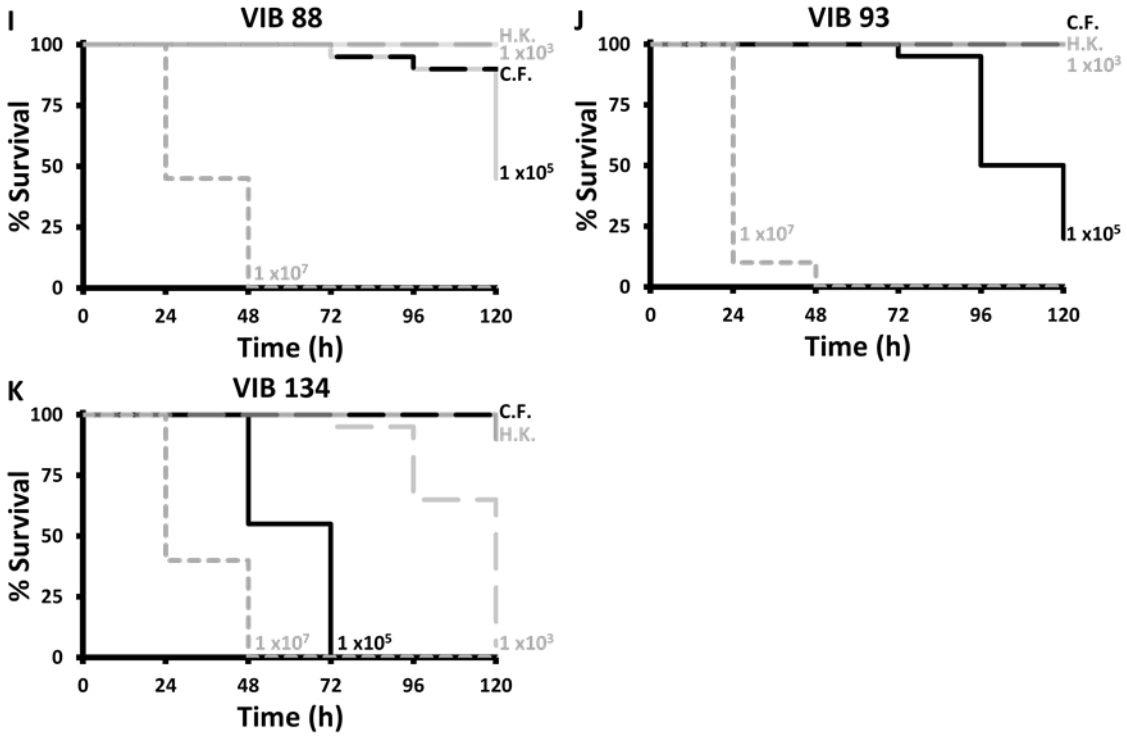

Figure 3.1. Survival of groups of *Galleria mellonella* larvae injected with culture filtrate (C.F.); 1 x10^3, 1 x10^5 and 1 x10^7 viable CFU; and 5 x10^7 heat-killed (H.K.) CFU of eleven wild-type *Vibrio anguillarum* isolates with different virulence during 120 h, namely VIB 1 (A), VIB 39 (B), VIB 44 (C), VIB 56 (D), VIB 64 (E), VIB 79 (F), VIB 85 (G), VIB 87 (H), VIB 88 (I), VIB 93 (J) and VIB 134 (K). For clarity, the unmanipulated and uninfected control groups data are not shown. n=20, except H.K. group where n=10.

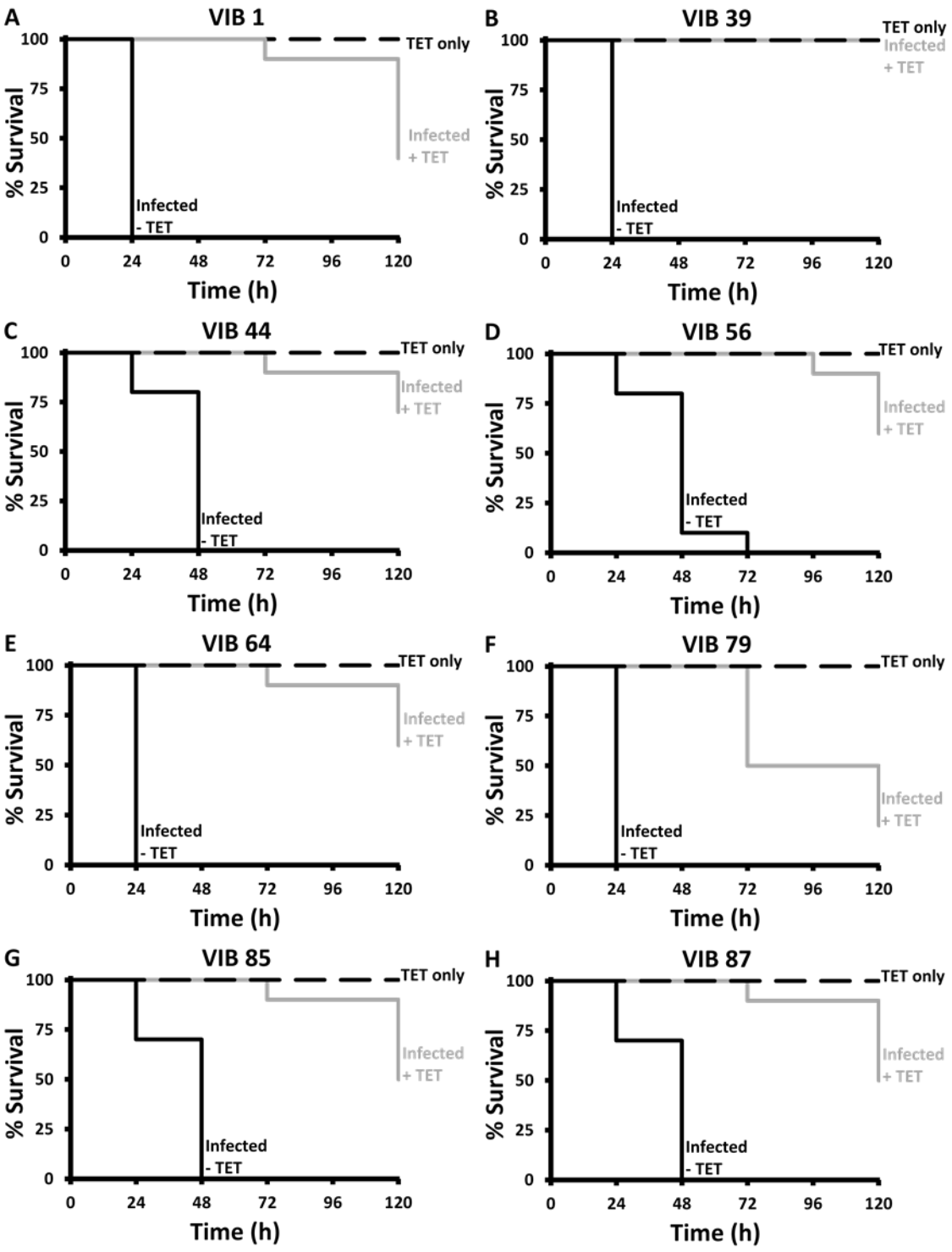
A
VIB 1
B
VIB 39
C
VIB 44
D
VIB 56
E
VIB 64
F
VIB 79
G
VIB 85
H
VIB 87
% Survival
Time (h)
TET only
Infected
+ TET
Infected
- TET
0
25
50
75
100
0
24
48
72
96
120

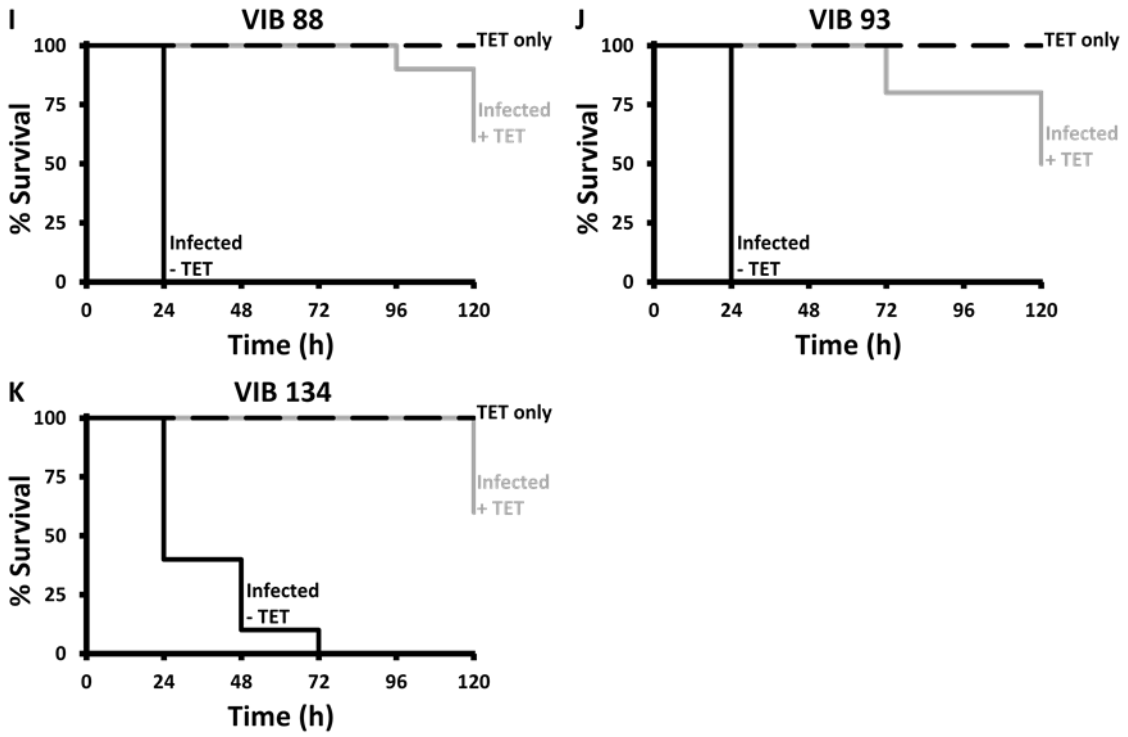

Figure 3.2. Survival of *Galleria mellonella* larvae injected with 1 x10^7 CFU of eleven wild-type *Vibrio anguillarum* isolates and treated at 2 h, 24 h and 48 h with tetracycline (1 µg/g of larva; Infected + TET) in 10 µL phosphate-buffered saline (PBS) over 120 hr: VIB 1 (A), VIB 39 (B), VIB 44 (C), VIB 56 (D), VIB 64 (E), VIB 79 (F), VIB 85 (G), VIB 87 (H), VIB 88 (I), VIB 93 (J) and VIB 134 (K). The infected control group was treated with PBS only (Infected - TET), while the TET only group controlled for the toxicity of the treatments. For clarity, the unmanipulated and uninfected control groups data are not shown. n=10.

that inhibited the growth of the bacterium (Figure 3.2). TET treatment of uninfected larvae had no significant effect on groups of larvae survival compared to PBS inoculated and unmanipulated control groups. (Figure 3.2).

3.3.5. Positive correlation in virulence of *V. anguillarum* isolates in *S. salar* and *G. mellonella* infection models.

The relative virulence of each isolate in *G. mellonella* was compared with virulence determined previously for each isolate in a *S. salar* infection model (Pedersen et al., 1997), and this confirmed a highly significant positive correlation (Pearson's correlation coefficient; $p < 0.01$) between relative virulence of the 11 wild-type isolates in *G. mellonella* larvae and fish models of infection, indicating that more virulent *V. anguillarum* strains in *S. salar* were also more virulent in the insect (Figure 3.3). Neither unmanipulated nor PBS inoculated controls had any significant effect on the survival of *G. mellonella* larvae.

3.3.6. Recovery of *Vibrio anguillarum* from infected *G. mellonella*.

Colonies recovered from *G. mellonella* larvae haemolymph infected with each of 11 *V. anguilarum* isolates were successfully subcultured onto TCBS, agglutinated using the MONO - *Va* reagent and produced PCR products of the expected size with primers rpoN-ang5' and rpoN2SMR, demonstrating that *V. anguillarum* survived within the larvae and was the likely causative agent of any infection.

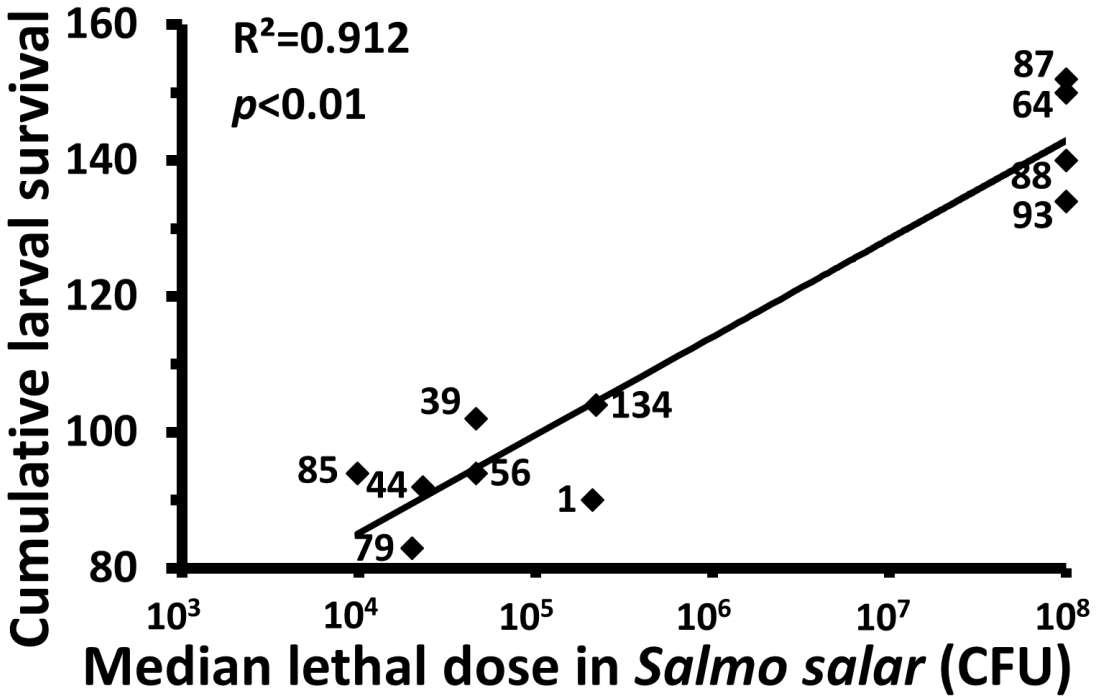

Figure 3.3. Pearson correlation of virulence of 11 wild-type serotype O1 *Vibrio anguillarum* isolates in the *Galleria mellonella* larva (calculated as cumulative larval survival) and in a *Salmo salar* infection model (median lethal doses determined after intraperitoneal injection by (Pedersen et al., 1997)). Median lethal doses for Vib64, Vib87, Vib88 and Vib93 were $>10^8$ CFU (the highest dose administered in the *S. salar* trials) but these have been plotted as 1 x10^8 CFU to allow for correlation. The number beside each point designates each 'VIB' isolate. n=11

Table 3.2. Burden of *V. anguillarum* viable colonies within infected *G. mellonella* presented as the ratio of colony forming units per mL (CFU/mL) recovered from haemolymph compared to whole body homogenate, of the same test animal, following homogenisation with a motorised pestle. Larvae were infected with 1×10^5 CFU of *V. anguillarum* VIB 79 and sampled 24 h post infection. Data shown are derived from the geometric average of 4 animals, with standard error, for each method.

Haemolymph (Log10 CFU/mL)	**Tissue (Log10 CFU/mL)**	**Ratio Haemolymph/tissue**
8.69 ± 0.20	7.79 ± 0.11	12.61 ± 5.36

3.3.7. *V. anguillarum* burden in haemolymph and tissue

Thirteen times more viable *V. anguillarum* VIB 79 colonies were recovered from haemolymph of infected *G. mellonella* larvae, compared to the tissue homogenised by motorised pestle (Table 3.2). This demonstrates that *V. anguillarum* cells are localised mainly within the intracellular haemolymph rather than the whole body homogenate. Taking these results into account bacterial burden was assayed from infected haemolymph, only, moving forward.

Assessment of the growth in the *G. mellonella* larva of the same 11 *V. anguillarum* wild-type isolates, that were investigated in Section 3.3.2., revealed that more virulent strains replicated faster and reached greater burden in the haemolymph than less virulent isolates (Figure 3.4). Indeed, within 48 h the more virulent isolates had increased to approximately 10^9–10^{10} CFU/mL in the larval haemolymph, whereas less virulent strains reached approximately 10^7-10^8 CFU/mL by this time (Figure 3.4). After 48 h it was not possible to obtain data for the more virulent strains as most larvae were dead, while the haemolymph burden of less virulent strains remained at approximately 10^7-10^8 CFU/mL for the duration of the experiment (Figure 3).

Additionally, mean bacterial burden in the haemolymph of dead larvae was determined and there was always greater than 5.72×10^9 CFU/mL (maximum 5.05×10^{10} CFU/mL) in these insects for the seven strains and

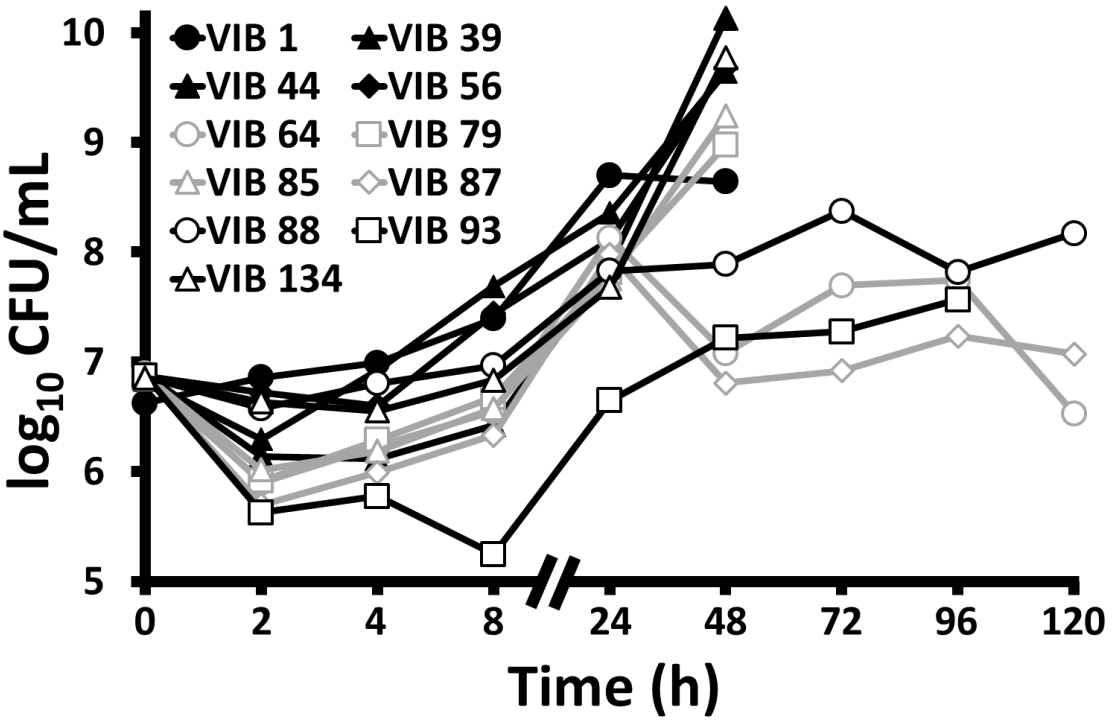

Figure 3.4. Replication of 11 wild-type *Vibrio anguillarum* isolates in the haemolymph of *Galleria mellonella* larvae during 120 h after injection at 0 h with 1 x10^5 CFU. Please note that the CFU/mL value at 0 h refers to the PBS inoculum whereas at the other sampling times the CFU/mL value refers to the haemolymph. It was not possible to obtain data for all strains at each sampling time after 48 h because most larvae were already dead and so were not sampled. Data points indicate geometric mean; n=4; For clarity, error bars have not been added.

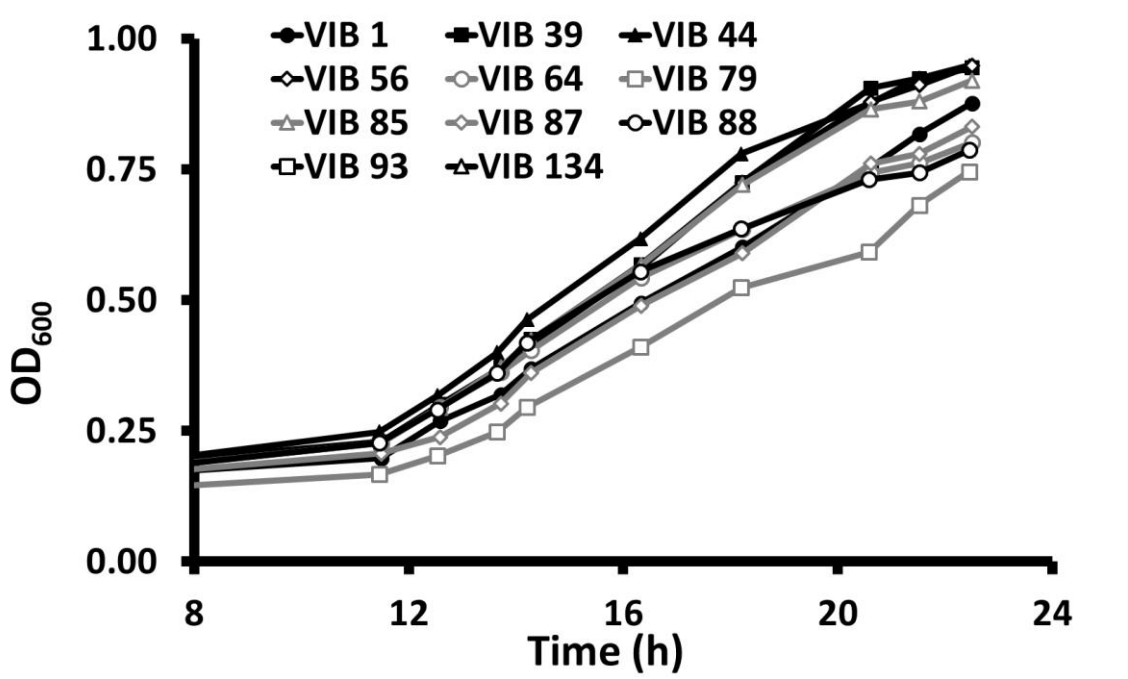

Figure 3.5. *In vitro* growth of 11 *Vibrio anguillarum* wild-type isolates in 96-well microtitre plates, measured as absorbance at 600nm (A_{600}) wavelength against incubation time. For clarity, error bars have not been added. n = 3.

times examined, indicating the likely breaching of a burden threshold before larval death ensued. Taken together with infection data, this evidence suggests that viable and replicating *V. anguillarum* cells are needed to establish a systemic infection of *G. mellonella*. To investigate whether the reduced growth of less virulent *V. angillarum* isolates was related to interactions with the *G. mellonella* host the same 11 *V. anguillarum* isolates were grown *in vitro*. Similar growth profiles were revealed for all 11 *V. anguillarum* isolates suggesting *G. mellonella* host mechanism slows or prevents replication of these strains (Figure 3.5).

3.3.8. Isogenic knockout Mutant challenge

To assess the role of various *V. anguillarum* virulence factors known to be important in fish infections, the virulence of pairs of parent strains and isogenic knockout mutant strains were compared in the larva model. First, the virulence of *V. anguillarum* NB10 was compared to a strain that had been cured of its virulence plasmid, pNB10-67, which encodes proteins involved in iron acquisition and transport and are known to play a crucial role in virulence of fish infections (Crosa et al., 1980; Weber et al., 2010). As expected, the strain cured of its virulence plasmid was significantly less virulent in the larva compared with the parent isolate (Table 3.3).

In *S. salar*, strains lacking the *rtxA* or *vah1* toxin genes are less virulent than their parent strains, and the reduced virulence of the Δ*rtxA* mutant was reflected in the larva model, though the Δ*vah1* mutant was equally as virulent as its parent (Table 3.3). A strain with inactivated haemolysin *plp*

Table 3.3. Comparison of virulence of *Vibrio anguillarum* parent and isogenic mutant strains lacking virulence factors in *Galleria mellonella* larva and fish models of infection. ↑, virulence of mutant greater than parent; ↓ virulence of mutant less than parent. In the larva model, the virulence change of the mutant compared to the parent was either not significant (n.s.) or significant ($p < 0.05$; Holm's corrected) using logrank test. n=20.

Knockout mutant	Parent	Inactivated/missing gene(s)	Gene function	Virulence change of mutant in fish	Virulence change of mutant in larvae	Reference
NB10 cured	NB10	Virulence plasmid (pJM1)	Iron-scavenging function	Not done	↓	Weber et al. (2010)
NB12	NB10	*empA*	Metalloprotease	↓ (*Oncorhynchus mykiss*)	↑	Milton et al. (1992)
M99	M93Sm	*empA*	Metalloprotease	n.s. (*S. salar*)	n.s.	Denkin and Nelson. (2004)
DM16	NB10	*flaA*	Flagellin protein	↓ (*O. mykiss*)	↑	Milton et al. (1996)
KD12	NB10	*flaD*	Flagellin protein	↓ (*O. mykiss*)	n.s.	McGee et al. (1996)
KD27	NB10	*flaE*	Flagellin protein	↓ (*O. mykiss*)	↑	McGee et al. (1996)
S123	M93Sm	*rtxA*	Repeat-in-toxin secreted toxin	↓ (*Salmo salar*)	↓	Li et al. (2008)
JR1	M93Sm	*vah1*	Secreted haemolysin	↓ (*S. salar*)	n.s.	Rock and Nelson. (2006)
S183	M93Sm	*rtxA* and *vah1*	Secreted toxin and haemolysin	↓ (*S. salar*)	↓	Li et al. (2008)
S262	M93Sm	*plp*	Secreted haemolysin	n.s. (*S. salar*)	n.s.	Li et al. (2013)

was not significantly attenuated in virulence in either fish or *G. mellonella* (Table 3.3). A double-knockout strain lacking both *rtxA* and *vah1* genes had attenuated virulence in the larva model, which confirmed earlier observations in fish (Table 3.3).

In fish, inactivation of *empA* (a metalloprotease possibly important for tissue invasion) in serotype O1 NB10 had reduced virulence, but this same mutant was more virulent compared to its parent strain in the larva model (Table 3.3). An Δ*empA* mutant in J-O-1 serotype M93Sm resulted in no change in virulence compared to its parent, which supported observations in fish. Finally, *V. anguillarum* strains lacking functional *flaA*, *flaD*, and *flaE* genes, which are necessary for flagella assembly and aid in adherence and colonisation of fish, show reduced virulence in fish, but these mutants did not show lower virulence in the larva compared with their respective parents (Table 3.2).

3.4. Discussion

Alternative infection models are becoming more important as experimentation on vertebrates becomes increasingly regulated, but few alternative infection models are available to study pathogens of animals produced in aquaculture. Hence, this present chapter aimed to validate *G. mellonella* as an alternative model to investigate the virulence of *V. anguillarum*, a key aquaculture pathogen that infects many species and reduces farm productivity (Austin et al., 1995; Frans et al., 2011; Paillard et al., 2004).

V. anguillarum was shown to establish systemic infections in *G. mellonella* larvae: the bacterium killed the larvae in a dose-dependent manner and replicated *in vivo*, while antibiotics rescued the insect from lethal bacterial inoculums. Virulence of all wild-type *V. anguillarum* isolates was assessed in *G. mellonella* at 15°C because the earlier *S. salar* trials (Pedersen et al., 1997) were performed at this temperature, thus mitigating the effects of differential expression of temperature-regulated bacterial virulence factors. Importantly, there was significant positive correlation between virulence of different wild-type *V. anguillarum* isolates in *S. salar* (native) and *G. mellonella* (alternative) infection models. *V. anguillarum* isolates with greater virulence replicated to a greater extent inside the insect haemolymph to bring about faster larval mortality than less virulent isolates, presumably by more effectively combating the innate immune defences to exploit the host.

Very few significant positive correlations between virulence in vertebrate hosts and *G. mellonella* have been published (Brennan et al., 2002; Jander et al., 2000; Olsen et al., 2011) despite the obvious validation benefits, possibly due to the undesirable number of animals required. To further reduce experimental vertebrate requirements, Jander et al. (2000) and Olsen et al. (2011) used previously published virulence data to generate a correlation. This approach was used successfully in this chapter, meaning that no fish were required for this present study. However long-term storage of isolates can lead to possible genotypic and phenotypic changes (Prakash et al., 2013), and this factor warrants consideration when

interpreting results. One alternative is a correlation comparing virulence in *G. mellonella* and cytopathology in cell culture simultaneously. This approach has been used to investigate virulence of *P. aeruginosa* using the HeLa cell line (Miyata et al., 2003); however, it doesn't account for numerous interactions which can only be studied within an *in vivo* system.

The data generated in this present study showed that certain virulence determinants were similarly important during fish and insect infections, including the pJM1-like virulence plasmid p67-NB10 (Crosa et al., 1980; Weber et al., 2010) and rtxA (a secreted toxin) (Li et al., 2008); however, some discrepancies were observed for the role of other virulence factors in the models, which is perhaps unsurprising given the physiological differences between the organisms. Indeed, some knockout strains were actually more virulent than the parent such as the NB12 Δ*empA* strain. However, Milton et al. (1992) first demonstrated a role in virulence for empA in *Oncorhynchus mykiss* infection, but a subsequent study with the Δ*empA* mutant prepared from a different *V. anguillarum* isolate was unable to confirm a role in virulence for this protein in *S. salar* when bacteria were introduced by intraperitoneal injection (Denkin and Nelson, 2004); a discrepancy that may be due to the use of different host species (Denkin and Nelson, 2004). However, the M99 Δ*empA* mutant was also no less virulent than its parent in this study (Denkin and Nelson, 2004). Different mechanisms of *V. anguillarum* EmpA post translational modification have been identified (Staroscik et al., 2005; Varina et al., 2008) with components of this system also possessing metalloprotease activity (Mo et al., 2010).

Therefore, it is possible that these systems may be involved in the differential virulence of *empA* knockout isolates in this and other studies (Denkin and Nelson, 2004).

The Δ*flaA* and Δ*flaE* flagellum mutants were also more virulent than parent strains in the larva compared with fish. In *V. anguillarum* infections of fish, flagella act in host attachment and dissemination (McGee et al., 1996; Ormonde et al., 2000) but, given the size of the larva and subversion of requirement for attachment due to direct injection into the haemolymph, these organelles may not be required for successful exploitation of the larva. Moreover, by knocking out flagellum protein genes, metabolic resources might be redirected to other virulence mechanisms that are more important during larva infection. The inability to evaluate the role of attachment and entry virulence factors, which are vital for infection (Weber et al., 2010), may at first seem to be a limitation of the *G. mellonella* model, and indeed it is, however many studies in fish and aquatic invertebrates also rely solely on injecting inocula through the external surface to establish an infection (Amparyup et al., 2009; Huang et al., 2010; Li et al., 2008; Pedersen et al., 1997; Wang et al., 2010). An additional consideration that might explain the differences observed between fish and larva models is that various fish models were used to confirm the role of a virulence factor and thus direct comparison to the larva may be considered inappropriate as we do not know the relative importance for these factors in different fish species (Table 3.3). In addition, a recent study of the mammalian pathogen *Candida albicans* in *G. mellonella* also found disparity in the importance of distinct virulence

factors in different hosts (Amorim-Vaz et al., 2015a). These findings do not prevent *G. mellonella* from being useful in virulence studies of *V. anguillarum*, but it does mean that caution is required when extrapolating results or using this model to investigate a specific virulence factor. Therefore, additional work may be needed to identify which particular virulence traits can be studied in this model.

In this chapter, the alternative host *G. mellonella* has been validated for the study of *V. anguillarum* and, importantly, demonstrated that some virulence mechanisms are conserved between native fish hosts and the insect. Furthermore, this insect has been established as an inexpensive and practical alternative host for challenge experiments comprising many experimental groups. Therefore, *G. mellonella* is an ideal host for a large-scale screen of virulence of *V. anguillarum* strains, such as mutants generated by random transposon mutagenesis.

Chapter 4. Identification of genes required for virulence in *Vibrio anguillarum* using transposon mutagenesis.

4.1. Introduction

The aim of this chapter was to prepare a library of random transposon insertion mutants of *Vibrio anguillarum* and screen these strains for attenuated virulence in the *Galleria mellonella* infection model. This would provide a means to further validate this alternative host as suitable for studying known *V. anguillarum* virulence factors, while also assessing its possible application to the discovery of novel virulence genes. Moreover, this initial screen of transposon insertion mutants has not been completed previously for any bacterial pathogen in the *G. mellonella* host and the full workflow (Figure 4.1) may be adapted and optimised for use with other important pathogens.

Random transposon mutagenesis has been used to study the genes responsible for various phenotypes of *V. anguillarum*, including iron transport, chemotaxis and O-antigen biosynthesis (Norqvist and Wolfwatz, 1993; O'Toole et al., 1996; Stork et al., 2004; Stork et al., 2007b; Tolmasky et al., 1988; Welch and Crosa, 2005). Furthermore, rainbow trout (*Oncorhynchus mykiss*) has been used previously as host to screen a *V. anguillarum* random transposon insertion library of 200 strains for attenuated virulence *in vivo*, which were evaluated subsequently as possible

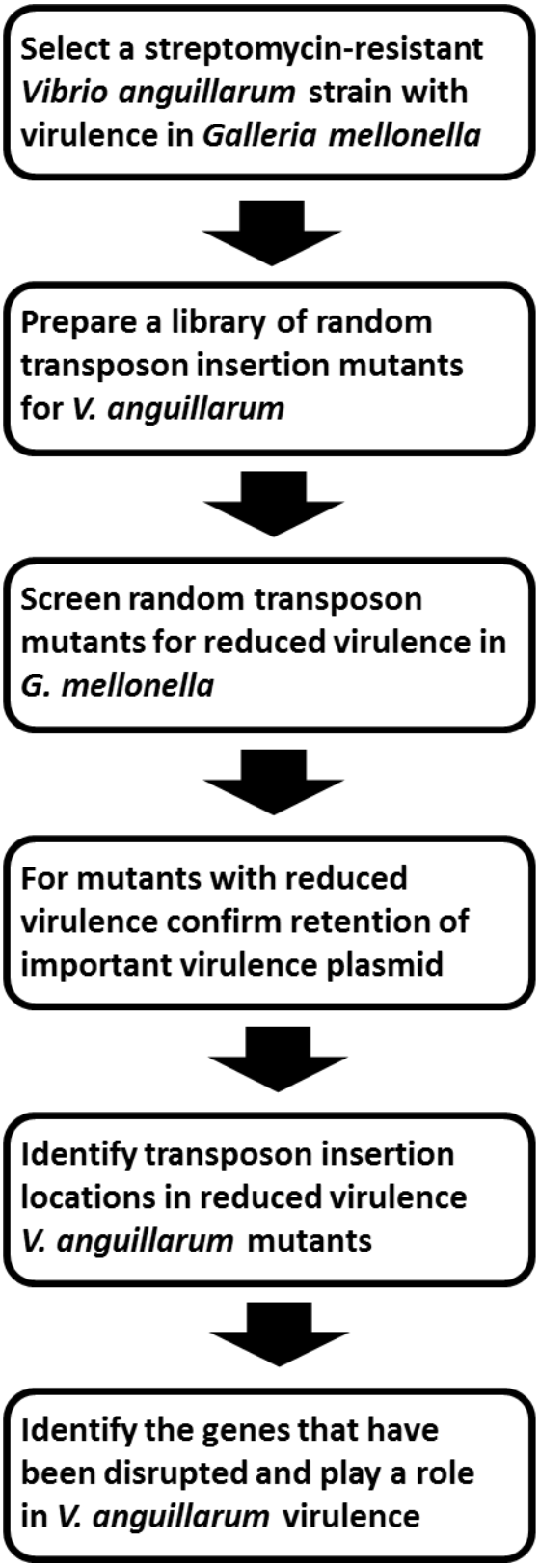

Figure 4.1. Workflow schematic illustrating the different stages required to complete a random transposon insertion mutant screen for *Vibrio anguillarum*.

targets for vaccine development (Norqvist et al., 1989). However, a screen of this nature remains logistically very challenging in fish and would require serious ethical consideration, but in *G. mellonella* this approach is practically achievable and ethically far more acceptable. The transposon mutagenesis system selected for this present study relies on a *mariner* transposon element, which inserts into DNA at TA dinucleotide recognition sequences (Tellier et al., 2015). *Mariner* elements are part of the IS630-Tc1-*mariner* (ITm) family of transposons found in most eukaryotic genomes, and these are all defined by a transposase gene that is bordered by a pair of terminal inverted repeats (Tellier et al., 2015). The transposon TnSC189 used in this present study was constructed with a selectable kanamycin-resistance marker flanked by FLP recombinase sites that was inserted into a *Himar1 mariner* element (Chiang and Rubin, 2002). This transposon was selected for its antibiotic resistance phenotype, compared to the recipient *V. anguillarum* NB10Sm strain. Furthermore, TA sites are relatively evenly distributed throughout most bacterial genomes and thus this system generates transposon insertion libraries with relatively random and even distribution throughout the genome (Chiang and Rubin, 2002; Robertson, 1995).

To generate a library of *V. anguillarum* random transposon mutants, the transposon was delivered to recipient *V. anguillarum* NB10Sm cells by *E. coli* SM10*λpir* donor cells that harbour the pSC189 mobilisable plasmid, which contains the *Himar1 mariner*-based TnSC189 transposon and the

hyperactive C9 transposase (Chiang and Rubin, 2002; Lampe et al., 1999). However, existing methods (Chiang and Rubin, 2002) had to be modified and optimised to successfully mutagenize *V. anguillarum* with TnSC189. First, an *E. coli* SM10λpir strain was cured of its pSC189 plasmid to produce a negative control for mating experiments. Second, before transposon mating experiments could begin, the *V. anguillarum* recipient isolate required an antibiotic resistance marker to select against the *E. coli* SM10λpir donor strain and therefore a spontaneous streptomycin-resistant (STR^r) *V. anguillarum* mutant was selected and characterised for virulence.

Transformed cells were selected on agar containing streptomycin (STR) and kanamycin (KAN) to select against donor cells and recipient cells that lack the TnSC189 transposon respectively, as TnSC189 carries a kanamycin-resistance cassette (Chiang and Rubin, 2002).

Once the random transposon library was generated, each mutant strain had to be assessed for virulence in the *G. mellonella* host and compared to the virulence of the wild-type parent. Mutants with attenuated virulence in this preliminary screen were re-tested to confirm the reduced virulence phenotype. The presence of the pJM1 like p67-NB10 virulence plasmid had to be confirmed in the reduced-virulence mutants, as absence of this genetic element abolishes virulence of *V. anguillarum* in *G. mellonella* (McMillan et al., 2015; Table 3.3). Furthermore, the transposon mutants had to be assessed for the absence of both the lysogenic Mu bacteriophage and the pSC189 plasmid back bone. The Mu bacteriophage is an additional genetic

element that can transfer from the chromosome of *E. coli* SM10*λpir* (pSC189) during mating and insert into the recipient cell DNA at a location different to the transposon, thereby potentially disrupting the function of another gene, which may also underlie a reduction in virulence by the strain (Ferrieres et al., 2010). Moreover, the conditionally replicative pSC189 plasmid is a member of the RK6 suicide plasmid family (Chiang and Rubin, 2002), where the plasmid can be carried by strains but it cannot replicate in the absence of the *pir*-encoded II protein, which is maintained in *trans* by the *E. coli* SM10λ*pir* donor (Ferrieres et al., 2010). Thus, the plasmid backbone is lost following recombination of the transposon into the DNA of the recipient cell.

Then, the locations of the transposon insertion in each reduced-virulence mutant were determined by amplification of the transposon-host DNA junction by arbitrary polymerase chain reaction (PCR) and comparison of the sequence with published *V. anguillarum* genomic sequence data (Holm et al., 2015). The location of the transposon insertion allows for determination of the disrupted gene in each mutant. Finally, strains with transposon insertions into putative novel virulence factor genes were investigated further through characterisation of *in vitro* phenotype differences compared to the parent strain, in an attempt to assist in efforts to determine the function of the disrupted gene.

4.2 Materials and Methods

4.2.1. Strains and plasmids

Additional isolates and plasmids (Table 4.1) were recovered and propagated according to the methods described in Section 2.2.2. Calibration and growth curves were determined for *E. coli* SM10*λpir* (pSC189) and *V. anguillarum* NB10Sm according to Sections 2.2.4 and Appendix III.

4.2.2. Susceptibility of test strains to antibiotics

Donor *E. coli* SM10λ*pir* (pSC189) [Chiang and Rubin, 2002] can be selected by ampicillin-resistant (AMP^r) and kanamycin-resistant (KAN^r) marker genes on the pSC189 plasmid (Chiang and Rubin, 2002) or a further KAN^r gene in the genomic DNA (Simon et al., 1983). The KAN^r marker on the pSC189 plasmid is transferred to the *V. anguillarum* host at the same time as the transposon. However, a suitable concentration of these antibiotics must be determined to ensure that wild-type *V. anguillarum* do not isolate onto media containing AMP or KAN. Furthermore, it is desirable that a spontaneous STR^r *V. anguillarum* mutant will be the recipient isolate for the TnSC189 transposon because *E. coli* SM10λpir (pSC189) is expected to be susceptible to STR, on account of neither strain or plasmid carrying a cassette conferring resistance to this antibiotic. However, susceptibility to STR had to be determined to confirm this as a suitable counter-selection strategy.

Minimum inhibitory concentration (MIC) and minimum bactericidal concentration (MBC) determinations were performed according to Section 3.2.1., except that MIC and MBC incubation conditions were altered (37°C, 24 h) for *E. coli* SM10λpir (pSC189) and *E. coli* TOP10, to reflect the optimal growth temperature for these isolates, and both were incubated using media not supplemented with NaCl. All assays were performed in duplicate.

To confirm AMP-resistant *E. coli* SM10*λpir* (pSC189) was suitable for mating with *V. anguillarum,* AMP MICs were established for virulent wild-type *V. anguillarum*. Furthermore, an AMP MIC, with maximum antibiotic concentration of 512 μg/mL, was determined for *E. coli* SM10*λpir* (pSC189) to evaluate whether an increase in AMP could be used to isolate this strain in the event that *V. anguillarum* had a degree of resistance to AMP.. To examine the suitability of STR to counter-select against the transposon donor strain, the MIC was established for *V. anguillarum* NB10 and *E. coli* SM10*λpir* (pSC189) with a maximum STR concentration of 512 μg/mL.

To investigate whether KAN concentration in transformant selection agar could be increased to a level preventing the growth of spontaneous *E. coli* SM10*λpir* (pSC189) mutants, MIC was performed against this strain. Moreover, *V. anguillarum* NB10 and *V. anguillarum* NB10Sm were examined in this assay to assess whether STR spontaneous mutation had increased resistance to KAN. To determine the MIC increase of recipient strains, after integration of TnSC189 transposon, a single *E. coli* transposon

Table 4.1. Bacterial isolates and plasmids used in Chapter 4.

Isolate or plasmid name	Characteristic(s)	Serotype	Culture medium[ab] or Donor	Source or Reference
Isolates				
Vibrio anguillarum				
Lab collection, University of Stirling, UK				
NB10Sm	Spontaneous streptomycin resistant derivative of NB10	O1	TSA20/TSB20 + STR^{200}	This study
VIB 1.1Sm	Spontaneous streptomycin resistant derivative of VIB 1	O1	TSA20/TSB20 + STR^{200}	This study
VIB 1.2Sm	Spontaneous streptomycin resistant derivative of VIB 1	O1	TSA20/TSB20 + STR^{200}	This study
VIB 1.3Sm	Spontaneous streptomycin resistant derivative of VIB 1	O1	TSA20/TSB20 + STR^{200}	This study
VIB 1.4Sm	Spontaneous streptomycin resistant derivative of VIB 1	O1	TSA20/TSB20 + STR^{200}	This study
VIB 1.5Sm	Spontaneous streptomycin resistant derivative of VIB 1	O1	TSA20/TSB20 + STR^{200}	This study
VIB 39Sm	Spontaneous streptomycin resistant derivative of VIB 39	O1	TSA20/TSB20 + STR^{200}	This study
VIB 44.1Sm	Spontaneous streptomycin resistant derivative of VIB 44	O1	TSA20/TSB20 + STR^{200}	This study
VIB 44.2Sm	Spontaneous streptomycin resistant derivative of VIB 44	O1	TSA20/TSB20 + STR^{200}	This study
VIB 44.3Sm	Spontaneous streptomycin resistant derivative of VIB 44	O1	TSA20/TSB20 + STR^{200}	This study
VIB 44.4Sm	Spontaneous streptomycin resistant derivative of VIB 44	O1	TSA20/TSB20 + STR^{200}	This study
VIB 44.5Sm	Spontaneous streptomycin resistant derivative of VIB 44	O1	TSA20/TSB20 + STR^{200}	This study
VIB 56.1Sm	Spontaneous streptomycin resistant derivative of VIB 56	O1	TSA20/TSB20 + STR^{200}	This study
VIB 56.2Sm	Spontaneous streptomycin resistant derivative of VIB 56	O1	TSA20/TSB20 + STR^{200}	This study
VIB 56.3Sm	Spontaneous streptomycin resistant derivative of VIB 56	O1	TSA20/TSB20 + STR^{100}	This study
VIB 56.4Sm	Spontaneous streptomycin resistant derivative of VIB 56	O1	TSA20/TSB20 + STR^{200}	This study
VIB 56.5Sm	Spontaneous streptomycin resistant derivative of VIB 56	O1	TSA20/TSB20 + STR^{100}	This study
VIB 79.1Sm	Spontaneous streptomycin resistant derivative of VIB 79	O1	TSA20/TSB20 + STR^{100}	This study
VIB 79.2Sm	Spontaneous streptomycin resistant derivative of VIB 79	O1	TSA20/TSB20 + STR^{100}	This study
VIB 79.3Sm	Spontaneous streptomycin resistant derivative of VIB 79	O1	TSA20/TSB20 + STR^{100}	This study
VIB 79.4Sm	Spontaneous streptomycin resistant derivative of VIB 79	O1	TSA20/TSB20 + STR^{100}	This study
VIB 79.5Sm	Spontaneous streptomycin resistant derivative of VIB 79	O1	TSA20/TSB20 + STR^{100}	This study

VIB 85.1Sm	Spontaneous streptomycin resistant derivative of VIB 85	O1	TSA20/TSB20 + STR^{200}	This study
VIB 85.2Sm	Spontaneous streptomycin resistant derivative of VIB 85	O1	TSA20/TSB20 + STR^{200}	This study
VIB 85.3Sm	Spontaneous streptomycin resistant derivative of VIB 85	O1	TSA20/TSB20 + STR^{200}	This study
VIB 85.4Sm	Spontaneous streptomycin resistant derivative of VIB 85	O1	TSA20/TSB20 + STR^{200}	This study
VIB 85.5Sm	Spontaneous streptomycin resistant derivative of VIB 85	O1	TSA20/TSB20 + STR^{200}	This study
VIB 134.1Sm	Spontaneous streptomycin resistant derivative of VIB 134	O1	TSA20/TSB20 + STR^{200}	This study
VIB 134.3Sm	Spontaneous streptomycin resistant derivative of VIB 134	O1	TSA20/TSB20 + STR^{200}	This study
NB10.4Sm	Spontaneous streptomycin resistant derivative of NB10	O1	TSA20/TSB20 + STR^{200}	This study
NB10.5Sm	Spontaneous streptomycin resistant derivative of NB10	O1	TSA20/TSB20 + STR^{200}	This study
Tn1- Tn350	NB10Sm derivatives with random TnSC189 insert within chromosomes or p67-NB10	O1	TSA20/TSB20 + STR^{100} + KAN^{100}	This study

Escherichia coli

Matthew K Waldor, Department of Microbiology and Immunobiology, Harvard Medical School, Boston, US

SM10λ*pir*	Standard plasmid for transfer of RK4 plasmids. Contains the *pir* gene (lysogenised with λ*pir* phage). KAN^R, *thi-1, thr, leu, tonA, lacY, supE, recA*::RP4-2-Tc::Mu, *pir.*	-	LBA + KAN^{100}	Simon et al., (1983)

Lab collection, University of Stirling, UK

TOP10	F'[*lacI*^{q} Tn10(tet^R)] *mcrA* Δ(*mrr-hsdRMS-mcrBC*) φ80*lacZ*ΔM15 ΔlacX74 *deoR nupG recA1 araD139* Δ(*ara-leu*)7697 *galU galK rpsL*(STR^r) *endA1* λ$^-$	-	LBA + STR^{100}	Invitrogen
TOP10Tn1-9	TOP10 derivative with random TnSC189 insert within genomic DNA	-	LBA + STR^{100} + KAN^{30}	This study

Plasmids

Matthew K Waldor, Department of Microbiology and Immunobiology, Harvard Medical School, Boston, US

pSC189	Cloning vector bearing the *mariner* transposon; R6K *ori*; AMP^r and KAM^R	SM10λ*pir*	Chiang and Rubin. (2002)

a TSA20, tryptone soya agar + 1.5 % NaCl; TSB20, tryptone soya broth + 1.5 % NaCl; LBA (20), Miller lysogeny agar (+ 1 % NaCl); LB (20) Miller lysogeny broth (+ 1 % NaCl).

b Concentrations of AMP, CHL, KAN and STR were added to medium at the concentrations (μg/mL) in superscript.

mutant isolate (*E. coli* TOP10Tn) and the *E. coli* TOP10 parent were also included.

4.2.3. Curing *E. coli* SM10λ*pir* of plasmid SC189

E. coli SM10*λpir* (pSC189) was grown overnight in Miller lysogeny broth (40°C, 150 rpm) with no antibiotic with the aim to select for strains lacking the plasmid. Ten-fold culture dilutions were prepared in phosphate-buffered saline (PBS) and for each concentration 40 µL was spread onto each of four LBA plates. Plates were incubated (37°C, 24 h) before colony numbers were enumerated, and then 100 distinct colonies were selected from Miller lysogeny agar (LBA) plates, and each streaked onto LBA + AMP200 and LBA + KAN100 before incubation (37°C, 24 h). E. coli TOP10 was streaked onto all plates as a negative control.

Colonies that failed to recover onto LBA + AMP^{200} were presumed to be cured of the pSC189 plasmid. These were picked individually from growth on LBA + KAN^{100} for DNA extraction following a previous method (Section 2.2.5.1), before confirmation of plasmid loss by PCR to amplify a *bla* gene fragment, as described in Section 4.2.7.2.

4.2.4. Generation and screening of *V. anguillarum* streptomycin-resistant mutants

4.2.4.1. Generation of *V. anguillarum* streptomycin-resistant mutants

To create a marker in *V. anguillarum*, for counter-selection of donor strain *E. coli* SM10*λpir* during conjugation experiments, spontaneous STR^r

mutants were selected on media containing STR. Cultures of virulent *V. anguillarum* serotype O1 isolates VIB 1, VIB 39, VIB 44, VIB 56, VIB 79, VIB 85, VIB 134 and NB10 (Table 2.1) were cultured, washed and suspended in 5 mL of PBS as described previously (Section 2.2.2). Absorbances (A_{600}) of cell suspensions were recorded and then 10 µL of each was plated in quadruplicate onto appropriate media, at 10^{-6} dilution in PBS, to enumerate input. Then, 3mL of each cell suspension was centrifuged (2600 ×*g*; 15 minutes; 4°C) and the pellet suspended in 100 µL PBS, which was then spread evenly across tryptone soya agar + 1.5 % NaCl (TSA20) + STR^{100}. The number of spontaneous mutant colony forming units (CFU), that formed following incubation (22°C, 72 h), was divided by input CFU to generate an estimate of mutation frequency.

Where available, five spontaneous mutants representing each isolate were selected and sub-cultured onto fresh TSA20 + STR^{100}. Single colonies from each newly sub-cultured isolate were patched onto TSA20 + STR^{200} and Thiosulphate-citrate-bile salts-sucrose agar (TCBS) plates. Henceforth isolates were recovered and grown in 100 or 200 µg /mL STR depending on their capacity to grow in this antibiotic. All isolates were grown in broth with the appropriate concentration of antibiotic and stored in cryotubes at -70°C in duplicate according to Section 2.2.2.

4.2.4.2. Spontaneous mutant challenge in wax moth

To identify any change in virulence of the spontaneous STR^r mutants, these strains were compared to wild-type parents in the *G. mellonella* host.

Briefly, 10^5 CFU of bacterial inoculums (prepared according to Section 2.2.2) were injected into groups of ten *G. mellonella* and survival assessed over 120 h according to Section 2.2.3. This experiment was performed only once, per mutant, except for *V. anguillarum* NB10 and the spontaneous STR^r mutant *V. anguillarum* NB10Sm whereby the trial was repeated; because this isolate (NB10Sm) was selected for transposon mating experiments. Inoculum sizes were confirmed by diluting and plating across agar according to Section 2.2.2.

4.3.4.3. *In vitro* growth of *V. anguillarum* NB10Sm

Growth curves (determined according to Appendix III) were prepared to investigate changes in replication rate between the spontaneous STR^r mutant *V. anguillarum* NB10Sm and the *V. anguillarum* NB10 parent.

4.2.5. Generation and validation of a *V. anguillarum* NB10Sm random transposon insertion mutant library

The *E. coli* SM10λ*pir* (pSC189) transposon delivery system was validated by mating with *E. coli* TOP10, and this confirmed that the pSC189 plasmid was able to transfer between these strains (Appendix VII). The donor *E. coli* SM10λ*pir* (pSC189) strain, the plasmidless *E. coli* SM10λ*pir* control donor strain and the *V. anguillarum* NB10Sm recipient cells were incubated (*E. coli*: 37°C, 150 rpm, 10 h; *V. anguillarum*: 22°C, 150 rpm, 18 h) to early stationary phase in 20 mL of appropriate broth (Table 4.1). Input CFU/mL for donor and recipient cultures were enumerated by plating at 10^{-5} and 10^{-6} onto LBA + AMP^{200} and TSA20 + STR^{200}, respectively. A suspension of

approximately equal CFU of donor and recipient cells (12 mL of donor and 3 mL of recipient culture) was prepared and then harvested by centrifugation (2600 ×*g*; 15 minutes; 4°C) before re-suspension in 1 mL PBS. Then, 100 µL of bacterial suspension was pipetted onto a 0.22-µm cellulose nitrate filter (Sartorius UK Ltd; Epsom, UK.) that had been placed on to the surface of an LBA20 agar plate, and this was repeated for a further nine filters and agar plates. In addition, a negative control was prepared with 6 mL of *E. coli* SM10λ*pir* and 1.5 mL of *V. anguillarum* NB10Sm cultures that were harvested by centrifugation (2600 ×*g*; 15 minutes; 4°C) and suspended in 500 µL of PBS, before 100 µL of bacterial suspension was pipetted onto each of four 0.22-µm cellulose nitrate filters (Sartorius) placed on the surface of separate LBA20 plates. All plates were incubated (30°C, 24 h; unsealed). This incubation temperature was selected because it is approximately equidistant between optimal growth temperature of *V. anguillarum* (22°C) and *E. coli* (37°C).

After incubation, the filters that had been inoculated with recipient and donor cells were transferred to 6 mL tryptone soya broth + 1.5 % NaCl (TSB20) and mixed by vortex for 30 s to resuspend the cells. Then 100 µL aliquots of this suspension and a single 10-fold dilution in PBS were plated onto each of ten TSA20 + KAN^{250} + STR^{200} agar plates. Bacterial suspensions were further diluted in PBS and plated onto LBA + AMP^{200} and TSA20 STR^{200}. Filters from the negative control mating were transferred to 3 mL of TSB20 and mixed by vortex for 30 s, and then plated onto TSA20 + KAN^{250} + STR^{200} in duplicate. All plates were incubated at 22°C, except LBA

plates that were incubated at 37°C. Transposition frequency was calculated as the ratio of CFU recovered on KAN^r + STR^r to STR^r agar from plated output cell suspensions. This experiment was performed in duplicate.

A total of 350 colonies were isolated onto fresh TSA20 + KAN^{250} + STR^{200} using sterile wooden cocktail sticks. DNA was extracted from 50 colonies selected at random (according to Section 2.2.5.1) and used to confirm the presence of the transposon as described in Section 4.2.7.

4.2.6. Individual transposon mutant challenge

4.2.6.1 Preparation of mutant inoculums for virulence assessment in *G. mellonella*

Next, the 350 transposon mutants were screened for attenuated virulence in *G. mellonella*. For this, inoculums were prepared in batches of 24 which consisted of a single wild-type parent *V. anguillarum* NB10Sm and 23 transposon insertion mutants derived from NB10Sm. For this, each *V. anguillarum* NB10Sm parent and transposon insertion mutant was inoculated into 1 mL of TSB20 + STR^{100} or TSB20 + KAN^{100} + STR^{100}, respectively, in separate wells of a polystyrene 24-well plate (Sarstedt AG and Co; Nümbrecht, Germany) using a sterile wooden cocktail stick. The plate was incubated (22°C, 230 rpm, 12–16 h) before the A_{600} of each well was determined with a Synergy HT microplate reader (Biotek UK; Swindon, UK.) after 10 s of agitation at medium speed. A_{600} was used to determine the volume of culture required to prepare an inoculum for each isolate at 1×10^9 CFU/mL in a fresh 24-well plate using the equation $y = (((7.64 \times 10^9)$

× x) – (2.65 ×10^9)); where y is the desired inoculum (1× 10^9) and x is A_{600} of the culture in the well. This equation was derived empirically using the method described in Section 2.2.4, except that cultures were grown in polystyrene 24-well plates (Sarstedt) and read with a microplate reader (Biotek) following 10 s of agitation at medium speed.

Cultures were diluted to ca. 1× 10^9 in TSB20 + STR^{100} (*V. anguillarum* NB10Sm parent) or TSB20 + KAN^{100} + STR^{100} (each transposon insertion mutant), A_{600} was recorded again, and then each suspension was diluted 1:100 in PBS to ca. 10^7 CFU/mL. For the first inoculum plate, all inoculums prepared were diluted in PBS and plated onto TSB20 + STR^{100} (*V. anguillarum* NB10Sm parent) or TSB20 + KAN^{100} + STR^{100} (transposon mutants) to provide an estimate for actual CFU/mL, but thereafter only one transposon insertion mutant (selected using a random number generator, https://www.random.org/) and the parent strain from each plate was diluted in PBS and plated on agar for colony enumeration. Meanwhile, 700 µL of each bacterial suspension at 1x 10^9 CFU/mL was added to 300 µL of 50% glycerol in separate wells of a sterile polypropylene 2.2-mL 96-well plate (Megablock®; Sarstedt). These plates were sealed with paraffin film (surface sterilised with 70% ethanol) and stored at -70°C so they could be recovered if required.

4.2.6.2 Assessment of virulence in *G. mellonella*

Each transposon insertion mutant was assessed for virulence in the *G. mellonella* model and compared to the virulence of the parent strain to

identify mutants with attenuated virulence. Briefly, ca. 1x 10^5 CFU of each strain was prepared in 10 µL PBS as described previously (Section 2.2.2), and this was injected into *G. mellonella* according to Section 2.2.3.1. Each transposon insertion mutant strain and the parent were injected into eight larvae. A control group injected with PBS only was prepared for each 24-well plate, while an 'unmanipulated' control group was also set up. Larvae were incubated for 5 days at 15°C and group survival was recorded every 24 h according to Section 2.2.3.1.

Transposon insertion mutants with significantly attenuated virulence (logrank test) compared to the *V. anguillarum* NB10Sm parent on the same plate were re-evaluated subsequently for virulence to confirm the observation. To do this, the strains were recovered from storage at -70°C and tested for virulence using a different batch of larvae.

4.2.7. PCR validation of *V. anguillarum* transposon mutants.

DNA was extracted according to Section 2.2.5.1 and all PCR reactions completed as described in Section 2.2.5.3. Approximate sizes of PCR products were assessed by gel electrophoresis according to Section 2.2.5.4. First, to confirm that isolated colonies were *V. anguillarum,* primers rpoN-ang5' and rpoN2SMR were used, following a previous method (Section 2.2.5.3), with the *V. anguillarum* NB10Sm parent as the positive and *V. ordalii* VIB 679 as the negative controls, respectively. Then, PCRs were completed to confirm that *V. anguillarum* NB10Sm transposon insertion mutants had incorporated the TnSC189 transposon into the host DNA and

retained their p67-NB10 virulence plasmid, while not replicating the plasmid pSC189 backbone and accepting any unwanted *Mu* transposition. These assays are illustrated in Figure 4.2.

4.2.7.1 Transposon integration into genomic DNA

To investigate whether suspected transposon insertion of *V. anguillarum* NB10Sm had incorporated TnSC189 into their genomic DNA, primers TnSC189F/R (Table 4.2) were used at an annealing temperature of 57°C, to amplify a TnSC189-specific sequence. *V. anguillarum* NB10Sm and *E. coli* SM10 *λpir* (pSC189 were used as positive and negative control respectively.

4.2.7.2. Loss of pSC189 plasmid backbone

To assess whether *E. coli* SM10*λpir* was cured of this plasmid and that the plasmid pSC189 backbone had been lost from all transformants, primers pSC189*bla*F/R (Table 4.2) were used, at an annealing temperature of 57°C, to amplify a section of the *bla* gene that encodes for the antibiotic resistance marker ß-lactamase on the plasmid backbone. *E. coli* SM10 *λpir* (pSC189) and *V. anguillarum* NB10Sm DNA were used as positive and negative controls respectively.

4.2.7.3. Retention of p67-NB10 virulence plasmid

Next, it was confirmed that each *V. anguillarum* transposon insertion mutant had retained the p67-NB10 virulence plasmid according to a previous method (Section 2.2.8). DNA extracted from the *V. anguillarum*

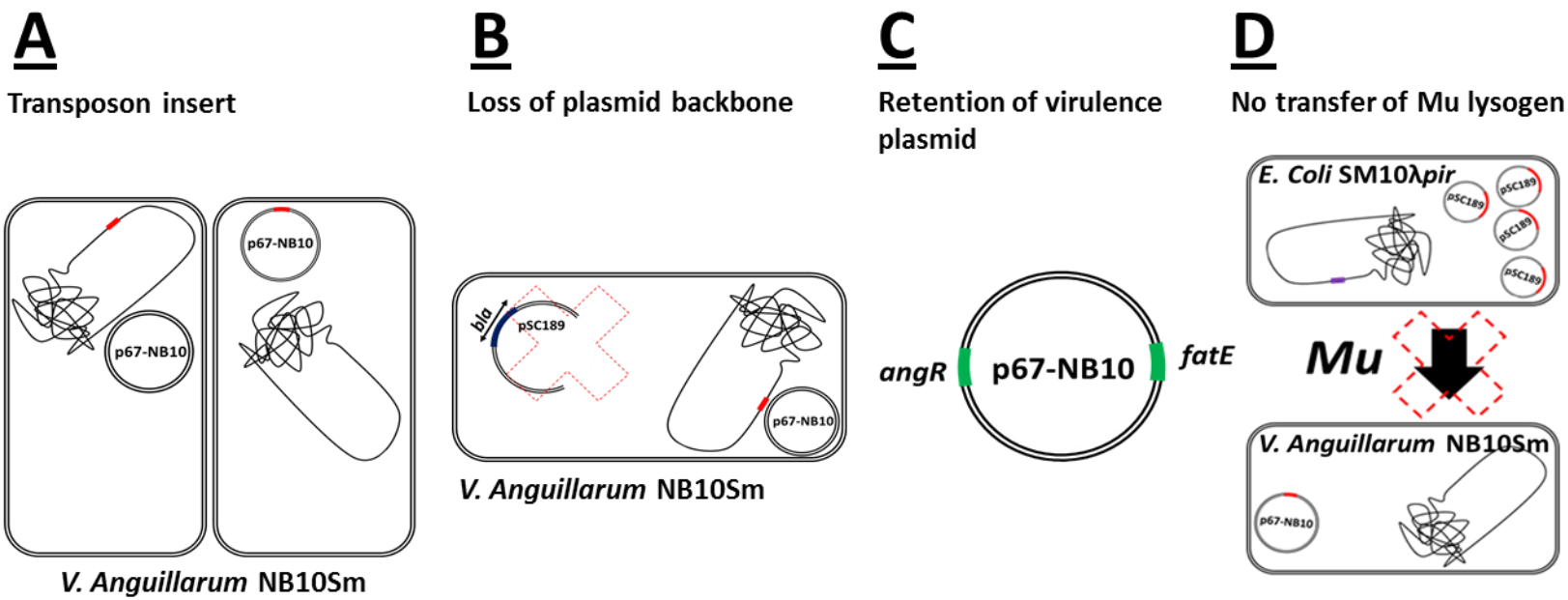

Figure 4.2. Diagrammatic representation of targets in PCR assays using template DNA from *V. anguillarum* NB10Sm transposon mutants to confirm the following. A) Transposon TnSC189 insertion into either plasmid or chromosomal DNA of *V. anguillarum* NB10Sm using primers TnSC189F/R. B) Loss of plasmid backbone using beta lactamase (*bla*) target and pSC189*bla*F/R. C) Retention of *V. anguillarum* NB10Sm p67-NB10 virulence plasmid using targets *angR* and *FatE* on the either side of the plasmid using primers sets angRSM/R and fatESMF/R. D) No unwanted transfer of lysogen *Mu* from *E. coli* SM10*λpir* to *V. anguillarum* NB10Sm using primers Mu1470bp.500-5 and Mu1470bp.500-3.

Table 4.2. Primers used to validate *V. anguillarum* NB10Sm transposon insertion mutants

Target	Primer	5'-3'	Amplicon length (bp)	Annealing temp. (°C)	Source or Reference
V. anguillarum specific *rpoN* – cellular factor σ^{54} subunit	**rpoN-ang5'** **rpoN2SMR**	**F:** GTTCATAGCATCAATGAGGAG **R:** TGCCGAGCAGATCAATATGT	**538**	**62**	**Gonzalez et al., 2003** **This study**
V. anguillarum angR on pJM1 like virulence plasmid	**angRSMF** **angRSMR**	**F:** AAGACGTGACCCGATTGCTT **R:** TATCGATGCTTCGGTGGCTC	**247**	**55**	**This study** **This study**
V. anguillarum fatE on pJM1 like virulence plasmid	**fatESMF** **fatESMR**	**F:** TTTTGTCCATGGCTTCACGC **R:** TGGATGACAAGCACTACGGC	**454**	**57**	**This study** **This study**
TnSC189 *mariner* transposon	**TnSC189F** **TnSC189R**	**F:** GTAACGCACTGAGAAGCCCT **R:** TAAGCCCACTGCAAGCTACC	**440**	**57**	**This study** **This study**
Lysogen Mu	**Mu1470bp.500-5** **Mu1470bp.500-3**	**F:** GTTACTTTTCAAAATTTAAAC **R:** CGCAGATAATCTGCAATCAG	**990**	**50**	**Ferrieres et al., 2010** **Ferrieres et al., 2010**
bla – β-lactamase antibiotic marker	**pSC189*bla*F** **pSC189*bla*R**	**F:** TCCTTGAGAGTTTTCGCCCC **R:** CTCCGGTTCCCAACGATCAA	**358**	**56**	**This study** **This study**

NB10Sm parent and plasmidless *V. anguillarum* M93Sm were used as positive and negative controls respectively.

4.2.7.4. Non-transfer of bacteriophage Mu

Finally, DNA in each *V. anguillarum* transposon insertion mutant was screened for the presence of the unwanted Mu mobile genetic element by amplifying a Mu-specific sequence using primers Mu1470bp.500-5 and Mu1470bp.500-3 (Table 4.2.) at an annealing temperature of 50°C and an increased PCR extension time of 1 minute. DNA extracted from *E. coli* SM10 *λpir* (pSC189) and *V. anguillarum* NB10Sm were used as positive and negative controls respectively.

4.2.8. Identification of transposon insert locations by arbitrary PCR

4.2.8.1. Arbitrary PCR to amplify the transposon-host DNA junction in transposon mutants

To amplify the transposon-host DNA junction, a two round arbitrary PCR was performed using the primers listed in Table 4.3. and following the workflow described in Figure 4.3 and below. DNA was extracted from each transposon insertion mutant according to Section 2.2.5.1.

Briefly, the first PCR step (Figure 4.3.) was completed with forward primer IR2 (which is complementary to a specific sequence of the transposon) and the ARB6 reverse primer, which included a section of 10 random nucleotides and a specific five nucleotide tag at the 3' end. DNA template for each

Table 4.3. Primers used for arbitrary PCR amplification of transposon-host DNA junctions in *V. anguillarum* NB10Sm transposon insertion mutants with attenuated virulence in the *G. mellonella* host.

Primer	5'- 3'	Reference
ARB6	GGCCACGCGTCGACTAGTACNNNNNNNNNNACGCC	O'Toole et al. (1998)
ARB2	GGCCACGCGTCGACTAGTAC	O'Toole et al. (1998)
IR2	CTGACCGCTTCCTCGTGCTTTACGG	Bernier et al. (2013)
IR2 60-5	TTCTGAGCGGGACTCTGGGGTACG	Bernier et al. (2013)

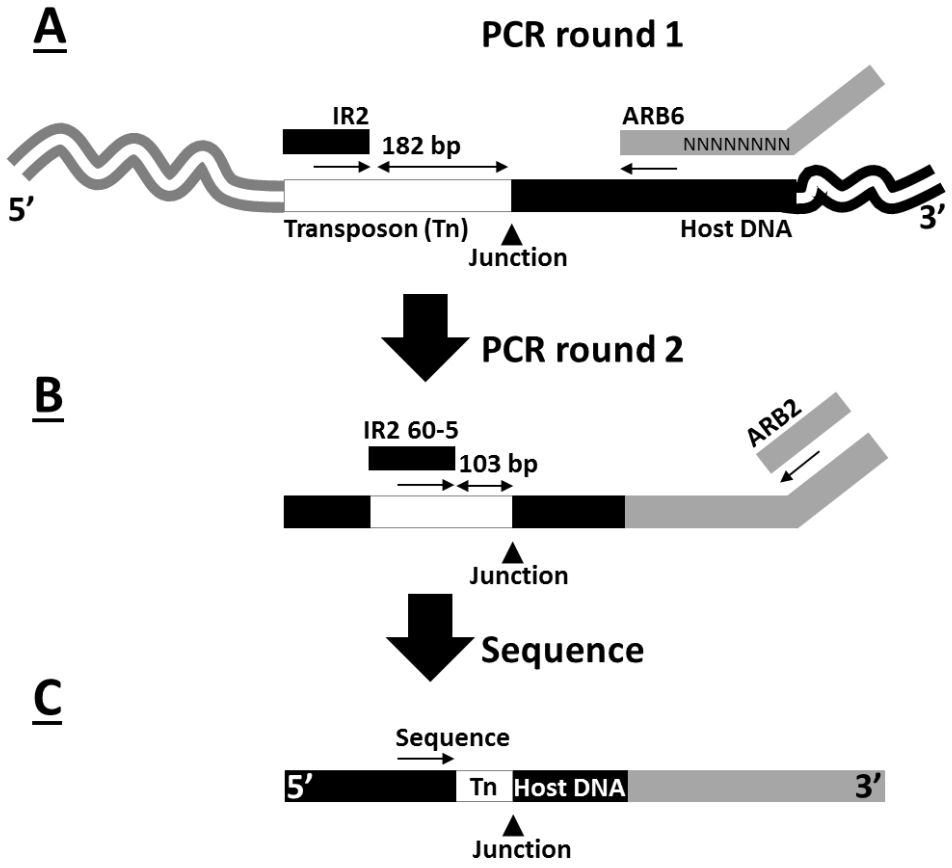

Figure 4.3. Diagrammatic representation of arbitrary PCR and sequencing workflow to identify transposon insertion locations in *Vibrio anguillarum* NB10Sm mutants. A) A first round of PCR amplifies products using an arbitrary primer (ARB 6) with a five nucleotide (nt) 3' end motif preceded by a chain of 10 randomised nts (producing many millions of different combinations in every PCR reaction) and a 20-nt overhang. The five nucleotide motif is complementary to multiple locations in bacterial DNA and, combined with the correct randomised nt sequence, will anneal to several locations, generating many possible different PCR products, including one of 400-600 bp which includes the transposon/genomic DNA junction. The second primer (IR2) is complementary to the 5' end of the Tn189 transposon. B) Then, a second round of PCR using the ARB 2 primer, complementary to ABR6 3' tail (20-nt overhang) and the IR2-60-5 primer, complementary to the transposon but closer to the transposon/genomic DNA junction than IR2, to enrich the first round PCR product containing the transposon insert. C) Finally, products are sequenced beginning at the 5' end travelling through the transposon/genomic DNA junction and then sequences are aligned to identify the transposon insertion location using BLASTn.

sample to be sequenced, which included *E. coli* SM10λ*pir* (pSC189) and each of the *V. anguillarum* transposon insertion mutants with attenuated virulence, were amplified in 20 µL reactions containing 10 µL 2× MyTaq mix (Bioline Reagents Ltd; London, UK.), 0.8 µL of each primer at 10 pmol/µL (final concentration of 0.4 pmol/µL), 4 µL of 50 ng/µL of sample DNA, and made up to 20 µL with nuclease-free water. PCR reaction conditions were: 95°C for 2 minutes; then 6 cycles of 95°C for 15 s, 30°C for 15 s, and 72°C for 1 minute; followed by 30 cycles of 95°C for 15 s, 52°C for 15 s, and 72°C for 1 minute; before a final single extension of 72°C for 5 minutes and cooling to 10°C for 10 s.

First-round PCR products were used as template for a second round of PCR (Figure 4.3.) using IR2.60-5 and ARB2 primers which were complementary to the transposon downstream (i.e., closer to the transposon-genomic DNA junction) of the sequence that corresponds to the IR2 primer, and 5' end of ARB6 respectively. Reactions contained 25 µL 2× MyTaq mix (Bioline), 2 µL of each primer at 10 pmol/µL (final concentration of 0.4 pmol/µL), 2.5 µL of first-round PCR product and were made up to 50 µL with nuclease-free water. PCR conditions were 95°C for 2 minutes; followed by 35 cycles of 95°C for 15 s, 52°C for 15 s and 72°C for 1 minute; then a final single extension of 72°C for 5 minutes and cooling to 10°C for 10 s.

4.2.8.2. PCR clean-up

Second-round PCR products were cleaned using a GeneJET PCR purification kit (ThermoFisher Scientific Inc., Renfrew, UK) with all steps

performed at room temperature. All centrifuge steps were at 13000 ×*g* for 60 s. Each PCR product (40 µL) was mixed 1:1 with binding buffer. Samples were transferred to a spin column and centrifuged before the flow-through was discarded. Then 700 µL of wash buffer was added and the column incubated for 10 minutes before centrifuging and discarding the flow-through. Columns were centrifuged again to remove residual wash buffer, and then the spin column was transferred to a 1.5 mL microfuge tube before 30 µL nuclease-free water was added to the spin column. Samples were incubated (room temperature, 5 minutes) before centrifuging and then collecting flow-through, pipetting this back onto the spin column membrane and centrifuging for a second time. DNA concentration of this final flow-through was analysed by NanoDrop (ThermoFisher) according to Section 2.2.5.1, and samples were stored at -20°C until prepared for sequencing.

4.2.8.3. Lightrun sequencing

Samples were sequenced (Figure 4.3.) using the Lightrun™ sequencing service (GATC Biotech, London, UK). Each sample comprised of 2.5 µL 10 µM IR2 60.5 primer and 250 ng of purified PCR product made up to 10 µL with nuclease-free water.

4.2.8.4. Identification of insert location

To identify where the TnSC189 transposon had inserted into the genomic DNA of each *V. anguillarum* NB10Sm transposon insertion mutant, the full Lightrun™ product and the TnSC189 sequence were aligned using Bioedit (http://www.mbio.ncsu.edu/BioEdit/bioedit.html) Then, the first 100-bp of

V. anguillarum genomic DNA, downstream of the transposon insertion junction, was aligned to the published *V. anguillarum* NB10 genome (Holm et al., 2015) by BLASTn® (https://blast.ncbi.nlm.nih.gov/Blast.cgi) to identify the transposon insertion location and to determine its orientation.

4.2.9. Characterisation of three *V. anguillarum* random transposon insertion mutants

Transposon insertion mutants *V. anguillarum* NB10SmTn73 (Tn73), NB10SmTn100 (Tn100) and NB10SmTn205 (Tn205) were selected for further characterisation as the transposon appeared to have inserted into putative novel virulence factors and uncharacterised genes.

4.2.9.1 Retention of transposon insertions in the strains during *in vivo* infection of *G. mellonella*

First, to confirm that the transposon insertion was retained in Tn73, Tn100 and Tn205 strains during *in vivo* infection of *G. mellonella*, bacterial suspensions of each of these strains were prepared (according to Section 2.2.2) and for each strain 10 µL was administered to a separate *G. mellonella* larva, as described previously (Section 2.2.3.1). Haemolymph was collected from each larva at 72 h, diluted in PBS and plated in quadruplicate onto TSA20 + PEN^{2} and TSA20 + KAN^{100} + STR^{100}, according to Section 3.2.3, to confirm that similar CFU formed on the standard and transposon insertion mutant selection agar. DNA was extracted from a single colony recovered from each inoculated group of *G. mellonella* following the method of Section 2.2.5.1. DNA extracts were assessed by PCR

and agarose gel as described previously (Sections 2.2.5.3 and 2.2.5.4) using primers TnSC189F/R (Table 4.2) to confirm that each strain had retained the transposon insertion after injection into *G. mellonella*. Then, to confirm that the transposon was inserted at the expected location in each mutant, genomic DNA, arbitrary PCR, PCR clean-up, Lightrun™ sequencing (GATC) and sequence alignment were completed as in Section 4.2.8.

4.2.9.2. *In vitro* growth of transposon insertion mutants compared to the parent strain

To investigate whether the transposon insertion mutants were attenuated in virulence due to a reduced replication rate, bacterial inoculums were prepared to determine *in vitro* growth curves for Tn73, Tn100 and Tn205 and compared to the parent strain following the method of Appendix III.

4.2.9.3. *In silico* analysis of an uncharacterised protein of Tn100

To further investigate the function of the gene disrupted by transposon insertion in Tn100, the complete coding sequence, of this gene, was subjected to BLASTn (BLAST®) analysis against *Vibrio* (taxid:662). Furthermore, the full predicted amino acid sequence (Genbank: CDQ50179.1) was screened with BLASTp, () against all bacterial (taxid:2) non-redundant protein sequences, and a tree of significant alignments was produced using the fast minimum evolution method set to 0.6 sequence difference (BLAST®). Then, the protein sequence was run through the Pfam database (Finn et al., 2016) to identify any known protein families or domains and submitted to PHYRE2 protein fold recognition server

(www.sbg.bio.ic.ac.uk/**phyre2**/) which predicted a 3-dimensional protein structure.

4.2.9.4. Biolog profiles

Biolog GEN III Microplate™ (catalogue number 1030; Hayward, USA) is a 96-well phenotypic fingerprinting system for identification of Gram-positive and Gram-negative bacteria using 71 carbon source assays and 23 chemical, pH and NaCl sensitivity tests. Thus, this system can identify a number of possible metabolic or growth inhibition response differences between the Tn100 mutant and its parent strain NB10Sm. The GEN III Microplate™ assay was performed for Tn100 and the parent isolate. Briefly, these two strains were re-isolated onto TSA20 from TSA20 + STR^{200} (NB10Sm) TSA20 + KAN^{100} + STR^{100} (Tn100) and cultured for (28°C, 36 h). Then 3-4 colonies of each strain were scraped into separate vials of Inoculating Fluid (IF) A (catalogue number 72401; Biolog) using a sterile inoculation loop and mixed by vortex before A_{600} was read against IF A as reference. If required, additional colonies were added until the A_{600} was 0.01–0.02 AU. An aliquot of 100 µL of bacterial suspension was added to each well of the GEN III Microplate™ before incubation (28°C, 24 h). After this incubation, A_{590} of each well was read on a Synergy HT (Biotek UK., Swindon, UK) plate reader after shaking (10 s, medium speed).

Carbon source assays were deemed to be positive (i.e., the culture was able to metabolise the well contents) when the well contents turned purple in colour after incubation, by reduction of tetrazolium dyes, and were graded

semi-quantitatively based on A_{590} readings compared to negative control: – (no change), 0 – 0.150 AU; +, 0.150 – 0.299 AU; ++, 0.300 – 0.449, +++, 0.450 – 0.599; ++++, > 0.600. Assay outcomes within one grade of intensity difference between the two isolates were classified as being in agreement, with the exception that cases where one strain produced a very weak positive (+) compared a negative (-) result from the other strain were recorded as being borderline or a possible difference.

For chemical pH and NaCl sensitivity assays, a positive (+) result was recorded when the isolate produced a similar intensity of purple colour compared to the positive control well. A result was recorded as negative when the intensity of the purple colour was reduced compared to the positive control well. Semi-quantitative results were reported based on A_{590} readings (–, < 0.700; +, ≥0.700).

4.2.10. Statistical analysis

The significance of group survival differences between each group of larvae injected with a transposon insertion mutant strain and the group injected with the parent strain was compared by the logrank test (Mantel, 1966). $p < 0.05$ was considered to indicate a significant difference between two groups and no account was taken for multiple comparisons.

4.3 Results

4.3.1. Curing *E. coli* SM10*λpir* of pSC189 plasmid.

Following incubation of *E. coli* SM10λpir (pSC189) at the increased temperature of 40°C, nine colonies (from a total of 100 sub-cultured onto LBA + 200 µg /mL AMP; Figure 4.4) failed to grow compared to every colony transferred onto LBA + KAN. None of these nine colonies generated PCR products in an assay specific for sections of the specific *bla* sequence located on the pSC189 plasmid (Figure 4.5), suggesting that the plasmid had been cured successfully from these strains. Thus, one of these cured strains was used as a negative control donor in subsequent mating experiments for *V. anguillarum*.

4.3.2. Antibiotic selection of *V. anguillarum* transposon insertion mutants

Minimum inhibitory concentration (MIC) and minimum bactericidal concentration (MBC) assays showed that the eight selected *V. anguillarum* strains had MICs of 32 µg/mL against AMP (MBCs: 32 to >128 µg/mL) compared to *E. coli* SM10*λpir* (pSC189) which grew in the presence of AMP even at 512 µg/mL (Table 4.4). Thus, the concentration of AMP used in the agar to select against *V. anguillarum* cells was increased to 200 µg/mL where required.

MICs against KAN for the *V. anguillarum* strains were 16–128 µg/mL (Table 3.1 and Table 4.5). However, KAN sensitivity of *E.coli* TOP10 with and without TnSC189 demonstrated a 250-fold decrease in susceptibility, as conferred by the KAN^r gene associated with the transposon, with an MIC of

Figure 4.4. Photograph of *Escherichia coli* SM10λ*pir* colonies sub-cultured onto antibiotic selective agar plate to identify strains cured of the pSC189 plasmid. Colonies recovered from an *E. coli* SM10λ*pir* (pSC189) culture after growth in Miller lysogeny broth at 40°C without ampicillin (AMP) selection were then sub-cultured onto Miller lysogeny agar containing 200 µg/mL AMP. Blank sections (92 and 98) confirm that the strains streaked in these sections of the agar had lost their AMP resistance phenotype (which is conferred by the presence of the pSC189 plasmid), suggesting these strains had been cured of the pSC189 plasmid. AMP-susceptible *E. coli* TOP10 was included as a negative control.

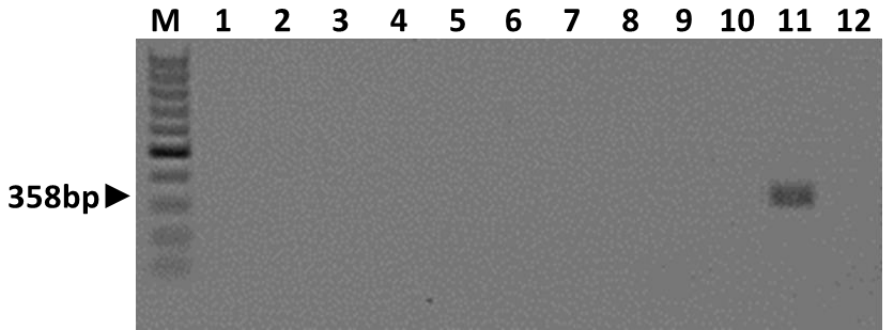

Figure 4.5. Agarose gel electrophoresis of *Escherichia coli* SM10λ*pir* isolates, to confirm loss of AMP^r pSC189 plasmid following curing experiments, using primers pSC189*bla*F and TnSC189R. M, 100bp DNA ladder (B); lanes 1-9, AMP susceptible SM10λ*pir* isolates; lane 10, TOP10 positive control; lane 11, *E. coli* SM10λ*pir* (pSC189) negative control; lane 12, no template control.

Table 4.4. Minimum inhibitory concentrations (MICs) and minimum bactericidal concentrations (MBCs) of 8 *Vibrio anguillarum* isolates and *E. coli* SM10*λpir* to ampicillin (AMP) following 24 h incubation. Minimum bactericidal concentration was calculated after plating the highest four antibiotic concentrations with no visible signs of growth following the initial 24 h incubation. Where an MIC or MBC could not be determined a '>' symbol indicates that growth was visible in the well with highest AMP concentration or that < 99.9% of the inoculum was killed in the well containing the greatest concentration of AMP tested. Assays were performed in duplicate and where the values differed by a 2-fold dilution it is the greater value that is reported.

Species	Isolate name	MIC (µg/mL)	MBC (µg/mL)
V. anguillarum	VIB 1	32	128
V. anguillarum	VIB 39	32	64
V. anguillarum	VIB 44	32	64
V. anguillarum	VIB 56	32	64
V. anguillarum	VIB 79	32	> 128
V. anguillarum	VIB 85	32	64
V. anguillarum	VIB 134	32	64
V. anguillarum	NB10	32	64
E. coli	SM10λ*pir* (pSC189)	>512	> 512

Table 4.5. Minimum inhibitory concentrations (MICs) and minimum bactericidal concentrations (MBCs) against kanamycin (KAN) of *Vibrio anguillarum* NB10 and the spontaneous streptomycin-resistant mutant (*V. anguillarum* NB10Sm), and *Escherichia coli* SM10λ*pir* (pSC189) (transposon donor), *Escherichia coli* TOP10 (transposon recipient) and the same isolate with the TnSC189 transposon integrated into the chromosome (TOP10Tn). Where MBC could not be determined a '>' symbol indicates that less than 99.9% of the inoculum was killed in the well containing the greatest concentration of KAN tested. Assays were completed in duplicate and where the values differed by a 2-fold dilution it is the greater value that is reported.

Species	Strain name	MIC (μg/mL)	MBC (μg/mL)
V. anguillarum	NB10	32	64
V. anguillarum	NB10Sm	32	64
E. coli	SM10λ*pir* (pSC189)	512	>512
E. coli	TOP10	2	4/8
E. coli	TOP10Tn	512	>512

512 μg/mL when TnSC189 was present compared to a MIC of 2 μg/mL when it was absent (Table 4.5). Thus, *V. anguillarum* transposon insertion mutants were isolated onto agar with a much greater concentration of KAN than the 30 μg/mL used previously (Chiang and Rubin, 2002); therefore, the KAN concentration in the transposon insertion mutant selection agar was increased to 250 μg/mL to select against non-recipient *V. anguillarum* NB10Sm cells.

4.3.3. Generation of *V. anguillarum* streptomycin-resistant (STR^r) spontaneous mutant for subsequent use in transposon insertion mutant library preparation

Streptomycin was selected as the antibiotic to select against *E. coli* in subsequent transposon insertion mutant library preparation as *E. coli* SM10*λpir* (pSC189) is known to be susceptible to this antibiotic (MIC = 4 μg/mL; Section 3.3.1) and spontaneous resistance can be selected in *V. anguillarum* (Denkin and Nelson, 1999). Thus, it was necessary to select for a spontaneously STR^r in *V. anguillarum* mutant for use as the recipient cells in transposon insertion mutant library preparation.

To this end, colonies were recovered from agar containing STR that had been inoculated with suspensions of different isolates of *V. anguillarum* to select for spontaneous STR^r mutants (Table 4.6). For each representative *V. anguillarum* strain, five colonies (except VIB 39 where only one colony was recovered onto agar + STR plate) were sub-cultured onto agar + STR. In some cases, the colonies grew after transfer to this fresh agar and these

Table 4.6. Spontaneous mutation frequency of selected *Vibrio anguillarum* isolates following selection onto 1.5% NaCl-supplemented tryptone soy agar (TSA20) containing 100 µg/mL of streptomycin (STR) and incubation for 72 h at 22°C. Mutation frequency was calculated as recovered CFU / input CFU.

Isolate	Input CFU	Recovered CFU	Mutation frequency
VIB 1	2.66×10^{10}	1672	6.28×10^{-08}
VIB 39	1.79×10^{10}	1	5.58×10^{-11}
VIB 44	1.26×10^{10}	7	5.56×10^{-10}
VIB 56	1.58×10^{10}	854	5.40×10^{-08}
VIB 79	1.73×10^{10}	1034	5.97×10^{-08}
VIB 85	1.51×10^{10}	871	5.78×10^{-08}
VIB 134	1.34×10^{10}	1026	7.69×10^{-08}
NB10	1.23×10^{10}	312	2.54×10^{-08}

strains also grew when sub-cultured onto TCBS agar, which confirmed that each of these progeny strains could grow in this concentration of STR and that each strain was a *Vibrio* spp., respectively. However, some isolates failed to recover onto TSA20 + STR^{200} but could grow at a lower concentration of STR (100 μg/mL) (Table 4.1). Moreover, five progeny isolates failed to culture in broth and were omitted from further investigation.

To check that the STR^r mutants retained their virulence in *G. mellonella*, these mutant strains (up to a maximum of five progeny strains from each parent) were challenged in *G. mellonella* and larval survival compared between respective progeny and parent strains. Nine isolates had significantly attenuated in virulence and so these strains were not used further (Table 4.7). The progeny strain selected for subsequent transposon mutagenesis library preparation was *V. anguillarum* NB10Sm because this strain showed no significant attenuation in virulence in *G. mellonella* when assessed in two independent trials (Figure 4.6) and a published genome is available (Holm et al., 2015). Moreover, MIC of *V. anguillarum* NB10Sm against KAN remained unchanged compared to the parent strain (Table 4.5). Still, *in vitro* growth of *V. anguillarum* NB10Sm was considerably slower than the *V. anguillarum* NB10 parent (Figure 4.7), but this was deemed to be of limited importance compared to the benefits of using this strain.

Table 4.7. Virulence of various *Vibrio anguillarum* parent and spontaneous STR^r mutants in *G. mellonella*. No significant difference (✓) or significant difference (×) in virulence between the groups (n=10, except *V. anguillarum* NB10Sm where n=20) injected with the parent and progeny strains (p = < 0.05 by log rank test); no account taken for multiple comparisons.

Parent strain name	Spontaneous mutant strain name	Virulence agreement (✓/×)
VIB 1	VIB 1.1Sm	✓
VIB 1	VIB 1.2Sm	✓
VIB 1	VIB 1.3Sm	✓
VIB 1	VIB 1.4Sm	✓
VIB 1	VIB 1.5Sm	✓
VIB 39	VIB 39Sm	×
VIB 44	VIB 44.1Sm	✓
VIB 44	VIB 44.2Sm	×
VIB 44	VIB 44.3Sm	✓
VIB 44	VIB 44.4Sm	✓
VIB 44	VIB 44.5Sm	✓
VIB 56	VIB 56.1Sm	✓
VIB 56	VIB 56.2Sm	✓
VIB 56	VIB 56.3Sm	✓
VIB 56	VIB 56.4Sm	✓
VIB 56	VIB 56.5Sm	×
VIB 79	VIB 79.1Sm	✓
VIB 79	VIB 79.2Sm	✓
VIB 79	VIB 79.3Sm	✓
VIB 79	VIB 79.4Sm	✓
VIB 79	VIB 79.5Sm	✓
VIB 85	VIB 85.1Sm	×
VIB 85	VIB 85.2Sm	✓
VIB 85	VIB 85.3Sm	✓
VIB 85	VIB 85.4Sm	×
VIB 85	VIB 85.5Sm	×
VIB 134	VIB 134.1Sm	×
VIB 134	VIB 134.3Sm	✓
NB10	NB10Sm	✓
NB10	NB10.4Sm	×
NB10	NB10.5Sm	×

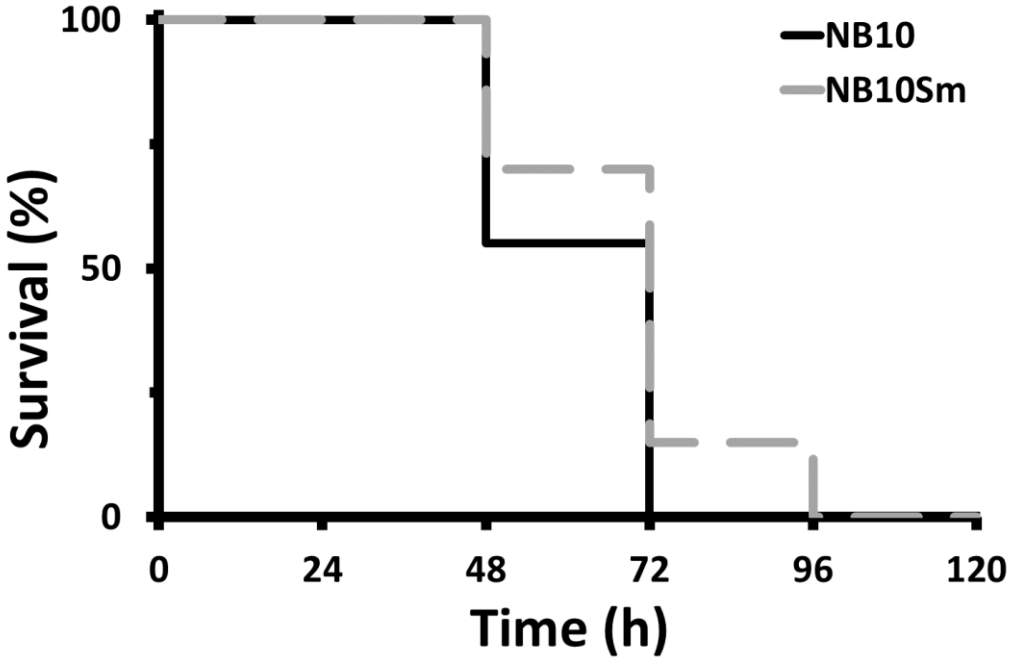

Figure 4.6. Survival of *Galleria mellonella* injected with 1 x10^5 CFU of spontaneous streptomycin-resistant mutant strain *Vibrio anguillarum* NB10Sm and the *V. anguillarum* NB10 parent strain during 120 h at 15°C. For clarity, data for the unmanipulated and uninfected PBS only control groups are not shown. This data was generated from two independent trails. n=20.

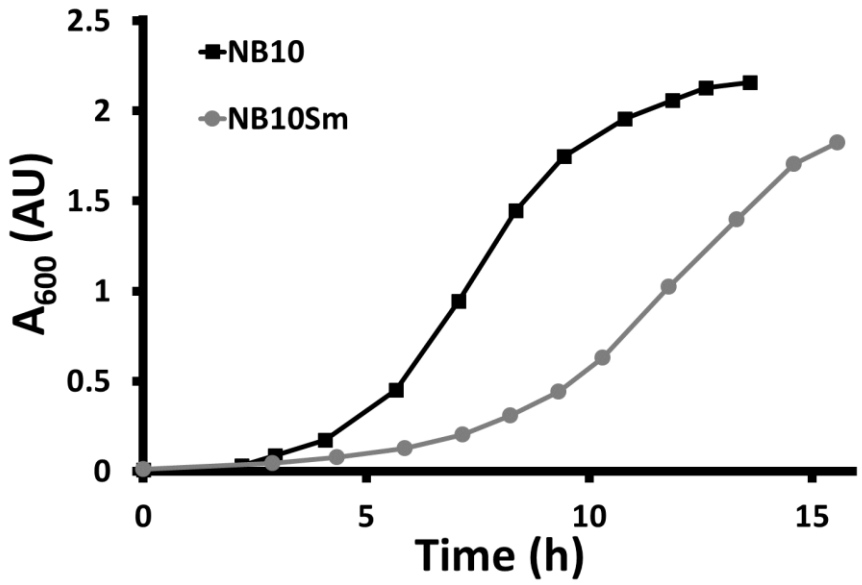

Figure 4.7. Growth of spontaneous STR^r mutant *V. anguillarum* NB10Sm compared to the *V. anguillarum* NB10 parent strain as determined by culture absorbance at 600 nm (A_{600}) over time. Data plotted as mean ± standard error of mean (error bars are too small to be visible). n=3.

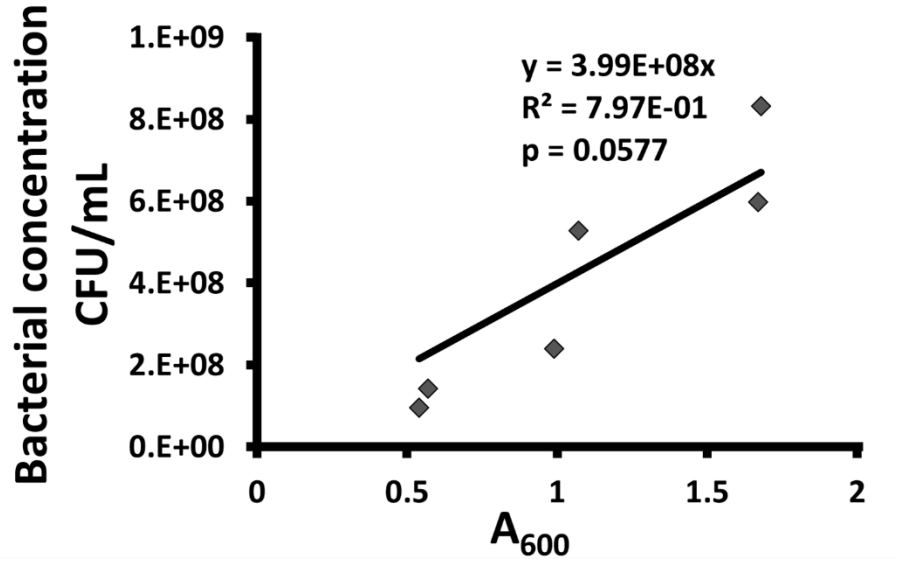

Figure 4.8. Correlation between colony forming units per mL (CFU/mL) and culture absorbance at 600 nm (A_{600}) for *E. coli* SM10 (pSC189). n=6.

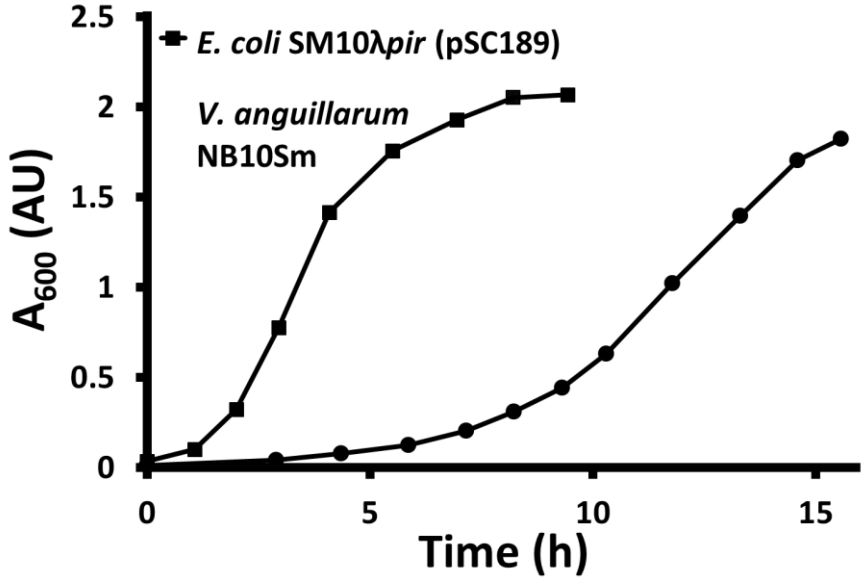

Figure 4.9. Growth of transposon donor strain *E. coli* SM10λ*pir* and *V. anguillarum* NB10Sm recipient as measured by absorbance at 600 nm (A_{600}). Data plotted as mean ± standard error (error bars are too small to be visible). n=3.

4.3.4. Generation and selection of *V. anguillarum* transposon mutants

Analysis of the calibration curve for the *E. coli* SM10 (pSC189) donor (Figure 4.8) indicated that approximately four times more *V. anguillarum* NB10Sm CFU (Figure 2.3) were present in a culture at the same A_{600} value. Therefore, to achieve a 1:1 (donor:recipient) ratio of CFU for transposon mating a 1:4 mixture of donor to recipient culture was required. Furthermore, growth curves produced for both donor and recipient strains (Figure 4.9) indicated that *E. coli* SM10 (pSC189) reached stationary phase approximately 8 h before *V. anguillarum* NB10Sm, therefore incubations were synchronised to generate cultures in the desired phases of growth for mating.

The TnSC189 transposon carried on the pSC189 plasmid was transferred successfully into *V. anguillarum* NB10Sm genomic DNA at a frequency of 1.16×10^{-6} and this generated approximately 60,000 mutant colonies from the single mating performed. Three hundred and fifty colonies (presumptive transposon insertion mutants) were picked from the TSA20 + KAN^{250} + STR^{200} agar used to select the mutants and separately patched onto TSA20+ KAN^{250} + STR^{200} to confirm the resistance phenotypes. Each of the 350 colonies grew successfully after this sub-culture step.

4.3.5. Virulence assessment of transposon insertion mutants in *G. mellonella*

The 350 *V. anguillarum* NB10Sm transposon insertion mutants were assessed for virulence in *G. mellonella*, and larval survival compared to the

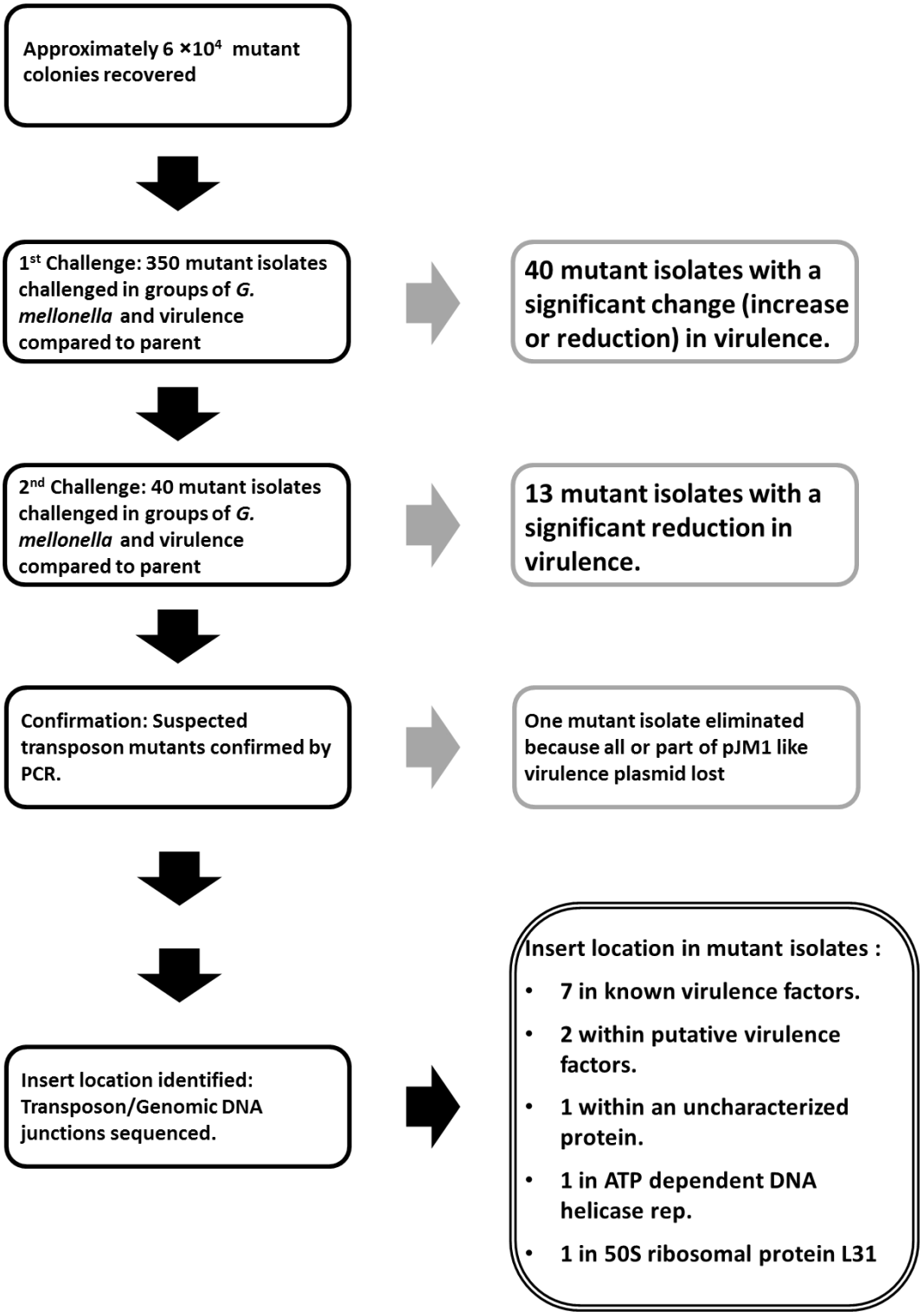

Figure 4.10. Transposon mutagenesis workflow illustrating the different stages of experiment and at which point groups of mutants were rejected.

V. anguillarum NB10Sm parent over a 120 h period. First-round trials identified 40 transposon mutants with significantly different virulence compared to the parent strain (Figure 4.10). However, when these strains were investigated in a subsequent trial, only 13 strains showed virulence that differed significantly from the parent strain. In all cases the virulence of the transposon insertion mutant was reduced compared to the parent (Figure 4.10).

4.3.6. Examination of transposon mutants by PCR.

DNA extracted from 50 of the 350 transposon insertion mutants each generated products in PCR assays that confirmed that these strains were *V. anguillarum* and had incorporated the TnSC189 transposon into the genomic DNA. These PCR assays were also completed for DNA extracted from the 13 transposon mutants with significantly attenuated virulence in *G. mellonella*, and each of these strains was also confirmed to be *V. anguillarum* and contain the TnSC189 transposon as expected (Figure 4.11). As expected, in all the *V. anguillarum*-specific PCR assays DNA from the positive control *V. anguillarum* NB10Sm parent produced products of the expected size; however, no products were amplified from the negative control *E. coli* SM10*λpir* (pSC189) DNA. Furthermore and as expected, DNA extracted from the positive control *E. coli* SM10*λpir* (pSC189) strain generated products of the expected sizes in all TnSC189 transposon transfer confirmation assays, while nothing was amplified from negative control

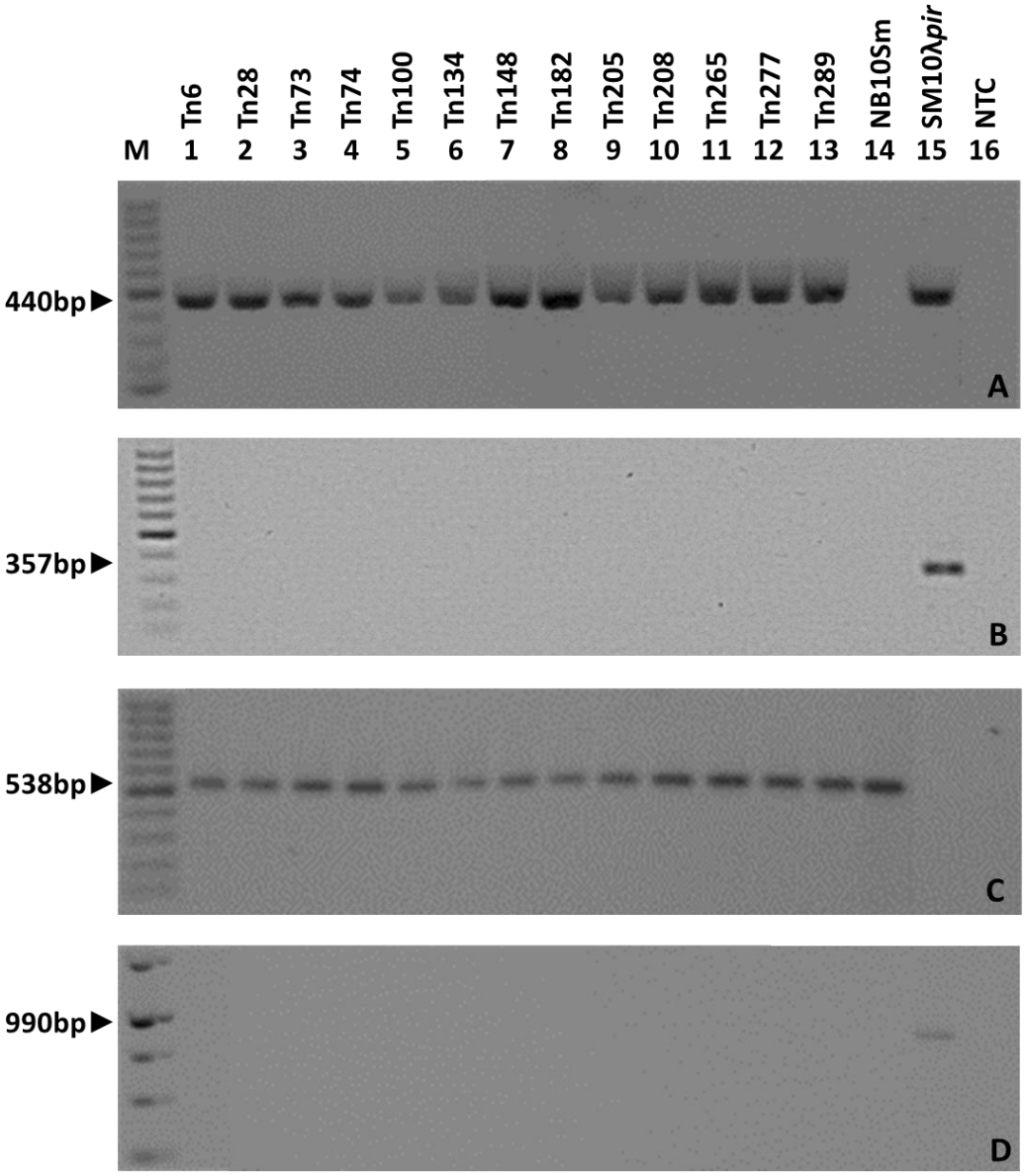

Figure 4.11. Agarose gel electrophoresis of PCR products from presumed *Vibrio anguillarum* NB10Sm transposon insertion mutants to confirm that: (A) the Tn189 transposon had inserted into *V. anguillarum* NB10Sm genomic DNA using TnSC189F and TnSC189R primers; (B) confirmation of loss of plasmid backbone using pSC189*bla*F and pSC189*bla*R primers; (C) confirmation of recovered strains as *V. anguillarum*, using rpoN-ang5' and rpoN2SMR primers; (D) confirmation that Mu lysogen had not transferred into the recipent *V. anguillarum* genomic DNA using Mu1470bp.500-5 and Mu1470bp.500-3 primers; M, 100-bp DNA ladder (A-C), or 1-kb DNA ladder (D); lane 1-13, *V. anguillarum* NB10Sm transposon insertion mutants (named above lanes); lane 14, *V. anguillarum* NB10Sm; lane 15, *E. coli* SM10λpir (pSC189); lane 16, no template control.

V. anguillarum NB10Sm parent. The no template controls did not generate PCR products in the assays.

Further PCR assays using DNA samples extracted from the transposon insertion mutants with significantly attenuated virulence in *G. mellonella*, following two challenges, confirmed that the pSC189 plasmid backbone had been lost as desired. Moreover, the troublesome Mu element had not transferred, while in both assays the positive control strain *E. coli* SM10*λpir* (pSC189) produced single products as expected (Figure 4.11). Again, and as expected, no product was produced from negative control *V. anguillarum* NB10Sm strain for these assays (Figure 4.11). However, *V. anguillarum* Tn134 failed to generate PCR products of the expected sizes corresponding to *fatE* or *angR* sequences present on the p67-NB10-like virulence plasmid (Figure 4.12), indicating the loss of this plasmid, and so this strain was discarded. The other 12 presumed transposon insertion mutants and the positive control *V. anguillarum* NB10Sm strain generated products of the expected sizes in both PCR assays (Figure 4.12), while the two negative control strains *E. coli* SM10*λpir* (pSC189) and plasmidless *V. anguillarum* M93Sm did not yield PCR products. Thus, with the exception of *V. anguillarum* Tn134, 12 transposon insertion mutants had retained the p67-NB10 virulence plasmid.

4.3.7. Identification of transposon insertion locations

Arbitrary PCR was used to amplify the transposon-host DNA junction in each of the 12 *V. anguillarum* NB10Sm transposon insertion mutants. The

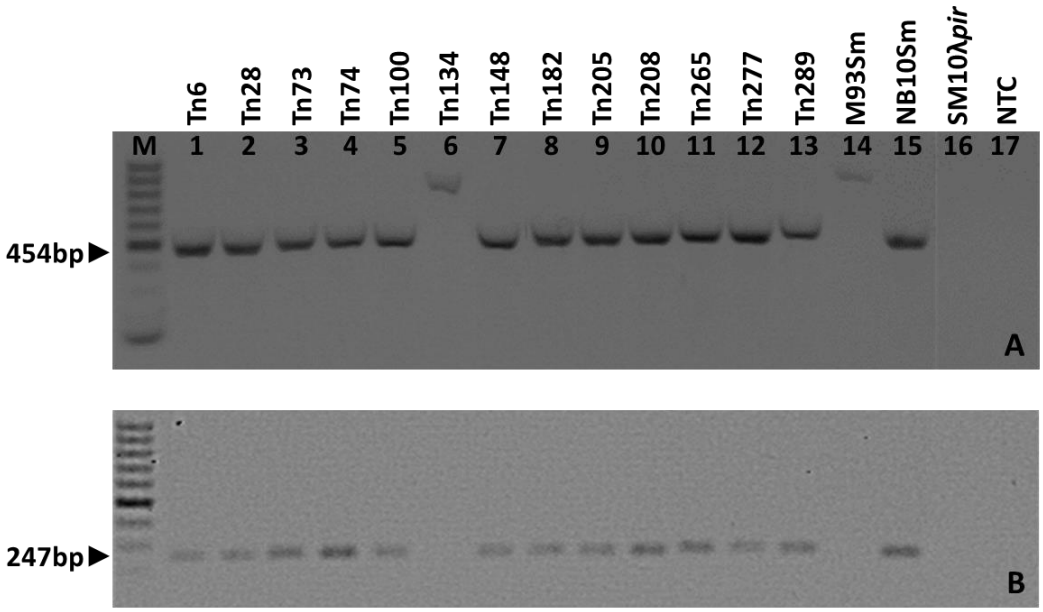

Figure 4.12. Agarose gel electrophoresis of PCR products from *Vibrio anguillarum* NB10Sm transposon insertion mutants to confirm retention of the pJM1-like virulence plasmid p67-NB10 using two primer sets, fatESMF and fatESMR (A), and angRSMF and angRSMR (B), which are specific for genes on opposite sides of this plasmid. M, 100-bp DNA ladder; lane 1-13, *V. anguillarum* NB10Sm transposon insertion mutants (named above lanes); lane 14, plasmid-less *V. anguillarum* M93Sm; lane 15, *V. anguillarum* NB10Sm lane 16, *E. coli* SM10λpir (pSC189); lane 17, no template control.

Table 4.8. Transposon insertion locations in the *V. anguillarum* NB10Sm genomic DNA. Protein product and function, if known, is present, as is the P significance value of virulence in *G. mellonella* between each transposon mutant strain and the *V. anguillarum* NB10Sm parent when tested by logrank. Insert locations were identified by BLASTn analysis of the first 100-bp of Lightrun™ sequence DNA downstream of transposon insert location, and in all cases this produced a 100% identity match against *V. anguillarum* NB10 genomic DNA.

Isolate	P value	Gene, insert location[a] and orientation (+/-)[b]	Product	Function	Reference
Tn6	0.003	*rpmE*, chromosome 1, 2795761, -	50S ribosomal protein L31	Binds 23S rRNA	Eistetter et al. (1999)
Tn28	0.0001	*angB/G*, p67-NB10, 7569, -	Isochorismate lyase	Involved in anguibactin biosynthesis	Welch et al. (2000)
Tn73	0.03	*wbhK*; chromosome 1, 2890365, +	Probable aminotransferase	Involved with lipopolysaccharide synthesis	Stroeher et al. (1998)
Tn74	0.00007	*Rep*; chromosome 1, 3033078, -	ATP dependent DNA helicase rep	Initiates unwinding of nicks in DNA	Gilchrist and Denhardt (1987)
Tn100	0.0003	Unknown; chromosome 1, 1499726, +	Putative uncharacterised protein	Unknown	-
Tn148	0.0004	*angN*: p67-NB10, 42771, +	Non-ribosomal peptide sythetase	Anguibactin biosynthesis	Di Lorenzo et al. (2003)
Tn182	0.03	*vah1*; chromosome 2, 269255, -	Haemolysin	Haemolytic activity	Li et al. (2011); Mou et al. (2013); Rock and Nelson (2006)
Tn205	0.0004	*cyaA*; chromosome 1, 85286, +	Class II Adenylate cyclase	Secreted toxin in some bacteria. Putative virulence factor in *V. anguillarum* 775	Rodkhum et al. (2006)
Tn208	0.0002	*angN*: p67-NB10, 43273, +	Non-ribosomal peptide sythetase	Anguibactin biosynthesis	Di Lorenzo et al. (2003)
Tn265	0.03	*vah1*; chromosome 2, 270954, -	Haemolysin	Haemolytic activity	Li et al. (2011); Mou et al. (2013); Rock and Nelson (2006)
Tn277	0.0003	*angR*: p67-NB10, 38149, -	Non-ribosomal peptide sythetase	Regulation of anguibactin biosynthesis and iron transport genes.	Wertheimer et al. (1999)
Tn289	0.009	*angB/G*[c]: p67-NB10, 7229, +	Isochorismate lyase	Involved in anguibactin biosynthesis	Welch et al. (2000)

a Insert location defined as number of t nucleotide directly after insert based on NB10 chromosome 1 (Accesion number LK021130), NB10 chromosome 2 (Accesion number LK021129) and p67-NB10 virulence plasmid (Accesion number LK021128).
b + transposon insert location on forward strand, - transposon insert location on reverse strand.
c Insert location 24 nucelotides before coding sequence start.

sequenced PCR products were used to identify the location of each transposon-host DNA junction by alignment to the *V. anguillarum* NB10 genome. By this method, two transposon insertions were detected within genes coding for an ATP-dependent DNA helicase rep and 50S ribosomal protein L31 (Tn6 and Tn74, respectively) on chromosome I (Table 4.8). A further seven locations were mapped to genes encoding known *V. anguillarum* virulence factors: five were located on the p67-NB10 virulence plasmid (Tn28, Tn148, Tn208, Tn277 and Tn289) and the remaining two were located on chromosome II (Tn182 and Tn265; Table 4.8). A further two transposon insertion locations on chromosome I were in genes encoding for putative virulence factors (Tn73 and Tn205; Table 4.8) (Rodkhum et al., 2006b; Stroeher et al., 1998). Finally, one transposon insertion location on chromosome I was in the middle of a gene that encodes a putative uncharacterised protein (Tn100; Table 4.8).

4.3.8. Further characterisation of Tn73, Tn100 and Tn205 *V. anguillarum* transposon insertion mutants

Isolates Tn73 and Tn205 with inserts in putative virulence factors, and mutant Tn100 with the transposon disrupting an uncharacterized protein, were studied further. Growth curves for these three isolates showed similar growth rates compared to the *V. anguillarum* NB10Sm parent strain (Figure 4.13).

BLASTn analysis of the full nucleotide sequence coding for the putative uncharacterised protein of Tn100 revealed strong similarities in the final

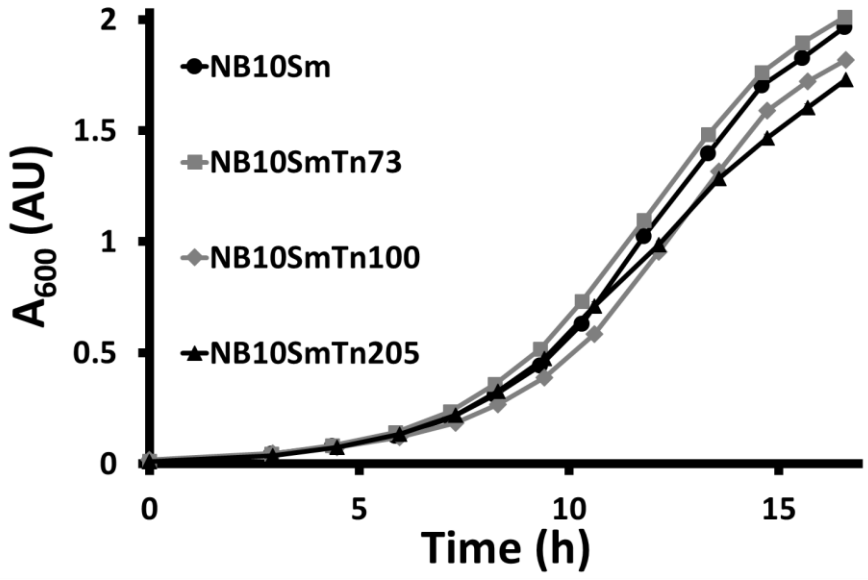

Figure 4.13. Growth of three transposon insertion mutants *V. anguillarum* (Tn73, Tn100 and Tn205) compared to the *V. anguillarum* NB10Sm parent, as measured by absorbance at 600 nm (A_{600}) during 16 hours. Data plotted as mean ± standard error (error bars are too small to be visible ible). n=3.

MSSKTFKITVIAASILAATQAHAALYQIVEVTPGNLVANEYYGRAIQKDNLSANPLGCFT
AGNSCNTFAFGGDTLNGSDGISYHDEVPFKMDNRFVYQDIDDLKNYCSNELGYSTCEAWA
DKQWHGFEYNNVETGGLKRERDAWDNGSYLQNAAAFVNSSQVVLTFGSIANTQNTVLTGL
DGTYAFGITSSGYTQSGSNYALGYRQRGFYNGNILNPPTDTTIVKDTNNKIVEKMGRTFA
YDVFNDGTHNFVVGSASVSPYLTGNGDDDNKDYNGDVNTCVSDGLDPQLTRQCQNFAFAT
QAYMWDTASISTGYRVTGWVGDVEANRSGYSAQASVRGAAVPTSGSYANKSVMAGFNTYR
DDNVFRMQATVFYPNASYDVTTPKHDMWSSKVITGTELKVDGDVIYSNSLATDINNHLIV
IGETKRKGDKPESGAAANRIFVADANSGTPVANYLSGGIFFTGAGGEAKAINNFNEIVGQ
IDAEKGREDGGKQRRHRGFIYPFNGTGSNAARMALFQNQGWWLDDLTNGGAYSQHNNQFR
IFEASDINDDGVIAASAFKCTGGYDDFSHNSYCTSGSESVVAIKLIPIAGAAASGIEVRS
TALPPVERK**GGSMGWITLTLLALFGFRRK**

Figure 4.14 Predicted amino acid sequence of putative uncharacterised protein into which theTnSC189 transposon was found to have inserted in *V. anguillarum* Tn100. The GlyGly-CTERM sorting domain is highlighted in bold. The transposon insertion occurred between G and T residues underlined in the sequence.

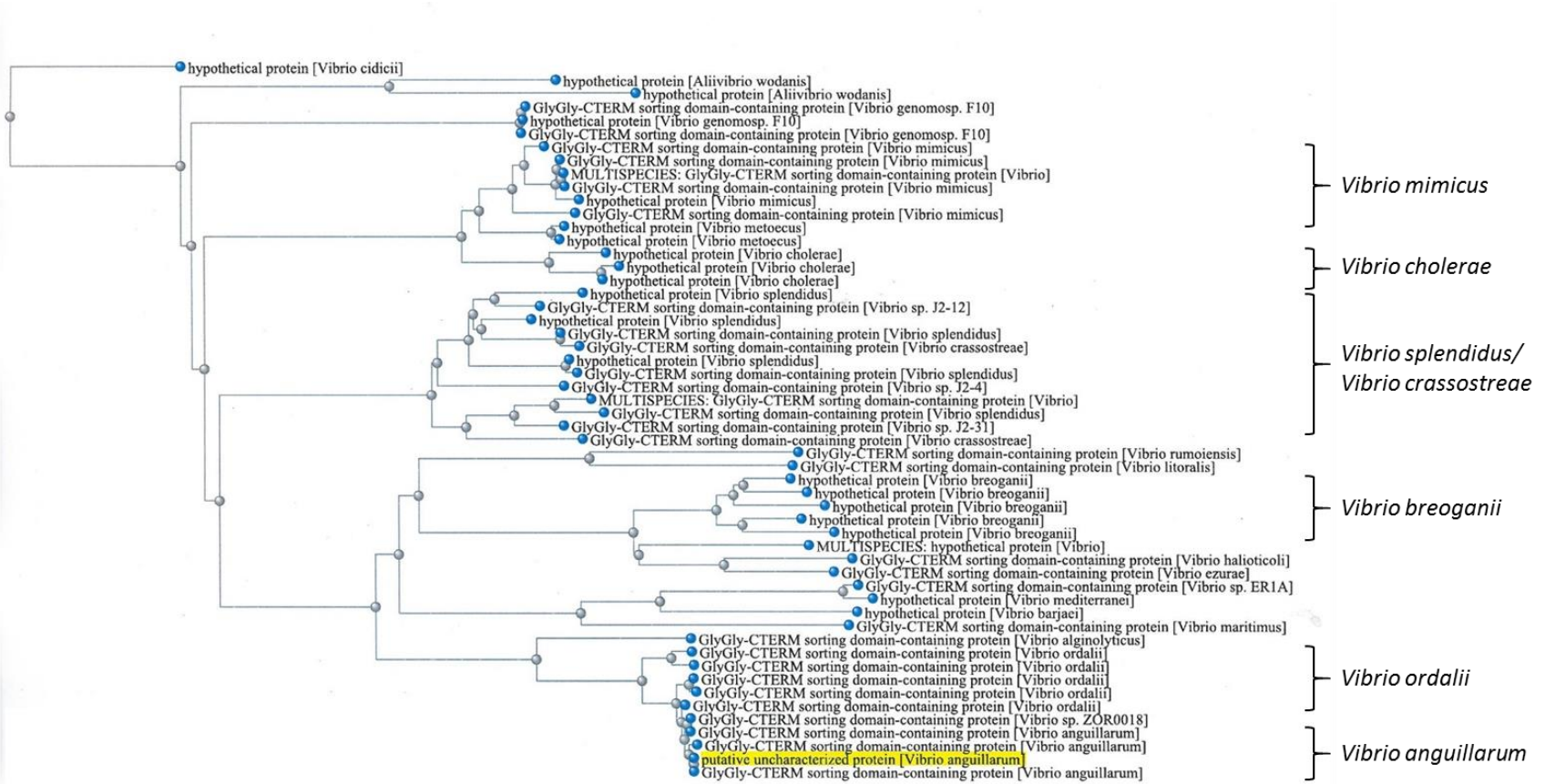

Figure 4.15 Similarity tree of the putative uncharacterised protein found in *V. anguillarum* Tn100 (highlighted in yellow; Genbank: CDQ50179.1) to proteins found in other *Vibrio* spp. The tree was produced after BLASTp analysis of whole protein sequences using the refseq_protein database against all bacteria (taxid 2), and using the fast minimum evolution method with 0.6 maximum difference. For clarity specific *Vibrio* spp. clades have been labelled.

25% of the nucleotide sequence with genes found in many other *Vibrio spp.* Meanwhile, BLASTp alignment of the complete predicted amino acid sequence (Figure 4.14) confirmed that many *Vibrio spp.* produce a protein with a similar sequence, although none of these products have been annotated in any database and these have been described as putative or hypothetical proteins. Furthermore, this BLASTp analysis was used to generate a similarity tree (Figure 4.15) which revealed that the Tn100 putative protein showed greatest similarity with a GlyGly-CTERM sorting domain-containing protein found in *V. ordalii*. Furthermore, the common motif amongst many of these proteins, including that found in *V. anguillarum* NB10 where it is the last 20 amino acid residues (Figure 4.14), is the GlyGly-CTERM sorting domain. Pfam analysis placed the protein within the uncharacterised DUF (Domain of Unknown Function) 3466 family of proteins. Finally, predicted protein structure was generated and this revealed that the protein most likely forms a classic alpha helix and contains a transmembrane domain (Figure 4.16).

Bacterial suspensions of *V. anguillarum* Tn100 and the *V. anguillarum* NB10Sm parent were screened in 94 separate assays to identify phenotypic differences between these strains with respect to carbon utilisation and metabolism in the presence of various cellular inhibitors. Compared to the *V. anguillarum* NB10Sm parent, *V. anguillarum* Tn100 had reduced capacity to utilise two carbon sources and an inability to use nine other carbon sources. However, Tn100 grew in the presence of formic acid

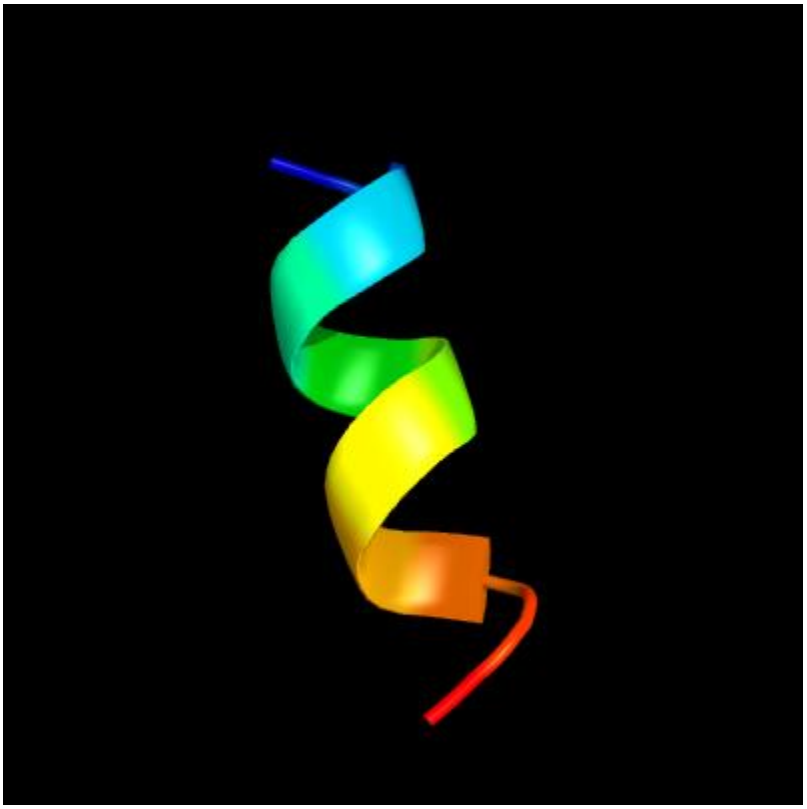

Figure 4.16. Predicted structure of putative uncharacterised protein into which transposon TnSC189 inserted in *V. anguillarum* Tn100. This model was generated using the PHYRE2 protein fold recognition server (www.sbg.bio.ic.ac.uk/**phyre2/**), and the confidence attributed to this assignment is 42.3%.

Table 4.9. Abilities of the *Vibrio anguillarum* NB10Sm parent and the transposon insertion mutant *V. anguillarum* Tn100 to utilise various carbon sources in the GEN III Microplate™ assay. Positive (+) results were recorded when the strain reduced tetrazolium dyes to produce a purple colour. The metabolic responses were graded semi-quantitatively based on A590 readings and compared to a negative control well: (- (no change), 0–150; +, 0.150–0.299; ++, 0.300–0.449, +++, 0.450–0.599; ++++, >0.600). Assays with the same score or within one score of intensity between the two isolates were classified as being in agreement. Cases where one strain produced a very weak positive (+) compared to a negative (–) for the other strain were recorded as a borderline difference (\). n = 2.

Phenotypic test	NB10Sm	Tn100	Agreement
Negative control	-	-	✓
Dextrin	++++	++++	✓
D-Maltose	++++	++++	✓
D-Trahalose	-	-	✓
D-Cellobiose	++++	++++	✓
Gentiobiose	+	-	\
Sucrose	++++	++++	✓
D-Turanose	-	-	✓
Stachyose	-	-	✓
D-Raffinose	-	-	✓
α-D-Lactose	-	-	✓
D-Mellibiose	+	-	✓
B-Methyl-D-Glucoside	++++	++++	✓
D-Salicin	++	+	✓
N-Acetyl-D-Glucosamine	++++	++++	✓
N-Acetyl-β-D-Mannosamine	+++	+++	✓
N-Acetyl-D-Galactosamine	-	-	✓
N-Acetyl-Neurominic Acid	-	-	✓
α-D-Glucose	++++	++++	✓
D-Mannose	++++	++++	✓
D-Fructose	++++	++++	✓
D-Galactose	++++	++++	✓

3-Methyl-Glucose	++	+	✓
D-Fucose	+	-	\
L-Fucose	+	+	✓
L-Rhamnose	++	-	×
Inosine	++++	++++	✓
D-Sorbital	++++	++++	✓
D-Mannitol	++++	++++	✓
D-Arabitol	++	+	✓
myo-Inositol	+	+	✓
Glycerol	++++	++++	✓
D-Glucose-6-PO_4	++++	++++	✓
D-Fructose-6-PO_4	+++	++++	✓
D-Aspartic Acid	+	-	\
D-Serine	-	-	✓
Gelatine	++++	+++	✓
Glycyl-L-Proline	++++	++++	✓
L-Alanine	++++	++++	✓
L-Arginine	++	+	✓
L-Aspartic Acid	++++	++++	✓
L-Glutamic Acid	++++	++++	✓
L-Histidine	++++	+	×
L-Pyroglutamic Acid	++	++	✓
L-Serine	++++	++++	✓
Pectin	++++	+++	✓
D-Galacturonic Acid	++	+	✓
D-Galactonic Acid Lactone	++	+	✓
D-Gluconic Acid	++++	++++	✓
D-Glucuronic Acid	+	+	✓
Glucuronamide	+	-	\
Mucic Acid	+	-	\
Quinic Acid	+	-	\
D-Saccharic Acid	-	-	✓
p-Hydroxy-Phenylacetic Acid	-	-	✓
Methyl Pyruvate	++++	+++	✓

D-Lactic Acid Methyl Ester	++++	++	×
L-Lactic Acid	++++	++++	✓
Citric Acid	++++	-	×
α-Keto-Glutaric Acid	+	-	\
D-Malic Acid	+++	+++	✓
L-Malic Acid	++++	++++	✓
Bromo-Succinic Acid	++++	++++	✓
Tween 40	++++	++++	✓
γ-Amino-Butyric Acid	-	-	✓
α-Hydroxy-Butyric Acid	++	++	✓
β-Hydroxy-D,L-Butyric Acid	+	-	\
α-Keto-Butyric Acid	++	-	×
Acetoacetic Acid	++	+++	✓
Propionic Acid	-	-	✓
Acetic Acid	++++	++	×
Formic Acid	-	++++	×

Table 4.10. *Vibrio anguillarum* spontaneous mutant NB10Sm and transposon mutant derivative Tn100 sensitivities to selected chemicals, pH and differential NaCl concentrations were assayed on the colorimetric Biolog GEN III Microplate™ (Biolog). A positive (+) result was recorded when isolates produced a similar intensity of purple colour, from the reducing tetrazolium dyes, compared to the positive control well. A result was recorded as negative (-) when purple colour was reduced. Results were calculated semi quantitatively based on A590 readings (+, 0.7 and above; -, < 0.7). n = 2. Mean of both positive control A590 readings was 0.853. n = 2.

Phenotypic test	NB10Sm	Tn100	Agreement
Positive control	+	+	✓
pH 6	+	+	✓
pH 5	-	-	✓
1%NaCl	+	+	✓
4%NaCl	+	+	✓
8%NaCl	+	+	✓
1% Sodium Lactate	+	+	✓
Fusidic Acid	+	+	✓
D-Serine	-	-	✓
Troleandomycin	+	+	✓
Rifamycin SV	+	+	✓
Minocycline	-	-	✓
Lincomycin	-	+	×
Guanidine HCl	+	+	✓
Niaproof 4	+	-	×
Vancomycin	+	+	✓
Tetrazolium Violet	+	+	✓
Tetrazolium Blue	+	+	✓
Nalidixic Acid	-	-	✓
Lithium Chloride	+	+	✓
Potassium Tellurite	-	-	✓
Aztreonam	+	+	✓
Sodium Butyrate	-	-	✓
Sodium Bromate	-	-	✓

whereas the *V. anguillarum* NB10Sm parent did not (Table 4.9). Surprisingly Tn100 was not susceptible to lincomycin, despite no growth of *V. anguillarum* NB10Sm in the presence of this inhibitor (Table 4.10). Moreover, the *V. anguillarum* NB10Sm parent was able to metabolise in the presence of anionic surfactant Niaproof 4, while *V. anguillarum* Tn100 was unable to proliferate.

4.4 Discussion

Random transposon mutagenesis is a powerful method for identifying the function of uncharacterised genes and novel virulence mechanisms (Judson and Mekalanos, 2000), and this approach has been used successfully with various bacterial pathogens, including *V. anguillarum* (Norqvist and Wolfwatz, 1993; O'Toole et al., 1996; Stork et al., 2004; Stork et al., 2007b; Tolmasky et al., 1988; Welch and Crosa, 2005). However, screening large numbers of transposon insertion mutants within a fish model to identify strains with reduced virulence is impractical and would be ethically difficult to justify nowadays, but greater understanding of *V. anguillarum* virulence remains a key goal. To circumvent these problems, a new approach was developed to generate random transposon insertion mutants of *V. anguillarum* and screen these for attenuated virulence in a *G. mellonella* host (developed in Chapter 3). Such an approach allowed for the identification of virulence genes, including putative novel virulence factors.

First, it was necessary to develop a procedure to generate random transposon insertion mutants for *V. anguillarum*. This entailed the selection

of a spontaneous STR^r strain that remained virulent in *G. mellonella* and could be used for transposon mating. This validation was essential as spontaneous single nucleotide mutations can have pleiotropic effects, such as reduced growth rate (Robinson et al., 2015), which could lead to a reduction in virulence during infection. Indeed, the STR^r *V. anguillarum* NB10Sm isolate used in this present study replicated at a slower rate when compared to its NB10 parent, although virulence remained unchanged. Furthermore, challenge in wax moth revealed attenuated virulence in other spontaneous STR^r *V. anguillarum* NB10 mutants, and this maybe due to a reduction in growth. The spontaneous STR^r *V. anguillarum* NB10Sm strain probably contains a point mutation in *rpsL* gene that confers the resistance phenotype. Streptomycin is an aminoglycoside antibiotic that binds to the S12 protein of the 30S ribosomal subunit to disrupt protein translation (Robinson et al., 2015). Bacterial resistance often results from a point mutation in S12 that is encoded by *rpsL* or the 16S rRNA gene *rrs* (Olkkola et al., 2010). However, *V. anguillarum* has seven copies of *rrs* (Kalia et al., 2015) and thus STR^r resulting from *rrs* mutations are unlikely when several copies of this gene are present (Springer et al., 2001).

Transposon insertion mutants of *V. anguillarum* NB10Sm were screened in *G. mellonella* and 13 had attenuated virulence. In one of these mutants (Tn134), the pJM1-like p67-NB10 virulence plasmid (Crosa, 1980; Holm et al., 2015) had been lost and thus the reduction in observed virulence was likely due to the loss of this plasmid. This could be verified by targeted

knockout of the gene in Tn134 into which TnSC189 had inserted, followed by challenge in wax moth to compare virulence between this mutant, NB10Sm, Tn134 and NB10 cured isolates. Loss of this indigenous plasmid can be spontaneous or, alternatively, the increased temperature for transposon mating (30°C compared to 22°C) may have caused cellular stress and induced some cells to multiply without the plasmid (Trevors, 1986). Confirmation of the presence of this plasmid is a valuable quality control step, as highlighted by a previous study where the inability of a *V. anguillarum* NB10 alternative σ54 sigma factor *rpoN* transposon mutant to propagate under low iron conditions was ultimately found to be due to the loss of the p67-NB10 virulence plasmid rather than a transposon insertion in *rpoN* (O'Toole et al., 1996; O'Toole et al., 1997).

Transposon insertion locations were identified for the remaining 12 *V. anguillarum* NB10Sm transposon insertion mutants (Table 4.8), of which one (Tn100) was found to be located within the middle of a putative gene on chromosome I that encodes for an uncharacterised protein. Analysis revealed a strong similarity between the predicted amino acid sequence of the final 25% of this protein and several other *Vibrio* spp. proteins. Moreover, many of these proteins, including that encoded by Tn100, had a common 20-amino acid GlyGly-CTERM domain motif at the C terminus. This motif is a membrane anchor putatively required for the post-translational processing of secreted proteins by serine proteases called rhombosortases (Haft and Varghese, 2011; Rather, 2013). Between one and

thirteen copies of the GlyGly-CTERM domain motif are found in other bacterial genomes and, in cases where there is only one rhombosortase, this is located adjacent or close by the GlyGly-CTERM protein target (Haft and Varghese, 2011). Interestingly, nucleotide analysis revealed only a single GlyGly-CTERM domain motif in *V. anguillarum* and a putative (serine) protease LA homologue (Figaj et al., 2014) located 1.2 kb and three genes distant. Furthermore, three chymotrypsin subfamily A serine proteases (VesA, VesB and VesC), all with GlyGly-CTERM domain motifs, are found in *Vibrio cholerae* (Sikora et al., 2011), and one of these (VesB) is secreted via the type II sectretion system and is involved in the post-translational processing of the cholera toxin (Gadwal et al., 2014).

Sequencing of the remaining 11 transposon/genomic DNA junctions revealed a single insertion each into genes encoding a DNA helicase rep and an RNA subunit (Eistetter et al., 1999; Gilchrist and Denhardt, 1987), and single insertions into seven genes encoding known virulence factors in *V. anguillarum* (Di Lorenzo et al., 2003; Rock and Nelson, 2006; Welch et al., 2000; Wertheimer et al., 1999) (Table 4.8). Finally, single insertions were located in two other genes encoding virulence factors: the mutant Tn73 contained a transposon insertion within the *wbhK* gene, which encodes a probable aminotransferase involved with lipopolysaccharide synthesis (Stroeher et al., 1998), while Tn205 contained a transposon insertion within the *cyaA* gene, which encodes a class II adenylate cyclase. Moreover, *cyaA* was identified to be putative virulence factor in *V. anguillarum* by *in silico*

detection of this gene, as it shares high sequence similarity with virulence factors in other bacteria (Rodkhum et al., 2006a); however, this present study confirms that these genes have the potential to play a role in virulence during infection, albeit in an insect host. In *Vibrio vulnificus* knockout of *cyaA* gene results in pleiotropic reductions in virulence, suggesting a role in regulation (Kim et al., 2005). Still, the roles of *wbhK* and *cyaA* in fish infections remain to be determined.

Additional future work to further characterise and confirm the role of genes disrupted by transposon mutagenesis in the *V. anguillarum* mutants should ensure that isolates have only incorporated single copies of the TnSC189 transposon into their genomic DNA, and this is traditionally assayed by Southern blots (Agnoli et al., 2012); However, a more efficient solution might be comparative genomic analysis (Busschaert et al., 2015), a procedure which can identify all genetic disparities between a transposon-mutated isolate and its wild-type parent. Thus, this latter technique could also elucidate single nucleotide polymorphisms potentially responsible for STR^r. Furthermore, targeted mutation and trans-complementation of these putative virulence genes and the uncharacterised putative virulence gene in the *V. anguillarum* NB10Sm parent will be necessary to confirm these genes as virulence factors (O'Toole et al., 1997). Moreover, knockout of the putative uncharacterised protein of Tn100 and the putative (serine) protease LA homologue could elucidate the relationship between these proteins and their role in virulence. Finally, further study of transposon

mutant growth *in vivo* would confirm whether the observed reductions in virulence in *G. mellonella* are related to reduced growth of the strains *in vivo*.

In summary, these experiments have demonstrated successfully that *G. mellonella* can be used to identify *V. anguillarum* virulence genes by screening a library of random transposon insertion mutants for attenuated virulence. This primary screen in *G. mellonella* is ethically more acceptable, practically feasible and more financially attractive than studies in fish, and it permits the screening of hundreds of strains for virulence attenuation prior to subsequent confirmation in fish trials. This approach has the potential to be applied to other pathogens, including other bacterial pathogens of fish, for the discovery of novel virulence factors and to rapidly improve our understanding of microbial pathogenesis and virulence.

Chapter 5. Determination of genes required for growth and virulence of *Vibrio anguillarum* by transposon insertion sequencing

5.1. Introduction

Chapter 4 established that individual *Vibrio anguillarum* transposon mutants could be screened in a *Galleria mellonella* infection model to identify genes with roles in virulence. Of course, it would be more desirable to screen large numbers of transposon mutants simultaneously in a single infection to identify suites of genes with roles in virulence. Thus, the aim of this chapter was to prepare and screen a large-library of random transposon insertion mutants to determine genes required for growth and virulence of *V. anguillarum* during infection. To do this, a transposon insertion sequencing (Tn-seq) approach was selected and this method combines two powerful components of the molecular toolkit: random transposon mutagenesis and massively parallel sequencing (Loman et al., 2012; van Opijnen et al., 2009; van Opijnen and Camilli, 2013). A related technique has been used profitably in *Vibrio cholerae* and used to produce fitness values and predict essentiality of genes (Chao et al., 2013; Kamp et al., 2013). Furthermore, one of these studies demonstrated successfully that this technique could be used to identify genes required for survival *in vivo* (Kamp et al., 2013). However, Tn-seq has not been performed previously for *V. anguillarum*.

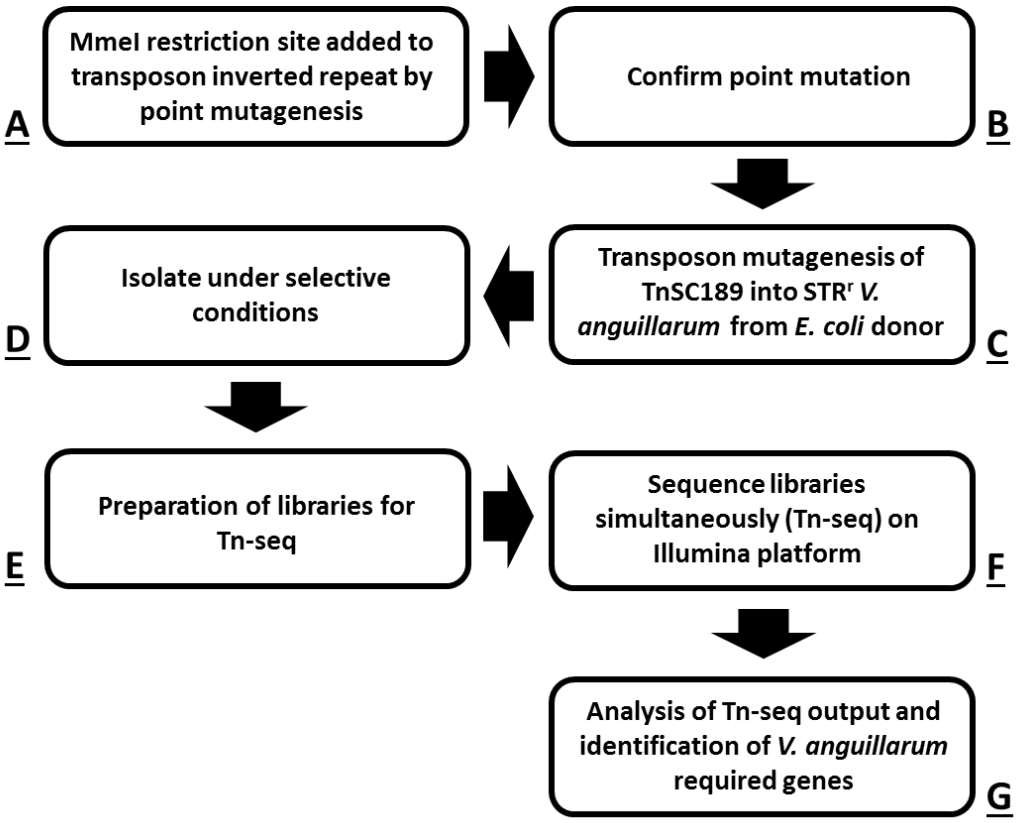

Figure 5.1. Transposon sequencing (Tn-seq) workflow. First, an MmeI restriction site was added to transposon TnSC189 by introducing a point mutation to the 5' end of the inverted repeat (A). The introduction of this point mutation was confirmed by digesting with MmeI and sequencing of this section of the plasmid (B). Then the mutagenized TnSC189 transposon was introduced into streptomycin-resistant *V. anguillarum* NB10 recipients from the *E. coli* SM10 donor (C). Transformants were isolated using antibiotic selection and then collected to give a library of *V. anguillarum* random transposon insertion mutants (D). DNA was extracted from the libraries and fragments containing transposon-genome junctions were prepared by digesting with the MmeI restriction enzyme (E). Next, DNA from each library was sequenced using the Illumina® MiSEQ platform, to produce 50-bp reads (F) and locations for each transposon insertion were mapped to the reference *V. anguillarum* sequence. Genes without any transposon insertions were considered to be required genes for growth on TSA + Streptomycin (G).

The pSC189 plasmid that carries the *mariner*-based TnSC189 transposon (Chiang and Rubin, 2002) was used to create random insertion mutants according to Section 4.2.5. An overview of the approach to determine the required genes for *V. anguillarum* NB10Sm can be found in Figure 5.1. The characterisation of random transposon insertion mutant libraries of *V. anguillarum* NB10Sm, which includes identifying the genes required for growth on TSA is the first step to using this library to determine the genes important for virulence, and this pilot study will form the foundation for future investigations, which could include identifying the genes essential for survival within the *G. mellonella* or native fish host. Moreover, this powerful approach can be applied to various aspects of *V. anguillarum* biology.

5.2. Materials and methods

5.2.1. Isolates and plasmids

Additional isolates and plasmids (Table 5.1) were recovered and propagated according to the methods described in Section 2.2.2. Plasmid DNA was isolated and then confirmed by linearisation of plasmids by BamHI digestion and gel electrophoresis according to the method of Appendix VIII. Plasmid restriction sites were located *in silico* using Bioedit software (http://www.mbio.ncsu.edu/BioEdit/bioedit.html, Ibis Biosciences; Carlsbad US).

Table 5.1. Isolates and plasmids used in this Chapter.

Isolate or plasmid	Characteristic(s)[a]	Culture medium[bc] or Donor[d]	Source or Reference
Isolates			
Vibrio anguillarum			
Laboratory collection, University of Stirling, UK			
NB10Sm	Spontaneous STR^r resistant derivative of serotype O1 NB10	TSA20/TSB20 + STR^{200}	This study
Escherichia coli			
Matthew K Waldor, Department of Microbiology and Immunobiology, Harvard Medical School, Boston, US			
SM10λ*pir*	Standard plasmid for transfer of RK4 plasmids. Contains the *pir* gene (lysogenised with λ*pir* phage). KAN^r, *thi-1, thr, leu, tonA, lacY, supE, recA*::RP4-2-Tc::Mu, *pir.*	LBA/LB + KAN^{100}	Simon et al. (1983)
Plasmids			
Matthew K Waldor, Department of Microbiology and Immunobiology, Harvard Medical School, Boston, US			
pSC189	Cloning vector bearing the *mariner* transposon; R6K *ori*; AMP^r and KAN^r	SM10λ*pir*[d]	Chiang and Rubin. (2002)
Lab collection, University of Stirling, UK			
pSC189_5'	pSC189 with single point mutation in 5' end of transposon inverted repeat region	SM10λ*pir*[d]	This study

a AMP^r, ampicillin-resistant; KAN^r, kanamycin-resistant; STR^r, streptomycin-resistant.

b TSA20, tryptone soya agar + 1.5 % NaCl; TSB20, tryptone soya broth + 1.5 % NaCl; LBA (20), Luria-Bertani agar, Miller (+ 1 % NaCl); LB (20) Luria-Bertani broth, Miller (+ 1 % NaCl).

c AMP, KAN and STR were added to media in concentrations (μg/mL) indicated in superscript.

5.2.2. Preparation of competent *E. coli* cells

E. coli SM10*λpir* (Table 5.1) was cultured to late-exponential phase in 10 mL of LB + KAN^{100} (37 °C, 16 h, 150 rpm) before 1 mL of culture was inoculated into separate 100 mL of LB (in glass bottle) and incubated (37 °C, 150 rpm) to an absorbance at 600 nm (A_{600}) of 0.3-0.4. Then the culture was placed on ice for 30 minutes before splitting between two 50-mL centrifuge tubes. Cells were harvested by centrifugation (4°C, 10 minutes, 2600 ×*g*), the supernatants were discarded, while each cell pellet was re-suspended in 12.5 mL of ice-cold sterile 100 mM $CaCl_2$ and 40 mM $MgSO_4$ and placed on ice for 30 minutes. Each aliquot was centrifuged again (4°C, 10 minutes, 2600 ×*g*), the supernatants were discarded, and the cell pellets re-suspended in 2.5 mL each of ice-cold sterile 100 mM $CaCl_2$ and 40 mM $MgSO_4$, before addition of sterile 60% (v/v) glycerol in dH_2O to a final volume of 10% (v/v). Competent cell suspensions were aliquoted (250 µL) into pre-chilled cryotubes on dry ice and stored at –70°C.

5.2.3. DNA quantification by Qubit®

Double stranded DNA (dsDNA) was quantified using a Qubit® 2.0 fluorometer (ThermoFisher Scientific Inc.) with 100-µL volumes in colourless 0.5 mL Eppendorf tubes and the whole process was completed in the absence of natural sunlight. A mastermix comprising of 1:200 (v/v) Qubit® dsDNA HS (high sensitivity) reagent in Qubit® dsDNA HS buffer was prepared and mixed according to the manufacturer's instructions. Then 95 µL of this mastermix was added to 4 µL TE buffer in each tube and then

1 µL of sample to be tested was added. Control reactions contained 95 µL mastermix and 5 µL of either of two Qubit® HS standards. Each sample was mixed by inversion, centrifuged (1000 ×*g*, 10 s) and incubated at room temperature for 5 minutes. The fluorometer was calibrated against the two control reactions and then each sample was read to calculate the concentration from the calibration data.

5.2.4. Purification of PCR products using magnetic beads

PCR amplicons were purified using Agencourt AMPure XP magnetic beads (Beckman Coulter (UK) Ltd; High Wycombe, UK) to remove excess dNTPs, salts, primers and primer dimers and contaminants <100 bp in length. A volume of Agencourt AMPure XP magnetic beads equal to 1.8× the volume of reaction to be purified was added to each sample in 1.7 mL Eppendorf tubes, before mixing on an Intelli-mixer RM-2S (00 mode, 99 rpm, 2 minutes; ELMI, Riga, Latvia), centrifuging (1000 ×*g*, 5 s) and incubating (room temperature, 5 minutes). Then, Eppendorf tubes were placed on a magnetic stand (ThermoFisher Scientific Inc.), and samples allowed to clarify before removing the supernatant. Next, samples were washed twice by adding 200 µL of 80% ethanol in water, incubating for 30 s and supernatant discarded. Then, Eppendorf tubes were removed from magnetic stand and samples allowed to air dry (room temperature, 5 minutes) before re-suspending in a volume (stated within individual experiments) of 10 mM TRIS (pH 8.0) and mixing on the Intelli-mixer RM-2S as before. Again the Eppendorf tubes were placed on the magnetic stand and each sample

allowed to clear before the supernatant (which contains the DNA) was collected and transferred to a fresh tube.

5.2.5.1. Site-directed point mutagenesis of the pSC189 plasmid

To introduce an MmeI restriction enzyme recognition site within the inverted repeat sequence of the TnSC189 transposon on the pSC189 plasmid, it was necessary to make a single nucleotide alteration (Figure 5.2). Tn-seq employs an MmeI restriction site that can conveniently be added to either or both ends of the transposon inverted repeats (Crimmins et al., 2012; van Opijnen et al., 2009). Uniquely, the MmeI restriction enzyme cuts approximately 20 bp up- or downstream of its recognition site (Figure 5.2), depending on the orientation of this sequence. With this knowledge and once the TnSC189 transposon has inserted into the DNA of a host cell, an MmeI recognition site five bases upstream from the 5' end of this transposon will ensure that the cut is located within host DNA expediting the packaging of the transposon/genomic DNA junction into products which can be standardised and prepared for Tn-seq (Figure 5.3) in only a few days.

The Quikchange II Site-Directed Mutagenesis Kit protocol (Agilent Technologies; Santa Clara, US) was used to introduce the point mutation into the TnSC189 transposon, though non-proprietary reagents were used. Primers mmeI5'F and mmeI5'R (Table 5.2) were designed to anneal to the same sequence on opposite strands of the plasmid DNA, at the 5' end of transposon TnSC189 sequence, with the appropriate point mutation and at

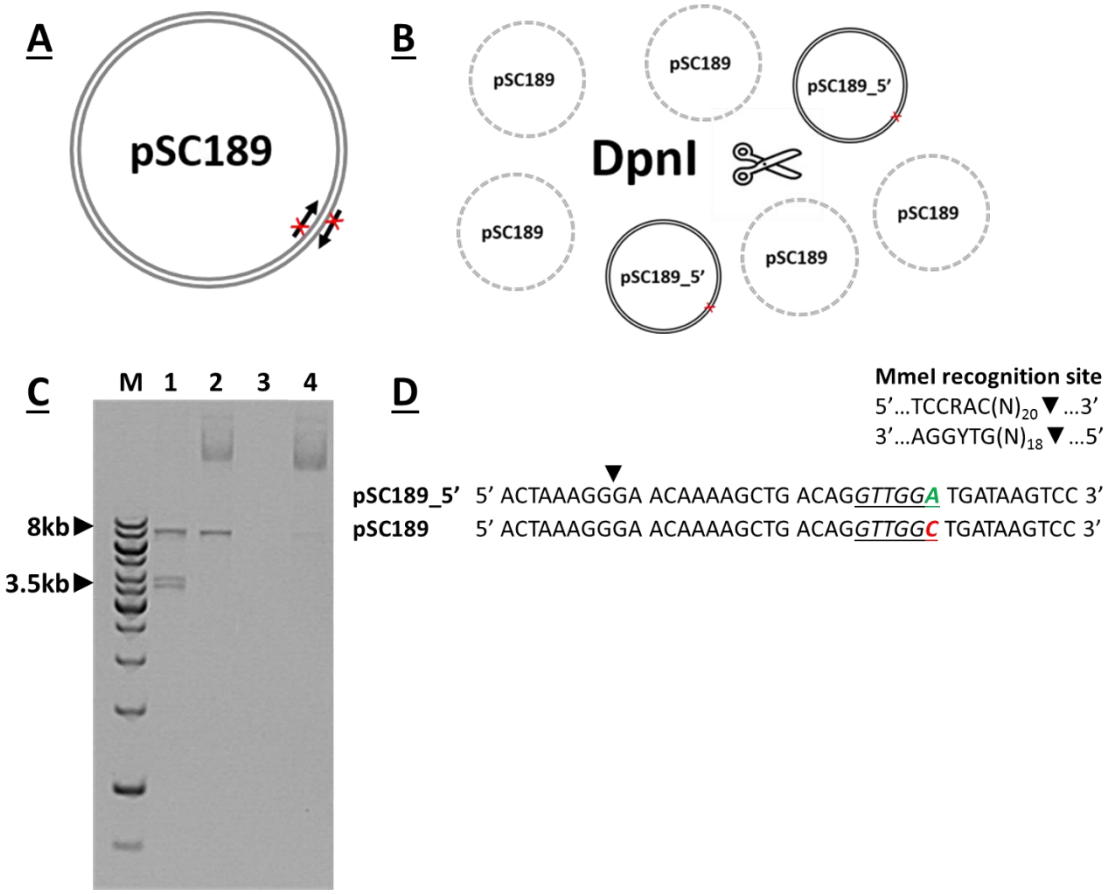

Figure 5.2. Point mutation of the pSC189 plasmid and confirmation of the C→A single substitution at the 5'-end of the inverted repeat region of the TnSC189 transposon within the plasmid to introduce an MmeI restiction site. A) mmeI5'F and mmeI5'R primers (which anneal to the same sequence on opposing strands of the plasmid) were used to amplify the entire pSC189 plasmid with a single base substitution within inverted repeat sequence at 5' end of transposon. B) Dam-methylated template DNA was removed by digestion with the DpnI restriction enzyme to leave the non-methylated amplified product pSC189_5'. C) Following transformation of the modified pSC189_5' plasmid back into *E. coli* SM10*λpir*, plasmid DNA was isolated and digested with the MmeI restriction enzyme, and then run on an agarose gel to confirm the presence of the additional MmeI cut site: M, 1kb DNA ladder; lane 1, pSC189_5'; lane 2, pSC189; lane 3, no template control; lane 4, no enzyme control. D) Finally, PCR of total DNA extracted from *E. coli* SM10*λpir* (pSC189) and *E. coli* SM10*λpir* (pSC189_5') with MmeI_Conf_5B'F and MmeI_Conf_5B'R primers were performed and the resulting products sequenced using the MmeI_Conf_5B'F primer to confirm that pSC189_5' had incorporated the single base substitution and an additional MmeI restriction site.

least 10 bases either side of this nucleotide complementary to target. Primers purified by polyacrylamide gel electrophoresis (PAGE) (Eurofins Genomics) were dissolved in nuclease free water to 10 pmol/μL. Plasmid DNA was amplified in 50 μL reactions prepared on ice, and each reaction contained 10 μL 5× HF Phusion Buffer (ThermoFisher Scientific Inc.), 125 ng of each primer (1.46 μL), 200 μM of each dNTP (1 μL, ThermoFisher Scientific Inc.), 6% dimethyl sulfoxide (3 μL, DMSO) (ThermoFisher Scientific Inc.), 20 ng of pSC189 plasmid DNA, and nuclease free water to a final volume of 49.5 μL. After mixing, by gentle flicking of bottom of tube, and briefly pulsing tubes in a centrifuge (3500 ×*g*), 0.5 μL Phusion HF polymerase (ThermoFisher Scientific Inc.) was added to a final concentration of 0.02 units/μL (U/μL) and the reaction mixed and centrifuged as before. Reactions were run in a thermocycler (TProfessional) with the lid heated to 99°C and according to this 2-step programme: 98ºC for 1 minute; then 18 cycles of denaturation at 98ºC for 10 s, and annealing and extension at 72°C for 5 minutes; followed by a final extension of 72ºC for 7 minutes; then 10ºC for 30 s to rapidly cool the reactions before placing on ice. The high primer T_m (Table 5.2) made it necessary to combine the annealing and extension step. A no template control (NTC) reaction that lacked plasmid DNA was also prepared.

5.2.5.2. Digestion of template DNA

Non-mutated template DNA is Dam-methylated (Siwek et al., 2012) and its destruction is essential to prevent transformation and selection of colonies

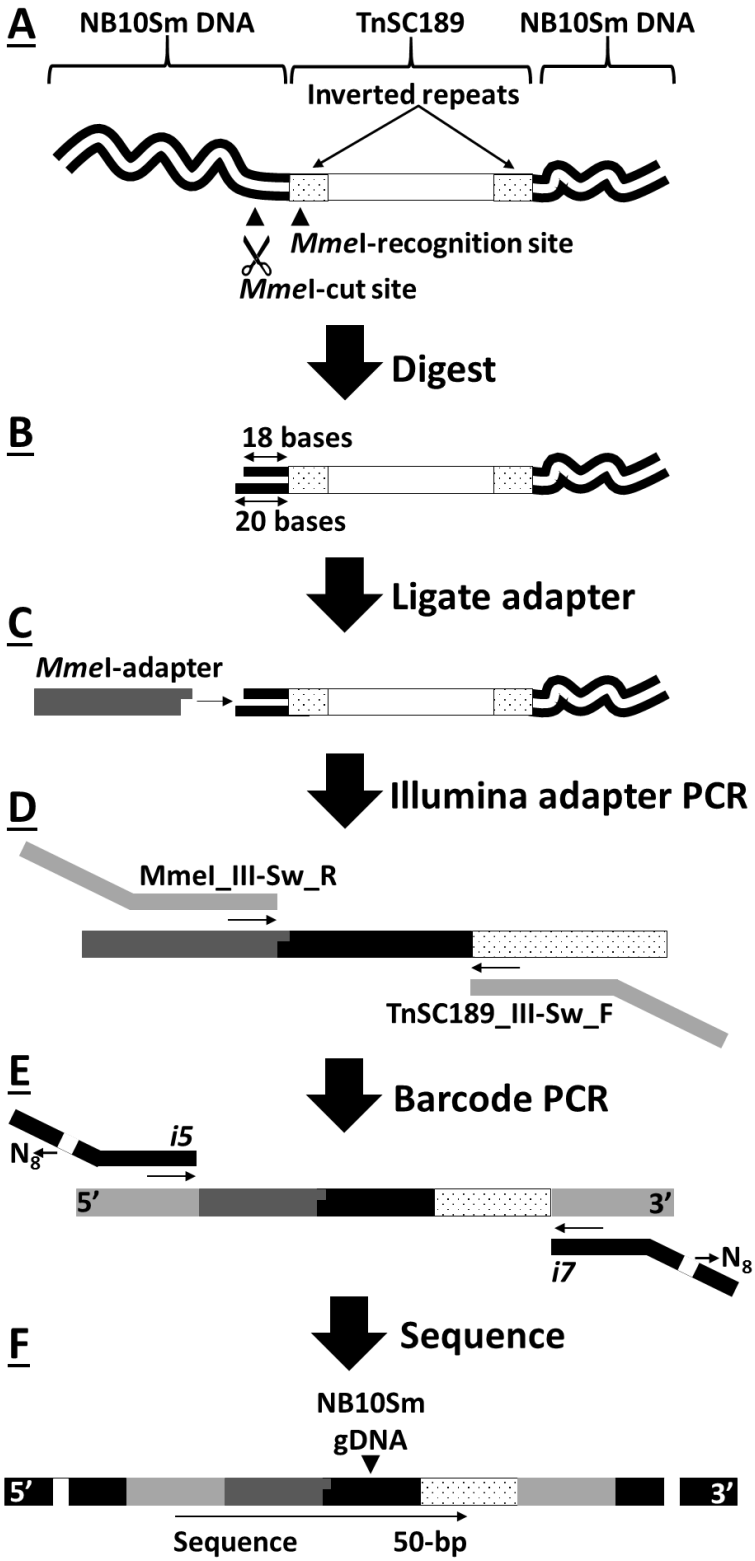
A
NB10Sm DNA
TnSC189
NB10Sm DNA
Inverted repeats
MmeI-recognition site
MmeI-cut site
Digest
B
18 bases
20 bases
Ligate adapter
C
MmeI-adapter
Illumina adapter PCR
D
MmeI_III-Sw_R
TnSC189_III-Sw_F
E
Barcode PCR
i5
N8
5'
3'
i7
N8
F
Sequence
NB10Sm
gDNA
5'
3'
Sequence
50-bp

Figure 5.3. Workflow of Tn-seq library preparation and sequencing, starting with the *V. anguillarum* NB10Sm pooled transposon mutant genomic DNA. The TnSC189 transposon inserted at a random location in the host genomic DNA of many thousands of *V. anguillarum* NB10Sm cells and this created a library of unique mutants (this was performed on three independent occasions). A) DNA was digested with the MmeI restriction enzyme, which has a recognition site in the 5' end inverted repeat region of TnSC189 insert. B) MmeI produces a staggered cut up- or downstream of the recognition site, depending on orientation. The MmeI restriction site on the TnSC189 transposon initiates a cut 18 nucleotides up-stream of recognition site on the leading strand, 14 of which are host DNA. C) A double-stranded adapter was ligated to the sticky ends resulting from cleavage by MmeI digestion to produce a substrate for Illumina primers to anneal to in the next step. D) PCR products were amplified with TnSC189_III-Sw_F and MmeI_III-Sw_R primers, which were designed to correspond to the inverted repeat region of TnSC189 and double-stranded adapter respectively. Thus, only DNA fragments containing the transposon insertion are amplified, and not any DNA fragments generated from cleavage of genomic DNA at naturally occurring MmeI cut sites in the NB10Sm genome (there are 2908 other MmeI recognition sequences in the *V. anguillarum* NB10Sm genome). Furthermore, each of these primers has an Illumina® adapter overhang that assists the next step. E) A further round of PCR amplified previous round products, with Illumina® Nextera v2 XT index primers (i5 – forward; i7 – reverse) required for multiplex sequencing by annealing these to the overhangs produced in the previous round. This produced products of 209 bp and each library contained has a unique tag for post-sequencing analysis. F) Libraries were sequenced from the 5' end, through the MmeI adapter and the *V. anguillarum* NB10Sm genomic DNA

Table 5.2. Oligonucleotides used in this Chapter.

Target	Primer	5'-3'[a]	Amplicon length (bp)	Annealing temperature (°C)	Source or Reference
TnSC189 inverted repeat 5' region	**mmel5'F** **mmel5'R**	**F:** GCTGACAGGTTGG**A**TGATAAGTCCCC[a] **R:** GGGGACTTATCA**T**CCAACCTGTCAGC[a]	6982	72	**This study** **This study**
pSC189 plasmid site directed mutagenesis confirmation.	MmeI_Conf_5B'F MmeI_Conf_5B'R	**F:** CACGACAGGTTTCCCGACTG **R:** ACCGAGATAGGGTTGAGTGTTG	441	57	**This study** **This study**
Adapters for ligation to MmeI sticky end.	**AP-A_bc-ACAC** **AP-b_bc-ACAC**	GTTCAGAGTTCTACAGTCCGACGATCACACnN 5phos/GTGTGATCGTCGGACTGTAGAACTCTGAACCTGTC/3phos	-	-	**van Opijnen and Camilli (2010)** **van Opijnen and Camilli (2010)**
TnSC189 inverted repeats and MmeI adapter	**TnSC189_III-Sw_F** **MmeI_III-Sw_R**	**F: GTCTCGTGGGCTCGGAGATGTGTATAAGAGACAG**AGACCGGGGACTTATCATcC[bc] **R: TCGTCGGCAGCGTCAGATGTGTATAAGAGACAG**GTTCAGAGTTCTACAGTCCgA[bc]	140	55	**This study** **This study**
Illumina® Nextera adapter and indexing primers	**Nextera XT index 1** **Nextera XT index 2**	**F:** CAAGCAGAAGACGGCATACGAGAT[i7][d]GTCTCGTGGGCTCGG **R:** AATGATACGGCGACCACCGAGATCTACAC[i5][d]TCGTCGGCAGCGTC	209	55	**Illumina** **Illumina**

a Nucleotides in bold indicate base change for site-directed mutagenesis
b Nucleotides in lower case indicate a phosphorothioate bond.
c Nucleotides in bold indicate Illumina® overhang adapter sequences
d 8 base Index sequences i7 and i5 are detailed in Table 5.4

without the required point mutation. To remove the DNA template, thus leaving only the amplified PCR products (Figure 5.2), 1 µL of DpnI (10 U/µL) [ThermoFisher Scientific Inc.], a restriction enzyme that digests Dam-methylated DNA, was added to each reaction. The tube contents were mixed by pipette aspiration and centrifuged (1 minute, 1000 ×*g*) before incubating at 37°C for 1 h. Following digestion, samples proceeded to the next step without heat denaturation of DpnI.

5.2.5.3. Plasmid transformation into delivery vector

Modified pSC189 plasmids (now expected to contain the point mutation) were transformed back into *E. coli* SM10*λpir*. Competent *E. coli* SM10*λpir* cells (prepared as described in Section 5.2.2) were thawed on ice and a 50 µL aliquot transferred to round-bottomed 15-mL culture tubes. Then, 0.85 µL of ß-mercaptoethanol (14.3 M) was added to each aliquot before incubating on ice for 10 minutes with occasional agitation by gently rotating the tubes. Then, 10 µL of the DpnI digested plasmid point mutagenesis reaction was added to each tube and the contents mixed by pipette aspiration before incubation for 30 minutes on ice. Sample tubes were heat shocked (42°C for 30 s) and then returned immediately to ice for 2 minutes. Thereafter, 500 µL of LB broth (pre-heated to 37°C) was added to each reaction and the tubes were incubated (37°C, 1 h, 225rpm). Then, the total volume of each reaction was spread equally across two LBA + AMP^{100} plates and these were incubated (37°C, 24 h).

5.2.5.4. Confirmation of point mutation and sequencing

To confirm that the desired point mutation had been introduced into pSC189_5' the following two step process was performed. First, pSC189_5' DNA and negative control pSC189 DNA was digested with the MmeI restriction enzyme and the resulting digestion products run on an agarose gel. For this, reactions of 50 µL were prepared containing 500 ng of plasmid DNA, 5 µL of 10× Cutsmart Buffer® (New England Biolabs® Inc; Ipswich, USA), 50 µM S-adenylosylmethionine (SAM; New England Biolabs®), 0.5 µL MmeI (2000 U/mL; New England Biolabs®), and the final volume made up with nuclease free water. The reactions were mixed by gently flicking the bottom of tube, and incubated (37°C, 15 minutes) before the digestion was deactivated (65°C, 20 minutes) and then cooled (10°C, 30 s). A NTC was also included, and products from digested samples and NTCs were run on agarose gels as described previously Appendix VIII.

Second, DNA from *E. coli* SM10 *λ pir* (pSC189_5') and the parent *E. coli* SM10 *λ pir* (pSC189) was used as templates for PCR to amplify products with MmeI_Conf_5B'F and MmeI_Conf_5B'R primers (Table 5.2). The PCR was performed at an annealing temperature of 57°C and in accordance with a method described previously (Section 2.2.5.3.), except that the volumes of each constituent in the reaction were doubled (total final volume = 20 µL). PCR with the template DNA from *E. coli* SM10 *λ pir* (pSC189_5') was performed in duplicate. PCR products were purified (as Section 4.2.8.3) and prepared for Lightrun™ (GATC Biotech, London, UK) sequencing as

described previously (Section 4.2.8.4.) using the MmeI_Conf_5B'F primer as template. Resulting sequences were aligned in Bioedit as described in Section 4.2.8.5.

5.2.6. Preparation of transposon mutant libraries

5.2.6.1 Transposon mutagenesis

To generate three large libraries of random insertion mutants, transposon mutagenesis was performed by a protocol modified from Section 4.2.5. The *E. coli* SM10 *λ pir* (pSC189_5') donor strain was cultured overnight to late exponential phase (37°C, 120 rpm) in 10 mL of LB + AMP^{100} in a universal bottle. Then 5 mL of this starter culture was used to inoculate 50 mL of LB + AMP^{100} in a 250-mL flask and incubated to stationary phase (37°C, 150 rpm, 4 h). The *V. anguillarum* NB10Sm recipient strain was cultured to stationary phase overnight (22°C, 150 rpm) in 50 mL of TSB20 + streptomycin STR^{200} in a 250-mL shakeflask. Donor and recipient cell cultures were prepared in triplicate, with each inoculated initially from separate single colonies. A plasmidless *E. coli* SM10 *λ pir* culture (to act as negative control for transposon mating) was prepared according to the same method as for the donor strain.

Cells from 9 mL of *V. anguillarum* NB10Sm culture and 18 mL of *E. coli* SM10 *λ pir* (pSC189_5') culture were harvested separately by centrifugation and washed in PBS as previously described (Section 2.2.2), except that the larger volume of *E. coli* SM10 *λ pir* (pSC189_5') required greater centrifugal

force (3400 ×*g*). Then, harvested *V. anguillarum* NB10Sm and *E. coli* SM10*λpir* (pSC189_5') were combined and re-suspended in 2.5 mL PBS. Aliquots of 100 µl combined bacterial suspension were pooled onto each of eighteen 0.22-µm cellulose nitrate filters (Sartorius UK Ltd; Epsom, UK) that had been placed onto Petri dishes containing LBA20. The liquid droplets were allowed to dry at room temperature for 1 h, before the agar plates were sealed with paraffin film and incubated (30°C, 24 h). This process was completed in triplicate for the three separate libraries. A single negative control mating of *E. coli* SM10λ*pir* with *V. anguillarum* NB10Sm was prepared as described above, except that only six 100 µL aliquots were inoculated onto filters. The CFU/mL of each bacterial strain in the inoculum 'input' pools was enumerated by preparing 10-fold dilutions and plating on LB + AMP^{100} for *E. coli* SM10 *λ pir* pSC189_5', LB + kanamycin $(KAN)^{100}$ for *E. coli* SM10 *λ pir* and TSA20 + STR^{200} for *V. anguillarum* NB10Sm.

Next, the filters from each independent mating for library preparation were placed into separate 7 mL aliquots of TSB20 and vortexed vigorously for 1 minute, before 250 µL of bacterial suspension was spread onto TSA20 + KAN^{250} + STR^{100} in each of 18 × 140-mm Petri dishes. Bacterial suspension was diluted 10-fold in PBS and 50 µL was spread onto TSA20 + KAN^{250} + STR^{100} in each of 4 × 90-mm Petri dishes. This process was repeated for the negative control mating, except that the filters were suspended in only 3 mL of TSB20 and bacterial suspension was plated crude, onto TSA20 + KAN^{250} + STR^{100} in each of 4 × 90-mm Petri dishes only. All transposon mutant selection plates were dried (room temperature, 1 h) before incubation (22°C,

72 h) to allow colonies to form. Remaining experimental bacterial suspensions were plated, following a previous method (Section 4.2.5.) to enumerate 'output' donor and recipient cells. Transposition frequency was calculated following a previous method (Section 4.2.5).

5.2.6.2. Library preparation

Following enumeration of colony forming units (CFU), 12 colonies from each mating were sub-cultured onto the same agar to confirm that they had retained their antibiotic resistance and thus, the transposon. Next, all colonies from each independent mating were collected by flooding each plate with 2 mL of TSB20 + KAN^{250} + STR^{100}, disrupting colonies with a sterile inoculation loop, and collecting by pipette before drawing up and pooling to give three independent random transposon mutant libraries. Each library was incubated (22°C, 1 h, 150 rpm), harvested (2600 ×*g*, 15 minutes, 20°C), re-suspended in TSB20 containing 15% (v/v) glycerol, and corrected to approximately 1 $\times 10^9$ CFU/mL in the same broth by measuring A_{600} following Section 2.2.2. These diluted transposon mutant libraries were pipetted into separate 1 mL aliquots and stored at -70°C.

5.2.7. Processing of random transposon mutant libraries for Tn-seq

5.2.7.1. Library selection

Duplicate aliquots for each of the three independent transposon mutant libraries were thawed on ice and then 0.5 mL of each aliquot was added to 5 mL TSB20 + KAN^{250} + STR^{100} in a Universal bottle. The cultures were

incubated (22°C, 150 rpm) until reaching an A_{600} of 0.1-0.2 AU (approximately 3 h). CFU/mL was enumerated for each culture by preparing 10-fold dilutions in PBS and plating on to TSB20 + KAN^{250} + STR^{100} as in section 2.2.2.

5.2.7.2. Library DNA Extraction

Bacteria in 3 mL of each culture were harvested by centrifuging (18000 ×*g*, 1 minute). The supernatants were discarded while the cells were re-suspended in 1 mL of STE buffer before centrifuging again (18000 ×*g*, 1 minute). The supernatants were discarded and each sample was re-suspended in 600 µL of 1% (v/v) sodium dodecyl sulphate (SDS) in SSTNE (NaCl -SDS-Tris-NaCl-EDTA) lysis buffer (Appendix II) Finally, 3 µL of proteinase K (10 mg/mL) was added to each sample and left to incubate overnight (55°C).

Each sample was cooled to room temperature and 10 µL of RNase A (2 mg/mL; ThermoFisher Scientific Inc.) was added before mixing by inversion, centrifuging (1000 ×*g*, 5 s) and incubating (37°C, 1 h). Then each sample was cooled to room temperature before 360 µL of 5 M NaCl was added, to precipitate proteins and mixed by vortex for 30 s, and then incubated on ice for 10 minutes. Samples were centrifuged (20000 ×*g*, 10 minutes) before the supernatant was transferred into a new Eppendorf tube and centrifuged again (20000 ×*g*, 10 minutes) to remove residual protein precipitate. Thereafter, the supernatant volume was transferred

into 600 µL of isopropanol and mixed by inversion six times to precipitate the DNA.

Precipitated DNA was harvested by centrifugation (20000 ×*g*, 10 minutes), and then the supernatant was removed by pipette and replaced with 1 mL of 70% ethanol. DNA pellets were re-suspended, by gentle flicking of bottom of tube, before the samples were incubated on a tube rotator (2 h, 12 rpm; Stuart; Bibby Scientific Ltd, Stone, UK). Each sample was centrifuged (20000 ×*g*, 10 minutes) before the supernatant was discarded, replaced with 900 µL of 70% ethanol, and incubated on the tube rotator (1.5 h, 12 rpm). Samples were centrifuged (20000 ×*g*, 10 minutes), the supernatant was removed by pipette, and the pellet was allowed to air dry for 5 minutes before 15 µL of elution buffer AE (Qiagen) was added. Each sample was incubated overnight at 4°C to allow the DNA to dissolve completely. DNA concentration and quality was measured spectrophotometrically against a blank of AE buffer as described previously (Section 2.2.5.1), and then the samples were stored at 4°C until needed.

5.2.7.3. Confirmation of DNA integrity

To confirm that DNA extracts had not excessively fragmented, degraded or been contaminated with RNA, samples were run on a 0.9% agarose gel made with 0.5× TAE and ethidium bromide (EtBr, to 0.08 µg/mL) following a previous method (Section 2.2.5.4). Samples of 6 µL were prepared to contain 50 ng of DNA in 5 µL nuclease free water and 1 µL of 6× loading dye. A marker of 100 ng of lambda DNA/HindIII (5 µL in TE, ThermoFisher

Scientific Inc.) and 1 µL of 6× loading dye was added to the gel to semi-quantify the DNA concentration in each sample. A negative control of DNA known to be contaminated with RNA (RP4; lab collection) was included for comparative purposes. The agarose gel was run at 75 V and photographed following a previous method (Section 2.2.5.4).

5.2.7.4. Library digestion and purification

Genomic DNA was cleaved close to one end of the TnSC189 transposon insertion site at the MmeI restriction site according to the method of van Opijnen and Camilli (2010) [Figure 5.1]. Briefly, for each library 3 µg of DNA was digested in reactions containing 3 µL MmeI (2000 U/mL) [New England Biolabs®], 20 µL of 10× Cutsmart Buffer® (New England Biolabs), 0.44 µL of 32 mM SAM (New England Biolabs®), and then volume was made up to 200 µL with nuclease free water before incubation (37°C, 2.5 h). To prevent re-ligation after digestion, 20 units of calf intestinal phosphatase (CIP; New England Biolabs®) was added to each reaction and incubated for a further hour at 37°C. Calf intestinal phosphatase catalyses the removal of phosphate groups from the 5' ends of DNA strands and so prevents re-ligation. DNA was purified to remove enzymes that could reduce the efficiency of downstream steps according to a method modified from Moore and Dowhan (2002). First, 200 µL of phenol/chloroform/isoamyl alcohol (25:24:1, v/v/v) was added to each reaction and these were mixed by vortex for 10 s before centrifugation (20000 ×*g*, 1 minute). Using wide-bore pipette tips, 150 µL of the top (aqueous) phase, containing the DNA, was

transferred to a fresh Eppendorf tube and to this was added 150 µL of phenol/chloroform/isoamyl alcohol (25:24:1, v/v/v). The sample was processed as above, except that only 100 µL of the top phase was collected. To precipitate the DNA in the sample, 3 M sodium acetate (pH 5.2) was added to 1/10 (v/v) and mixed by vortex, before addition of 250 µL of ice-cold 95% ethanol, incubation (-70°C, 30 minutes), centrifugation (20000 ×g, 10 minutes) and removal and disposal of the supernatant. The precipitated DNA was washed twice by adding 1 mL of 70% ethanol. The samples were incubated on a tube rotator (1 h, 12 rpm), centrifuged (20000 ×*g*, 10 minutes) and the supernatant discarded. Following a second wash of the DNA pellets, these were allowed to air dry for 5 minutes before 25 µL nuclease free water was added to dissolve the DNA overnight at 4°C. DNA concentration and quality was measured spectrophotometrically against a blank of nuclease free water as described previously (Section 2.2.5.1).

5.2.7.5. Ligation of adapter

To produce fragments that can be amplified by PCR, an adapter was ligated to the sticky end resulting from MmeI digestion according to a published protocol (Figure 5.3; van Opijnen and Camilli, 2010). Briefly, adapter oligonucleotides (AP-A_bc-ACAC and AP-b_bc-ACAC; Table 5.2) were synthesised by Eurofins Genomics and purified by high performance liquid chromatography (HPLC) before dissolving in 10 mM TRIS.Cl (pH 8.5) to 0.2 mM. Then 100 µL of each adapter oligonucleotide was mixed together and incubated (96°C, 2 minutes). This preparation was cooled at room

temperature for 20 minutes, before aliquots of 20 µL were prepared and frozen at -20°C.

To each whole sample of purified DNA from Section 5.2.7.4 was added 1 µL of the adapter oligonucleotide preparation , 400 U of T4 DNA ligase, 3 µL of 10× DNA ligase buffer (New England Biolabs®) and 1.2 µL of nuclease free water, and these were incubated (16°C, 16 h), and subsequently deactivated (65°C, 10 minutes).

5.2.7.6. Insert fragment amplification and addition of Nextera adapter sequences

The DNA fragments covering the junction between the inverted repeat of the TnSC189 transposon and the *V. anguillarum* NB10Sm genomic DNA were amplified and indexed in a two-step process (Figure 5.3). This first step used the HPLC-purified primers, TnSC189_III-Sw_F and MmeI_III-Sw_R (Eurofins Genomics) (Table 5.2), which were complementary to the inverted repeat region of the TnSC189 transposon and the adapter oligonucleotide (that has overhanging Illumina® adapter sequences), following a modified version of the Illumina® 16S Metagenomic DNA sequencing library preparation protocol (Illumina, 2016).

Primers were dissolved in 1× TE (pH 8.0) to 100 µM and stored at -20°C, and these stocks were diluted to 1 µM in nuclease free water when required. Each DNA sample was diluted to 5 ng/µL in 10 mM TRIS (pH 8.0) following dsDNA quantification by Qubit® analysis (Section 5.2.3). Then a 140-bp target sequence was amplified in 25-µL reactions containing 12.5 µL of Q5®

Hot start HF 2× Mastermix (New England Biolabs®), 5 µL each of the TnSC189_III-Sw_F and MmeI_III-Sw_R primers, 5 µL of nuclease free water and 2.5 µL of DNA sample. Reactions were run on a thermocycler (TProfessional) with the lid heated to 99°C according to the following conditions: 98ºC for 90 s; then 25 cycles of denaturation at 98ºC for 30 s, annealing at 55ºC for 30 s, and extension at 72ºC for 30 s; followed by a final extension of 72ºC for 5 minutes; then 10ºC for 30 s. A NTC was included.

Reactions were purified by paramagnetic bead (Section 5.2.4) and the dsDNA concentration quantified by Qubit® analysis (Section 5.2.3). Then each sample was run on an agarose gel to confirm that the majority of PCR products were of the expected size (144-bp). For this, each sample well of the gel contained 10 ng of DNA in 5 µL of nuclease free water and 1 µL of 6× loading dye, and the gel was prepared and run according to Section 5.2.7.3, except that the marker well contained 0.1 µg of a 100-bp ladder (ThermoFisher Scientific Inc.) 4.8 µL of nuclease free water and 1 µL of 6× loading dye. Additional controls consisted of template DNA only (to confirm that no non-specific amplification occurred), and the products of a PCR that had not been purified with magnetic beads (to confirm the purification had been successful).

A second PCR was performed to attach Illumina® index adapters to the PCR products (which had Illumina overhang adapter sequences attached above) (Figure 5.3). Each sample was amplified in duplicate using Nextera XT v2 index primers (Illumina®; San Diego, US) (Table5.2) with i7 and i5

Table 5.3. *Vibrio anguillarum* transposon (Tn) libraries and Illumina® Nextera XT index number and sequences, incorporated into sequencing adapter primers for sequencing on the MiSeq platform for each of three independent random transposon libraries that had been processed in duplicate. This produced a total of six libraries (1A, 1B, 2A, 2B, 3B and 3B) which were prepared in duplicate and sequenced to identify transposon/genomic DNA junctions at insertion locations.

Tn library	MiSeq index Number	i7 barcode	i7 sequence	i5 barcode	i5 sequence
1A	1	N701	TAAGGCGA	S502	CTCTCTAT
1B	2	N702	CGTACTAG	S503	TATCCTCT
2A	3	N703	AGGCAGAA	S505	GTAAGGAG
2B	4	N704	TCCTGAGC	S506	ACTGCATA
3A	5	N705	GGACTCCT	S507	AAGGAGTA
3B	6	N706	TAGGCATG	S508	CTAAGCCT
1A	7	N707	CTCTCTAC	S508	CTAAGCCT
1B	8	N710	CGAGGCTG	S507	AAGGAGTA
2A	9	N711	AAGAGGCA	S506	ACTGCATA
2B	10	N712	GTAGAGGA	S505	GTAAGGAG
3A	11	N714	GCTCATGA	S503	TATCCTCT
3B	12	N715	ATCTCAGG	S502	CTCTCTAT

barcodes (Table 5.3). Importantly, each of the biological (three independent libraries prepared in duplicate) and technical replicates (each of these six samples had been split into two aliquots as stated above) were barcoded uniquely to yield 12 sample libraries for sequencing. A 209-bp target was amplified in 25-µL PCRs prepared to contain 12.5 µL of Q5® Hot start HF 2× Mastermix (New England Biolabs®), 2.5 µL each of Nextera XT index 1 (i7) Nextera XT index 2 (i5) primers, 5 µL of nuclease free water and 2.5 µL of purified first round PCR products. Reactions were run on a thermocycler (TProfessional) with the lid heated to 99°C, and according to the following conditions: 98ºC for 90 s; then 8 cycles of denaturation at 98ºC for 30 s, annealing at 55ºC for 30 s, and extension at 72ºC for 30 s; followed by a final extension of 72ºC for 5 minutes; and then cooled (10ºC, 30 s).

Reactions were purified (as Section 5.2.4), dsDNA concentration quantified by Qubit® analysis (Section 5.2.3), and an aliquot of each sample run on agarose gel to confirm that products were the size (209-bp), according to the method earlier in this Section. A control of first round PCR product was included to confirm the size difference of products.

5.2.7.7. Processing and loading onto MiSeq

Libraries were initially standardised to 20 nM concentration in EB Buffer (Qiagen) using the following equation: nM = (((concentration in ng/µL) / (660 × amplicon length [bp]))×10^6), and then 3 µL of each library was pooled before the dsDNA concentration was determined again by Qubit®, (Section 5.2.3). To correct the final pooled sample to 10nM, 10 µL of the pooled

library sample was added to 12.9 µL of EB buffer and 2.5 µL of 1% (v/v) TWEEN®20 in nuclease free water. The library sample was further diluted 2:3 (Library: nuclease free water) before addition of 5 µL of 0.2 M NaOH and incubation (room temperature, 5 minutes). Then 990 µL of buffer HT1 (Illumina) was added to reduce the library sample concentration to 20 pM. From this, a sample for sequencing was prepared by adjusting to 11 pM using 300.3 µL of the 20 pM library sample, 270 µL of buffer HT1 and 29.7 µL (to a final concentration of 9% and 11pM) 20 pM PhiX (Illumina, 2016c). PhiX is a sequencing control added to libraries of low complexity to improve sequence read quality.

The sample was denatured (98°C, 2 minutes), incubated on ice for 5 minutes, and loaded onto the MiSeq platform (Illumina) prepared with a 50-cycle v2 reagent kit (Illumina) to generate up to 15 million reads.

5.2.8. Data analysis

First, primers and adapters were clipped from each of the single reads using the Cutadapt software (https://cutadapt.readthedocs.io/en/stable/). Then the unique variable read regions (which correspond to the genomic DNA that had been amplified) were aligned using Bowtie (http://bowtie-bio.sourceforge.net/index.shtml) to *V. anguillarum* 775 chromosome I (NC_015633) and chromosome II (NC_015637), *V. anguillarum* M3 pJM1-like virulence plasmid (NC_022225) and two smaller un-published plasmid sequences deposited in Genbank: pLO2 (NC_009351) and pJV (NC_019325). Then, transposon insert coverage maps were generated using GView v1.7.

(https://www.gview.ca/wiki/GView/WebHome; Petkau et al., 2010). Genes, excluding all transfer ribonucleic acids (tRNAs), were defined as putatively required if no transposon insertions were detected within the first 90% of the gene sequence, and then these identified genes were aligned to the putative essential genes of *V. cholerae* E7946 determined previously (Kamp et al., 2013) using BLASTn (only alignments with E value scores < 1×10^{-10} were considered to be homologous genes for this analysis). Quality control data for the sequencing were generated by the MiSeq platform and analysed according to Illumina (Illumina, 2016b).

5.3. Results

5.3.1. Site-directed point mutagenesis of the pSC189 plasmid

A single point mutation (C to A) was introduced successfully into the 5'-end inverted repeat of the TnSC189 transposon by PCR to generate the pSC189_5' plasmid. Transformation of the mutated pSC189_5' plasmid into *E. coli* SM10*λpir* yielded a single colony on LB +AMP^{100}.

The presence of the expected point mutation in the pSC189_5' plasmid of the single *E.coli* SM10*λpir* colony was confirmed by digestion with MmeI. *In silico* analysis of a sequenced pSC189 plasmid fragment, generated by PCR, revealed the presence of a single constitutive MmeI recognition site (Figure 5.2), which would lead to a staggered cut of the DNA at 18 nucleotides upstream on the leading strand at 5184 bp. Thus, if the single nucleotide substitution of pSC189_5' had been performed successfully and at the correct site, the plasmid would have gained a second MmeI restriction site

and so would produce two products of similar size on agarose gel when digested with this enzyme. Digestion with MmeI of PCR product from the pSC189_5' plasmid produced two bands compared to just one larger band for the pSC189 plasmid (Figure 5.2), thus indicating that the pSC189_5' plasmid had acquired the correct point mutation and an additional MmeI recognition site. However, a single larger molecular weight band was also visualised in the lane containing the pSC189_5' sample which is probably due to religation, while a large fragment also observed for the pSC189 plasmid is likely due to incomplete digestion (Figure 5.2). As expected, no DNA products were visualised in the no template control lane.

5.3.2. Preparation of transposon mutant libraries

Three independent random transposon insertion libraries of *V. anguillarum* NB10Sm were prepared and recovered on TSA20 + KAN^{250} + STR^{100}, and these were estimated from colony counts to contain 5500, 9900 and 15300 mutants, respectively (Table 5.4), although the transposition frequency for each of these matings was approximately 10 times lower than achieved previously (Section 4.3.4). As expected, no colonies were recovered on TSA20 + KAN^{250} + STR^{100} from the negative control mating, which was performed with *E. coli* SM10 λ pir lacking the plasmid pSC189. A selection of 12 transposon mutants, from each insertion library, grew after sub-culture on to fresh TSA20 + KAN^{250} + STR^{100}, thus confirming the expected antibiotic phenotype profile of successful transformants.

Table 5.4. Estimated number of *V. anguillarum* NB10Sm random transposon mutants recovered from matings with *E. coli* SM10 (pSC189_5') and pooled to form three independent libraries. Transposition frequency for each mating was calculated as the ratio of colony forming units (CFU) that recovered onto agar containing kanamycin (KAN) and streptomycin (STR) divided by CFU recovered onto agar containing STR only.

Library name	Number of colonies recovered from each library	Transposition frequency
1	9900	1.12×10^{-7}
2	15300	1.34×10^{-7}
3	5500	8.26×10^{-8}

5.3.3. Transposon library quality and yield

Spectrophotometric and agarose gel electrophoresis confirmed that the DNA extracted was of a purity and quality for subsequent processing and sequencing (Figure 5.4). Indeed, each transposon mutant library demonstrated similar yields and both A260/A230 and A260/A280 ratios (Table 5.5) indicating that all of the samples were of sufficient yield and purity for subsequent experimentation. All samples migrated on agarose gels to give well-defined bands indicating minimal fragmentation of DNA or RNA contamination (Figure 5.4). However, the intensity of bands suggested a yield as much as twice that estimated by NanoDrop spectrophotometry. The Lambda DNA/HindIII marker contains eight fragments of lambda DNA after HindIII digestion. The largest band (at 23130 bp) contributes approximately 50% of the total mass of all the Lambda DNA/HindIII fragments. Thus, when100 ng of marker is loaded the 23130 bp band should be comparable to 50 ng of DNA in the experimental sample. In addition to a faint band at the same position as all experimental samples, the negative control RP4 sample produced a fast-moving smear, which is characteristic of RNA contamination and this migrated past the second smallest band (564 bp) of the Lambda DNA/HindIII marker (Figure 5.4).

5.3.4. Ligation of Illumina and Illumina Nextera index adapters by PCR

Following successful MmeI adapter ligation using T4 DNA ligase, PCR amplification produced products containing the 5' end of transposon TnSC189 insert site and approximately 16 bp of genomic DNA; thus,

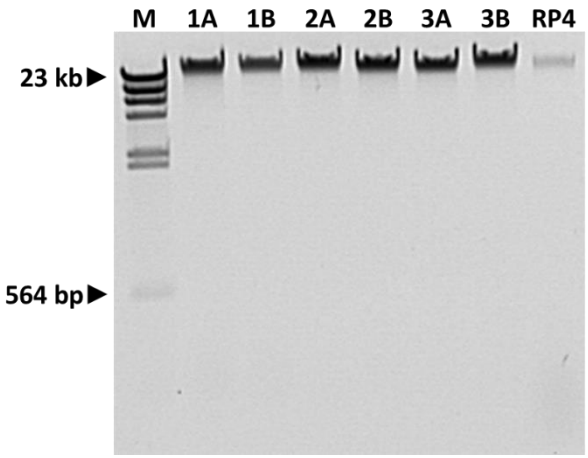

Figure 5.4. Image of agarose gel following electrophoresis of DNA extracted from each of three independent *Vibrio anguillarum* NB10Sm random transposon libraries: M, 100 ng of lambda DNA/HindIII marker; 1A, 1B, 2A, 2B, 3A and 3B, duplicate 50 ng samples (A and B) of DNA from each transposon library (1, 2 and 3 processed in duplicate); RP4, DNA sample contaminated with RNA, which produced a weak smear (not visible on this reproduced gel image).

Table 5.5. Transposon library DNA concentration and purity as measured spectrophotometrically by determining absorbance ratios at A_{260}/A_{280} and A_{260}/A_{230}. These products are derived from three separate transposon libraries processed in duplicate.

Library number	Yield (ng/µL)	Ratio (A_{260}/A_{280})	Ratio (A_{260}/A_{230})
1A	392.24	1.91	2.36
1B	451.4	1.85	2.34
2A	225.63	1.87	2.33
2B	279.96	1.98	2.27
3A	236.87	1.97	2.33
3B	239.64	2.16	2.31

selecting from the other 2908 possible fragments of NB10Sm DNA, produced during MmeI digestion. Moreover, the primers used for this Illumina adapter PCR step had tailed sequences to provide secondary PCR sites complementary to the Illumina® indexing primers used in the next step (Table 5.2). Quality control agarose gel electrophoresis of PCR products from each library sample (once these had been purified using magnetic beads) revealed the presence of a band at ca. 140 bp in each sample, which corresponded to the expected product size (Figure 5.5). Furthermore, the PCR amplified, but not purified, sample revealed a fast-migrating smear, which is indicative of dNTPs, primers and primer dimers, as might be expected. Although a similar smear was evident in the no template control lane, the smear was absent from bead-purified samples demonstrating the successful removal of contaminants that could disrupt downstream reactions. A final control reaction that contained template DNA only revealed a large, slow-migrating, smear. This is likely due to the many unamplified *V. anguillarum* NB10Sm genomic DNA fragments, generated after digestion with the MmeI restriction enzyme.

A further agarose gel confirmed the successful addition of the Illumina® Nextera XT index adapters, by PCR, to each of the library samples (Figure 5.6) generating products of 209 bp for sequencing. A size control (PCR sample 1A), from the previous round, further confirmed this due to its smaller size (140 bp compared to 209 bp).

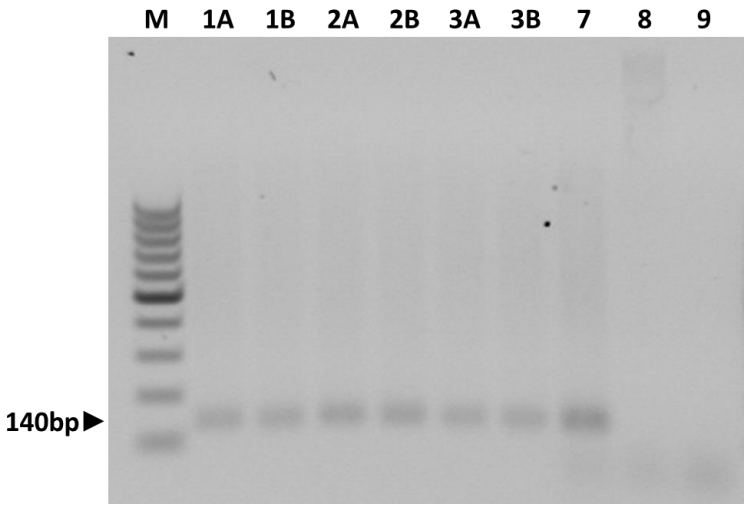

Figure 5.5. Image of agarose gel following electrophoresis of *Vibrio anguillarum* NB10Sm random transposon library products after the Illumina adapters had been ligated by PCR. Template DNA was amplified with TnSC189_III-Sw_F and MmeI_III-Sw_R primers, which also added tailed adaptor sequences to the DNA target fragments which consisted of transposon TnSC189-5' 5'-end inverted repeat, approximately 16 bp of genomic DNA, flanking the transposon insert, and the MmeI adapter. M, 100bp DNA ladder; lanes 1A, 1B, 2A, 2B, 3A and 3B, 10 ng of dsDNA random transposon library PCR product after purification with magnetic beads. These products are derived from three separate transposon libraries processed in duplicate; lane 7, 10 ng of sample 1A PCR product without purification; lane 8, 10 ng of sample 1A following ligation of MmeI adapter prior to PCR, showing a smear of non-specific restriction enzyme digest fragments (not visible on this reproduced gel image); lane 9, no template control.

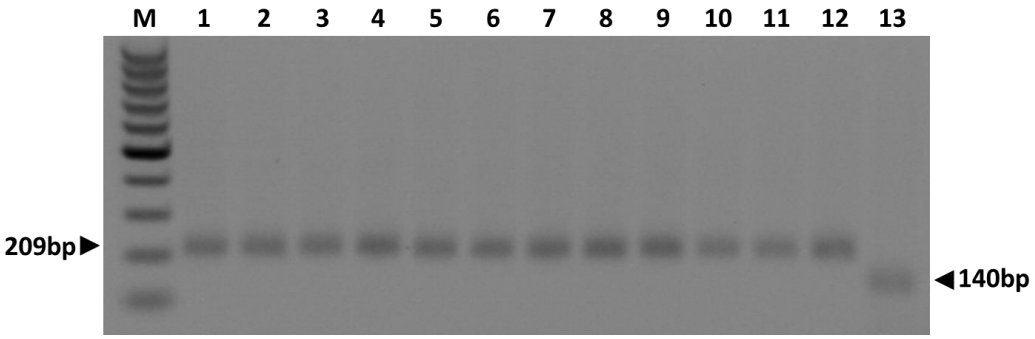

Figure 5.6. Image of agarose gel following electrophoresis of *Vibrio anguillarum* NB10Sm random transposon library products following index PCR. Template DNA was amplified with Illumina® Nextera XT v2 Index primers to incorporate unique pairs of indices to each library sample (Table 5.3) along with the required MiSeq sequencing adapters. M, 100bp DNA ladder; lanes 1 through 12, 10 ng of each dsDNA random transposon library PCR product after purification with magnetic beads; lane 13, 10 ng of sample 1A PCR product from previous adapter PCR step, to highlight the increased size of PCR product, in this second round, which demonstrates successful ligation of index primers.

5.3.5. MiSeq run performance and processing of raw reads

The MiSeq sequencing run was completed successfully, with a cluster density of 757k per mm^2 with 47.9% of reads passing filter, which generated 5,802,645 raw reads of which 74% had a quality score of >30; i.e. base call accuracy of 99.9% (Figure 5.7). Following trimming of reads to remove Illumina adapters, 81.5% remained after the cutadapt software removed sequences with no adapter (0.5%), or that were too short (0.5%) or long (18.1%).

5.3.6. Tn-seq analysis

Of the 4,727,608 reads that remained 71.36% aligned to the selected *V. anguillarum* chromosomal or plasmid DNA sequences. Coverage, measured as read frequency for each TA dinucleotide with a transposon insert, and distance between each TA dinucleotide with a hit are presented Table 5.6 and Table 5.7. The overall coverage, calculated as the proportion of TA dinucleotide sites determined to contain at least one insertion by the Tn189-5' transposon compared to the total number of possible insertion sites was 12.91% across all three libraries (Table 5.8). Moreover, the coverage of TA sites with insertions on chromosomes I and II were similar (12.62% and 12.86%, respectively) while the p67-NB10 plasmid had a greater coverage rate with transposon insertions in 25.23% of the total number of possible sites.

Next, the number of unique insertion sites was determined for each of the three independently prepared libraries (Table 5.9). Each library had been

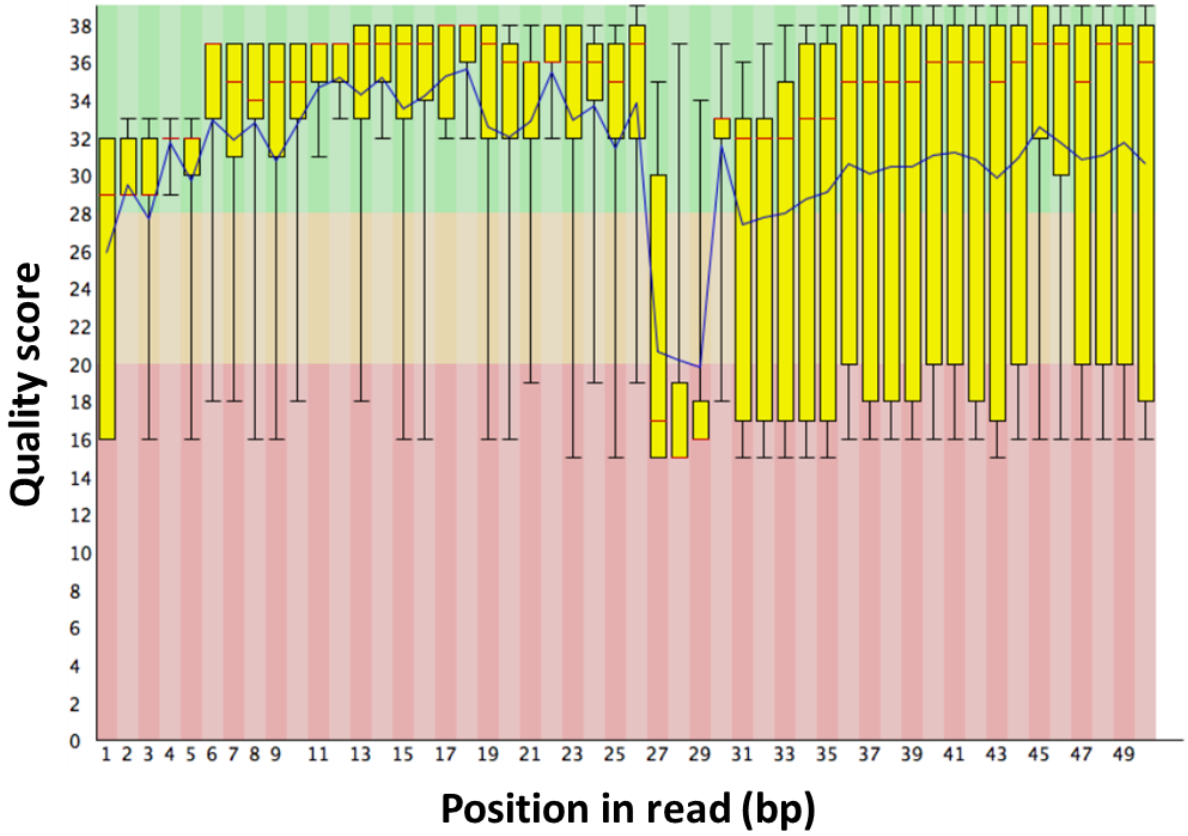

Figure 5.7. Mean quality score of reads in the sequencing run across all bases. Quality scores (QS) are based on the probability of an incorrect base call, so-called base call accuracy (bca), for each position in the sequencing read (bp) as follows: QS of 10 is 90% bca; QS of 20is 99% bca; QS of 30 is 99.9% bca; and QS of 40 is 99.99% bca.

Table 5.6. Coverage of TA dinucleotide transposon insertion sites in *Vibrio anguillarum* NB10Sm genomic DNA. Data are presented as the average (median and mean) number of reads mapped to each unique TA dinucleotide insertion site and the minimum and maximum number of individual insertion reads within a sample library. Each of the six libraries (three independent libraries prepared as duplicates) was indexed as duplicates and the data subsequently combined (Section 5.2.7.6). Please note these data disregard TA dinucleotide sites lacking transposon insertions.

Library	Median	Mean	Minimum	Maximum
Overall	4	48.73	1	8333
1a	6	30.62	1	979
1b	7	35.03	1	1179
2a	8	22.36	1	767
2b	8	22.36	1	808
3a	2	50.58	1	4742
3b	2	43.59	1	3581

Table 5.7. Distance between TA dinucleotide sites with transposon insert within *Vibrio anguillarum* NB10Sm genomic DNA. This is presented as the distance between each unique TA dinucleotide site containing a transposon insert. Each of the six libraries (three independent libraries prepared as duplicates) was indexed as duplicates and the data subsequently combined (Section 5.2.7.6). Please note these data disregard TA dinucleotide sites lacking transposon insertions.

Library	Median	Mean	Minimum	Maximum
Overall	32	67.28	1	5900
1a	113	242.3	1	6738
1b	114	247.9	1	6529
2a	73	167.7	1	6147
2b	75	170	1	6355
3a	242	479.1	1	8700
3b	235	500	1	9352

Table 5.8. Dinucleotide TA sites in *Vibrio anguillarum* NB10Sm identified to have been disrupted by transposon insertion (pooled data from all libraries). The number of potential TA dinucleotide insertion locations was determined in *V. anguillarum* 775 chromosomes I and II, *V. anguillarum* M3 pJM1-like virulence plasmid and two other accessory plasmids (Genbank accession numbers NC_009351 and NC_009325) on forward and reverse strands before calculation of the mean distances between insertions in nucleotides (nt). This enabled the calculation of the percentage of TA dinucleotide sites that had been disrupted by transposon insertion compared to the total number of possible TA insertion sites present in the total genomic DNA of *V. anguillarum* NB10Sm.

	NC_009351 plasmid	NC_015633 Chromosome I	NC_015637 Chromosome II	NC_019325 plasmid	NC_022225 pNB10-67	All
Sequence length (nt)	7941	3063912	988135	5389	66164	4131541
Insert sites on + strand	531	174820	57377	594	4443	237765
Insert sites (+ and – strand)	1062	349640	114754	1188	8886	475550
Mean distance between insert sites (nt)	7.48	8.76	8.61	4.54	7.45	8.69
Insert sites with transposon insertion	55	44117	14755	38	2429	61394
Insert sites without transposon insert	1007	305523	99999	1150	6457	414156
Insert sites by transposon insertion (%)	5.18	12.62	12.86	3.20	27.34	12.91

split into two aliquots during the collection of the colonies and then each of these was subsequently split into further duplicates when the index adaptors were ligated onto the DNA fragments in the samples. This revealed a very similar number of hits between duplicate samples, derived from the same library, suggesting a robust and accurate Tn-seq processing methodology. The total number of unique transposon insertions (i.e. mutants) in each of the three independent libraries was approximately twice the number of mutants estimated from colony counts, which may result from an inability to discriminate overlapping colonies on the agar plates when collecting the transposon mutants. As such, from sequencing data it was possible to discriminate a total of 61394 unique insert locations, compared to the 30700 mutant colonies estimated to have been collected from plates.

Further analysis of transposon insertion locations after mapping to chromosome I (Figure 5.8) and II (Figure 5.9) of *V. anguillarum* 775 (NC_015633, NC_015637), the pJM1-like virulence plasmid of *V. anguillarum* M3 (NC_022225, Figure 5.10), and two other *V. anguillarum* plasmids called pLO2 (NC_009351; Figure 5.11) and pJV (NC_019325, Figure 5.12) revealed 288 annotated genes (including protein coding sequences and ribosomal RNAs but excluding tRNAs; Appendix IX) that contained either no transposon insertions (178 genes), or just a single insertion within the first 90% of the coding sequence of the gene. These are suggested to be putative genes required for growth under the culture

Table 5.9 Number of different transposon Tn-seq insert reads mapped to *Vibrio anguillarum* genomic DNA. Transposon (Tn) insert reads were mapped to *Vibrio anguillarum* 775 chromosomes I and II, *V. anguillarum* M3 pJM1 like virulence plasmid and two further accessory plasmids (Genbank accession numbers NC_009351 and NC_009325) for each of three independent random transposon libraries that had been processed in duplicate. This produced a six libraries (1a, 1b, 2a, 2b, 3a and 3b) which were each processed in technical duplicate (12 libraries in total) and sequenced to identify transposon/genomic DNA junctions at insertion locations. Data for each library (and for all the libraries combined) is presented as the total number of unique TA dinucleotide insertion locations identified, and the number of genes containing or lacking at least one transposon insertion.

	NC_015633 Chromosome I	NC_015637 Chromosome II	NC_022225 pJM1 like	NC_009351 plasmid	NC_019325 plasmid	Total
1A (1)	9639	3195	777	11	3	13625
1A (7)	9852	3265	795	8	3	13923
1A (overall)	12167	3954	879	17	4	17021
Genes with a transposon insertion	2228	717	46	6	1	2998
Genes lacking a transposon insertion	570	141	13	4	5	733

	NC_015633 Chromosome I	NC_015637 Chromosome II	NC_022225 pJM1 like	NC_009351 plasmid	NC_019325 plasmid	Total
1B (2)	9775	3286	786	10	8	13865
1B (8)	9427	3170	770	8	5	13380
1B (overall)	11796	3949	867	15	11	16638
Genes with a transposon insertion	2217	701	46	6	4	2974
Genes lacking a transposon insertion	581	157	13	4	2	757

	NC_015633 Chromosome I	NC_015637 Chromosome II	NC_022225 pJM1 like	NC_009351 plasmid	NC_019325 plasmid	Total
2A (3)	15343	5247	1180	10	4	21784
2A (9)	13577	4586	1076	7	5	19251
2A (overall)	17390	5936	1260	16	8	24610
Genes with a transposon insertion	2352	767	45	6	2	3172

Genes lacking a transposon insertion	446	91	14	4	4	559

	NC_015633 Chromosome I	NC_015637 Chromosome II	NC_022225 pJM1 like	NC_009351 plasmid	NC_019325 plasmid	Total
2B (4)	13754	4743	1110	1	2	19610
2B (10)	14897	5078	1188	3	4	21170
2B (overall)	17166	5847	1256	4	6	24279
Genes with a transposon insertion	2341	770	46	3	3	3163
Genes lacking a transposon insertion	457	88	13	7	3	568

	NC_015633 Chromosome I	NC_015637 Chromosome II	NC_022225 pJM1 like	NC_009351 plasmid	NC_019325 plasmid	Total
3A (5)	4425	1555	268	1	1	6250
3A (11)	4794	1693	281	3	5	6776
3A (overall)	6144	2133	320	3	6	8606
Genes with a transposon insertion	1832	602	42	3	1	2480
Genes lacking a transposon insertion	966	256	17	7	5	1251

	NC_015633 Chromosome I	NC_015637 Chromosome II	NC_022225 pJM1 like	NC_009351 plasmid	NC_019325 plasmid	Total
3B (5)	3976	1365	251	2	4	5598
3B (12)	4912	1634	275	5	4	6830
3B (overall)	5960	1950	312	7	8	8237
Genes with a transposon insertion	1810	576	42	3	3	2434
Genes lacking a transposon insertion	988	282	17	7	3	1297

	NC_015633 Chromosome I	NC_015637 Chromosome II	NC_022225 pJM1 like	NC_009351 plasmid	NC_019325 plasmid	Total
ALL	44117	14755	2429	55	38	61394
Genes with a transposon insertion	2621	821	46	9	5	3502
Genes lacking a transposon insertion	177	37	13	1	1	229

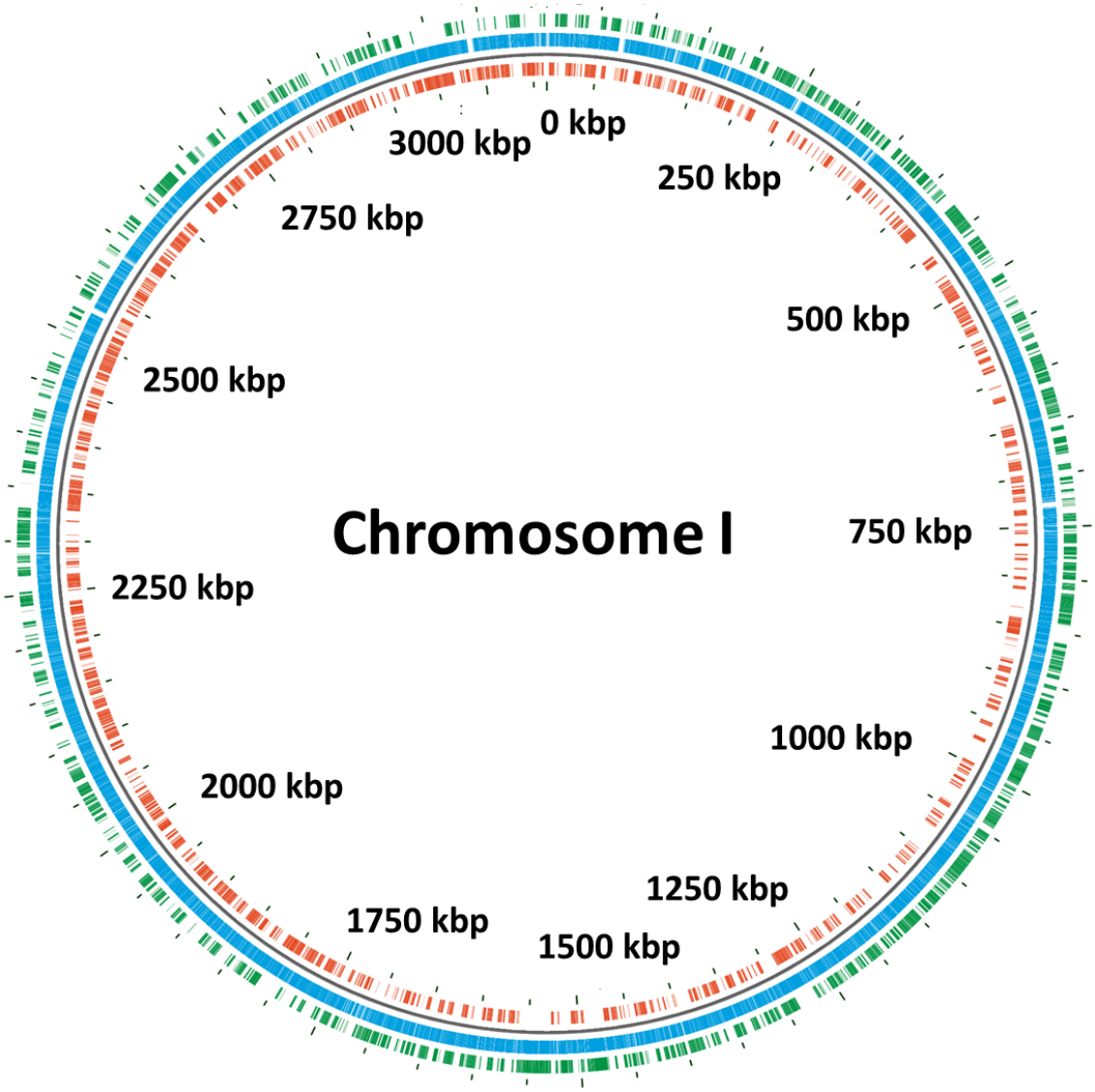

Figure 5.8. Coverage of transposon insertions into *V. anguillarum* NB10Sm Chromosome I. Blue lines indicate the position of each unique transposon insertion; dark green lines represent genes coded on the positive strand of the chromosome and that contain at least one transposon insertion; light green lines represent genes coded on the positive strand of the chromosome and that lack a transposon insertion; red lines represent genes coded on the negative strand of the chromosome and that contain at least one transposon insertion; pink lines represent genes coded on the negative strand of the chromosome and that lack a transposon insertion.

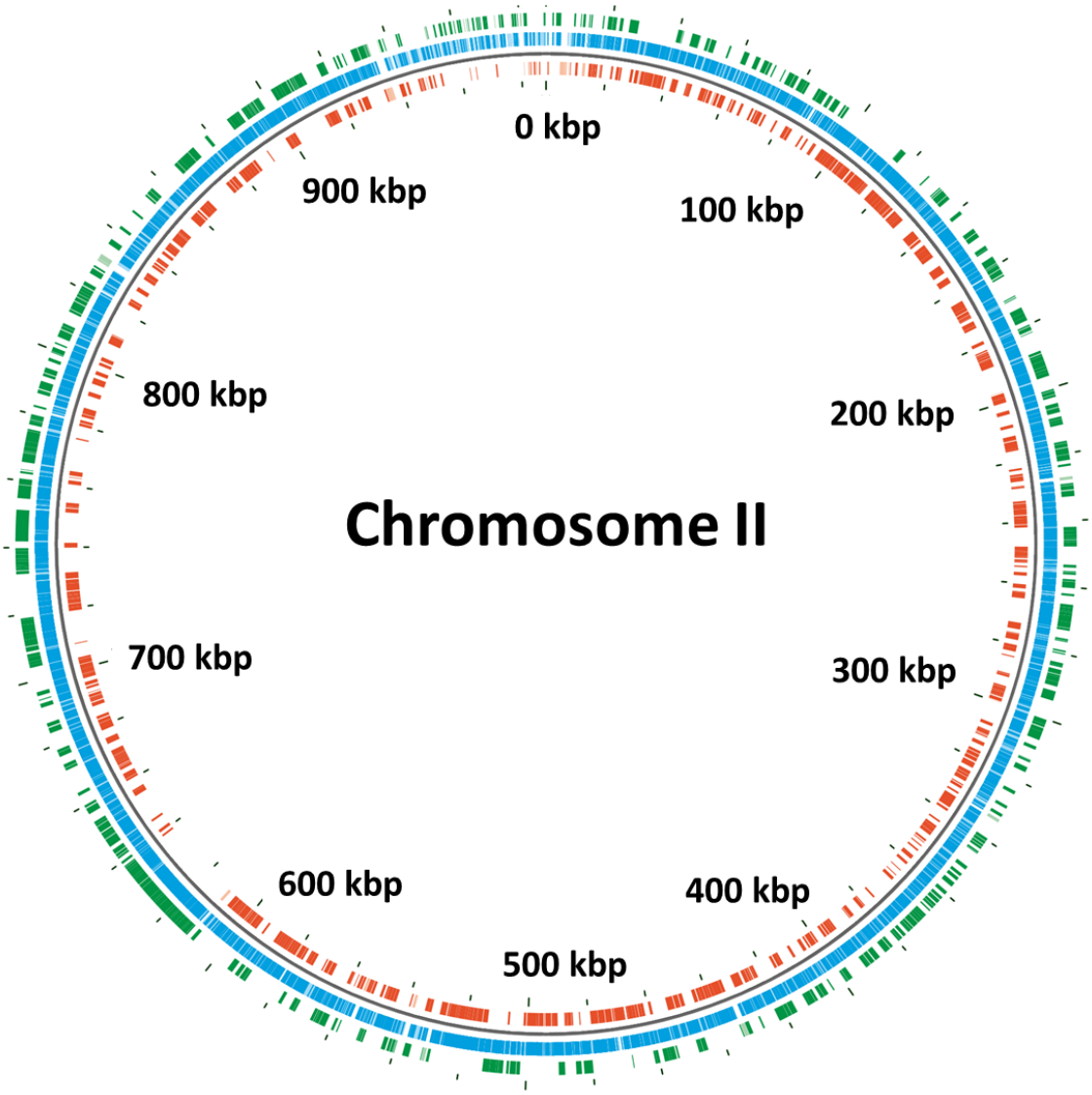

Figure 5.9. Coverage of transposon insertions into *V. anguillarum* NB10Sm Chromosome II. Blue lines indicate the position of each unique transposon insertion; dark green lines represent genes coded on the positive strand of the chromosome and that contain at least one transposon insertion; light green lines represent genes coded on the positive strand of the chromosome and that lack a transposon insertion; red lines represent genes coded on the negative strand of the chromosome and that contain at least one transposon insertion; pink lines represent genes coded on the negative strand of the chromosome and that lack a transposon insertion.

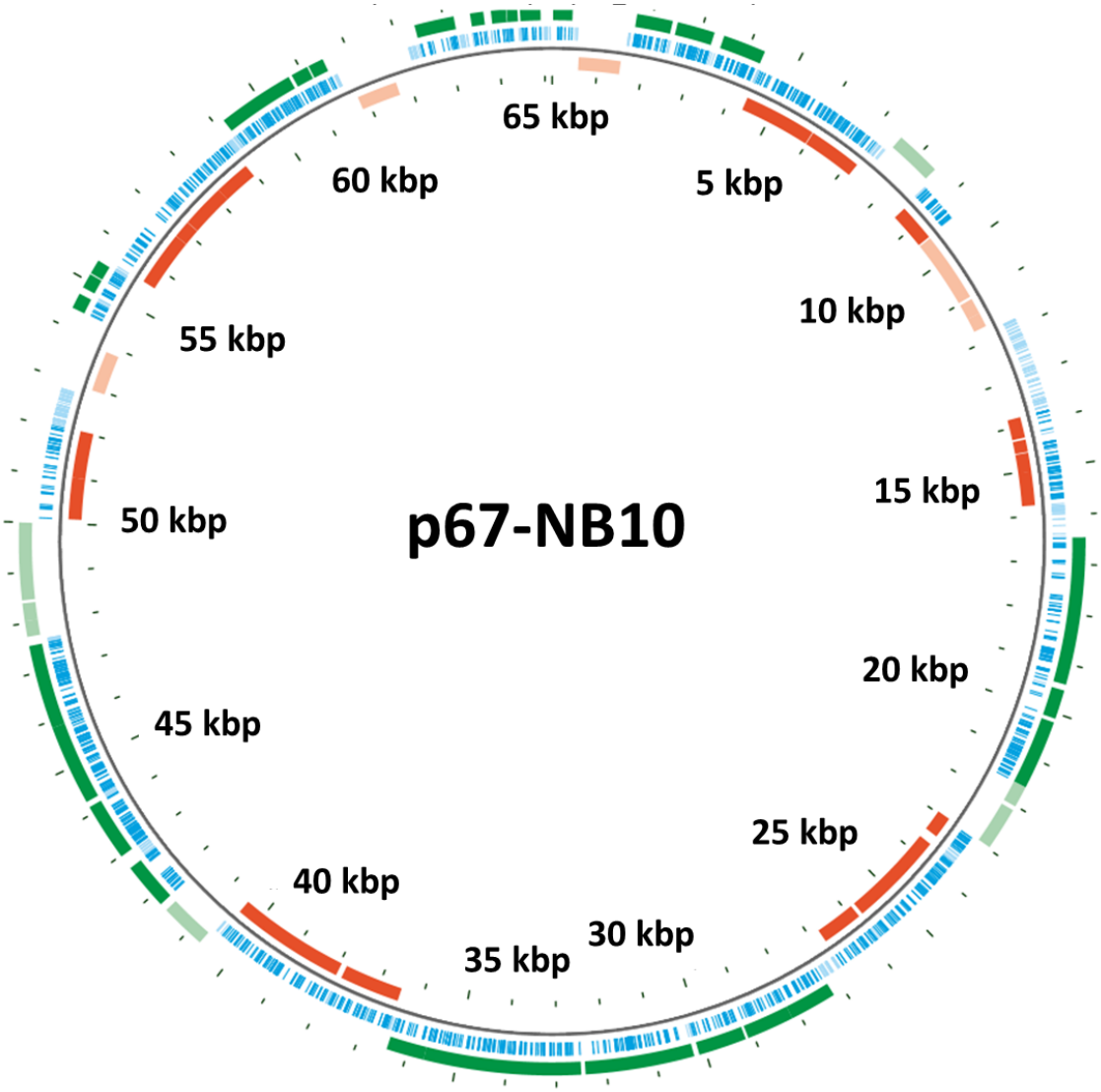

Figure 5.10. Coverage of transposon insertions into the *V. anguillarum* NB10Sm p67-NB10 virulence plasmid. Blue lines indicate the position of each unique transposon insertion; dark green lines represent genes coded on the positive strand of the plasmid and that contain at least one transposon insertion; light green lines represent genes coded on the positive strand of the plasmid and that lack a transposon insertion; red lines represent genes coded on the negative strand of the plasmid and that contain at least one transposon insertion; pink lines represent genes coded on the negative strand of the plasmid and that lack a transposon insertion.

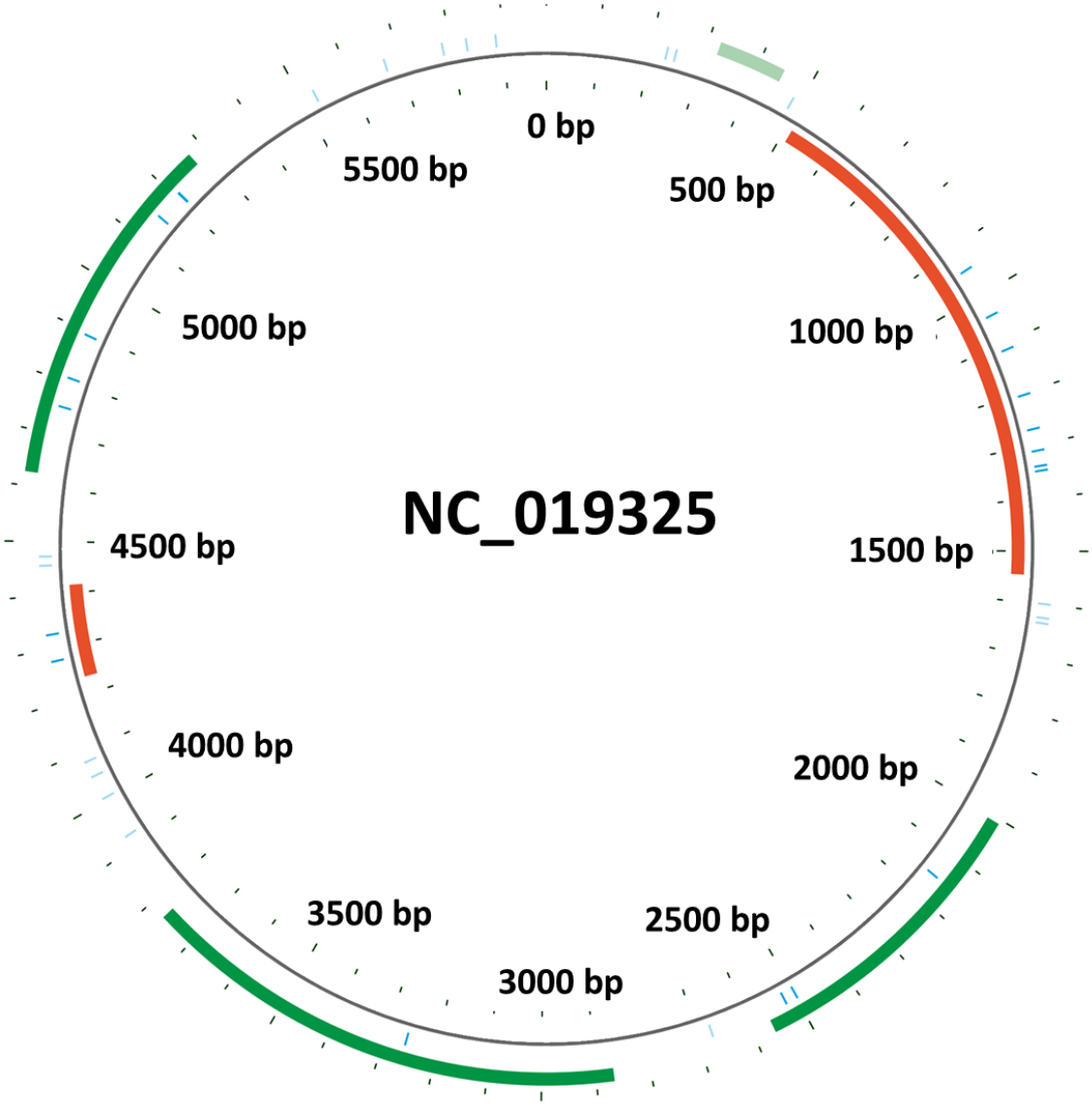

Figure 5.11. Coverage of transposon insertions into the *V. anguillarum* NB10Sm plasmid NC_019325. Blue lines indicate the position of each unique transposon insertion; dark green lines represent genes coded on the positive strand of the plasmid and that contain at least one transposon insertion; light green lines represent genes coded on the positive strand of the plasmid and that lack a transposon insertion; red lines represent genes coded on the negative strand of the plasmid and that contain at least one transposon insertion; pink lines represent genes coded on the negative strand of the plasmid and that lack a transposon insertion.

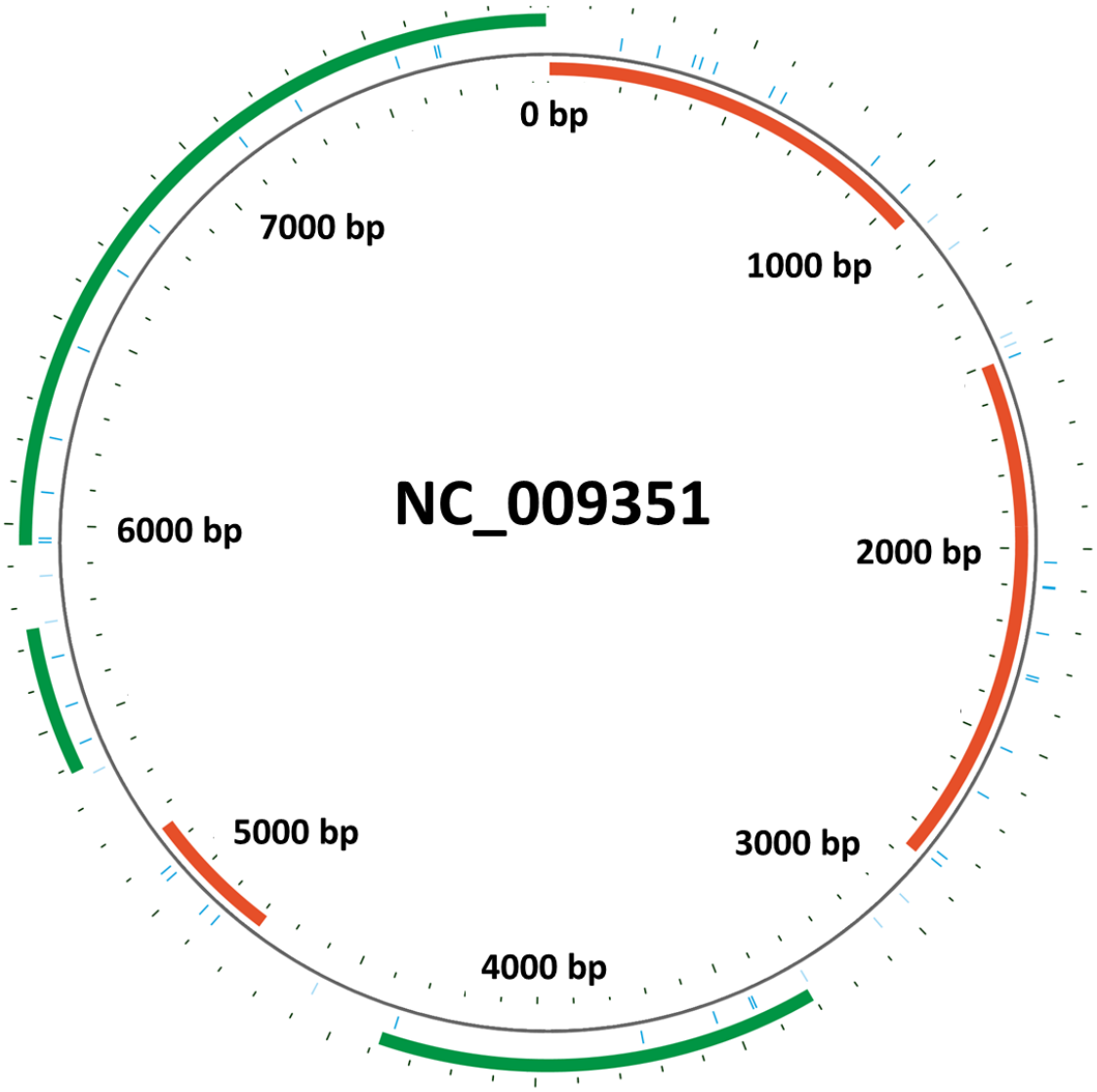

Figure 5.12. Coverage of transposon insertions into the *V. anguillarum* NB10Sm plasmid NC_009531. Blue lines indicate the position of each unique transposon insertion; dark green lines represent genes coded on the positive strand of the plasmid and that contain at least one transposon insertion; light green lines represent genes coded on the positive strand of the plasmid and that lack a transposon insertion; red lines represent genes coded on the negative strand of the plasmid and that contain at least one transposon insertion; pink lines represent genes coded on the negative strand of the plasmid and that lack a transposon insertion.

conditions used in this present study. The 'required' genes identified in *V. anguillarum* NB10Sm were compared to a 'required' gene set identified by a previous Tn-seq experiment on *V. cholerae* E7946 (Kamp et al., 2013), where 414 'required' genes were identified. Rather surprisingly there was little overlap between the two datasets, comparison of 'required' gene lists revealed that only 8 putatively 'required' genes, with sequence similarity BLASTn alignment E value of less than 1×10^{-10} (Figure 5.13 and Table 5.9), were shared between these two *Vibrio* species, and this increased only to 22 genes even when the genes with a single transposon insertion, within the first 90%, in *V. anguillarum* NB10Sm were considered to be 'required'.

5.4. Discussion

Required genes are those considered to be essential for growth and survival in optimum growth conditions such as rich media including TSA (Kwon et al., 2016). Once identified, required genes of pathogenic organisms can be investigated as potential drug targets or vaccine candidates (Klein et al., 2012). Thus, the recent development of Tn-seq and other transposon sequencing techniques (van Opijnen et al., 2009; van Opijnen and Camilli, 2013) provides a potentially powerful tool to be harnessed to elucidate required gene sets of pathogens (Le Breton et al., 2015; Lee et al., 2015; Verhagen et al., 2014).

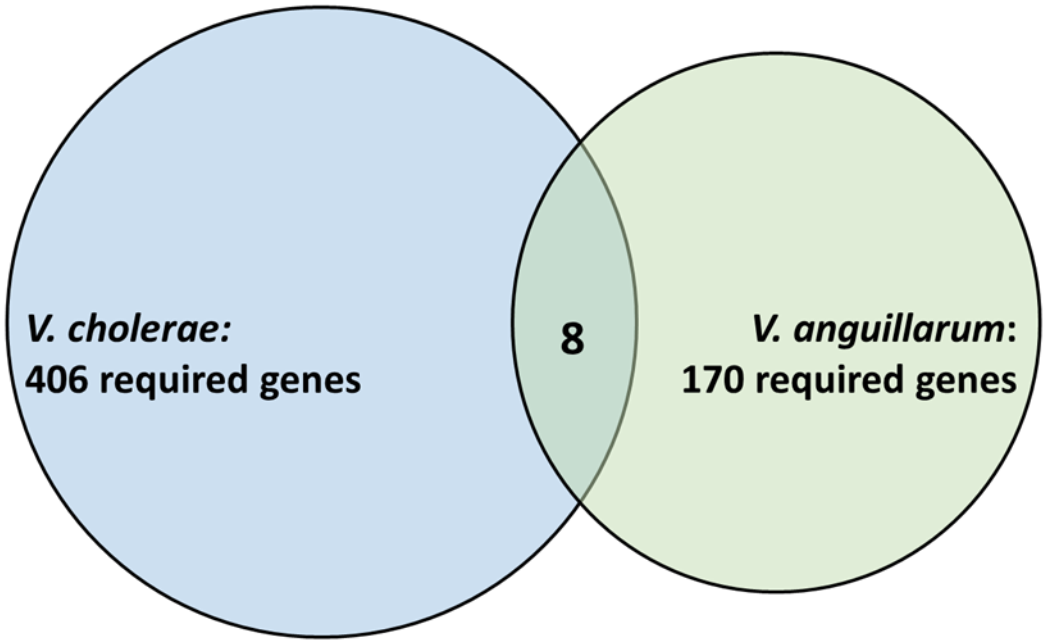

Figure 5.13. Putative required genes of *Vibrio anguillarum* NB10Sm and *Vibrio cholerae* E7946. Analysis of Tn-seq data of *V. anguillarum* NB10Sm random transposon insertion libraries revealed a total of 178 putative required genes that did not contain a transposon discounting the last 10% of sequence. This dataset was compared to a previous experiment which identified 414 *V. cholerae* required genes (Kamp et al,. 2013) and revealed that 8 of these genes had similar nucleotide sequences based on BLASTn alignment with an accepted E value of less than 1×10^{-10}. In both studies required loci were defined as genes with no transposon inserts after the last 10% had been trimmed.

Table 5.9. Putative required genes and gene products of *Vibrio anguillarum* NB10Sm with sequence similarity to a required gene of *Vibrio cholerae* E7946. Analysis of Tn-seq data of *V. anguillarum* NB10Sm random transposon insertion libraries revealed a total of 178 putative required genes that did not contain a transposon. This dataset was compared to a previous experiment which identified 414 *V. cholerae* required genes (Kamp et al,. 2013) and revealed that 8 of these genes had similar nucleotide sequences based on BLASTn alignment with an E value of less than 1×10^{-10}. In both studies required loci were defined as genes with no transposon insertions outside of the final 10% of the coding sequence.

Vibrio anguillarum		***Vibrio cholerae***	
Gene	**Product**	**Gene**	**Product**
rplT	50S ribosomal protein L20	-	hypothetical protein
-	50S ribosomal protein L10	*rplL*	50S ribosomal protein L7/L12
-	hypothetical protein	-	30S ribosomal protein S7
tuf	elongation factor Tu	-	Replicative DNA helicase
fliN	flagellar motor switch protein FliN	-	heme exporter protein D
-	23S ribosomal RNA	*ftsL*	Cell division protein
-	50S ribosomal protein L16	-	hypothetical protein
-	hypothetical protein	*rpsM*	50S ribosomal protein S13

This chapter has described a Tn-seq experiment to identify required genes of *V. anguillarum*, the first of its kind for a fish pathogen. However, following initial alignment of the Tn-seq data against the NB10 genome (Holm et al., 2015) it was revealed that the original parent isolate used was most likely not NB10. Thus, the alignment proceeded using sequences of *V. anguillarum* 775 chromosomes I and II (Naka and Crosa, 2011) and the M3 pJM1-like plasmid (Li et al., 2013a), in addition to two smaller unpublished plasmid sequences (Accession numbers NC_009351 and NC_019325) deposited in Genbank, which increased the number of reads aligned to 71.36% compared to 64.66% with NB10Sm. Despite this surprising discovery, it has little impact on the data generated in chapter 4 because all transposon insertion locations identified during that experiment were 100% homologous to the same sequence and gene (if applicable) in *V. anguillarum* 775.

Mapping of transposon insertion reads to the five *V. anguillarum* sequences, detailed above, revealed a total of 178 loci (excluding all tRNAs) with no transposon inserts and a further 110 with only a single insertion, when discounting the last 10% of sequence. Although this is a good initial indication of required genes in *V. anguillarum*, the combined libraries only covered 13% of the possible 550,000 TA dinucleotide transposon insertion sites which could mean that some genes are likely not disrupted by chance, particularly if they are especially short (Chao et al., 2016); thus, justifying the exclusion of tRNAs, which are all shorter than 100 bp from this present analysis. Therefore, a repeat of this experiment would benefit from the

generation and pooling of larger, fully-saturated transposon libraries to increase the accuracy of predicted putative required genes (Kwon et al., 2016). Alternatively, a selection of putative required genes could be confirmed by conventional knockout, as this process is essential for validation of libraries anyhow.

Quality of reads was not optimal in this initial Tn-seq study (Figure 5.7), and this may be related to the poor cluster density (757) then the low percentage of library products (< 50%) passing filter, which culminated in only 5 million usable reads from an anticipated >12 million reads for the V2 kit. In contrast, the manufacturer suggests low read quality scores are related to overclustering (Illumina, 2016d). Despite these disappointing results, the bacterial DNA reads were of high quality and suitable for further analysis. Furthermore, the drop in quality score between 27 and 29 bp (Figure 5.7) is within the MmeI adapter/genomic DNA junction region which may explain the poor readings. The system used in this present study employed adapters described previously (van Opijnen and Camilli, 2010). However, these contain indexing barcodes for a different Illumina platform and at present approximately 30 bases of identical sequence pass through filters before the variable region of genomic DNA is read. This is another important consideration and can be improved by designing a new MmeI adapter for ligation to MmeI cohesive ends before PCR amplification of Illumina-specific sequences. Designing a shorter MmeI adapter without these redundant indices would lead to sequencing reads of greater complexity earlier in the cycle and could improve base call accuracy.

The putative required set of 178 *V. anguillarum* genes revealed in this present study was compared to that of a previous collection of 414 required genes in *V. cholerae* (Kamp et al., 2013) for conserved nucleotide sequences between the two species. However, it is important to consider that the criteria used to generate these two libraries may not be identical, as the exact parameters to assign the required genes are not described in Kamp et al. (2013). Surprisingly, only 8 genes identified to be required in *V. anguillarum* (based on there being no transposon insertions within the coding sequence) displayed similarity to the genes in the required gene set of *V. cholerae* (Figure 5.13 and Tables 5.9). Most of these genes did not share functional similarity between the two species with the exception of a pair of 50S ribosomal subunits; however, this list could grow as hypothetical protein encoding genes are characterised. One gene that may be of interest is *fliN* as it encodes a protein involved with changing flagellar rotation direction and a knockout in *V. parahaemolyticus* revealed a loss of sodium-driven swimming motility (Boles and McCarter, 2000).

In a previous study, *groES* was identified as a putative required gene of *V. cholerae* (Kamp et al., 2013). Examination of the same gene in this present study of *V. anguillarum* revealed only a single transposon insertion. In addition to *V. cholerae*, *groES* of *V. anguillarum* has nucleotide sequence similarity of over 85% in eight other *Vibrio* spp., including *Vibrio parahaemolyticus and Vibrio ordalii* (Kim et al., 2010). Interestingly, *groES*, which is a co-chaperonin involved with protein folding in stress response to heat shock (Sagane et al., 2003), is already regarded as a promising drug

target in many species including, *Bacillus subtilis*, *Enterococcus faecium*, *Staphylococcus aureus*, *Pseudomonas aeruginosa*, after it was found to be a required gene in *E. coli* BL21(DE3) and proved to be susceptible to multiple inhibitors (Abdeen et al., 2016; Johnson et al., 2014). Further work on the *groES* gene of *V. anguillarum* could elucidate whether a similar strategy of targeted inhibition would be an effective strategy against this pathogen.

Furthermore, the identification of *groES* as a putative required gene, despite a single transposon insert within its sequence, highlights the difficulty in predicting exactly how to define required or essential genes. Insertions within the 5' and 3' ends of genes do not necessarily imitate true gene disruption (Chao et al., 2016). Thus, the terminal 5 -10% of all genes have been ignored in previous studies (Chao et al., 2013; Crimmins et al., 2012; van Opijnen et al., 2009). In this present study, it was decided to discount the final 10% of the sequence at the 3' end because abbreviated gene products may not lose their functionality (van Opijnen et al., 2009), although it must be emphasised that this was an arbitrary figure and not derived empirically. However, a more robust approach might be to evaluate gene fitness based on percentage of potential insert sites with a transposon disruption for each gene (Chao et al., 2016), although this approach requires highly saturated libraries making the approach taken in this present study more appropriate.

To conclude, this work has successfully demonstrated that Tn-seq can be applied to the fish pathogen, *V. anguillarum*. However, analysis of Tn-seq

data revealed double the number of insertion locations compared to the figure estimated using recovered colony counts (61394 compared to approximately 30700), a discrepancy that may have originated from multiple inserts within the same mutant strain (Klein et al., 2012) or colony overgrowth on agar selection plates. Therefore, library validation, using a subset of mutants, is required to confirm that only one transposon insertion is present in each isolate and this could be accomplished by restriction enzyme digest and Southern-hybridization (Bourhy et al., 2005). This technique can be developed in further applications including *in vitro* condition specific fitness screening using different media preparations (Lee et al., 2015) or analysis of genes required for survival *in vivo* in *Galleria mellonella* (Gebhardt et al., 2015). Optimisation of this process will produce a powerful tool to investigate the mechanisms underlying phenotype-genotype relationships of *V. anguillarum* and other pathogens.

Chapter 6. General discussion

Aquaculture plays an increasingly important role in global food production, but microbial diseases continue to cause considerable economic losses to producers and impact negatively on animal welfare (Lafferty et al., 2015). One such disease is vibriosis, which can be caused by *Vibrio anguillarum*, a key aquaculture pathogen that infects many species and can reduce farm productivity (Austin et al., 1995; Frans et al., 2011; Naka and Crosa, 2011). Generally, vaccines have mitigated this issue in Atlantic salmon production, but this bacterium is now a major pathogen of cleaner fish, which are cultured and employed to combat the problems caused by sea lice (Biering et al., 2016; Colquhoun and Lillehaug, 2014). To address microbial disease problems, there is a requirement for deeper understanding of the processes involved during infection, as this will lead to new and improved treatments, vaccinations and management practices. Alternative infection models are becoming more important as experimentation on vertebrates becomes increasingly regulated, in turn driving incentive to adhere to the principles of the 3Rs. However, few alternative infection models are available to study pathogens of aquaculture species. Therefore, there is a justified need to pursue alternative hosts to aid the study of microbial pathogens of farmed fish. Thus, the overall aim of this thesis was to explore new techniques to investigate the mechanisms underlying the virulence of the fish pathogen *V. anguillarum* and determine the genes required for survival *in vitro*.

To this end, two novel approaches were taken that had not been attempted previously with any fish pathogen: evaluation of the invertebrate

alternative host *Galleria mellonella* to investigate *V. anguillarum* virulence and its application in screening random transposon mutants, and the mass sequencing of these mutants to determine the required gene set for *V. anguillarum* under *in vitro* conditions.

First, *G. mellonella* was evaluated as an alternative host for studying *V. anguillarum* virulence (Chapter 3). *V. anguillarum* killed the larvae in a dose-dependent manner while the larvae could be rescued from lethal infective doses of *V. anguillarum* by treatment with penicillin to which the bacterium was susceptible. Furthermore, there was a highly significant and positive correlation between the virulence of 11 wild-type *V. anguillarum* isolates in *G. mellonella* and Atlantic salmon (Pedersen et al., 1997) models of infection. The differential virulence of these *V. anguillarum* isolates in *G. mellonella* was related to the replication rates inside the larvae, with more virulent isolates replicating faster than less virulent isolates. Moreover, the techniques needed to work with this model are acquired after only limited instruction and studies using this model are ethically more acceptable than working with vertebrate hosts (McMillan et al., 2015). Notably, the *G. mellonella* model presents a low biohazard risk because no liquid systems are required and the larvae are kept in Petri dishes with infected material made safe by autoclaving.

Next, a collection of 350 transposon mutants of a spontaneous streptomycin-resistant *V. anguillarum* NB10Sm strain were screened in *G. mellonella* for reduced virulence (Chapter 4). This approach contributed further evidence

to supporting the use of *G. mellonella* as a host for studying the virulence of *V. anguillarum*. Thirteen *V. anguillarum* transposon insertion mutants were attenuated in virulence compared to the parent strain and sequencing of the transposon insertion/genomic DNA junction in each isolate revealed disruptions in known (*vah1* and genes on p67-NB10) and putative (a putative secreted toxin *cyaA* and *wbhK* that is predicted to be involved in lipopolysaccharide synthesis) virulence genes (Naka et al., 2013a; Rock and Nelson, 2006; Rodkhum et al., 2006b; Stroeher et al., 1998). Furthermore, one transposon insertion was located within a gene coding for a putative uncharacterised protein with a GlyGly-CTERM domain motif in the C-terminus region, which may be implicated in the post-translational processing of secreted proteins by serine proteases (Rather, 2013). Interestingly, further analysis of DNA sequences surrounding this gene revealed a putative (serine) protease LA homologue (Figaj et al., 2014) just 1.2 kb and three genes downstream. All the known virulence factors identified by this approach were either located within three genes on the pJM1-like p67-NB10 virulence plasmid or inside a gene encoding for the haemolysin Vah1 on chromosome II (Holm et al., 2015; Rock and Nelson, 2006). Moreover, examination of *V. anguillarum* knockout mutants in *G. mellonella* also found that haemolysin and p67-NB10 plasmid virulence factors were conserved mechanisms for exploiting fish and *G. mellonella*, suggesting this alternative host may be useful for further study of these mechanisms (Chapter 3).

The haemolysins RtxA and Vah1, and the iron acquisition genes found on the pJM1-like plasmid, are important *V. anguillarum* virulence factors required for systemic infection of fish hosts (Li et al., 2008; Stork et al., 2002), and these proteins were important for infection of *G. mellonella* (Chapter 3; McMillan et al., 2015). In contrast, the metalloprotease-encoding *empA* gene is thought to assist host invasion through the gastrointestinal tract (Denkin and Nelson, 2004) and flagella genes (*flaA and flaE*) aid host attachment and invasion (Ormonde et al., 2000). Although, flagellum-mediated dissemination and persistence within host is perhaps required for virulence in fish (McGee et al., 1996), the small size of *G. mellonella* may render the need for this mechanism redundant and thus explain why knockout of these genes had no effect on virulence in the larva. Therefore, *G. mellonella* is probably better suited to discovery and characterisation of virulence factors necessary for systemic infection, compared to those required for attachment, invasion and dissemination. This illustrates an important potential limitation of *G. mellonella* in certain situations when investigating host-pathogen interactions.

The screen of random tagged-transposon insertion mutants of *V. anguillarum* showed that *G. mellonella* can be used to identify novel *V. anguillarum* virulence determinants and genes important for fitness within the larva (Chapter 4). Moreover, this approach identified a small number of genes that could realistically be validated in fish, which is the crucial next step in the process. Of course, observations in alternative hosts need to be assessed within the native host to confirm the role of specific

genes during infection, as disparities in the importance of certain virulence factors in different hosts were found in Chapter 3 and have been reported elsewhere (Amorim-Vaz et al., 2015a; Trevijano-Contador and Zaragoza, 2014). Therefore, the construction of targeted and trans-complemented mutant strains with disruptions in the gene encoding the putative novel virulence factor need to be prepared and tested in the native host. This must be performed to confirm the role in fish infections of the uncharacterised protein disrupted in the Tn100 mutant strain.

Transposon sequencing (Tn-seq; van Opijnen et al., 2009), a technique combining random tagged-transposon mutagenesis and massively parallel sequencing, was used to identify a subset of required genes of *V. anguillarum* NB10Sm under *in vitro* conditions (Chapter 5). This powerful high-throughput process allows for the identification of required genes of pathogenic organisms and the products of these genes can be investigated as potential vaccine candidates or drug targets (Klein et al., 2012). The initial Tn-seq screen performed in Chapter 5 gave 13% coverage of potential transposon insertions sites (out of a possible ca. 550,000) within the *V. anguillarum* genome. While this was sufficient to identify many potential required genes, improved read quality, and greater coverage and saturation of insertion locations, should allow far deeper understanding of the importance for certain sequences in the genome, particularly small non-coding regions and discrete regions within genes. Despite this, 178 *V. anguillarum* genes were found to have no transposon insertion within the first 90% of the coding sequence and these were identified as putative

required genes. Furthermore, eight of these *V. anguillarum* required genes shared sequence homology to protein coding genes within a *Vibrio cholerae* required gene set (Kamp et al., 2013), which was surprisingly low given the relatedness of these species. Additional work is required to more completely investigate the *V. anguillarum* dataset of required genes and determine if any of these show homology to *V. cholerae* genes not classified to be required. Moreover, future work will include correlation of the putative required genes of *V. anguillarum* with those of the 473 genes of the minimum required genome that was designed and synthesised to identify the core set of genes required for an independently replicating cell (Hutchison et al., 2016). Unexpectedly, 148 genes of the minimum required genome had unknown biological functions (Hutchison et al., 2016) and this emphasises the need to characterise similar genes in pathogenic bacteria.

Further work is required to improve the Tn-seq method, especially the sequencing efficiency and quality. Libraries at full, or close to full saturation, will greatly increase the power of this approach and reduce the chance of a gene not being targeted by the transposon. A method using an altered MmeI restriction enzyme site and ligation of adapter, required to enclose the MmeI cut-site and provide a substrate for sequencing primers to anneal, was discussed in Chapter 5. Tn-seq using MmeI to cut DNA close to the transposon insertion site has limitations, including the small length of informative sequencing reads (ca. 16-bp of genomic DNA); fluctuating efficiency of enzyme cleavage; and the formation of adapter dimers (Klein et al., 2012; Lazinski and Camilli, 2013). In contrast, Tn-seq and high-

throughput insertion tracking by deep-sequencing (HITS) (Gawronski et al., 2009; van Opijnen et al., 2009) transposon sequencing methods, which both use MmeI, benefit from producing reads of a similar size that prevents bias created by variable lengths of PCR products (Kwon et al., 2016). One method that would create a more streamlined and less labour intensive approach is homopolymer tail-mediated ligation PCR (HTML-PCR) (Klein et al., 2012; Lazinski and Camilli, 2013). This technique incorporates a homopolymer tail to 3' ends of the dsDNA containing the transposon insertion subsequent to sonication which causes fragmentation of DNA; ligation of oligonucleotides to 5' end; and a single PCR step to generate products for sequencing (Lazinski and Camilli, 2013). This approach was adapted for transposon library analysis with the addition of a further PCR step to select for fragments containing the insertion (Klein et al., 2012). Furthermore, homopolymer nucleotide extension is more efficient than adapter ligation (Chao et al., 2016) and would produce longer more complex reads which may help overcome the modest read quality experienced in this present study.

Subsequent to successful optimisation of the Tn-seq protocol the natural progression of this present research would involve passage of the *V. anguillarum* random tagged-transposon mutant library through *G. mellonella* to identify genes important for survival and replication within this host. This experiment would provide an effective novel system for identifying genes important to virulence, and this approach could be adapted to the study of other bacterial pathogens of fish. Random

transposon libraries have been screened through *G. mellonella* previously, and this method was used for *Acinteobacter baumannii* to identify the genes required for survival within the larvae and, importantly, both known virulence factors and novel genes were identified (Gebhardt et al., 2015). The rapid and efficient identification of novel genes required for survival and/or virulence *in vivo* using *G. mellonella* will be a valuable tool for advancing our understanding of pathogen biology. This approach will highlight genes warranting further investigation of function, mechanisms of inhibition, and virulence in native fish hosts. Thus, *G. mellonella*, which is simple to handle, challenge and keep compared to fish, could become an important weapon in our arsenal to tackle fish diseases.

In summary, this present study has shown that the alternative host *G. mellonella* is useful for investigating the virulence of the fish pathogen *V. anguillarum*, which could lead to a reduction in experimental fish use and fulfil the principles of the 3Rs. Furthermore, Tn-seq was applied successfully to identify the required genes of *V. anguillarum* under *in vitro* conditions. In conclusion, these two techniques have furthered our knowledge of *V. anguillarum* biology, particularly with respect to virulence and viability, and may assist in efforts to address the problems caused by this pathogen in aquaculture. Moreover, this entire system will likely be highly suited to the study of virulence in other fish and aquaculture pathogens.

References

Abdeen, S., N. Salim, N. Mammadova, C. M. Summers, R. Frankson, A. J. Ambrose, G. G. Anderson, P. G. Schultz, A. L. Horwich, E. Chapman, and S. M. Johnson, 2016, GroEL/ES inhibitors as potential antibiotics: Bioorganic & Medicinal Chemistry Letters, v. 26, p. 3127-3134.

Actis, L. A., M. E. Tolmasky, and J. H. Crosa. 2011. Vibriosis, p. 570–605. In P. T. K. Woo and D. W. Bruno (ed.), Fish diseases and disorders, vol. 3: viral, bacterial, and fungal infections, 2nd ed. CABI International, Oxfordshire, United Kingdom.

Agius, C., and R. J. Roberts, 2003, Melano-macrophage centres and their role in fish pathology: Journal of Fish Diseases, v. 26, p. 499-509.

Agnoli, K., S. Schwager, S. Uehlinger, A. Vergunst, D. F. Viteri, D. T. Nguyen, P. A. Sokol, A. Carlier, and L. Eberl, 2012, Exposing the third chromosome of *Burkholderia cepacia* complex strains as a virulence plasmid: Molecular Microbiology, v. 83, p. 362-378.

Alibaud, L., Y. Rombouts, X. Trivelli, A. Burguiere, S. L. G. Cirillo, J. D. Cirillo, J. F. Dubremetz, Y. Guerardel, G. Lutfalla, and L. Kremer, 2011, A *Mycobacterium marinum* TesA mutant defective for major cell wall-associated lipids is highly attenuated in *Dictyostelium discoideum* and zebrafish embryos: Molecular Microbiology, v. 80, p. 919-934.

Alsina, M., J. Martinez-Picado, J. Jofre, and A. R. Blanch, 1994, A medium for presumptive identification of *Vibrio-anguillarum*: Applied and Environmental Microbiology, v. 60, p. 1681-1683.

Amorim-Vaz, S., E. Delarze, F. Ischer, D. Sanglard, and A. T. Coste, 2015a, Examining the virulence of *Candida albicans* transcription factor mutants using *Galleria mellonella* and mouse infection models: Frontiers in Microbiology, v. 6, p. 39.

Amorim-Vaz, S., V. D. T. Tran, S. Pradervand, M. Pagni, A. T. Coste, and D. Sanglard, 2015b, RNA Enrichment Method for Quantitative Transcriptional Analysis of Pathogens In Vivo Applied to the Fungus *Candida albicans*: Mbio, v. 6, p. 16.

Amparyup, P., W. Charoensapsri, and A. Tassanakajon, 2009, Two prophenoloxidases are important for the survival of *Vibrio harveyi* challenged shrimp *Penaeus monodon*: Developmental and Comparative Immunology, v. 33, p. 247-256.

Austin, B., M. Alsina, D. A. Austin, A. R. Blanch, F. Grimont, P. A. D. Grimont, J. Jofre, S. Koblavi, J. L. Larsen, K. Pedersen, T. Tiainen, L. Verdonck, and J. Swings, 1995, Identification and typing of *Vibrio anguillarum* - a comparison of different methods: Systematic and Applied Microbiology, v. 18, p. 285-302.

Austin, B., D. A. Austin, A. R. Blanch, M. Cerda, F. Grimont, P. A. D. Grimont, J. Jofre, S. Koblavi, J. L. Larsen, K. Pedersen, T. Tiainen, L. Verdonck, and J. Swings, 1997, A comparison of methods for the typing of fish-pathogenic Vibrio spp: Systematic and Applied Microbiology, v. 20, p. 89-101.

Austin, B., and D. A. Austin. 2007. Bacterial fish pathogens: disease of farmed and wild fish, 4th ed. Praxis Publishing Ltd., Chichester, United Kingdom.

Balado, M., C. R. Osorio, and M. L. Lemos, 2006, A gene cluster involved in the biosynthesis of vanchrobactin, a chromosome-encoded siderophore produced by *Vibrio anguillarum*: Microbiology-Sgm, v. 152, p. 3517-3528.

Balado, M., C. R. Osorio, and M. L. Lemos, 2008, Biosynthetic and regulatory elements involved in the production of the siderophore vanchrobactin in *Vibrio anguillarum*: Microbiology-Sgm, v. 154, p. 1400-1413.

Balado, M., C. R. Osorio, and M. L. Lemos, 2009, FvtA Is the Receptor for the Siderophore Vanchrobactin in *Vibrio anguillarum*: Utility as a Route of Entry for Vanchrobactin Analogues: Applied and Environmental Microbiology, v. 75, p. 2775-2783.

Balboa, S., A. L. Dieguez, A. Doce, J. L. Barja, and J. L. Romalde, 2012, Evaluation of different culture media for the isolation and growth of the fastidious *Vibrio tapetis*, the causative agent of brown ring disease: Journal of Invertebrate Pathology, v. 111, p. 74-81.

Balboa, S., H. W. Ferguson, and J. L. Romalde, 2007, Phenotypic, serological and genetic characterization of *Pseudomonas anguilliseptica* strains isolated from cod, *Gadus morhua* L., in northern Europe: Journal of Fish Diseases, v. 30, p. 657-664.

Banno, Y., T. Shimada, Z. Kajiura, and H. Sezutsu, 2010, The Silkworm-An Attractive BioResource Supplied by Japan: Experimental Animals, v. 59, p. 139-146.

Banville, N., N. Browne, and K. Kavanagh, 2012, Effect of nutrient deprivation on the susceptibility of *Galleria mellonella* larvae to infection: Virulence, v. 3, p. 497-503.

Barancin, C. E., J. C. Smoot, R. H. Findlay, and L. A. Actis, 1998, Plasmid-mediated histamine biosynthesis in the bacterial fish pathogen *Vibrio anguillarum*: Plasmid, v. 39, p. 235-244.

Bergin, D., M. Brennan, and K. Kavanagh, 2003, Fluctuations in haemocyte density and microbial load may be used as indicators of fungal pathogenicity in larvae of *Galleria mellonella*: Microbes and Infection, v. 5, p. 1389-1395.

Bergman, A.M., 1909 Die rote Beulenkrankheit des Aals. Bericht aus der Koniglichen Bayerischen Versuchsstation v. 2, p. 10-54.

Bernier, S. P., D. Lebeaux, A. S. DeFrancesco, A. Valomon, G. Soubigou, J. Y. Coppee, J. M. Ghigo, and C. Beloin, 2013, Starvation, Together with the SOS Response, Mediates High Biofilm-Specific Tolerance to the Fluoroquinolone Ofloxacin: Plos Genetics, v. 9.

Biering, E., O. Vaagnes, B. Krossoy, S. Gulla, and D. J. Colquhoun, 2016, Challenge models for atypical *Aeromonas salmonicida* and *Vibrio anguillarum* in farmed Ballan wrasse (*Labrus bergylta*) and preliminary testing of a trial vaccine against atypical *Aeromonas salmonicida*: Journal of fish diseases, v. 39, p. 1257-61.

Boesen, H. T., K. Pedersen, J. L. Larsen, C. Koch, and A. E. Ellis, 1999, *Vibrio anguillarum* resistance to rainbow trout (*Oncorhynchus mykiss*) serum: Role of O-antigen structure of lipopolysaccharide: Infection and Immunity, v. 67, p. 294-301.

Boles, B. R., and L. L. McCarter, 2000, Insertional inactivation of genes encoding components of the sodium-type flagellar motor and switch of *Vibrio parahaemolyticus*: Journal of Bacteriology, v. 182, p. 1035-1045.

Bolinches J., M. L. Lemos, B. Fouz, M. Cambra, J. L. Larsen and A. E. Toranzo, 1990. Serological relationship among *Vibrio anguillarum* strains. J Aquatic Animal Health 2:21–29.

Bourhy, P., H. Louvel, I. Saint Girons, and M. Picardeau, 2005, Random insertional mutagenesis of *Leptospira interrogans*, the agent of leptospirosis, using a mariner transposon: Journal of Bacteriology, v. 187, p. 3255-3258.

Brackman, G., S. Celen, U. Hillaert, S. Van Calenbergh, P. Cos, L. Maes, H. J. Nelis, and T. Coenye, 2011, Structure-Activity Relationship of Cinnamaldehyde Analogs as Inhibitors of AI-2 Based Quorum Sensing and Their Effect on Virulence of Vibrio spp: Plos One, v. 6, p. 10.

Brennan, M., D. Y. Thomas, M. Whiteway, and K. Kavanagh, 2002, Correlation between virulence of *Candida albicans* mutants in mice and *Galleria mellonella* larvae: Fems Immunology and Medical Microbiology, v. 34, p. 153-157.

Browne, N., C. Surlis, A. Maher, C. Gallagher, J. C. Carolan, M. Clynes, and K. Kavanagh, 2015, Prolonged pre-incubation increases the susceptibility of *Galleria mellonella* larvae to bacterial and fungal infection: Virulence, v. 6, p. 458-465.

Brucker, R. M., L. J. Funkhouser, S. Setia, R. Pauly, and S. R. Bordenstein, 2012, Insect Innate Immunity Database (IIID): An Annotation Tool for Identifying Immune Genes in Insect Genomes: Plos One, v. 7.

Brutinel, E. D., and J. A. Gralnick, 2012, Anomalies of the anaerobic tricarboxylic acid cycle in *Shewanella oneidensis* revealed by Tn-seq: Molecular Microbiology, v. 86, p. 273-283.

Busschaert, P., I. Frans, S. Crauwels, B. Zhu, K. Willems, P. Bossier, C. Michiels, K. Verstrepen, B. Lievens, and H. Rediers, 2015, Comparative genome sequencing to assess the genetic diversity and virulence attributes of 15 *Vibrio anguillarum* isolates: Journal of Fish Diseases, v. 38, p. 795-807.

Callaway, R., A. P. Shinn, S. E. Grenfell, J. E. Bron, G. Burnell, E. J. Cook, M. Crumlish, S. Culloty, K. Davidson, R. P. Ellis, K. J. Flynn, C. Fox, D. M. Green, G. C. Hays, A. D. Hughes, E. Johnston, C. D. Lowe, I. Lupatsch, S. Malham, A. F. Mendzil, T. Nickell, T. Pickerell, A. F. Rowley, M. S. Stanley, D. R. Tocher, J. F. Turnbull, G. Webb, E. Wootton, and R. J. Shields, 2012, Review of climate change impacts on marine aquaculture in the UK and Ireland: Aquatic Conservation-Marine and Freshwater Ecosystems, v. 22, p. 389-421.

Canestrini, G., 1893, La malattia dominate delle anguille. Atti Institute Veneto Service, v. 7, p. 809-814.

Castillo, A., P. D. Alvise, R. Xu, F. Zhang, M. Middelboe, and L. Gram, 2017, Comparative genome analyses of Vibrio anguillarum strains reveal a link with pathogenicity traits: mSystems 2:e00001-17. https://doi.org/10.1128/mSystems.00001-17.

Chamilos, G., M. S. Lionakis, R. E. Lewis, and D. P. Kontoyiannis, 2007, Role of mini-host models in the study of medically important fungi: Lancet Infectious Diseases, v. 7, p. 42-55.

Chao, M. C., S. Abel, B. M. Davis, and M. K. Waldor, 2016, The design and analysis of transposon insertion sequencing experiments: Nature Reviews Microbiology, v. 14, p. 119-128.

Chao, M. C., J. R. Pritchard, Y. J. J. Zhang, E. J. Rubin, J. Livny, B. M. Davis, and M. K. Waldor, 2013, High-resolution definition of the *Vibrio cholerae* essential gene set with hidden Markov model-based analyses of transposon-insertion sequencing data: Nucleic Acids Research, v. 41, p. 9033-9048.

Chao, M. C., S. J. Zhu, S. Kimura, B. M. Davis, E. E. Schadt, G. Fang, and M. K. Waldor, 2015, A Cytosine Methytransferase Modulates the Cell Envelope Stress Response in the Cholera Pathogen: Plos Genetics, v. 11.

Chen, Q., L. A. Actis, M. E. Tolmasky, and J. H. Crosa, 1994, Chromosome-mediated 2,3-dihydroxybenzoic acid is a precursor in the biosynthesis of the plasmid-mediated siderophore anguibactin in *Vibrio-anguillarum*: Journal of Bacteriology, v. 176, p. 4226-4234.

Chiang, S. L., and E. J. Rubin, 2002, Construction of a mariner-based transposon for epitope-tagging and genomic targeting: Gene, v. 296, p. 179-185.

Choi, J. Y., C. D. Sifri, B. C. Goumnerov, L. G. Rahme, F. M. Ausubel, and S. B. Calderwood, 2002, Identification of virulence genes in a pathogenic

strain of *Pseudomonas aeruginosa* by representational difference analysis: Journal of Bacteriology, v. 184.

Choi, K. H., and K. J. Kim, 2009, Applications of Transposon-Based Gene Delivery System in Bacteria: Journal of Microbiology and Biotechnology, v. 19, p. 217-228.

Colquhoun, D. J., and A. Lillehaug, 2014, Vaccination against Vibriosis, *in* R. Gudding, A. Lillehaug, and O. Evensen, eds., Fish Vaccination: Oxford, Blackwell Science Publ, p. 172-184.

Cook, S. M., and J. D. McArthur, 2013, Developing *Galleria mellonella* as a model host for human pathogens: Virulence, v. 4, p. 350-3.

Covington, E. D., C. B. Gelbmann, N. J. Kotloski, and J. A. Gralnick, 2010, An essential role for UshA in processing of extracellular flavin electron shuttles by *Shewanella oneidensis*: Molecular Microbiology, v. 78, p. 519-532.

Craig, N. L., 1997, Target site selection in transposition: Annual Review of Biochemistry, v. 66, p. 437-474.

Crimmins, G. T., S. Mohammadi, E. R. Green, M. A. Bergman, R. R. Isberg, and J. Mecsas, 2012, Identification of MrtAB, an ABC Transporter Specifically Required for *Yersinia pseudotuberculosis* to Colonize the Mesenteric Lymph Nodes: Plos Pathogens, v. 8.

Crisafi, F., R. Denaro, M. Genovese, M. Yakimov, and L. Genovese, 2014, Application of relative real-time PCR to detect differential expression of virulence genes in *Vibrio anguillarum* under standard and stressed growth conditions: Journal of Fish Diseases, v. 37, p. 629-640.

Crosa, J. H., 1980, A plasmid associated with virulence in the marine fish pathogen *Vibrio anguillarum* specifies an iron sequestering system: Nature (London), v. 284, p. 566-568.

Crosa, J. H., L. L. Hodges, and M. H. Schiewe, 1980, Curing of a plasmid is correlated with an attenuation of virulence in the marine fish pathogen *Vibrio anguillarum*: Infection and Immunity, v. 27, p. 897-902.

Croxatto, A., V. J. Chalker, J. Lauritz, J. Jass, A. Hardman, P. Williams, M. Camara, and D. L. Milton, 2002, VanT, a homologue of *Vibrio harveyi* LuxR, regulates serine, metalloprotease, pigment, and biofilm production in *Vibrio anguillarum*: Journal of Bacteriology, v. 184, p. 1617-1629.

Croxatto, A., J. Lauritz, C. Chen, and D. L. Milton, 2007, *Vibrio anguillarum* colonization of rainbow trout integument requires a DNA locus involved in exopolysaccharide transport and biosynthesis: Environmental Microbiology, v. 9, p. 370-382.

Croxatto, A., J. Pride, A. Hardman, P. Williams, M. Camara, and D. L. Milton, 2004, A distinctive dual-channel quorum-sensing system operates in *Vibrio anguillarum*: Molecular Microbiology, v. 52, p. 1677-1689.

Cytrynska, M., P. Mak, A. Zdybicka-Barabas, P. Suder, and T. Jakubowicz, 2007, Purification and characterization of eight peptides from *Galleria mellonella* immune hemolymph: Peptides, v. 28, p. 533-546.

Defoirdt, T., P. Bossier, P. Sorgeloos, and W. Verstraete, 2005, The impact of mutations in the quorum sensing systems of *Aeromonas hydrophila*, *Vibrio anguillarum* and *Vibrio harveyi* on their virulence towards gnotobiotically cultured *Artemia franciscana*: Environmental Microbiology, v. 7, p. 1239-1247.

Delarze, E., F. Ischer, D. Sanglard, and A. T. Coste, 2015, Adaptation of a Gaussia princeps Luciferase reporter system in *Candida albicans* for in vivo detection in the *Galleria mellonella* infection model: Virulence, v. 6, p. 684-693.

Denkin, S. M., and D. R. Nelson, 1999, Induction of protease activity in *Vibrio anguillarum* by gastrointestinal mucus: Applied and Environmental Microbiology, v. 65, p. 3555-3560.

Denkin, S. M., and D. R. Nelson, 2004, Regulation of *Vibrio anguillarum* empA metalloprotease expression and its role in virulence: Applied and Environmental Microbiology, v. 70, p. 4193-4204.

Desalermos, A., B. B. Fuchs, and E. Mylonakis, 2012, Selecting an Invertebrate Model Host for the Study of Fungal Pathogenesis: Plos Pathogens, v. 8.

Desbois, A. P., and P. J. Coote, 2011, Wax moth larva (*Galleria mellonella*): an in vivo model for assessing the efficacy of antistaphylococcal agents: Journal of Antimicrobial Chemotherapy, v. 66, p. 1785-1790.

Desbois, A. P., and P. J. Coote, 2012, Utility of Greater Wax Moth Larva (*Galleria mellonella*) for Evaluating the Toxicity and Efficacy of New Antimicrobial Agents: Advances in Applied Microbiology, v. 78, v. 78.

Desbois, A. P., and S. McMillan, 2015, Paving the way to acceptance of *Galleria mellonella* as a new model insect: Virulence, v. 6, p. 410-411.

Di Lorenzo, M., M. Stork, and J. H. Crosa, 2011, Genetic and biochemical analyses of chromosome and plasmid gene homologues encoding ICL and ArCP domains in *Vibrio anguillarum* strain 775: Biometals, v. 24, p. 629-643.

Di Lorenzo, M., M. Stork, M. E. Tolmasky, L. A. Actis, D. Farrell, T. J. Welch, L. M. Crosa, A. A. Wertheimer, Q. Chen, P. Salinas, L. Waldbeser, and J. H. Crosa, 2003, Complete sequence of virulence plasmid pJM1 from the marine fish pathogen *Vibrio anguillarum* strain 775: Journal of Bacteriology, v. 185, p. 5822-5830.

Dorer, M. S., and R. R. Isberg, 2006, Non-vertebrate hosts in the analysis of host-pathogen interactions: Microbes and Infection, v. 8, p. 1637-1646.

Dorr, T., F. Delgado, B. D. Umans, M. A. Gerding, B. M. Davis, and M. K. Waldor, 2016, A Transposon Screen Identifies Genetic Determinants of *Vibrio cholerae* Resistance to High-Molecular-Weight Antibiotics: Antimicrobial Agents and Chemotherapy, v. 60, p. 4757-4763.

Dorr, T., A. Moll, M. C. Chao, F. Cava, H. Lam, B. M. Davis, and M. K. Waldor, 2014, Differential Requirement for PBP1a and PBP1b in In Vivo and In Vitro Fitness of *Vibrio cholerae*: Infection and Immunity, v. 82, p. 2115-2124.

Eistetter, A. J., P. D. Butler, R. R. Traut, and T. G. Fanning, 1999, Characterization of *Escherichia coli* 50S ribosomal protein L31: Fems Microbiology Letters, v. 180, p. 345-349.

FAO. 2012. Improving biosecurity through prudent and responsible use of veterinary medicines in aquatic food production. FAO Fisheries and Aquaculture Technical Paper No. 547. p. 208.

FAO. 2016a. The State of World Fisheries and Aquaculture 2016. Contributing to food security and nutrition for all. Rome. p. 200.

FAOb. 2016b. FAO yearbook. Fishery and Aquaculture Statistics 2014. Rome. p. 76.

FEAP (Federation of European Aquaculture Producers). 2015. European Aquaculture Production Report 2005-2014. http://www.feap.info/Default.asp?SHORTCUT=582

Fernandez, J., and R. Avendano-Herrera, 2009, Analysis of 16S-23S rRNA gene internal transcribed spacer of *Vibrio anguillarum* and *Vibrio ordalii* strains isolated from fish: Fems Microbiology Letters, v. 299, p. 184-192.

Ferrieres, L., G. Hemery, T. Nham, A. M. Guerout, D. Mazel, C. Beloin, and J. M. Ghigo, 2010, Silent Mischief: Bacteriophage Mu Insertions Contaminate Products of *Escherichia coli* Random Mutagenesis Performed Using Suicidal Transposon Delivery Plasmids Mobilized by Broad- Host-

Range RP4 Conjugative Machinery: Journal of Bacteriology, v. 192, p. 6418-6427.

Figaj, D., A. Gieldon, A. Polit, A. Sobiecka-Szkatula, T. Koper, M. Denkiewicz, B. Banecki, A. Lesner, J. Ciarkowski, B. Lipinska, and J. Skorko-Glonek, 2014, The LA Loop as an Important Regulatory Element of the HtrA (DegP) Protease from *Escherichia coli* structural and functional studies: Journal of Biological Chemistry, v. 289, p. 15880-15893.

Finn, R. D., P. Coggill, R. Y. Eberhardt, S. R. Eddy, J. Mistry, A. L. Mitchell, S. C. Potter, M. Punta, M. Qureshi, A. Sangrador-Vegas, G. A. Salazar, J. Tate, and A. Bateman, 2016, The Pfam protein families database: towards a more sustainable future: Nucleic Acids Research, v. 44, p. D279-D285.

Frans, I., K. Dierckens, S. Crauwels, A. Van Assche, J. Leisner, M. H. Larsen, C. W. Michiels, K. A. Willems, B. Lievens, P. Bossier, and H. Rediers, 2013, Does Virulence Assessment of *Vibrio anguillarum* Using Sea Bass (*Dicentrarchus labrax*) Larvae Correspond with Genotypic and Phenotypic Characterization?: Plos One, v. 8.

Frans, I., C. W. Michiels, P. Bossier, K. A. Willems, B. Lievens, and H. Rediers, 2011, *Vibrio anguillarum* as a fish pathogen: virulence factors, diagnosis and prevention: Journal of Fish Diseases, v. 34, p. 643-661.

Froquet, R., N. Cherix, S. E. Burr, J. Frey, S. Vilches, J. M. Tomas, and P. Cosson, 2007, Alternative host model to evaluate Aeromonas virulence: Applied and Environmental Microbiology, v. 73, p. 5657-5659.

Fujiwara-Nagata, E., K. Kogure, K. Kita-Tsukamoto, M. Wada, and M. Eguchi, 2003, Characteristics of Na+-dependent respiratory chain in *Vibrio anguillarum*, a fish pathogen, in comparison with other marine Vibrios: Fems Microbiology Ecology, v. 44, p. 225-230.

Fuchs, B. B., E. O'Brien, J. B. El Khoury, and E. Mylonakis, 2010, Methods for using *Galleria mellonella* as a model host to study fungal pathogenesis: Virulence, v. 1, p. 475-482.

Gadwal, S., K. V. Korotkov, J. R. Delarosa, W. G. J. Hol, and M. Sandkvist, 2014, Functional and Structural Characterization of *Vibrio cholerae* Extracellular Serine Protease B, VesB: Journal of Biological Chemistry, v. 289, p. 8288-8298.

Gallagher, L. A., J. Shendure, and C. Manoil, 2011, Genome-Scale Identification of Resistance Functions in *Pseudomonas aeruginosa* Using Tn-seq: Mbio, v. 2.

Gawronski, J. D., S. M. S. Wong, G. Giannoukos, D. V. Ward, and B. J. Akerley, 2009, Tracking insertion mutants within libraries by deep sequencing and a genome-wide screen for Haemophilus genes required in the lung: Proceedings of the National Academy of Sciences of the United States of America, v. 106, p. 16422-16427.

Gebhardt, M. J., L. A. Gallagher, R. K. Jacobson, E. A. Usacheva, L. R. Peterson, D. V. Zurawski, and H. A. Shuman, 2015, Joint Transcriptional Control of Virulence and Resistance to Antibiotic and Environmental Stress in Acinetobacter baumannii: Mbio, v. 6.

Gilchrist, C. A., and D. T. Denhardt, 1987, *Escherichia-coli* rep gene - sequence of the gene, the encoded helicase, and its homology with uvrd: Nucleic Acids Research, v. 15, p. 465-475.

Glavis-Bloom, J., M. Muhammed, and E. Mylonakis, 2012, Of Model Hosts and Man: Using *Caenorhabditis elegans*, *Drosophila melanogaster* and *Galleria mellonella* as Model Hosts for Infectious Disease Research, *in* E. Mylonakis, F. M. Ausubel, M. Gilmore, and A. Casadevall, eds., Recent Advances on Model Hosts: Advances in Experimental Medicine and Biology, v. 710: Berlin, Springer-Verlag Berlin, p. 11-17.

Gonzalez, S. F., C. R. Osorio, and Y. Santos, 2003, Development of a PCR-based method for the detection of *Listonella anguillarum* in fish tissues and blood samples: Diseases of Aquatic Organisms, v. 55, p. 109-115.

Goodman, A. L., N. P. McNulty, Y. Zhao, D. Leip, R. D. Mitra, C. A. Lozupone, R. Knight, and J. I. Gordon, 2009, Identifying Genetic Determinants Needed to Establish a Human Gut Symbiont in Its Habitat: Cell Host & Microbe, v. 6, p. 279-289.

Gottig, S., T. M. Gruber, B. Stecher, T. A. Wichelhaus, and V. A. J. Kempf, 2015, In Vivo Horizontal Gene Transfer of the Carbapenemase OXA-48 During a Nosocomial Outbreak: Clinical infectious diseases : an official publication of the Infectious Diseases Society of America, v. 60, p. 1808-15.

Gratacap, R. M. L., 2008, Characterisation of *Vibrio anguillarum* for the development of vaccine in cod (*Gadus morhua*). PhD Thesis. Institute of Aquaculture, University of Stirling, Scotland, UK

Grisez, L., and F. Ollevier, 1995, Comparative serology of the marine fish pathogen *Vibrio-anguillarum*: Applied and Environmental Microbiology, v. 61, p. 4367-4373.

Gudmundsdottir, S., B. Magnadottir, B. Bjornsdottir, H. Arnadottir, and B. K. Gudmundsdottir, 2009, Specific and natural antibody response of cod juveniles vaccinated against *Vibrio anguillarum*: Fish & Shellfish Immunology, v. 26, p. 619-624.

Guijarro, J. A., D. Cascales, A. I. Garcia-Torrico, M. Garcia-Dominguez, and J. Mendez, 2015, Temperature-dependent expression of virulence genes in fish-pathogenic bacteria: Frontiers in Microbiology, v. 6, p. 11.

Gutierrez, M. G., D. R. Yoder-Himes, and J. M. Warawa, 2015, Comprehensive identification of virulence factors required for respiratory melioidosis using Tn-seq mutagenesis: Frontiers in Cellular and Infection Microbiology, v. 5.

Haft, D. H., and N. Varghese, 2011, GlyGly-CTERM and Rhombosortase: A C-Terminal Protein Processing Signal in a Many-to-One Pairing with a Rhomboid Family Intramembrane Serine Protease: Plos One, v. 6, p. 11.

Handfield, M., A. Progulske-Fox, and J. D. Hillman, 2005, In vivo induced genes in human diseases: Periodontology 2000, v. 38, p. 123-134.

Hao, B., Z. L. Mo, P. Xiao, H. J. Pan, X. Lan, and G. Y. Li, 2013, Role of alternative sigma factor 54 (RpoN) from *Vibrio anguillarum* M3 in protease secretion, exopolysaccharide production, biofilm formation, and virulence: Applied Microbiology and Biotechnology, v. 97, p. 2575-2585.

Hardman, A. M., G. Stewart, and P. Williams, 1998, Quorum sensing and the cell-cell communication dependent regulation of gene expression in pathogenic and non-pathogenic bacteria: Antonie Van Leeuwenhoek International Journal of General and Molecular Microbiology, v. 74, p. 199-210.

Harvie, E. A., J. M. Green, M. N. Neely, and A. Huttenlocher, 2013, Innate Immune Response to *Streptococcus iniae* Infection in Zebrafish Larvae: Infection and Immunity, v. 81, p. 110-121.

Hirono, I., T. Masuda, and T. Aoki, 1996, Cloning and detection of the hemolysin gene of *Vibrio anguillarum*: Microbial Pathogenesis, v. 21, p. 173-182.

Hoffmann, J. A., J. M. Reichhart, and C. Hetru, 1996, Innate immunity in higher insects: Current Opinion in Immunology, v. 8, p. 8-13.

Holm, K. O., K. Nilsson, E. Hjerde, N. P. Willassen, and D. L. Milton, 2015, Complete genome sequence of *Vibrio anguillarum* strain NB10, a virulent isolate from the Gulf of Bothnia: Standards in Genomic Sciences, v. 10, p. 12.

Holm, S., 1979, A simple sequentially rejective multiple test procedure: Scandinavian Journal of Statistics, v. 6, p. 65-70.

Hong, G. E., D. G. Kim, J. Y. Bae, S. H. Ahn, S. C. Bai, and I. S. Kong, 2007, Species-specific PCR detection of the fish pathogen, *Vibrio anguillarum*, using the amiB gene, which encodes N-acetylmuramoyl-L-alanine amidase: Fems Microbiology Letters, v. 269, p. 201-206.

Huang, W. B., H. L. Ren, S. Gopalakrishnan, D. D. Xu, K. Qiao, and K. J. Wang, 2010, First molecular cloning of a molluscan caspase from variously colored abalone (*Haliotis diversicolor*) and gene expression analysis with bacterial challenge: Fish & Shellfish Immunology, v. 28, p. 587-595.

Hudson, M. E., 2008, Sequencing breakthroughs for genomic ecology and evolutionary biology: Molecular Ecology Resources, v. 8, p. 3-17.

Hurst, M. R. H., A. K. Beattie, S. A. Jones, P.-C. Hsu, J. Calder, and C. van Koten, 2015, Temperature-Dependent *Galleria mellonella* Mortality as a Result of *Yersinia entomophaga* Infection: Applied and Environmental Microbiology, v. 81, p. 6404-6414.

Hutchison, C. A., III, R.-Y. Chuang, V. N. Noskov, N. Assad-Garcia, T. J. Deerinck, M. H. Ellisman, J. Gill, K. Kannan, B. J. Karas, L. Ma, J. F. Pelletier, Z.-Q. Qi, R. A. Richter, E. A. Strychalski, L. Sun, Y. Suzuki, B. Tsvetanova, K. S. Wise, H. O. Smith, J. I. Glass, C. Merryman, D. G. Gibson, and J. C. Venter, 2016, Design and synthesis of a minimal bacterial genome: Science, v. 351, p. 1414-U73.

Illumina, 2016a. http://www.illumina.com/content/dam/illumina-support/documents/documentation/chemistry_documentation/16s/16s-metagenomic-library-prep-guide-15044223-b.pdf

Illumina, 2016b. http://www.illumina.com/documents/products/technotes/technote_Q-Scores.pdf

Illumina 2016c. https://support.illumina.com/content/dam/illumina-support/documents/documentation/system_documentation/miseq/miseq-denature-dilute-libraries-guide-15039740-01.pdf

Illumina, 2016d https://www.illumina.com/content/dam/illumina-marketing/documents/products/other/miseq-overclustering-primer-770-2014-038.pdf

Jander, G., L. G. Rahme, and F. M. Ausubel, 2000, Positive correlation between virulence of *Pseudomonas aeruginosa* mutants in mice and insects: Journal of Bacteriology, v. 182.

Jedani, K. E., U. H. Stroeher, and P. A. Manning, 2000, Distribution of IS1358 and linkage to *rfb*-related genes in *Vibrio anguillarum*: Microbiology-Uk, v. 146, p. 323-331.

Jensen, R. L., K. S. Pedersen, V. Loeschcke, H. Ingmer, and J. J. Leisner, 2007, Limitations in the use of *Drosophila melanogaster* as a model host for gram-positive bacterial infection: Letters in Applied Microbiology, v. 44, p. 218-223.

Jha, J. K., J. H. Baek, T. Venkova-Canova, and D. K. Chattoraj, 2012, Chromosome dynamics in multichromosome bacteria: Biochimica Et Biophysica Acta-Gene Regulatory Mechanisms, v. 1819, p. 826-829.

Jiang, H., A. Vilcinskas, and M. R. Kanost, 2010, Immunity in lepidopteran insects: Invertebrate Immunity, v. 708, p. 181-204.

Johnson, C. M., and A. D. Grossman, 2014, Identification of host genes that affect acquisition of an integrative and conjugative element in *Bacillus subtilis*: Molecular Microbiology, v. 93, p. 1284-1301.

Johnson, S. M., O. Sharif, P. A. Mak, H. T. Wang, I. H. Engels, A. Brinker, P. G. Schultz, A. L. Horwich, and E. Chapman, 2014, A biochemical screen for GroEL/GroES inhibitors: Bioorganic & Medicinal Chemistry Letters, v. 24, p. 786-789.

Judson, N., and J. J. Mekalanos, 2000, Transposon-based approaches to identify essential bacterial genes: Trends in Microbiology, v. 8, p. 521-526.

Junqueira, J. C., 2012, *Galleria mellonella* as a model host for human pathogens: Virulence, v. 3, p. 474-476.

Kaito, C., N. Akimitsu, H. Watanabe, and K. Sekimizu, 2002, Silkworm larvae as an animal model of bacterial infection pathogenic to humans: Microbial Pathogenesis, v. 32, p. 183-190.

Kaito, C., K. Kurokawa, Y. Matsumoto, Y. Terao, S. Kawabata, S. Hamada, and K. Sekimizu, 2005, Silkworm pathogenic bacteria infection model for identification of novel virulence genes: Molecular Microbiology, v. 56, p. 934-944.

Kaito, C., H. Yoshikai, and K. Sekimizu, 2012, Utilization of a silkworm model for understanding host-pathogen interactions: Isj-Invertebrate Survival Journal, v. 9, p. 163-168.

Kalia, V. C., P. Kumar, R. Kumar, A. Mishra, and S. Koul, 2015, Genome Wide Analysis for Rapid Identification of Vibrio Species: Indian Journal of Microbiology, v. 55, p. 375-383.

Kamp, H. D., B. Patimalla-Dipali, D. W. Lazinski, F. Wallace-Gadsden, and A. Camilli, 2013, Gene Fitness Landscapes of *Vibrio cholerae* at Important Stages of Its Life Cycle: Plos Pathogens, v. 9, p. 11.

Kaplan, E. L., and P. Meier, 1958, Nonparametric-estimation from incomplete observations: Journal of the American Statistical Association, v. 53, p. 457-481.

Kavanagh, K., and E. P. Reeves, 2004, Exploiting the potential of insects for in vivo pathogenicity testing of microbial pathogens: Fems Microbiology Reviews, v. 28, p. 101-112.

Khalil, S., E. Jacobson, M. C. Chambers, and B. P. Lazzaro, 2015, Systemic Bacterial Infection and Immune Defense Phenotypes in *Drosophila Melanogaster*: Jove-Journal of Visualized Experiments.

Kidwell, M. G., and D. R. Lisch, 2001, Perspective: Transposable elements, parasitic DNA, and genome evolution: Evolution, v. 55, p. 1-24.

Kim, D. G., Y. R. Kim, E. Y. Kim, H. M. Cho, S. H. Ahn, and I. S. Kong, 2010, Isolation of the groESL cluster from *Vibrio anguillarum* and PCR detection targeting groEL gene: Fisheries Science, v. 76, p. 803-810.

Kim, Y. R., S. Y. Kim, C. M. Kim, S. E. Lee, and J. H. Rhee, 2005, Essential role of an adenylate cyclase in regulating *Vibrio vulnificus* virulence: Fems Microbiology Letters, v. 243, p. 497-503.

Kitao, T., T. Aoki, M. Fukudome, K. Kawano, Y. Wada, and Y. Mizuno, 1983, Serotyping of *Vibrio-anguillarum* isolated from diseased fresh-water fish in Japan: Journal of Fish Diseases, v. 6, p. 175-181.

Kleckner, N., J. Roth, and D. Botstein, 1977, Genetic engineering in Vivo using translocatable drug-resistance elements: Journal of Molecular Biology, v. 116, p. 125-159.

Klein, B. A., E. L. Tenorio, D. W. Lazinski, A. Camilli, M. J. Duncan, and L. T. Hu, 2012, Identification of essential genes of the periodontal pathogen *Porphyromonas gingivalis*: Bmc Genomics, v. 13.

Kobayashi T., Enomoto S., Sakazaki R. and Kuwahara S. (1963) Jap. J. Bacteriol. 18. 10-11, 387-311.

Konkel, M. E., and K. Tilly, 2000, Temperature-regulated expression of bacterial virulence genes: Microbes and Infection, v. 2, p. 157-166.

Kwon, Y. M., S. C. Ricke, and R. K. Mandal, 2016, Transposon sequencing: methods and expanding applications: Applied Microbiology and Biotechnology, v. 100, p. 31-43.

Lafferty, K. D., C. D. Harvell, J. M. Conrad, C. S. Friedman, M. L. Kent, A. M. Kuris, E. N. Powell, D. Rondeau, and S. M. Saksida, 2015, Infectious diseases affect marine fisheries and aquaculture economics: Annual review of marine science, v. 7, p. 471-96.

Lampe, D. J., B. J. Akerley, E. J. Rubin, J. J. Mekalanos, and H. M. Robertson, 1999, Hyperactive transposase mutants of the Himar1 mariner transposon: Proceedings of the National Academy of Sciences of the United States of America, v. 96, p. 11428-11433.

Land, M., L. Hauser, S. R. Jun, I. Nookaew, M. R. Leuze, T. H. Ahn, T. Karpinets, O. Lund, G. Kora, T. Wassenaar, S. Poudel, and D. W. Ussery, 2015, Insights from 20 years of bacterial genome sequencing: Functional & Integrative Genomics, v. 15, p. 141-161.

Langridge, G. C., M.-D. Phan, D. J. Turner, T. T. Perkins, L. Parts, J. Haase, I. Charles, D. J. Maskell, S. E. Peters, G. Dougan, J. Wain, J. Parkhill, and A. K. Turner, 2009, Simultaneous assay of every Salmonella Typhi gene using one million transposon mutants: Genome Research, v. 19, p. 2308-2316.

Larsen, M. H., N. Blackburn, J. L. Larsen, and J. E. Olsen, 2004, Influences of temperature, salinity and starvation on the motility and chemotactic response of *Vibrio anguillarum*: Microbiology-Sgm, v. 150, p. 1283-1290.

Larsen, J. L., K. Pedersen, and I. Dalsgaard, 1994, *Vibrio anguillarum* serovars associated with vibriosis in fish: Journal of Fish Diseases, v. 17, p. 259-267.

Lazinski, D. W., and A. Camilli, 2013, Homopolymer tail-mediated ligation PCR: a streamlined and highly efficient method for DNA cloning and library construction: Biotechniques, v. 54, p. 25-+.

Le Breton, Y., A. T. Belew, K. M. Valdes, E. Islam, P. Curry, H. Tettelin, M. E. Shirtliff, N. M. El-Sayed, and K. S. McIver, 2015, Essential Genes in the

Core Genome of the Human Pathogen *Streptococcus pyogenes*: Scientific Reports, v. 5.

Lee, S. A., L. A. Gallagher, M. Thongdee, B. J. Staudinger, S. Lippman, P. K. Singh, and C. Manoil, 2015, General and condition-specific essential functions of *Pseudomonas aeruginosa*: Proceedings of the National Academy of Sciences of the United States of America, v. 112, p. 5189-5194.

Lehane, L., and G. T. Rawlin, 2000, Topically acquired bacterial zoonoses from fish: a review: Medical Journal of Australia, v. 173, p. 256-259.

Lemos, M. L., M. Balado, and C. R. Osorio, 2010, Anguibactin- versus vanchrobactin-mediated iron uptake in *Vibrio anguillarum*: evolution and ecology of a fish pathogen: Environmental Microbiology Reports, v. 2, p. 19-26.

LeRoux, F., K. M. Wegner, C. Baker-Austin, L. Vezzulli, C. R. Osorio, C. Amaro, J. M. Ritchie, T. Defoirdt, D. Destoumieux-Garzon, M. Blokesch, D. Mazel, A. Jacq, F. Cava, L. Gram, C. C. Wendling, E. Strauch, A. Kirschner, and S. Huehn, 2015, The emergence of Vibrio pathogens in Europe: ecology, evolution, and pathogenesis (Paris, 11-12th March 2015): Frontiers in Microbiology, v. 6.

Li, G., Z. Mo, J. Li, P. Xiao, and B. Hao, 2013a, Complete Genome Sequence of *Vibrio anguillarum* M3, a Serotype O1 Strain Isolated from Japanese Flounder in China: Genome announcements, v. 1.

Li, L., X. Y. Mou, and D. R. Nelson, 2011, HlyU Is a Positive Regulator of Hemolysin Expression in *Vibrio anguillarum*: Journal of Bacteriology, v. 193, p. 4779-4789.

Li, L., X. Y. Mou, and D. R. Nelson, 2013b, Characterization of Plp, a phosphatidylcholine-specific phospholipase and hemolysin of *Vibrio anguillarum*: Bmc Microbiology, v. 13.

Li, L., J. L. Rock, and D. R. Nelson, 2008, Identification and characterization of a repeat-in-toxin gene cluster in *Vibrio anguillarum*: Infection and Immunity, v. 76, p. 2620-2632.

Li, X., T. Defoirdt, and P. Bossier, 2015, Relation between virulence of Vibrio anguillarum strains and response to the host factors mucin, bile salts and cholesterol: Journal of Applied Microbiology, v. 119, p. 25-32.

Lin, C. Y., C. Y. Chiang, and H. J. Tsai, 2016, Zebrafish and Medaka: new model organisms for modern biomedical research: Journal of Biomedical Science, v. 23, p. 11.

Lindell, K., A. Fahlgren, E. Hjerde, N. P. Willassen, M. Fallman, and D. L. Milton, 2012, Lipopolysaccharide O-antigen prevents phagocytosis of *Vibrio anguillarum* by rainbow trout (*Oncorhynchus mykiss*) skin epithelial cells: Plos One, v. 7, p. 13.

Lionakis, M. S., and D. P. Kontoyiannis, 2010, The growing promise of Toll-deficient *Drosophila melanogaster* as a model for studying Aspergillus pathogenesis and treatment: Virulence, v. 1, p. 488-499.

Liu, Q., Y. Ma, L. Y. Zhou, and Y. X. Zhang, 2005, Gene cloning, expression and functional characterization of a phosphopantetheinyl transferase from *Vibrio anguillarum* serotype O1: Archives of Microbiology, v. 183, p. 37-44.

Loh, J. M. S., N. Adenwalla, S. Wiles, and T. Proft, 2013, *Galleria mellonella* larvae as an infection model for group A Streptococcus: Virulence, v. 4, p. 419-428.

Loman, N. J., C. Constantinidou, J. Z. M. Chan, M. Halachev, M. Sergeant, C. W. Penn, E. R. Robinson, and M. J. Pallen, 2012, High-throughput bacterial genome sequencing: an embarrassment of choice, a world of opportunity: Nature Reviews Microbiology, v. 10, p. 599-606.

Ma, L., J. X. Chen, R. Liu, X. H. Zhang, and Y. A. Jiang, 2009, Mutation of *rpoS* gene decreased resistance to environmental stresses, synthesis of

extracellular products and virulence of *Vibrio anguillarum*: Fems Microbiology Ecology, v. 70, p. 286-292.

Macdonell, M. T., and R. R. Colwell, 1985, Phylogeny of the vibrionaceae, and recommendation for 2 new genera, listonella and shewanella: Systematic and Applied Microbiology, v. 6, p. 171-182.

Magnadottir, B., 2006, Innate immunity of fish (overview): Fish & Shellfish Immunology, v. 20, p. 137-151.

Mancuso, M., M. Genovese, M. C. Guerrera, G. Casella, L. Genovese, G. Piccolo, and G. Maricchiolo, 2015, First episode of vibriosis in wild specimens of *Pagellus bogaraveo* (Brunnich, 1768) in the Mediterranean Sea: Cahiers De Biologie Marine, v. 56, p. 355-361.

Mantel, N., 1966, Evaluation of survival data and two new rank order statistics arising in its consideration., Cancer chemotherapy reports. Part 1, p. 163-170.

Mazoy, R., C. R. Osorio, A. E. Toranzo, and M. L. Lemos, 2003, Isolation of mutants of *Vibrio anguillarum* defective in haeme utilisation and cloning of *huvA*, a gene coding for an outer membrane protein involved in the use of haeme as iron source: Archives of Microbiology, v. 179, p. 329-338.

McGee, K., P. Horstedt, and D. L. Milton, 1996, Identification and characterization of additional flagellin genes from *Vibrio anguillarum*: Journal of Bacteriology, v. 178, p. 5188-5198.

McMillan, S., D. Verner-Jeffreys, J. Weeks, B. Austin, and A. P. Desbois, 2015, Larva of the greater wax moth, *Galleria mellonella*, is a suitable alternative host for studying virulence of fish pathogenic *Vibrio anguillarum*: Bmc Microbiology, v. 15, p. 10.

Meeske, A. J., L. T. Sham, H. Kimsey, B. M. Koo, C. A. Gross, T. G. Bernhardt, and D. Z. Rudner, 2015, MurJ and a novel lipid II flippase are required for cell wall biogenesis in Bacillus subtilis: Proceedings of the

National Academy of Sciences of the United States of America, v. 112, p. 6437-6442.

Meijer, A. H., and H. P. Spaink, 2011, Host-Pathogen Interactions Made Transparent with the Zebrafish Model: Current Drug Targets, v. 12, p. 1000-1017.

Metalnikoff, S. 1906. The immunity of the *Galleria mellonella* with regards to tuberculous bacillus. *Comptes Rendus Des Seances De La Societe De Biologie Et De Ses Filiales,* 58**,** 518-519.

Mikkelsen, H., V. Lund, R. Larsen, and M. Seppola, 2011, Vibriosis vaccines based on various sero-subgroups of *Vibrio anguillarum* O2 induce specific protection in Atlantic cod (*Gadus morhua* L.) juveniles: Fish & Shellfish Immunology, v. 30, p. 330-339.

Mikkelsen, H., V. Lund, L. C. Martinsen, K. Gravningen, and M. B. Schroder, 2007, Variability among *Vibrio anguillarum* O2 isolates from Atlantic cod (*Gadus morhua* L.): Characterisation and vaccination studies: Aquaculture, v. 266, p. 16-25.

Miller, R. A., P. S. Gaunt, R. Reimschuessel, J. Carson, C. Gieseker, P. R. Smith, I. Dalsgaard, J. P. Hawke, T. Somsiri and C. Wu, 2014, Methods for broth dilution susceptibility testing of bacteria isolated form aquatic animals; Approved guideline – 2nd Ed. Clinical and laboratory standards institute (CLSI)., PA, USA.

Milton, D. L., 2006, Quorum sensing in vibrios: Complexity for diversification: International Journal of Medical Microbiology, v. 296, p. 61-71.

Milton, D. L., A. Hardman, M. Camara, S. R. Chhabra, B. W. Bycroft, G. Stewart, and P. Williams, 1997, Quorum sensing in *Vibrio anguillarum:* Characterization of the *vanI/vanR* locus and identification of the

autoinducer N-(3-oxodecanoyl)-L-homoserine lactone: Journal of Bacteriology, v. 179, p. 3004-3012.

Milton, D. L., A. Norqvist, and H. Wolf-Watz, 1992, Cloning of a metalloprotease gene involved in the virulence mechanism of *Vibrio anguillarum*: Journal of Bacteriology, v. 174, p. 7235-7244.

Milton, D. L., A. Norqvist, and H. Wolfwatz, 1995, Sequence of a novel virulence-mediating gene, virc, from *Vibrio anguillarum*: Gene, v. 164, p. 95-100.

Milton, D. L., R. O'Toole, P. Horstedt, and H. WolfWatz, 1996, Flagellin A is essential for the virulence of *Vibrio anguillarum*: Journal of Bacteriology, v. 178, p. 1310-1319.

Miyamoto, N., and M. Eguchi, 1996, Development of monoclonal antibodies that specifically react with a fish pathogen, *Vibrio anguillarum* serotype J-O-1: Fisheries Science, v. 62, p. 710-714.

Miyashita, A., S. Iyoda, K. Ishii, H. Hamamoto, K. Sekimizu, and C. Kaito, 2012, Lipopolysaccharide O-antigen of enterohemorrhagic *Escherichia coli* O157:H7 is required for killing both insects and mammals: Fems Microbiology Letters, v. 333, p. 59-68.

Miyata, S., M. Casey, D. W. Frank, F. M. Ausubel, and E. Drenkard, 2003, Use of the *Galleria mellonella* caterpillar as a model host to study the role of the type III secretion system in *Pseudomonas aeruginosa* pathogenesis: Infection and Immunity, v. 71, p. 2404-2413.

Miyazaki, S., Y. Matsumoto, K. Sekimizu, and C. Kaito, 2012, Evaluation of *Staphylococcus aureus* virulence factors using a silkworm model: Fems Microbiology Letters, v. 326, p. 116-124.

Mo, Z.-l., S.-y. Chen, and P.-j. Zhang, 2002, Properties of proteolytic toxin of *Vibrio anguillarum* from diseased flounder: Chinese Journal of Oceanology and Limnology, v. 20, p. 316-322.

Mo, Z.-l., X.-g. Tan, Y.-l. Xu, and P.-j. Zhang, 2001, A *Vibrio anguillarum* strain associated with skin ulcer on cultured flounder, *Paralichthys olivaceus*: Chinese Journal of Oceanology and Limnology, v. 19, p. 319-326.

Mo, Z. L., D. S. Guo, Y. X. Mao, X. H. Ye, Y. X. Zou, P. Xiao, and B. Hao, 2010, Identification and characterization of the *Vibrio anguillarum prtV* gene encoding a new metalloprotease: Chinese Journal of Oceanology and Limnology, v. 28, p. 55-61.

Moore, D., and D. Dowhan, 2002, Purification and concentration of DNA from aqueous solutions: Current protocols in molecular biology / edited by Frederick M. Ausubel ... [et al.], v. Chapter 2, p. Unit 2.1A-Unit 2.1A.

Morey, M., A. Fernandez-Marmiesse, D. Castineiras, J. M. Fraga, M. L. Couce, and J. A. Cocho, 2013, A glimpse into past, present, and future DNA sequencing: Molecular Genetics and Metabolism, v. 110, p. 3-24.

Morgan, R. D., E. A. Dwinell, T. K. Bhatia, E. M. Lang, and Y. A. Luyten, 2009, The MmeI family: type II restriction-modification enzymes that employ single-strand modification for host protection: Nucleic Acids Research, v. 37, p. 5208-5221.

Mou, X. Y., E. J. Spinard, M. V. Driscoll, W. J. Zhao, and D. R. Nelson, 2013, H-NS Is a Negative Regulator of the Two Hemolysin/Cytotoxin Gene Clusters in *Vibrio anguillarum*: Infection and Immunity, v. 81, p. 3566-3576.

Mourino, S., C. R. Osorio, and M. L. Lemos, 2004, Characterization of heme uptake cluster genes in the fish pathogen *Vibrio anguillarum*: Journal of Bacteriology, v. 186, p. 6159-6167.

Mourino, S., I. Rodriguez-Ares, C. R. Osorio, and M. L. Lemos, 2005, Genetic variability of the heme uptake system among different strains of the fish pathogen *Vibrio anguillarum*: Identification of a new heme receptor: Applied and Environmental Microbiology, v. 71, p. 8434-8441.

Mowlds, P., A. Barron, and K. Kavanagh, 2008, Physical stress primes the immune response of *Galleria mellonella* larvae to infection by Candida albicans: Microbes and Infection, v. 10, p. 628-634.

Mowlds, P., and K. Kavanagh, 2008, Effect of pre-incubation temperature on susceptibility of *Galleria mellonella* larvae to infection by *Candida albicans*: Mycopathologia, v. 165, p. 5-12.

Naka, H., Q. Chen, Y. Mitoma, Y. Nakamura, D. McIntosh-Tolle, A. E. Gammie, M. E. Tolmasky, and J. H. Crosa, 2012, Two replication regions in the pJM1 virulence plasmid of the marine pathogen *Vibrio anguillarum*: Plasmid, v. 67, p. 95-101.

Naka, H., and J. H. Crosa, 2011, Genetic Determinants of Virulence in the Marine Fish Pathogen *Vibrio anguillarum*: Fish Pathology, v. 46, p. 1-10.

Naka, H., and J. H. Crosa, 2012, Identification and characterization of a novel outer membrane protein receptor FetA for ferric enterobactin transport in *Vibrio anguillarum* 775 (pJM1): Biometals, v. 25, p. 125-133.

Naka, H., G. M. Dias, C. C. Thompson, C. Dubay, F. L. Thompson, and J. H. Crosa, 2011, Complete Genome Sequence of the Marine Fish Pathogen *Vibrio anguillarum* Harboring the pJM1 Virulence Plasmid and Genomic Comparison with Other Virulent Strains of *V. anguillarum* and *V. ordalii*: Infection and Immunity, v. 79, p. 2889-2900.

Naka, H., M. Q. Liu, L. A. Actis, and J. H. Crosa, 2013a, Plasmid- and chromosome-encoded siderophore anguibactin systems found in marine vibrios: biosynthesis, transport and evolution: Biometals, v. 26, p. 537-547.

Naka, H., M. Q. Liu, and J. H. Crosa, 2013b, Two ABC transporter systems participate in siderophore transport in the marine pathogen *Vibrio anguillarum* 775 (pJM1): Fems Microbiology Letters, v. 341, p. 79-86.

Naka, H., C. S. Lopez, and J. H. Crosa, 2008, Reactivation of the vanchrobactin siderophore system of *Vibrio anguillarum* by removal of a

chromosomal insertion sequence originated in plasmid pJM1 encoding the anguibactin siderophore system: Environmental Microbiology, v. 10, p. 265-277.

Naka, H., C. S. Lopez, and J. H. Crosa, 2010, Role of the pJM1 plasmid-encoded transport proteins FatB, C and D in ferric anguibactin uptake in the fish pathogen Vibrio anguillarum: Environmental Microbiology Reports, v. 2, p. 104-111.

Neumann, N. F., J. L. Stafford, D. Barreda, A. J. Ainsworth, and M. Belosevic, 2001, Antimicrobial mechanisms of fish phagocytes and their role in host defense: Developmental and Comparative Immunology, v. 25, p. 807-825.

Norqvist, A., A. Hagstrom, and H. Wolfwatz, 1989, Protection of rainbow-trout against vibriosis and furunculosis by the use of attenuated strains of *Vibrio anguillarum*: Applied and Environmental Microbiology, v. 55, p. 1400-1405.

Norqvist, A., B. Norrman, and H. Wolfwatz, 1990, Identification and characterization of a zinc metalloprotease associated with invasion by the fish pathogen *Vibrio anguillarum*: Infection and Immunity, v. 58, p. 3731-3736.

Norqvist, A., and H. Wolfwatz, 1993, characterization of a novel chromosomal virulence locus involved in expression of a major surface flagellar sheath antigen of the fish pathogen *Vibrio anguillarum*: Infection and Immunity, v. 61, p. 2434-2444.

Nuidate, T., N. Tansila, S. Saengkerdsub, J. Kongreung, D. Bakkiyaraj, and V. Vuddhakul, 2016, Role of Indole Production on Virulence of *Vibrio cholerae* Using *Galleria mellonella* Larvae Model: Indian Journal of Microbiology, v. 56, p. 368-374.

O'Reilly, L. P., C. J. Luke, D. H. Perlmutter, G. A. Silverman, and S. C. Pak, 2014, C. elegans in high-throughput drug discovery: Advanced Drug Delivery Reviews, v. 69, p. 247-253.

O'Toole, G. A., L. A. Pratt, P. I. Watnick, D. K. Newman, V. B. Weaver, and R. Kolter, 1999, Genetic approaches to study of biofilms: Biofilms, v. 310, p. 91-109.

O'Toole, R., D. L. Milton, P. Horstedt, and H. Wolf-Watz, 1997, RpoN of the fish pathogen *Vibrio (Listonella) anguillarum* is essential for flagellum production and virulence by the water-borne but not intraperitoneal route of inoculation: Microbiology-Sgm, v. 143, p. 3849-3859.

O'Toole, R., D. L. Milton, and H. WolfWatz, 1996, Chemotactic motility is required for invasion of the host by the fish pathogen *Vibrio anguillarum:* Molecular Microbiology, v. 19, p. 625-637.

Okada, K., T. Iida, K. Kita-Tsukamoto, and T. Honda, 2005, Vibrios commonly possess two chromosomes: Journal of Bacteriology, v. 187, p. 752-757.

Olkkola, S., P. Juntunen, H. Heiska, H. Hyytiainen, and M. L. Hanninen, 2010, Mutations in the *rpsL* Gene Are Involved in Streptomycin Resistance in *Campylobacter coli*: Microbial Drug Resistance, v. 16, p. 105-110.

Olsen, R. J., M. E. Watkins, C. C. Cantu, S. B. Beres, and J. M. Musser, 2011, Virulence of serotype M3 Group A Streptococcus strains in wax worms (*Galleria mellonella* larvae): Virulence, v. 2, p. 111-119.

Ormonde, P., P. Horstedt, R. O'Toole, and D. L. Milton, 2000, Role of motility in adherence to and invasion of a fish cell line by *Vibrio anguillarum*: Journal of Bacteriology, v. 182, p. 2326-2328.

Ott, L., A. McKenzie, M. T. Baltazar, S. Britting, A. Bischof, A. Burkovski, and P. A. Hoskisson, 2012, Evaluation of invertebrate infection models for

pathogenic corynebacteria: Fems Immunology and Medical Microbiology, v. 65, p. 413-421.

Paillard, C., F. Le Roux, and J. J. Borrego, 2004, Bacterial disease in marine bivalves, a review of recent studies: Trends and evolution: Aquatic Living Resources, v. 17, p. 477-498.

Pang, M. D., X. Q. Lin, M. Hu, J. Li, C. P. Lu, and Y. J. Liu, 2012, Tetrahymena: An alternative model host for evaluating virulence of *Aeromonas* strains: Plos One, v. 7.

Pardo, B. G., A. Machordom, F. Foresti, F. Porto-Foresti, M. F. C. Azevedo, R. Banon, L. Sanchez, and P. Martinez, 2005, Phylogenetic analysis of flatfish (Order Pleuronectiformes) based on mitochondrial 16s rDNA sequences: Scientia Marina, v. 69, p. 531-543.

Pearson, K., 1895, Notes on regression and inheritance in the case of two parents: Proceedings of the Royal Society of London, v. 58, p. 240-242.

Pedersen, K., B. Austin, D. A. Austin, and J. L. Larsen, 1999a, Vibrios associated with mortality in cultured plaice *Pleuronectes platessa* fry: Acta Veterinaria Scandinavica, v. 40, p. 263-270.

Pedersen, K., L. Gram, D. A. Austin, and B. Austin, 1997, Pathogenicity of *Vibrio anguillarum* serogroup O1 strains compared to plasmids, outer membrane protein profiles and siderophore production: Journal of Applied Microbiology, v. 82, p. 365-371.

Pedersen, K., L. Grisez, R. van Houdt, T. Tiainen, F. Ollevier, and J. L. Larsen, 1999b, Extended serotyping scheme for *Vibrio anguillarum* with the definition and characterization of seven provisional O-serogroups: Current Microbiology, v. 38, p. 183-189.

Peeler, E. J., and S. W. Feist, 2011, Human intervention in freshwater ecosystems drives disease emergence: Freshwater Biology, v. 56, p. 705-716.

Petkau, A., M. Stuart-Edwards, P. Stothard, and G. Van Domselaar, 2010, Interactive microbial genome visualization with GView: Bioinformatics, v. 26, p. 3125-3126.

Pfeffer, C., and J. D. Oliver, 2003, A comparison of thiosulphate-citrate-bile salts-sucrose (TCBS) agar and thiosulphate-chloride-iodide (TCI) agar for the isolation of Vibrio species from estuarine environments: Letters in Applied Microbiology, v. 36, p. 150-151.

Prakash, O., Y. Nimonkar, and Y. S. Shouche, 2013, Practice and prospects of microbial preservation: Fems Microbiology Letters, v. 339, p. 1-9.

Pritchard, J. R., M. C. Chao, S. Abel, B. M. Davis, C. Baranowski, Y. J. J. Zhang, E. J. Rubin, and M. K. Waldor, 2014, ARTIST: High-Resolution Genome-Wide Assessment of Fitness Using Transposon-Insertion Sequencing: Plos Genetics, v. 10, p. 15.

Ramarao, N., C. Nielsen-Leroux, and D. Lereclus, 2012, The insect *Galleria mellonella* as a powerful infection model to investigate bacterial pathogenesis: Journal of visualized experiments : JoVE, p. e4392.

Rather, P., 2013, Role of rhomboid proteases in bacteria: Biochimica Et Biophysica Acta-Biomembranes, v. 1828, p. 2849-2854.

Riquelme, S., M. Varas, C. Valenzuela, P. Velozo, N. Chahin, P. Aguilera, A. Sabag, B. Labra, S. A. Alvarez, F. P. Chavez, and C. A. Santiviago, 2016, Relevant Genes Linked to Virulence Are Required for *Salmonella Typhimurium* to Survive Intracellularly in the Social Amoeba Dictyostelium discoideum: Frontiers in Microbiology, v. 7.

Robertson, H. M., 1995, The tc1-mariner superfamily of transposons in animals: Journal of Insect Physiology, v. 41, p. 99-105.

Robinson, L. J., A. D. S. Cameron, and J. Stavrinides, 2015, Spontaneous and on point: Do spontaneous mutations used for laboratory experiments

cause pleiotropic effects that might confound bacterial infection and evolution assays?: Fems Microbiology Letters, v. 362, p. 6.

Rock, J. L., and D. R. Nelson, 2006, Identification and characterization of a hemolysin gene cluster in *Vibrio anguillarum*: Infection and Immunity, v. 74, p. 2777-2786.

Rodkhum, C., I. Hirono, J. H. Crosa, and T. Aoki, 2005, Four novel hemolysin genes of *Vibrio anguillarum* and their virulence to rainbow trout: Microbial Pathogenesis, v. 39, p. 109-119.

Rodkhum, C., I. Hirono, J. H. Crosa, and T. Aoki, 2006a, Multiplex PCR for simultaneous detection of five virulence hemolysin genes in *Vibrio anguillarum*: Journal of Microbiological Methods, v. 65, p. 612-618.

Rodkhum, C., I. Hirono, M. Stork, M. Lorenzo, J. H. Crosa, and T. Aoki, 2006b, Putative virulence-related genes in *Vibrio anguillarum* identified by random genome sequencing: Journal of Fish Diseases, v. 29, p. 157-166.

Romalde, J. L., B. Magarinos, B. Fouz, I. Bandin, S. Nunez, and A. E. Toranzo, 1995, Evaluation of bionor mono-kits for rapid detection of bacterial fish pathogens: Diseases of Aquatic Organisms, v. 21, p. 25-34.

Ruiz, P., M. Poblete-Morales, R. Irgang, A. E. Toranzo, and R. Avendano-Herrera, 2016, Survival behaviour and virulence of the fish pathogen *Vibrio ordalii* in seawater microcosms: Diseases of Aquatic Organisms, v. 120, p. 27-38.

Sagane, Y., K. Hasegawa, S. Mutoh, H. Kouguchi, T. Suzuki, H. Sunagawa, T. Nakagawa, A. Kamaguchi, S. Okasaki, K. Nakayama, T. Watanabe, K. Oguma, and T. Ohyama, 2003, Molecular characterization of GroES and GroEL homologues from *Clostridium botulinum*: Journal of Protein Chemistry, v. 22, p. 99-108.

Schaeck, M., W. Van den Broeck, K. Hermans, and A. Decostere, 2013, Fish as Research Tools: Alternatives to *In Vivo* Experiments: Atla-Alternatives to Laboratory Animals, v. 41, p. 219-229.

Schiewe, M. H., J. H. Crosa, and E. J. Ordal, 1977, Deoxyribonucleic-acid relationships among marine vibrios pathogenic to fish: Canadian Journal of Microbiology, v. 23, p. 954-958.

Schiewe, M. H., T. J. Trust, and J. H. Crosa, 1981, *Vibrio-ordalii*-sp-nov - a causative agent of vibriosis in fish: Current Microbiology, v. 6, p. 343-348.

Schulenburg, H., C. L. Kurz, and J. J. Ewbank, 2004, Evolution of the innate immune system: the worm perspective: Immunological Reviews, v. 198, p. 36-58.

Shewan, J. M., W. A. Hodgkiss, 1954, Method for the rapid differentiation of certain non-pathogenic, asporogenous bacilli: Nature, v. 173 p. 208-9

Sikora, A. E., R. A. Zielke, D. A. Lawrence, P. C. Andrews, and M. Sandkvist, 2011, Proteomic Analysis of the *Vibrio cholerae* Type II Secretome Reveals New Proteins, Including Three Related Serine Proteases: Journal of Biological Chemistry, v. 286, p. 16555-16566.

Silva-Rubio, A., R. Avendano-Herrera, B. Jaureguiberry, A. E. Toranzo, and B. Magarinos, 2008, First description of serotype O3 in *Vibrio anguillarum* strains isolated from salmonids in Chile: Journal of Fish Diseases, v. 31, p. 235-239.

Simon, R., U. Priefer, and A. Puhler, 1983, A broad host range mobilization system for *in vivo* genetic-engineering - transposon mutagenesis in gram-negative bacteria: Bio-Technology, v. 1, p. 784-791.

Siwek, W., H. Czapinska, M. Bochtler, J. M. Bujnicki, and K. Skowronek, 2012, Crystal structure and mechanism of action of the N6-methyladenine-dependent type IIM restriction endonuclease R.DpnI: Nucleic Acids Research, v. 40, p. 7563-7572.

Skipper, K. A., P. R. Andersen, N. Sharma, and J. G. Mikkelsen, 2013, DNA transposon-based gene vehicles - scenes from an evolutionary drive: Journal of Biomedical Science, v. 20.

Smoot, L. M., J. C. Smoot, M. R. Graham, G. A. Somerville, D. E. Sturdevant, C. A. L. Migliaccio, G. L. Sylva, and J. M. Musser, 2001, Global differential gene expression in response to growth temperature alteration in group A Streptococcus: Proceedings of the National Academy of Sciences of the United States of America, v. 98, p. 10416-10421.

Sorensen, U. B. S., and J. L. Larsen, 1986, Serotyping of *Vibrio anguillarum*: Applied and Environmental Microbiology, v. 51, p. 593-597.

Springer, B., Y. G. Kidan, T. Prammananan, K. Ellrott, E. C. Bottger, and P. Sander, 2001, Mechanisms of streptomycin resistance: Selection of mutations in the 16S rRNA gene conferring resistance: Antimicrobial Agents and Chemotherapy, v. 45, p. 2877-2884.

Staroscik, A. M., S. M. Denkin, and D. R. Nelson, 2005, Regulation of the *Vibrio anguillarum* metalloprotease EmpA by posttranslational modification: Journal of Bacteriology, v. 187, p. 2257-2260.

Steenbergen, J. N., J. D. Nosanchuk, S. D. Malliaris, and A. Casadevall, 2003, *Cryptococcus neoformans* virulence is enhanced after growth in the genetically malleable host *Dictyostelium discoideum*: Infection and Immunity, v. 71, p. 4862-4872.

Steenbergen, J. N., H. A. Shuman, and A. Casadevall, 2001, *Cryptococcus neoformans* interactions with amoebae suggest an explanation for its virulence and intracellular pathogenic strategy in macrophages: Proceedings of the National Academy of Sciences of the United States of America, v. 98, p. 15245-15250.

Steinum, T. M., S. Karatas, N. T. Martinussen, P. M. Meirelles, F. L. Thompson, and D. J. Colquhoun, 2016, Multilocus sequence analysis of close

relatives *Vibrio anguillarum* and *Vibrio ordalii*: Applied and Environmental Microbiology, v. 82, p. 5496-5504.

Stroeher, U. H., K. E. Jedani, and P. A. Manning, 1998, Genetic organization of the regions associated with surface polysaccharide synthesis in *Vibrio cholerae* O1, O139 and *Vibrio anguillarum* O1 and O2: a review: Gene, v. 223, p. 269-282.

Stork, M., M. Di Lorenzo, S. Mourino, C. R. Osorio, M. L. Lemos, and J. H. Crosa, 2004, Two *tonB* systems function in iron transport in *Vibrio anguillarum*, but only one is essential for virulence: Infection and Immunity, v. 72, p. 7326-7329.

Stork, M., M. Di Lorenzo, T. J. Welch, and J. H. Crosa, 2007a, Transcription termination within the iron transport-biosynthesis operon of *Vibrio anguillarum* requires an antisense RNA: Journal of Bacteriology, v. 189, p. 3479-3488.

Stork, M., M. Di Lorenzo, T. J. Welch, L. M. Crosa, and J. H. Crosa, 2002, Plasmid-mediated iron uptake and virulence in *Vibrio anguillarum*: Plasmid, v. 48, p. 222-228.

Stork, M., B. R. Otto, and J. H. Crosa, 2007b, A novel protein, TtpC, is a required component of the TonB2 complex for specific iron transport in the pathogens *Vibrio anguillarum* and *Vibrio cholerae*: Journal of Bacteriology, v. 189, p. 1803-1815.

Stroeher, U. H., K. E. Jedani, and P. A. Manning, 1998, Genetic organization of the regions associated with surface polysaccharide synthesis in *Vibrio cholerae* O1, O139 and Vibrio anguillarum O1 and O2: a review: Gene, v. 223, p. 269-282.

Sullivan, C., and C. H. Kim, 2008, Zebrafish as a model for infectious disease and immune function: Fish & Shellfish Immunology, v. 25, p. 341-350.

Tellier, M., C. C. Bouuaert, and R. Chalmers, 2015, Mariner and the ITm Superfamily of Transposons: Microbiology Spectrum, v. 3, p. 19.

Thompson, F. L., C. C. Thompson, G. M. Dias, H. Naka, C. Dubay, and J. H. Crosa, 2011, The genus *Listonella* MacDonell and Colwell 1986 is a later heterotypic synonym of the genus *Vibrio* Pacini 1854 (Approved Lists 1980) - a taxonomic opinion: International Journal of Systematic and Evolutionary Microbiology, v. 61, p. 3023-3027.

Tiainen, T., K. Pedersen, and J. L. Larsen, 1997, Immunological reactivity of *Vibrio anguillarum* sero-subgroups O2a and O2b, and comparison of their lipopolysaccharide profiles: Current Microbiology, v. 34, p. 38-42.

Tinsley, J. W., A. R. Lyndon, and B. Austin, 2011, Antigenic and cross-protection studies of biotype 1 and biotype 2 isolates of *Yersinia ruckeri* in rainbow trout, *Oncorhynchus mykiss* (Walbaum): Journal of Applied Microbiology, v. 111, p. 8-16.

Tolmasky, M. E., L. A. Actis, and J. H. Crosa, 1988, Genetic-analysis of the iron uptake region of the *Vibrio anguillarum* plasmid pJM1 - molecular-cloning of genetic-determinants encoding a novel trans activator of siderophore biosynthesis: Journal of Bacteriology, v. 170, p. 1913-1919.

Tolmasky, M. E., L. A. Actis, and J. H. Crosa, 1995, A histidine-decarboxylase gene encoded by the *Vibrio anguillarum* plasmid pJM1 is essential for virulence - histamine is a precursor in the biosynthesis of anguibactin: Molecular Microbiology, v. 15, p. 87-95.

Tolmasky, M. E., A. M. Wertheimer, L. A. Actis, and J. H. Crosa, 1994, Characterization of the *Vibrio-anguillarum* fur gene - role in regulation of expression of the FatA outer-membrane protein and catechols: Journal of Bacteriology, v. 176, p. 213-220.

Treasurer, J. W., 2012, Diseases of north European wrasse (Labridae) and possible interactions with cohabited farmed salmon, *Salmo salar* L: Journal of Fish Diseases, v. 35, p. 555-562.

Trevijano-Contador, N., and O. Zaragoza, 2014, Expanding the use of alternative models to investigate novel aspects of immunity to microbial pathogens: Virulence, v. 5, p. 454-456.

Trevors, J. T., 1986, Plasmid curing in bacteria: Fems Microbiology Letters, v. 32, p. 149-157.

Tsai, C. J. Y., J. M. S. Loh, and T. Proft, 2016, *Galleria mellonella* infection models for the study of bacterial diseases and for antimicrobial drug testing: Virulence, v. 7, p. 214-229.

van Opijnen, T., K. L. Bodi, and A. Camilli, 2009, Tn-seq: high-throughput parallel sequencing for fitness and genetic interaction studies in microorganisms: Nature Methods, v. 6, p. 767-U21.

van Opijnen, T., and A. Camilli, 2010, Genome-wide fitness and genetic interactions determined by Tn-seq, a high-throughput massively parallel sequencing method for microorganisms: Current protocols in microbiology, v. Chapter 1, p. Unit1E.3-Unit1E.3.

van Opijnen, T., and A. Camilli, 2012, A fine scale phenotype-genotype virulence map of a bacterial pathogen: Genome Research, v. 22, p. 2541-2551.

van Opijnen, T., and A. Camilli, 2013, Transposon insertion sequencing: a new tool for systems-level analysis of microorganisms: Nature Reviews Microbiology, v. 11.

van Soest, J. J., O. W. Stockhammer, A. Ordas, G. V. Bloemberg, H. P. Spaink, and A. H. Meijer, 2011, Comparison of static immersion and intravenous injection systems for exposure of zebrafish embryos to the natural pathogen *Edwardsiella tarda*: Bmc Immunology, v. 12, p. 15.

Varina, M., S. M. Denkin, A. M. Staroscik, and D. R. Nelson, 2008, Identification and characterization of epp, the secreted processing protease for the *Vibrio anguillarum* EmpA metalloprotease: Journal of Bacteriology, v. 190, p. 6589-6597.

Verhagen, L. M., M. I. de Jonge, P. Burghout, K. Schraa, L. Spagnuolo, S. Mennens, M. J. Eleveld, C. E. van der Gaast-de Jongh, A. Zomer, P. W. M. Hermans, and H. J. Bootsma, 2014, Genome-Wide Identification of Genes Essential for the Survival of *Streptococcus pneumoniae* in Human Saliva: Plos One, v. 9, p. 11.

Vogel, H., B. Altincicek, G. Glockner, and A. Vilcinskas, 2011, A comprehensive transcriptome and immune-gene repertoire of the lepidopteran model host *Galleria mellonella*: Bmc Genomics, v. 12.

Wang, Y., Z. Xu, A. Jia, J. Chen, Z. Mo, and X. Zhang, 2009, Genetic diversity between two *Vibrio anguillarum* strains exhibiting different virulence by suppression subtractive hybridization: Weishengwu Xuebao, v. 49, p. 363-370.

Wang, Y., X. H. Zhang, and B. Austin, 2010, Comparative analysis of the phenotypic characteristics of high- and low-virulent strains of *Edwardsiella tarda*: Journal of Fish Diseases, v. 33, p. 985-994.

Weber, B., C. Chen, and D. L. Milton, 2010, Colonization of fish skin is vital for *Vibrio anguillarum* to cause disease: Environmental Microbiology Reports, v. 2, p. 133-139.

Weber, B., A. Croxatto, C. Chen, and D. L. Milton, 2008, RpoS induces expression of the *Vibrio anguillarum* quorum-sensing regulator VanT: Microbiology-Sgm, v. 154, p. 767-780.

Welch, T. J., S. H. Chai, and J. H. Crosa, 2000, The overlapping angB and angG genes are encoded within the trans-acting factor region of the

virulence plasmid in *Vibrio anguillarum*: Essential role in siderophore biosynthesis: Journal of Bacteriology, v. 182, p. 6762-6773.

Welch, T. J., and J. H. Crosa, 2005, Novel role of the lipopolysaccharide O1 side chain in ferric siderophore transport and virulence of *Vibrio anguillarum:* Infection and Immunity, v. 73, p. 5864-5872.

Wertheimer, A. M., W. Verweij, Q. Chen, L. M. Crosa, M. Nagasawa, M. E. Tolmasky, L. A. Actis, and J. H. Crosa, 1999, Characterization of the *angR* gene of *Vibrio anguillarum*: Essential role in virulence: Infection and Immunity, v. 67, p. 6496-6509.

Wilson, B. R., A. R. Bogdan, M. Miyazawa, K. Hashimoto, and Y. Tsuji, 2016, Siderophores in Iron Metabolism: From Mechanism to Therapy Potential: Trends in Molecular Medicine, v. 22, p. 1077-1090.

Wu, H., Y. Ma, Y. Zhang, and H. Zhang, 2004, Complete sequence of virulence plasmid pEIB1 from the marine fish pathogen *Vibrio anguillarum* strain MVM425 and location of its replication region: Journal of Applied Microbiology, v. 97, p. 1021-1028.

Wu, H. J., A. H. J. Wang, and M. P. Jennings, 2008, Discovery of virulence factors of pathogenic bacteria: Current Opinion in Chemical Biology, v. 12, p. 93-101.

Xu, J., J. Kim, T. Danhorn, P. M. Merritt, and C. Fuqua, 2012, Phosphorus limitation increases attachment in Agrobacterium tumefaciens and reveals a conditional functional redundancy in adhesin biosynthesis: Research in Microbiology, v. 163, p. 674-684.

Xu, Z. N., Y. Wang, Y. Han, J. X. Chen, and X. H. Zhang, 2011, Mutation of a novel virulence-related gene *mltD* in *Vibrio anguillarum* enhances lethality in zebra fish: Research in Microbiology, v. 162, p. 144-150.

Yanik, M. F., C. B. Rohde, and C. Pardo-Martin, 2011, Technologies for Micromanipulating, Imaging, and Phenotyping Small Invertebrates and

Vertebrates, *in* M. L. Yarmush, J. S. Duncan, and M. L. Gray, eds., Annual Review of Biomedical Engineering, Vol 13: Annual Review of Biomedical Engineering, v. 13: Palo Alto, Annual Reviews, p. 185-217.

Yanischperron, C., J. Vieira, and J. Messing, 1985, Improved m13 phage cloning vectors and host strains - nucleotide-sequences of the m13mp18 and puc19 vectors: Gene, v. 33, p. 103-119.

Yook, K., T. W. Harris, T. Bieri, A. Cabunoc, J. Chan, W. J. Chen, P. Davis, N. de la Cruz, A. Duong, R. Fang, U. Ganesan, C. Grove, K. Howe, S. Kadam, R. Kishore, R. Lee, Y. Li, H.-M. Muller, C. Nakamura, B. Nash, P. Ozersky, M. Paulini, D. Raciti, A. Rangarajan, G. Schindelman, X. Shi, E. M. Schwarz, M. A. Tuli, K. Van Auken, D. Wang, X. Wang, G. Williams, J. Hodgkin, M. Berriman, R. Durbin, P. Kersey, J. Spieth, L. Stein, and P. W. Sternberg, 2012, WormBase 2012: more genomes, more data, new website: Nucleic Acids Research, v. 40, p. D735-D741.

Zak, O., and T. O'reilly, 1991, Animal-models in the evaluation of antimicrobial agents: Antimicrobial Agents and Chemotherapy, v. 35, p. 1527-1531.

Zhang, Z., Z. Mo, S. Chen, Y. Zou, and P. Zhang, 2015, Construction and characterization of the angR mutant of *Vibrio anguillarum* via insertional inactivation: Journal of Environmental Biology, v. 36, p. 807-811.

Zou, Y. X., Z. L. Mo, B. Hao, X. H. Ye, D. S. Guo, and P. J. Zhang, 2010, Screening of genes expressed in vivo after infection by *Vibrio anguillarum* M3: Letters in Applied Microbiology, v. 51, p. 564-569.

Appendix I

Consumables and equipment suppliers

Agilent Technologies., Santa Clara, US.

Beckman Coulter (UK) Ltd., High Wycombe, UK

Bibby Scientific Ltd., Stone, UK

Bioline Reagents Ltd., London, UK.

Biolog., Hayward, US

Biometra GmbH., Göttingen, Germany.

Bionor Laboratories AS., Skien, Norway.

BioSpec products, Inc., Bartlesville, USA

Biotek UK., Swindon, UK.

Cecil Instruments Ltd., Cambridge, UK.

ELMI., Riga, Latvia

Eurofins Genomics., Ebersberg, Germany

Fisher Scientific UK Ltd., Loughborough, Leicestershire, UK.

GATC Biotech., London, UK.

Hamilton., Ghiroda, Romania.

Ibis Biosciences., Carlsbad, US.

IKA®-Werke GmbH &Co. KG., Staufen, Germany.

Illumina®., San Diego, US

Invitrogen (See ThermoFisher)

Kimble Chase., Rockwood, US.

Microsoft., Redmond, US.

Millipore Ltd., Watford, Hertfordshire, UK.

New England Biolabs® Inc., Ipswich, USA

Qiagen Ltd., Manchester, UK

Sarstedt AG and Co., Nümbrecht, Germany

Sartorius UK Ltd., Epsom, UK.

Sigma-Aldrich Ltd., Poole, Dorset, UK.

Syngene., Cambridge, UK

ThermoFisher Scientific Inc. (nanodrop), Wilmington, US.

ThermoFisher Scientific Inc., Renfrew, UK.

UK Waxworms Ltd., Sheffield, UK.

Appendix II

Molecular buffers and reagents

All molecular buffers and reagents were prepared in RNase free glass or plastic ware and using nuclease free water.

All stock solutions were prepared using nuclease free water and autoclaved at 121°C for 15 minutes unless stated.

0.5 M EDTA (ethylenediaminetetraacetic acid) [pH8.0], 1 L

	Mass/ volume	Final molar (M) concentration
EDTA.Na_2.2H_2O (disodium ethylenediaminetetraacetate 2H_20)	186.2 g	0.5

EDTA.Na_2.2H_2O was added to 800 mL nuclease free water and placed on magnetic stirrer without heating. NaOH pellets were added gradually until pH8.0 was reached and all EDTA.Na_2.2H_2O was dissolved and then made up to 1 L with nuclease free water.

50 ×TAE (Tris-acetate-EDTA) Buffer (pH 8.3), 1 L

	Mass/ volume	Final molar (M) concentration
Tris base	242 g	2
Glacial acetic acid (100%)	57.1 mL	1
0.5 M Na_2EDTA (pH8.0)	100 mL	0.05

Tris base was dissolved in 750 mL of nuclease free water using a magnetic stirrer then glacial acetic acid and EDTA were added before solution was corrected to pH 8.3, then made up to 1 L with nuclease free water and autoclaved. 50 ×TAE was diluted as required in nuclease free water.

STE (NaCl-Tris-EDTA) buffer, 100 mL

	Volume	Final milli-molar (mM) concentration
1M Tris (pH 8.0)	1 mL	10
0.5 M Na_2EDTA (pH8.0)	200 µL	1
5M NaCl	2 mL	100

This solution was made up to 100 mL with nuclease free water

TE (Tris-EDTA) buffer, 100 mL

	Volume	Final milli-molar (mM) concentration
1M Tris (pH 8.0)	1 mL	10
0.5 M Na_2EDTA (pH8.0)	200 µL	1

This solution was made up to 100 mL with nuclease free water.

SSTNE (NaCl -SDS-Tris-NaCl-EDTA; Pardo et al., 2005) buffer, 1 L

	Volume	Final milli-molar (mM) concentration
NaCl	17.5 g	0.3
Tris base	6.5 g	0.054
0.2 M Na_2EDTA (pH8.0)	1 mL	0.2
EGTA (Ethylene glycol-bis[2-aminoethylether]-N,N,N',N'-tetraacetic acid)	76 mg	0.2
Spermidine	72 mg	0.5
Spermine	52 mg	0.257

All ingredients were dissolved in 800 mL of nuclease free water, using a magnetic stirrer, then corrected to 1 L and stored at 4°C after autoclaving.

Pardo, B. G., A. Machordom, F. Foresti, F. Porto-Foresti, M. F. C. Azevedo, R. Banon, L. Sanchez, and P. Martinez, 2005, Phylogenetic analysis of flatfish (Order Pleuronectiformes) based on mitochondrial 16s rDNA sequences: Scientia Marina, v. 69, p. 531-543.

Appendix III

Growth curves in shakeflask

To best predict an appropriate time to harvest bacterial cultures, during late exponential phase, growth curves were determined for isolates of interest. Each isolate was cultured in appropriate broth and conditions (Table 2.1 or Table 4.1, Section 2.2.2) to late exponential phase in a Universal bottle before washing the cells, re-suspending in PBS, and correcting to an A_{600} of 0.88 AU for *Vibrio* spp. and 1.2 AU for *E. coli* (approximately 10^9 CFU/mL and 5×10^8 CFU/mL, respectively).

Bacterial suspension was added to a 250-mL shakeflask, dressed with a non-absorbent cotton wool bung and an aluminium foil cover, to a final concentration of 5×10^6 CFU/mL in 50mL of medium. Each culture was mixed and 1 mL of culture was removed aseptically and A_{600} determined against a blank of appropriate medium. Cultures were incubated at the appropriate conditions (Section 2.2.2) with A_{600} determined every hour until stationary phase.

Values from triplicate flasks inoculated at the same time were combined to generate the growth curve plotting A_{600} of bacterial suspensions against time.

Appendix IV

Hamilton® syringe wash procedure

A wash regime was developed and evaluated for the injection procedure to reduce the opportunity for carryover of bacterial inoculums between experimental groups. Briefly, *V. anguillarum* VIB 1 was grown, washed and re-suspended in PBS, at a concentration of 10^9 CFU/mL, as previously described (Section 2.2.2). Using a 50-µL syringe (Ghiroda, Romania), 10 µL of bacterial suspension was drawn up and discharged into a discard jar. The syringe was then washed six times in 1% (w/v) sodium hypochlorite followed by six consecutive washes of 70% ethanol, in DH_2O, then rinsed six times with PBS. For each wash or rinse stage the syringe barrel was completely filled and discharged into a discard jar. Following the final rinse 10 µL of PBS was drawn up, from a fresh aliquot, and plated onto TSA20. This wash and rinse treatment was completed a further three times, plating fresh PBS after each cycle.

The complete process was then repeated, using the same bacterial suspension, but reducing the number of each wash and rinse stage by one. This was repeated, reducing wash and rinse stages by one after each complete quadruplicate treatment until the syringe was washed only once with 1% (w/v) sodium hypochlorite then 70% ethanol followed by a single rinse in PBS. A final treatment comprised one 70% ethanol wash only followed by a single rinse in PBS.

Results

No *V. anguillarum* colonies were recovered onto TSA20 agar following every syringe wash and rinse regime, excluding the single 70% ethanol wash and PBS rinse which produced too many colonies to reliably count. Therefore, all challenge experiments were performed with a wash and rinse regime comprising three each of 1% (w/v) sodium hypochlorite and 70% ethanol followed by 6 rinses in sterile PBS. The increase in washes will prevent any aberration in carryover, impacting a larval challenge, and the additional rinse cycles will remove any toxic wash chemicals from the syringe.

Appendix V

Heat killing of *Vibrio anguillarum*

To assess the best conditions for heat inactivation of *Vibrio anguillarum* isolates (Table 2.1.) VIB 44, VIB 64, VIB 79, AND VIB 87, were grown to stationary phase, in 15mL of TSA20, then washed and re-suspended in 15 mL PBS following Section 2.2.2. Each bacterial suspension was split into 3 aliquots of 5 mL, in glass Universal bottles, and placed in a water bath at 60°C. At 20 minute intervals a single aliquot of each isolate bacterial suspension was removed from water bath and 10 μL plated into TSA20, before refrigerating. This produced samples that had been heat killed for 20, 40 and 60 minutes. After 72 h refrigeration samples were again plated onto TSA20 as above to confirm that no cells had reactivated.

Results

No cells were recovered from any samples. Therefore *V. anguillarum* heat killing conditions were set at 60°C for 25 minutes.

Appendix VI

Effect of penicillin in media

Briefly, *V. anguillarum* VIB 79 was grown, washed and re-suspended in PBS, at a concentration of 10^7 CFU/mL, as previously described (2.2.2), before a group of 4 larvae were challenged and incubated following the method in a previous section (3.2.3.1). Control groups of four PBS injected, and un-manipulated larvae were also included. After 24 h incubation haemolymph from all experimental and control animals was plated at three 1:10 dilutions (10^{-2} - 10^{-5}) as previously described (3.2.3.1) onto TSA20 and TSA20 + PEN to investigate whether the PEN produced any differences in recovery. Colonies were counted, and plates examined for contamination, after 48 h incubation at 22°C.

Results

Addition of PEN to TSA20 had no effect on *V. anguillarum* recovery, when compared to colonies recovered onto TSA20 only, but prevented the growth of most contaminating microbes introduced from the larva surface or gut. Moreover, any contaminating colonies were obvious and did not affect CFU determinations.

Appendix VII

Mariner Transposon mutagenesis of *E. coli* recipient

To confirm that *E. coli* SM10*λpir* (pSC189) was capable of transferring this plasmid to a donor strain, it was mated with the *E. coli* TOP10 strain that had been used by researchers during the construction of this *mariner* transposon system (Chiang and Rubin, 2002). Donor and recipient cultures were incubated (37°C, 150 rpm, 4 h) in appropriate media with selective antibiotics (Table 4.1). Both cultures were diluted and plated onto appropriate media to confirm input CFU according to section 2.2.2. A 1.6 mL volume of each culture was washed once in PBS, as described previously (2.2.2.), before harvesting cells by centrifugation (2600 ×*g*; 15 minutes; 4°C) and suspending the cell pellet in 400 µL of LB. Then, 100 µL of this cell suspension was spread onto LBA on three plates, and incubated (37°C, 6 h) before all colonies were scraped from the agar surface and suspended in 7.5 mL LB. Factor ten dilutions of this bacterial suspension, from 10^{-1} - 10^{-6} were prepared in PBS, and 20 µL of each concentration plated onto LBA + STR^{200} + KAN^{30}, LBA + STR^{200} and LBA + AMP^{100} + KAN^{30}. Transposition frequency was calculated as the ratio of CFU recovered on KAN^r + STR^r to STR^r agar from plated output cell suspensions. This experiment was performed in duplicate.

To confirm that colonies that isolated onto transformant selection media had integrated the TnSC189 transposon in their genetic material, 12 colonies were re-isolated onto LBA + KAN^{250} + STR^{100} and then LBA +

AMP^{100}, onto which transposon mutants shouldn't recover if the plasmid backbone has been correctly lost.

Results

Following PCR confirmation that donor *E. coli* SM10*λpir* carried the pSC189 plasmid containing the TnSC189 transposon (Figure 4.3), *E. coli* TOP10 was successfully mutagenized following the protocol (Chiang and Rubin, 2002), thus confirming the integrity of the transposon system. However, thousands of micro-colonies grew on media containing 30 μg/mL KAN and 100 μg/mL STR spread with both mating experimental mating mixture and control of *E coli* TOP10 only, therefore suggesting that *E coli* TOP10 spontaneously mutates under KAN selection and indicated that a higher concentration of KAN should be used to eliminate these spontaneous mutants. Despite this, exconjugants were easily distinguishable from spontaneous mutants, due to their larger colony size, and nine of 12 colonies successfully re-isolated onto LBA + KAN^{250} + STR^{100} and subsequently were confirmed to contain the TnSC189 transposon by PCR (Figure 4.4); however, the same nine colonies failed to recover onto LBA + AMP^{100} indicating that they had lost the pSC189 plasmid backbone. Furthermore, no DNA extracted from the nine transposon mutant isolates produced products corresponding to the Mu lysogen, thus suggesting this genetic element had not transferred into the recipient cells (Figure 4.4). Mutation efficiency was low (2.65×10^{-6}) compared with 3×10^{-3} reported for this system previously (Chiang and Rubin, 2002).

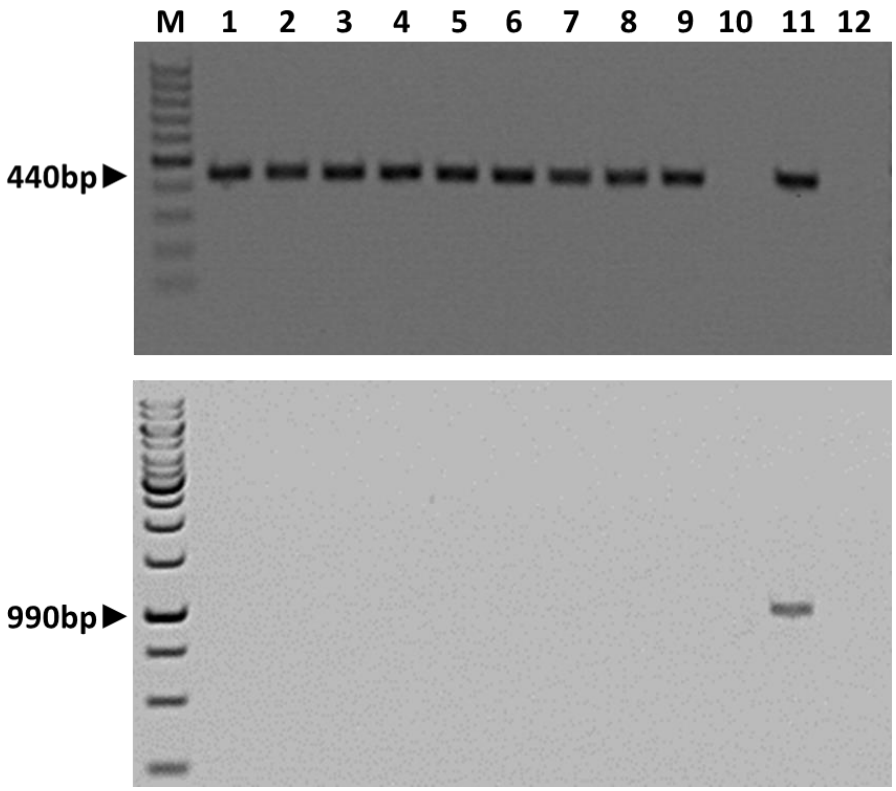

Figure. Image of Agarose gel following electrophoresis of PCR products derived from DNA extracted from *Escherichia coli* TOP10 transposon mutants to confirm that: (A) transposon has inserted into TOP10 genomic DNA, using primers TnSC189F and TnSC189R; (B) lysogenic Mu has not transferred from *E. coli* SM10λpir chromosome into TOP10 genomic DNA, using primers Mu1470bp.500-5 and Mu1470bp.500-3. M, 100bp (A) or 1kb DNA ladder (B); lanes 1-9, TOP10 isolates with suspected TnSC189 insert; lane 10, TOP10; lane 11, *E. coli* SM10λpir (pSC189); lane 12, no template control.

Appendix VIII

1. Isolation of pSC189 and pUC18 plasmids

The pSC189 plasmid was isolated with a QIAprep® Spin Miniprep Kit (Qiagen Ltd; Manchester, UK) according to the manufacturer. All reagents and buffers were supplied with the kit and any additions to these were completed prior to plasmid isolation, following the manufacturer's instructions. *E. coli* SM10*λpir* (pSC189) was cultured in 10 mL Miller lysogeny broth (LB) + 100 μg/mL ampicillin (AMP^{100}) (37°C, 14 h, 250 rpm) and the cells, in six 1.5 ml aliquots, were collected by centrifugation (room temperature, 3 minutes, 6800 ×*g*). Supernatants were discarded and 125 μL of LyseBlue reagent diluted in P1 buffer (1:1000) was added to each pellet. The pellet was resuspended by aspirating with a pipette, before 125 μL of P2 buffer was added and the tube contents mixed by gentle inversion. Samples were incubated for 3 minutes and then 175 μL of P3 buffer was added and mixed by inversion before centrifugation (20°C, 10 minutes, 17900 ×*g*). The supernatants were pooled into three aliquots in fresh microcentrifuge tubes before centrifugation (20°C, 5 minutes, 17900 ×*g*) to remove any insoluble impurities.

Supernatant from one aliquot was added to an assembled spin column and collection tube, which was centrifuged (20°C, 30 s, 17900 ×*g*) and the flow-through discarded. This process was repeated with the supernatants from the other two aliquots using the same spin column and conditions, except that the very last centrifugation step was for 60 s. Then, 0.5 mL of PB wash

buffer was added to the spin column, a centrifugation step was performed (20°C, 60 s, 17900 ×*g*) and then the flow-through was discarded. A final wash of 0.75 mL of PE buffer was added to the spin column before centrifugation (20°C, 1 minute, 17900 ×*g*), discard of the supernatant, and a second centrifugation step (20°C, 60 s, 22000 ×*g*).

The spin column was transferred to a fresh Eppendorf tube and 50 µL of EB buffer was added before incubation for 5 minutes followed by centrifugation (20°C, 60 s, 17900 ×*g*). Flow-through was collected and reloaded on to the spin column before a second identical centrifugation step. Plasmid DNA concentration and quality of the flow-through was analysed by NanoDrop 1000 spectrophotometer (ThermoFisher Scientific Inc; Wilmington, US.) and using buffer EB as a blank. The plasmid DNA was stored at -20°C until needed.

pUC18 plasmid DNA was isolated from *E. coli* TOP10 using the same protocol as above, except that only a single 1.5 mL aliquot of culture was processed because this plasmid is at high copy number in the host cell compared to the pSC189 plasmid due to differing origins of replication (*Ori*). In addition, the PB wash buffer step was omitted, as this is required only for strains that are *endA*$^{+}$ endonuclease positive.

2. Linearisation of plasmids by BamHI digestion.

To confirm the size of plasmid DNA, plasmid samples were digested with the BamHI restriction enzyme (ThermoFisher Scientific Inc., Renfrew, UK) and run on agarose gel. For this, plasmid samples were diluted to 20 ng/μL in nuclease free water. Restriction enzyme reactions were prepared in reactions to contain 10 μL of plasmid DNA, 7.5 μL of nuclease free water and 2 μL of 10× BamHI buffer (ThermoFisher Scientific Inc.) then mixed by flicking bottom of tube and briefly centrifuged (5 s, 3500 ×*g*), before 0.5 μL of BamHI (10 U/μL) was added to each reaction. The tube contents were mixed, by flicking bottom of tube, and briefly centrifuged (5 s, 3500 ×*g*), before incubation (37°C, 1 h). A control reaction lacking BamHI was prepared, while a further control lacked plasmid DNA (no template control). Reactions were inactivated by adding 0.8 μL of 0.5 M EDTA (pH8.0) to a final concentration of 20 mM, then to 5 μL of each sample was added 1 μL 6× loading dye (ThermoFisher Scientific Inc.) and this was run on a 1.5% (w/v) agarose gel made with 0.75 × TAE as previously described (Section 2.2.5.4.). To the first well of the gel was added 2 μL of 1-kb ladder (0.1 μg/μL) (ThermoFisher Scientific Inc.) in 6 μL of a 1× loading dye.

Results: BamHI digestion of plasmid DNA

To confirm expected plasmid size, pSC189 plasmid was digested with the BamHI restriction enzyme and this yielded two product bands when visualised on an agarose gel, suggesting the presence of two BamHI

recognition sites. However, bioinformatics analysis of the plasmid sequence with Bioedit suggested that only one BamHI recognition site should be present (beginning at nucleotide position 5810). Furthermore, the combined size of the two BamHI digested pSC189 bands (approximately 7700 bp) exceeded the published 6982 bp size (Chiang and Rubin., 2002). While both of these unexpected results suggest an additional insert into pSC189, which requires further investigation, it was beyond the scope of the present study, and was not expected to exert a detrimental impact on subsequent experiments. The pUC18 control plasmid was also digested with BamHI and this yielded a single band of the expected size (2686 bp) when visualised on agarose gel, which was in agreement with the *in silico* identification of a single BamHI recognition site in this plasmid. Undigested pSC189 yielded two bands: the first of which migrated approximately the same distance as the 8-kb band of the ladder while the second band migrated a much greater distance, and this profile is characteristic of supercoiled and nicked plasmid DNA respectively.

Chiang, S. L., and E. J. Rubin, 2002, Construction of a mariner-based transposon for epitope-tagging and genomic targeting: Gene, v. 296, p. 179-185.

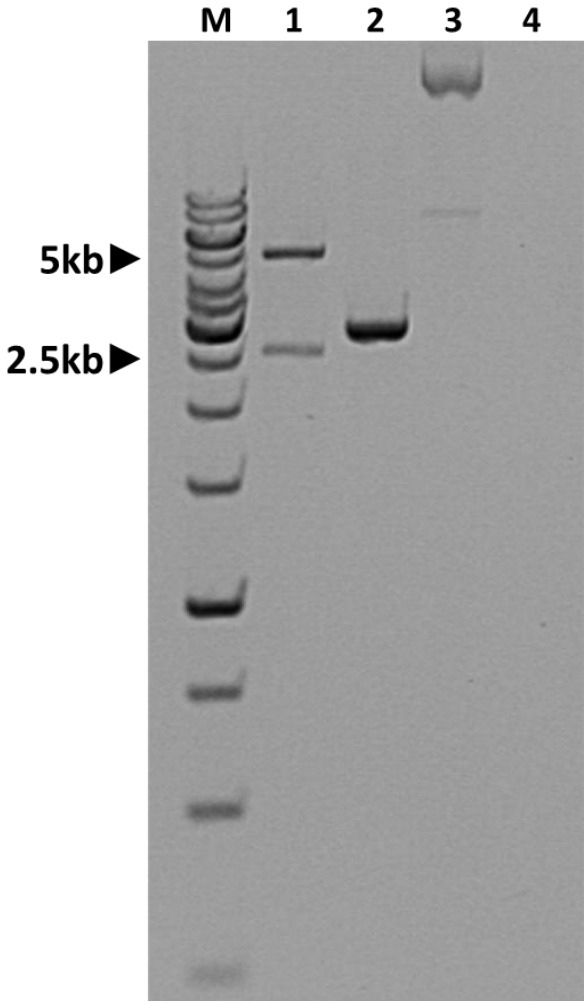

Figure. Agarose gel electrophoresis of pSC189 and pUC18 plasmids, following digestion with the BamHI restriction enzyme at 37°C for 1 h to confirm expected plasmid sizes: M, 1kb DNA ladder; lane 1, pSC189; lane 2, pUC18; lane 3, pSC189 no enzyme control; lane 4, no template control

Appendix IX.

Essential genes of *Vibrio anguillarum* NB10Sm identified in this study

	Chromosome (1 or 2)/ or plasmid	Gene	Protein	Gene ID	start	end	Gene size	strand
VAA_RS00300	1		5S ribosomal RNA	10773845	69454	69569	116	-
VAA_RS00305	1		23S ribosomal RNA	10773846	69636	72554	2919	-
VAA_RS00315	1		16S ribosomal RNA	10773848	73010	74567	1558	-
VAA_RS00320	1		hypothetical protein	10773849	74589	74768	180	-
VAA_RS00380	1		hypothetical protein	10773860	84944	85153	210	+
VAA_RS00555	1		IS5 family transposase	10773897	121431	122351	921	-
VAA_RS00570	1		hypothetical protein	10773900	123961	124278	318	+
VAA_RS00575	1		hypothetical protein	10773901	124275	124628	354	+
VAA_RS00580	1		transposase	10773902	124688	126229	1542	+
VAA_RS00710	1		23S ribosomal RNA	10773932	150294	153211	2918	-
VAA_RS00725	1		hypothetical protein	10773935	155228	155407	180	-
VAA_RS00845	1		transposase	10773964	177887	179428	1542	-
VAA_RS00850	1		transposase	10773965	179488	179841	354	-
VAA_RS00855	1		transposase	10773966	179838	180155	318	-
VAA_RS00960	1		hypothetical protein	10773986	204880	205065	186	-
VAA_RS00965	1		sulfurtransferase TusA	10773987	205199	205447	249	+
VAA_RS01170	1		16S ribosomal RNA	10774031	248905	250462	1558	+
VAA_RS01185	1		23S ribosomal RNA	10774034	251007	253925	2919	+
VAA_RS01190	1		5S ribosomal RNA	10774035	253992	254107	116	+
VAA_RS01580	1		transposase	10774115	332429	333970	1542	-

VAA_RS01585	1		transposase	10774116	334030	334383	354	-
VAA_RS01590	1		hypothetical protein	10774117	334380	334697	318	-
VAA_RS01615	1		hypothetical protein	10774122	338005	338322	318	+
VAA_RS01620	1		transposase	10774123	338319	338672	354	+
VAA_RS01625	1		transposase	10774124	338732	340273	1542	+
VAA_RS01650	1		IS5 family transposase	10774129	347226	348146	921	-
VAA_RS01765	1		IS5 family transposase	10774154	377585	378505	921	-
VAA_RS01785	1		excisionase	10774158	385083	385367	285	-
VAA_RS01845	1		transcriptional regulator	10774170	398907	399236	330	-
VAA_RS01900	1	rpmB	50S ribosomal protein L28	10774180	409272	409508	237	+
VAA_RS02160	1		hypothetical protein	10774233	462789	463037	249	-
VAA_RS02200	1		hypothetical protein	10774241	471804	472346	543	+
VAA_RS02935	1		50S ribosomal protein L16	10774395	634078	634488	411	+
VAA_RS02940	1		50S ribosomal protein L29	10774396	634488	634679	192	+
VAA_RS02950	1		50S ribosomal protein L14	10774398	635094	635465	372	+
VAA_RS02965	1	rpsN	30S ribosomal protein S14	10774401	636377	636682	306	+
VAA_RS02995	1		50S ribosomal protein L15	10774407	638714	639148	435	+
VAA_RS03420	1		hypothetical protein	10774497	720622	720831	210	-
VAA_RS03440	1		16S ribosomal RNA	10774501	725771	727328	1558	+
VAA_RS03465	1		23S ribosomal RNA	10774506	728144	731063	2920	+
VAA_RS03470	1		5S ribosomal RNA	10774507	731130	731245	116	+
VAA_RS03480	1		5S ribosomal RNA	10774509	731420	731535	116	+
VAA_RS03555	1		cell division protein ZapA	10774525	748350	748658	309	-
VAA_RS03800	1		hypothetical protein	23440775	804131	804340	210	-
VAA_RS04085	1		DUF3545 domain-containing protein	10774635	874401	874580	180	-
VAA_RS04155	1		hypothetical protein	10774650	893176	893388	213	-
VAA_RS05185	1	fliN	flagellar motor switch protein FliN	10774862	1096758	1097168	411	+
VAA_RS05490	1		DNA repair ATPase	10774923	1161149	1161673	525	+

VAA_RS05685	1	acyl carrier protein	23440785	1202074	1202307	234	+
VAA_RS06570	1	transposase	10775144	1397424	1398965	1542	-
VAA_RS06575	1	transposase	10775145	1399025	1399378	354	-
VAA_RS06580	1	hypothetical protein	10775146	1399375	1399692	318	-
VAA_RS06615	1	IS5 family transposase	10775152	1405736	1406656	921	-
VAA_RS07255	1	transposase	10775288	1560677	1562218	1542	-
VAA_RS07265	1	hypothetical protein	10775290	1562631	1562948	318	-
VAA_RS07305	1	hypothetical protein	10775299	1569997	1570311	315	-
VAA_RS07705	1	hypothetical protein	10775382	1669173	1669394	222	+
VAA_RS07850	1	hypothetical protein	23440810	1708082	1708186	105	+
VAA_RS07875	1	IS5 family transposase	10775419	1712857	1713777	921	+
VAA_RS07890	1	transposase	10775422	1718148	1718501	354	-
VAA_RS07895	1	hypothetical protein	10775423	1718498	1718815	318	-
VAA_RS07910	1	hypothetical protein	10775427	1723105	1723422	318	+
VAA_RS07915	1	transposase	10775428	1723419	1723772	354	+
VAA_RS07920	1	transposase	10775429	1723832	1725373	1542	+
VAA_RS08225	1	cytochrome-c oxidase	10775491	1787572	1787748	177	-
VAA_RS08445	1	IS91 family transposase	23440816	1840112	1841002	891	-
VAA_RS08730	1	IS5 family transposase	10775594	1901285	1902205	921	-
VAA_RS08905	1	IS5 family transposase	10775630	1943336	1944256	921	+
VAA_RS09020	1	trimethylamine N-oxide reductase system protein *torE*	10775654	1968500	1968676	177	-
VAA_RS09500	1	hypothetical protein	23440820	2076427	2076615	189	+
VAA_RS10100	1	molybdopterin synthase sulfur carrier subunit	10775878	2208882	2209127	246	-
VAA_RS10185	1	IS91 family transposase	23440832	2234291	2235181	891	+
VAA_RS10405	1	IS91 family transposase	23440834	2287528	2288418	891	+
VAA_RS10535	1	hypothetical protein	10775970	2317377	2317655	279	+
VAA_RS10850	1	amelogenin	10776038	2385669	2385989	321	-
VAA_RS10930	1	hypothetical protein	23440842	2398470	2398655	186	-

VAA_RS11010	1		IS5 family transposase	10776069	2415532	2416452	921	-
VAA_RS11195	1		IS5 family transposase	10776108	2452530	2453450	921	-
VAA_RS11245	1		IS5 family transposase	10776118	2462263	2463183	921	-
VAA_RS11530	1		5S ribosomal RNA	10776176	2526185	2526300	116	-
VAA_RS11535	1		23S ribosomal RNA	10776177	2526367	2529285	2919	-
VAA_RS11555	1		16S ribosomal RNA	10776181	2529994	2531565	1572	-
VAA_RS11705	1		30S ribosomal protein S20	23440850	2568580	2568840	261	+
VAA_RS11740	1		transposase	10776223	2575251	2576123	873	-
VAA_RS11745	1		transposase	10776224	2576120	2576428	309	-
VAA_RS11765	1		transposase	10776228	2577921	2579462	1542	-
VAA_RS11775	1		hypothetical protein	10776230	2579875	2580192	318	-
VAA_RS11825	1		hypothetical protein	10776241	2585718	2586035	318	+
VAA_RS11830	1		hypothetical protein	10776242	2586032	2586385	354	+
VAA_RS11835	1		transposase	10776243	2586445	2587986	1542	+
VAA_RS12715	1		hypothetical protein	10776421	2785632	2785949	318	+
VAA_RS12720	1		transposase	10776422	2785946	2786299	354	+
VAA_RS12725	1		transposase	23440861	2786359	2787899	1541	+
VAA_RS12735	1		glycine/betaine ABC transporter	10776425	2788662	2788961	300	+
VAA_RS12795	1		glycine/betaine ABC transporter	10776439	2802647	2802946	300	+
VAA_RS12800	1		transposase	10776440	2802967	2803803	837	+
VAA_RS12940	1		transposase	10776470	2832064	2832372	309	+
VAA_RS12945	1		transposase	10776471	2832369	2833242	874	+
VAA_RS13305	1	rpmA	50S ribosomal protein L27	10776546	2904196	2904453	258	-
VAA_RS13335	1		hypothetical protein	23440872	2909724	2909912	189	-
VAA_RS13370	1		hypothetical protein	10776559	2916967	2917170	204	-
VAA_RS13385	1		transcriptional regulator	10776562	2919187	2919396	210	+
VAA_RS13635	1		tRNA-Asp	10776612	2986459	2986535	77	-
VAA_RS13640	1		5S ribosomal RNA	10776613	2986565	2986680	116	-

VAA_RS13645	1		23S ribosomal RNA	10776614	2986747	2989665	2919	-
VAA_RS13655	1		16S ribosomal RNA	10776616	2990088	2991659	1572	-
VAA_RS13660	1		hypothetical protein	10776617	2991681	2991860	180	-
VAA_RS13805	1		hypothetical protein	23440874	3016306	3016494	189	-
VAA_RS13940	1		50S ribosomal protein L10	10776675	3052385	3052873	489	-
VAA_RS13965	1	*tuf*	elongation factor Tu	10776680	3055625	3056809	1185	-
VAA_RS14020	1		5S ribosomal RNA	10776692	3062762	3062877	116	-
VAA_RS14045	2		transposase	10776698	767	1084	318	-
VAA_RS14065	2		transposase	10776704	4561	6102	1542	-
VAA_RS14070	2		transposase	10776705	6162	6515	354	-
VAA_RS14075	2		transposase	10776706	6512	6829	318	-
VAA_RS14080	2		hypothetical protein	10776708	7450	7680	231	-
VAA_RS14115	2		IS5 family transposase	10776715	11986	12906	921	-
VAA_RS15085	2		IS91 family transposase	23440895	226877	227767	891	+
VAA_RS15420	2		transcriptional regulator	23440897	299529	299756	228	-
VAA_RS15560	2		IS5 family transposase	10777009	332888	333808	921	+
VAA_RS15995	2		hypothetical protein	23440902	432258	433504	1247	+
VAA_RS16370	2		IS91 family transposase	23440909	530579	531469	891	+
VAA_RS16395	2		IS91 family transposase	23440910	537488	538378	891	-
VAA_RS16495	2		IS91 family transposase	23440912	554448	555338	891	-
VAA_RS16610	2		phage-shock protein	10777228	579986	580360	375	-
VAA_RS16740	2		IS5 family transposase	10777255	609976	610896	921	-
VAA_RS17580	2		hypothetical protein	10777427	829688	830005	318	+
VAA_RS17585	2		hypothetical protein	10777428	830002	830355	354	+
VAA_RS17590	2		transposase	10777429	830415	831956	1542	+
VAA_RS18020	2	*rplT*	50S ribosomal protein L20	10777519	933742	934095	354	+
VAA_RS18030	2		transposase	10777521	934703	936244	1542	-
VAA_RS18035	2		transposase	10777522	936253	936657	405	-

VAA_RS18040	2		transposase	10777523	936654	936971	318	-
VAA_RS18045	2		ribosomal small subunit pseudouridine synthase	10777524	937028	937222	195	+
VAA_RS18100	2		hypothetical protein	10777542	948280	948564	285	-
VAA_RS18120	2		RecA regulator	10777551	951601	952035	435	+
VAA_RS18185	2		hypothetical protein	23440934	963445	963672	228	+
VAA_RS18190	2		hypothetical protein	10777573	964167	964451	285	+
VAA_RS18240	2		hypothetical protein	23440936	972653	972868	216	+
VAA_RS18255	2		hypothetical protein	10777600	977616	977831	216	+
VAA_RS18275	2		hypothetical protein	23440938	980325	980765	441	+
VAA_RS18280	2		hypothetical protein	10777606	980876	981073	198	-
VAA_RS18295	2		hypothetical protein	10777608	982307	982921	615	-
VAA_RS18310	2		excinuclease	23440941	984712	985152	441	-
langO2_p10	pNC_009351	*mobD*	mobD protein	4991489	7500	7865	366	+
UQY_1 "1391	pNC_019325		hypothetical protein	13919012	322	447	126	+
N175_RS1829	p67-NB10		IS5 family transposase	-	578	1498	921	-
N175_RS1832	p67-NB10		IS5 family transposase	-	7513	8433	921	+
N175_RS1833	p67-NB10		transposase	-	9429	10970	1542	-
N175_RS1834	p67-NB10		transposase	-	11030	11383	354	-
N175_RS1834	p67-NB10		transposase	-	11380	11697	318	-
N175_RS1838	p67-NB10		hypothetical protein	-	21576	22010	435	+
N175_RS1839	p67-NB10		IS5 family transposase	-	22095	22961	867	+
N175_RS1845	p67-NB10		IS5 family transposase	-	40680	41600	921	+
N175_RS1847	p67-NB10		hypothetical protein	-	47728	48045	318	+
N175_RS1848	p67-NB10		hypothetical protein	-	48042	48395	354	+
N175_RS1848	p67-NB10		transposase	-	48455	49996	1542	+
N175_RS1850	p67-NB10		IS91 family transposase	-	52957	53847	891	-
N175_RS1856	p67-NB10		IS91 family transposase	-	61814	62704	891	-
langO2_p05	pNC_009351		hypothetical protein	4991484	4018	4383	366	+

VAA_RS01225	1		thiamine biosynthesis protein ThiS	10774042	259377	259586	210	+
VAA_RS02560	1		hypothetical protein	10774318	555887	556225	339	-
VAA_RS02915	1		50S ribosomal protein L2	10774391	631882	632706	825	+
VAA_RS03605	1		RNA polymerase sigma factor RpoE	10774535	756677	757249	573	+
VAA_RS05010	1		oxidoreductase	10774823	1063543	1063770	228	+
VAA_RS05335	1		succinate dehydrogenase cytochrome b556 large SUBUNIT	10774893	1122890	1123282	393	+
VAA_RS07095	1		hypothetical protein	10775255	1523934	1524215	282	+
VAA_RS09685	1		transcriptional regulator HU subunit alpha	10775795	2116092	2116364	273	-
VAA_RS12660	1	*rpsU*	30S ribosomal protein S21	10776411	2774346	2774561	216	+
VAA_RS12750	1		transcriptional regulator	10776429	2792729	2792893	165	-
VAA_RS12980	1		stress protein	10776479	2840037	2840333	297	-
VAA_RS13160	1		YggU family protein	10776517	2884412	2884702	291	+
VAA_RS13740	1		YggU family protein	10776634	3006683	3006985	303	-
VAA_RS14310	2		thiol:disulfide oxidoreductase	10776754	47264	47932	669	-
VAA_RS14655	2		chemotaxis protein CheC	10776824	123458	123823	366	-
VAA_RS16000	2		hypothetical protein	10777101	433634	433972	339	+
VAA_RS17400	2		LysR family transcriptional regulator	10777390	781135	782013	879	-
VAA_RS17940	2		nitrate reductase catalytic subunit	10777502	916646	916951	306	-
VAA_RS18075	2		prevent-host-death family protein	10777533	943478	943729	252	+